University of Reading

Fifty years of research on the Madden-Julian Oscillation: recent progress, challenges and perspectives

Article

Accepted Version

Jiang, X., Adames, Á. F., Kim, D., Maloney, E. D., Lin, H., Kim, H., Zhang, C., DeMott, C. A. and Klingaman, N. P. ORCID: https://orcid.org/0000-0002-2927-9303 (2020) Fifty years of research on the Madden-Julian Oscillation: recent progress, challenges and perspectives. Journal of Geophysical Research: Atmospheres, 125 (17). e2019JD030911. ISSN 2169-8996 doi: 10.1029/2019JD030911 Available at https://centaur.reading.ac.uk/91428/

It is advisable to refer to the publisher's version if you intend to cite from the work. See Guidance on citing.

To link to this article DOI: http://dx.doi.org/10.1029/2019JD030911

Publisher: American Geophysical Union

All outputs in CentAUR are protected by Intellectual Property Rights law, including copyright law. Copyright and IPR is retained by the creators or other copyright holders. Terms and conditions for use of this material are defined in the End User Agreement.

University of Reading

www.reading.ac.uk/centaur

CentAUR

Central Archive at the University of Reading

Reading's research outputs online

Fifty Years of Research on the Madden-Julian Oscillation: Recent Progress, Challenges, and Perspectives

Xianan Jiang[1,2], Ángel F. Adames[3], Daehyun Kim[4], Eric D. Maloney[5], Hai Lin[6], Hyemi Kim[7], Chidong Zhang[8], Charlotte A. DeMott[5], and Nicholas P. Klingaman[9]

[1]*Joint Institute for Regional Earth System Science & Engineering, University of California, Los Angeles, California, USA*

[2]*Jet Propulsion Laboratory, California Institute of Technology, Pasadena, California, USA*

[3]*Department of Climate and Space Science and Engineering, University of Michigan, Ann Arbor, Michigan, USA*

[4]*Department of Atmospheric Sciences, University of Washington, Seattle, Washington, USA*

[5]*Department of Atmospheric Science, Colorado State University, Fort Collins, Colorado, USA*

[6] *Recherche en prévision numérique atmosphérique, Environment and Climate Change Canada, Dorval, Canada*

[7]*School of Marine and Atmospheric Sciences, Stony Brook University, Stony Brook, New York, USA*

[8]*NOAA/Pacific Marine Environmental Laboratory, Seattle, Washington, USA*

[9]*National Centre for Atmospheric Science and Department of Meteorology, University of Reading, Reading, UK*

Special Collection on "*Grand Challenges in the Earth and Space Sciences*"
J. Geophysical Research - Atmosphere

Submitted 02/2020
Revised 06/2020

**Corresponding author address:* Dr. Xianan Jiang, Jet Propulsion Laboratory, California Institute of Technology, MS 233-300, 4800 Oak Grove Drive, Pasadena, CA 91109. Email: xianan@ucla.edu. Copyright © 2020. All rights reserved.

Abstract

Since its discovery in the early 1970s, the crucial role of the Madden-Julian Oscillation (MJO) in the global hydrological cycle and its tremendous influence on high-impact climate and weather extremes have been well recognized. The MJO also serves as a primary source of predictability for global Earth system variability on subseasonal time scales. The MJO remains poorly represented in our state-of-the-art climate and weather forecasting models, however. Moreover, despite the advances made in recent decades, theories for the MJO still disagree at a fundamental level. The problems of understanding and modeling the MJO have attracted significant interest from the research community. As a part of the AGU's Centennial collection, this article provides a review of recent progress, particularly over the last decade, in observational, modeling, and theoretical study of the MJO. A brief outlook for near-future MJO research directions is also provided.

Keywords: Madden-Julian Oscillation, tropical convection, climate modeling, seasonal-to-subseasonal prediction

1. Introduction

Motivated by the desire to explain the newly discovered Quasi-biennial Oscillation (QBO) in the 1960s (*Reed et al.*, 1961), and particularly inspired by Taroh Matsuno's seminal work on analytical solutions of equatorial waves (*Matsuno*, 1966), Roland Madden and Paul Julian analyzed 10-year radiosonde observations collected from Canton Island to find evidence for equatorial synoptic waves. What they found instead was an oscillatory signal in surface pressure and zonal winds with mysterious periodicity of 30-60 days (*Madden and Julian*, 1971). In their follow-up study that analyzed observations collected in 20 stations across the tropics, Madden and Julian (1972) found that this 30-60 day oscillation is part of a slowly eastward propagating (~ 5 m s^{-1}), planetary-scale phenomenon that features large-scale convective fluctuations and associated vertically overturning circulation anomalies. This large-scale phenomenon is now widely known as the Madden-Julian Oscillation (MJO; see *Lau and Waliser*, 2012 for details on historical MJO research).

Since its discovery, the detailed structure and evolution of the MJO have been extensively characterized, particularly by taking advantage of contemporary observations in recent decades, including those from satellites, in-situ field experiments, and modern reanalysis datasets. For example, as shown in Fig. 1, the recent high-resolution precipitation data from the Tropical Rainfall Measuring Mission (TRMM) satellite provides excellent detail of the MJO's horizontal structure during its life cycle beyond that depicted by Madden and Julian (1972). These details include the MJO's asymmetry about the equator associated with the Inter-tropical Convergence Zone (ITCZ) and South Pacific Convergence Zone (SPCZ), and strong disruptions by tropical land masses including the Maritime Continent.

Meanwhile, the crucial role of the MJO in Earth's hydrological cycle has been gradually recognized by numerous studies subsequent to Madden and Julian's pioneering work. Widespread influences of the MJO on global climate and weather extremes have been documented (see extensive reviews by *Lau and Waliser*, 2012; *Zhang*, 2013), including the onset and demise of global monsoons (e.g., *Lau and Chan*, 1986; *Hendon and Liebmann*, 1990; *Webster et al.*, 1998; *Sultan et al.*, 2003; *Jiang et al.*, 2004; *Wang*, 2006; *Lorenz and Hartmann*, 2006; *Wheeler et al.*, 2009; *Mo et al.*, 2012), the genesis and tracks of tropical cyclones (e.g., *Nakazawa*, 1988; *Mo*, 2000; *Higgins and Shi*, 2001; *Liebmann et al.*, 1994; *Maloney and Hartmann*, 2000; *Bessafi and*

Wheeler, 2006; *Aiyyer and Molinari*, 2008; *Klotzbach*, 2010; *Jiang et al.*, 2012), the frequency of extreme temperature and precipitation events (e.g., *Zhu et al.*, 2003; *Bond and Vecchi*, 2003; *Jeong et al.*, 2005; *Park et al.*, 2010; *Guan et al.*, 2012; *Zheng et al.*, 2018; *Lin et al.*, 2019b), tornadoes (*Tippett*, 2018; *Gensini et al.*, 2019), polar sea ice (*Henderson et al.*, 2016; *Lee and Seo*, 2019), and chemical and biological components in the atmosphere and oceans (e.g., *Waliser et al.*, 2005; *Tian et al.*, 2007; *Tian et al.*, 2011; *Li et al.*, 2010). The MJO also interacts with other prominent modes of climate variability, including the El Niño / Southern Oscillation (ENSO; e.g., *Takayabu et al.*, 1999; *McPhaden*, 1999; *Kessler and Kleeman*, 2000; *Hendon et al.*, 2007), Arctic Oscillation (AO; *L'Heureux and Higgins*, 2008), North Atlantic Oscillation (NAO; *Cassou*, 2008; *Lin et al.*, 2009), and Indian Ocean Dipole (IOD; *Rao and Yamagata*, 2004). It has also been suggested that the recent rapid warming over the Arctic, a.k.a., Arctic amplification, could be partially attributed to the enhanced moisture transport and warm temperature advection by planetary Rossby waves that are associated with the increase in the frequency of MJO convective activity over the Maritime Continent (MC) and western Pacific (*Yoo et al.*, 2011; *Lee et al.*, 2011; *Yoo et al.*, 2012; *Seo et al.*, 2016). The MJO influences sudden stratospheric warming events, which can distort or completely reverse the stratospheric polar vortex, thus producing a negative phase of the Northern Annular Mode (*Garfinkel et al.*, 2014; *Garfinkel and Schwartz*, 2017; *Kang and Tziperman*, 2017; 2018a; b).

With its far-reaching impacts on global climate and weather patterns, and its quasi-periodic occurrence on intraseasonal time scales, the MJO provides a primary source of predictability for extended-range weather forecasts, and thereby fills the gap between deterministic weather forecasts and climate prediction (e.g., *Waliser*, 2012; *Gottschalck et al.*, 2010; *NAS*, 2010; Vitart et al., 2012; *NASEM*, 2016). Motivated by recent coordinated community efforts that target enhancing accuracy and socio-economic utility of seasonal-to-subseasonal (S2S) forecasts (e.g., *Vitart and Robertson*, 2018), great enthusiasm has developed for improving extended-range prediction of MJO-related extreme weather activity (e.g., *Xiang et al.*, 2015a; *Baggett et al.*, 2017; *Jiang et al.*, 2018b; *Baggett et al.*, 2018; *Lee et al.*, 2018; *Mundhenk et al.*, 2018; *Wang et al.*, 2018d; *Lin*, 2018; *DeFlorio et al.*, 2019; *Xiang et al.*, 2020; *Gensini et al.*, 2019).

Despite its critical role in the global climate system, the MJO remains poorly represented in recent generations of GCMs (Hung et al., 2013; Jiang et al., 2015; Ahn et al., 2017; *Ahn et al.*, 2020b; see the detailed review in Section 3.3). In the few GCMs that are able to capture the bulk

characteristics of the MJO, the reasons for their good MJO simulations are not well understood (e.g., *Klingaman et al.*, 2015a). The improved MJO representation achieved by tuning GCM parameters can occur at the expense of degrading the model mean state and other climate phenomena (e.g., *Kim et al.*, 2011b; *Mapes and Neale*, 2011b). Meanwhile, MJO prediction skill still remains limited in most climate and weather forecasting models (see Section 3.4), with a typical skill of 3-5 weeks (e.g., Seo et al., 2009; Vitart and Molteni, 2010; Rashid et al., 2011; *Wang et al.*, 2014; *Neena et al.*, 2014; *Kim et al.*, 2014c; *Xiang et al.*, 2015b; *Kim et al.*, 2018), in contrast to its estimated intrinsic potential predictability of about 5-7 weeks (e.g., *Waliser et al.*, 2003; *Neena et al.*, 2014; *Ding et al.*, 2010).

The challenges in simulating and predicting the MJO create an urgent demand for improved understanding of its fundamental physics. Since the call for intensified research on MJO physics and dynamics at a Trieste workshop in 2006 (*ICTP*, 2006), the MJO has been a central focus of multinational research projects endorsed by the World Weather Research Program (WWRP), the World Climate Research Program (WCRP), and by International and US CLIVAR (Climate Variability and Predictability) (see a review by *Zhang et al.*, 2013). These international efforts have included the Intraseasonal Variability Hindcast Experiment (*Neena et al.*, 2014), the Year of Tropical Convection (YOTC) virtual field campaign (*Waliser et al.*, 2012; Moncrieff et al., 2012), the Dynamics of the MJO (DYNAMO) field campaign over the Indian Ocean (Yoneyama et al., 2013; see Section 3.1.1), the WCRP/WWRP YOTC MJO Task Force (MJOTF, now under the Working Group on Numerical Experimentation, WGNE) and the Global Energy and Water Exchanges (GEWEX) Atmospheric System Study (GASS) MJO model comparison project (Petch et al., 2011; *Klingaman et al.*, 2015a), the Subseasonal to Seasonal (S2S) Prediction Project (Vitart et al., 2012; 2017), the Years of the Maritime Continent (YMC) field campaign (see Section 3.6.3), and the Subseasonal Experiment (SubX) (*Pegion et al.*, 2019). Meanwhile, to address specific issues related to biases in MJO simulations and predictions, the MJOTF has promoted efforts to develop advanced MJO process-oriented diagnostics (*Waliser et al.*, 2009; *Kim et al.*, 2009; *Gottschalck et al.*, 2010; *Wheeler and Maloney*, 2013; see details in Sections 3.3 and 3.4).

Because of the extensive efforts in the weather and climate research community listed above, recent decades have seen significant advances towards improved MJO understanding and prediction, although continued efforts are still warranted as outlined in Section 4. The growing use

of models that employ cloud-permitting resolutions either in the form of the super-parameterization (*Randall et al.*, 2003) or global cloud-resolving models (GCRMs; *Miura et al.*, 2007; *Miyakawa et al.*, 2014) have provided powerful tools to understand MJO physics and act as a benchmark for conventional GCM parameterization schemes. Theoretical understanding of the MJO has also been significantly advanced in recent decades. In particular, moisture mode theory (*Neelin and Yu*, 1994; *Raymond and Fuchs*, 2009; *Sobel and Maloney*, 2013; *Adames and Kim*, 2016) has provided critical insights into key processes regulating MJO variability in observations and simulations of current and future climate (*Kim et al.*, 2014a; *Kim et al.*, 2017; *Gonzalez and Jiang*, 2019; *DeMott et al.*, 2018; *Jiang et al.*, 2018a; *Adames et al.*, 2017a; *Maloney et al.*, 2019a; *Rushley et al.*, 2019) and processes responsible for model deficiencies in simulating and predicting the MJO (*Jiang*, 2017; *Gonzalez and Jiang*, 2017; *Kim*, 2017; *Lim et al.*, 2018; *DeMott et al.*, 2019). New observations from recent in-situ field experiments have meanwhile provided an unprecedented opportunity to document key processes during an MJO life cycle (e.g., *Yoneyama et al.*, 2013). The recently identified strong connection between the MJO and QBO has also inspired great interest in exploring the role of stratosphere-troposphere interactions in shaping the year-to-year variability of MJO activity (e.g., *Yoo and Son*, 2016; *Son et al.*, 2017; *Zhang and Zhang*, 2018).

Much of the earlier research on the MJO has been summarized in detail by several previous review articles or books, including Madden and Julian (1994), Zhang (2005), and Lau and Waliser (2012). This article provides a comprehensive review of recent progress on MJO research as a part of the AGU's Centennial collection, motivated by the aforementioned recent exciting developments in MJO research. We mainly focus on progress achieved in the years following those previous reviews, although some important aspects of MJO research earlier in time are included for completeness. In Section 2, several scientific issues related to the essential physics of the MJO are briefly discussed, which provides background for detailed discussion in the following sections. Major progress made over the most recent decade is reviewed in Section 3, including that related to MJO observations (3.1), theoretical understanding (3.2), modeling (3.3), prediction (3.4), air-sea interactions (3.5), MC interactions (3.6), tropical-extratropical interactions (3.7), QBO connections (3.8), and changes under a future climate (3.9). An outlook for future MJO studies is presented in Section 4. A brief summary is given in Section 5.

2. Scientific issues of the MJO

Based on numerous observational studies of MJO structure and evolution, a typical longitude-height profile of the MJO is given by the schematic in Fig. 2 from Kiladis et al. (2009). Vigorous deep convective clouds, enhanced column moisture, and strong upward motion and overturning circulations prevail near the MJO convection center. The region to the east of MJO convection is characterized by enhanced lower-tropospheric moisture anomalies (e.g., *Kemball-Cook and Weare*, 2001; *Sperber*, 2003; *Kiladis et al.*, 2005; *Tian et al.*, 2010; *Johnson and Ciesielski*, 2013), warm sea surface temperature (SST; *Hendon and Glick*, 1997; *Woolnough et al.*, 2000; *Shinoda et al.*, 1998), boundary layer (BL) convergence (*Sperber*, 2003; *Kiladis et al.*, 2005), and a bottom-heavy heating structure (e.g., *Lin et al.*, 2004; *Kiladis et al.*, 2005; *Jiang et al.*, 2011) dominated by shallow cumuli/congestus clouds (*Johnson et al.*, 1999; *Kikuchi and Takayabu*, 2004; *Chen and Del Genio*, 2009b; *Tromeur and Rossow*, 2010; *Powell and Houze*, 2013; *Xu and Rutledge*, 2014), characteristic of free tropospheric moistening that supports MJO eastward propagation. To the west of MJO convection can be found extensive trailing stratiform-type clouds (*Lin et al.*, 2004; *Kiladis et al.*, 2005) that interact with atmospheric radiation (*Del Genio and Chen*, 2015; *Kim et al.*, 2015) and enhanced low-level westerly winds that amplify surface turbulent fluxes (*Hendon and Glick*, 1997). Precipitation from these upper-tropospheric stratiform clouds fall through relatively dry lower levels, cooling the environment through evaporation, leading to a vertical dipole stratiform heating structure, i.e., heating in the upper troposphere and cooling in the lower troposphere (e.g., *Lin et al.*, 2004; *Benedict and Randall*, 2007).

The prominent east-west asymmetry in dynamic and thermodynamic fields of the observed MJO has been one of the key constraints in the development of MJO theories. The fact that the MJO does not appear in the solutions of the dry shallow-water system on an equatorial beta-plane linearized about a resting atmosphere (e.g., *Wheeler and Kiladis*, 1999) has led to the hypothesis that incorporating moisture and its interactions with convection and large-scale dynamics and/or nonlinear interaction among multi-scale waves are key to MJO dynamics. In the following sections, several critical processes associated with the MJO are briefly outlined, which serve as background for the detailed reviews on various MJO aspects in Section 3.

2.1 Moisture-convection feedback

Observational studies indicate that organized convection over tropical oceans exhibits great sensitivity to tropospheric humidity. In a dry environment, a rising convective parcel can lose its

buoyancy quickly due to dilution by turbulent entrainment and resulting evaporative cooling within the parcel, limiting the depth of convective penetration, and favoring shallow cumuli. As a result, heavy area-averaged rainfall associated with oceanic deep convection mostly occurs in moist environments as shown in Fig. 3 (*Bretherton et al.*, 2004; *Peters and Neelin*, 2006; *Thayer-Calder and Randall*, 2009; *Adames*, 2017; *Rushley et al.*, 2018; *Kuo et al.*, 2019). A particularly strong coupling between moisture and convection is observed for MJO wavenumbers and frequencies (*Yasunaga and Mapes*, 2012), illuminating the crucial role of the convection-moisture feedbacks for the MJO. For example, one measure of convective sensitivity to atmospheric moisture, the convective moisture adjustment time scale, defined as the time it takes for convection to remove a given moisture perturbation (*Bretherton et al.*, 2004; *Sobel and Maloney*, 2012), is highly related to MJO rainfall variability (*Jiang et al.*, 2016; *Adames*, 2017).

As shown in Fig. 2, shallow cumulus clouds are prevalent prior to the development of deep MJO convection. These shallow cumuli moisten the atmosphere through detrainment and rain evaporation as well as associated BL convergence, generating a more humid atmosphere that favors the development of deeper convective elements. This recharging process for tropospheric moisture gradually moistens the atmosphere column and favors onset of the deep convective phase of the MJO. Precipitation and compensating convective and mesoscale downdrafts accompany the drying phase of the MJO leading to the suppressed MJO phase. Replicating the interactions between environmental moisture and convection has proven challenging for convection parameterization schemes (e.g., Derbyshire et al., 2004; *Del Genio*, 2012; *Kim et al.*, 2014b). In many GCMs, ubiquitous deep convection still occurs even when the column is relatively dry (*Del Genio et al.*, 2012; *Thayer-Calder and Randall*, 2009; *Rushley et al.*, 2018). Therefore, the MJO moistening phase during the shallow-to-deep convective transition is not well depicted, which can lead to a weak model MJO. Indeed, MJO simulations have been improved in many modeling studies by increasing the sensitivity of convection to environmental moisture (see Section 3.3), suggesting that moisture-convection coupling during the transition phase is critical to the MJO.

2.2 Convection-circulation feedback and the gross moist stability

A growing body of evidence supports the "moisture mode" paradigm of the MJO (see detailed review in Section 3.2), in which MJO convection is tightly coupled to column moisture and the variability of convection is largely regulated by processes that control the variability of column-

integrated moisture or moist static energy (MSE). Diagnosis of processes regulating column MSE anomalies have thus been widely applied for understanding the essential physics regulating MJO amplitude and propagation.

The MSE budget of the MJO in observations and model simulations suggests that feedbacks between MJO convection and large-scale circulation anomalies play a crucial role for MJO stability and propagation. From the moisture mode perspective, a dominant process regulating MJO eastward propagation is through the horizontal advection of the background lower-tropospheric MSE by the anomalous MJO circulation, which exhibits an east-west asymmetry about MJO convection center associated with a Kelvin wave response to the east and Rossby wave response to the west of MJO convection (*Wang and Li*, 1994; *Hendon and Salby,* 1994; *Wang et al.*, 2018a). Horizontal MSE advection leads to the build-up of MSE to the east of MJO deep convection and decrease to the west, thus promoting the eastward propagation of the MJO (e.g., *Maloney*, 2009; *Maloney et al.*, 2010; *Andersen and Kuang, 2012*; *Kim et al., 2014*; *Sobel et al.*, 2014; *Chikira*, 2014; *Adames and Wallace*, 2015; *Arnold et al.*, 2015; *Jiang*, 2017; *Gonzalez and Jiang, 2019).*

Since a typical profile of mean MSE in the tropics is characterized by a minimum in the mid-troposphere, anomalous low-level convergence and mid-level divergence associated with shallow and congestus clouds to the east of MJO deep convection import high MSE air at low levels, and export low MSE air at mid-levels. This is reflected in a net import of moisture, under which the column MSE will grow and convection will intensify in time. Meanwhile, a top-heavy stratiform heating to the west of MJO deep convection induces a circulation that tends to export MSE, thus effectively drying the column and weakening MJO convection (*Raymond et al.*, 2009). The transition from shallow / congestus clouds to deep clouds and then to stratiform clouds as shown in Fig. 2, could therefore also be critical in moistening and supporting convection to the east of the MJO convective center, and drying and suppressing convection to the west, thus promoting the eastward propagation of MJO convection (e.g., *Hsu and Li*, 2012; *Sobel et al.*, 2014; *Yokoi and Sobel*, 2015; *Wang et al.*, 2017; *Inoue and Back*, 2015b).

The efficiency of the large-scale circulation in exporting MSE from a convecting column can be diagnosed with a metric known as the gross moist stability (GMS) (*Neelin and Held*, 1987; *Raymond et al.*, 2009), defined as column MSE export through vertical and/or horizontal MSE advection per unit convective activity, and can be used as a metric for MJO instability. It is

hypothesized that the GMS should be small or negative in order to sustain strong MJO convection (*Raymond and Fuchs*, 2009; *Raymond et al.*, 2009; *Hannah and Maloney*, 2011; *Sobel and Maloney*, 2012; *Benedict et al.*, 2014; *Inoue and Back*, 2015a).

2.3 Cloud-radiation feedbacks

The critical role for cloud-radiative feedbacks to the MJO is now widely recognized (e.g., *Raymond*, 2001; *Lee et al.*, 2001; *Sobel and Gildor*, 2003; *Stephens et al.*, 2004; *Bony et al.*, 2015; *Kim et al.*, 2015). Reduced column radiative cooling (a positive heating anomaly) dominated by long-wave radiative effects due to increased cloudiness and moisture during periods of active MJO convection (*Lin and Mapes*, 2004; *Jiang et al.*, 2011; *Ma and Kuang,* 2011; *Del Genio and Chen*, 2015; *Ciesielski et al.*, 2017) is considered to be an important anomalous MSE source for destabilizing MJO convection (*Andersen and Kuang*, 2012; *Arnold and Randall*, 2015; *Jiang*, 2017). Even when the GMS is weakly positive by the aforementioned convection-circulation feedback, the MJO can still be destabilized by anomalous column radiative heating, which generates a negative effective GMS (*Sobel and Maloney,* 2013; *Hannah and Maloney*, 2014; *Adames and Kim*, 2016).

Associated with the shallow-to-deep convective transition during an MJO life cycle, a vertical tilting structure in radiative heating is also observed, largely associated with the water vapor effects (*Ciesielski et al.*, 2017). While the maximum radiative heating associated with the MJO slightly lags peak MJO convection (*Jiang et al.*, 2011; *Kim et al.*, 2015; *Ciesielski et al.*, 2017), various observational and modeling studies report that the column-integrated radiation enhances the convective heating in the context of total apparent heating anomalies by 15-25% (e.g., Lee et al., 2001; Lin and Mapes, 2004; *Jiang et al.*, 2011; Andersen and Kuang, 2012; *Johnson et al.*, 2015; *Ciesielski et al.*, 2017). In the stratiform region, with warm anomalies in the upper-troposphere and cold anomalies in the lower–troposphere, strong top-heavy radiative heating may also destabilize the MJO by the stratiform instability mechanism (*Mapes*, 2000; *Khouider and Majda*, 2006; *Kuang*, 2008; *Seo and Wang*, 2010; *Del Genio and Chen*, 2015). The critical role of convection-radiative feedbacks to the MJO will be discussed in detail in Sections 3.2 and 3.3.

2.4 Multi-scale interactions of the MJO

The MJO convective envelope consists of multi-scale elements (e.g., Nakazawa, 1988; *Hendon and Liebmann*, 1994; *Kiladis et al.*, 2009), with scales ranging from mesoscale convective

303 systems (MCSs) to synoptic scale waves, with the latter often referred to as the convectively
304 coupled equatorial waves (CCEWs). Figure 4 illustrates the multi-scale structure of convective
305 activity along the equator associated with two MJO events during the 2018/2019 winter. This
306 multiscale structure includes embedded fast eastward-propagating moist Kelvin waves and
307 associated 2-day westward-propagating inertio-gravity waves (Takayabu, 1994; Liebmann et al.,
308 1997; Haertel and Kiladis, 2004; *Hendon and Liebmann*, 1994; Chen and Houze, 1997), westward
309 propagating Mixed Rossby-Gravity waves that are particularly active over the western Pacific, and
310 diurnally-migrating convective signals originated over the MC region (e.g., *Yang and Slingo*,
311 2001a; *Love et al.*, 2011).

312 The dynamical structures and cloud morphology of the MCSs and CCEWs display a large
313 degree of self-similarity to the MJO (Fig. 2), with shallow convection at their leading edge,
314 followed by deep convection and then stratiform precipitation (*Mapes et al.*, 2006; *Kiladis et al.*,
315 2009). Due to these vertical tilting structures, in addition to their contribution to convective heating
316 on the MJO (*Tao et al.*, 2016), these organized MCSs and CCEWs within the MJO envelope affect
317 the MJO circulation through upscale transport of momentum (Moncrieff, 1992; Majda and Biello,
318 2004; Biello and Majda, 2005; *Majda and Stechmann*, 2009; *Tung and Yanai*, 2002a; b; Houze et
319 al., 2000; Khouider et al., 2012; Wang and Liu, 2011; Miyakawa et al., 2014; *Oh et al.*, 2015a; *Oh*
320 *et al.*, 2015b). The MJO-associated anomalous circulation can also regulate MCS and CCEW
321 activities by favoring particular types of convective systems and propagation directions (e.g.,
322 *Straub and Kiladis*, 2003; *Masunaga et al.*, 2006; *Majda and Stechmann*, 2009; 2012; *Han and*
323 *Khouider*, 2010; *Guo et al.*, 2014), although the underlying mechanisms are not fully understood.
324 This feedback represents a two-way interaction between small-scale convective elements and the
325 MJO.

326 Diagnosis based on reanalysis products and models reveal that organized synoptic eddies
327 contribute to MJO eastward propagation through anomalous moistening to the east and drying to
328 the west of MJO convection (e.g., Maloney, 2009; Andersen and Kuang, 2012; Benedict et al.,
329 2015; Jiang, 2017). The moistening and drying are largely considered to be driven by anomalous
330 poleward moisture transport by synoptic eddies. To the east of MJO convection, synoptic eddy
331 activity tends to be reduced within anomalous MJO easterlies possibly through the barotropic
332 kinetic energy conversion processes (Maloney and Hartmann 2001; Maloney and Dickinson 2003;

Andersen and Kuang, 2012). This reduction in eddy activity suppresses the entrainment of dry air into the Tropics by these eddies, representing an anomalous moistening. However, further investigation is needed to fully understand the importance of synoptic eddies to the MJO.

Lastly, the build-up of moisture during the MJO preconditioning phase is often accompanied by the emergence of an early-afternoon secondary peak in the diurnal cycle of oceanic convection (e.g., *Ruppert and Johnson*, 2015). The early afternoon peak is thought to arise from a reduction of convective inhibition due to enhanced heat and moisture fluxes in response to oceanic diurnal warm layers (Bernie et al., 2005; Bellenger and Duvel, 2009; *Moum et al.*, 2014a; *Ruppert and Johnson*, 2015; Section 3.5). The diurnal cycle over MC islands is also considered important for the so-called "barrier" effect of the MC on MJO propagation (Section 3.6).

3. Recent progress in understanding, modeling, and predicting the MJO

3.1 Observation of key MJO processes

3.1.1 Recent results from in situ observations

In situ observations help advance our fundamental understanding of the MJO. Our ability of numerically simulating and predicting the MJO critically depends on our knowledge of detailed physical processes that can be gained only through in situ observations. Sustained observing systems, such as the tropical mooring arrays in the Pacific and Indian Ocean (*Hayes et al.*, 1991) and the Department of Energy Atmospheric Radiation Measurement (ARM) Program tropical sites at Manus and Nauru (*Long et al.*, 2013), have provided large samples for robust statistics. Special field campaigns provided comprehensive in situ observations for the MJO study. The Tropical Ocean Global Atmosphere Coupled Ocean-Atmosphere Response Experiment (TOGA COARE, *Webster and Lukas*, 1992) covered for the first time several MJO events in the equatorial western Pacific. Dynamics of the MJO (DYNAMO), designed specifically for the study of MJO initiation over the Indian Ocean (*Yoneyama et al.*, 2013), covered three MJO events (*Gottschalck et al.*, 2013). (Note the DYNAMO field campaign was joined by three other projects: The Cooperative Indian Ocean Experiment on Intraseasonal Variability in the Year 2011, the ARM MJO Investigation Experiment, and the Littoral Air-Sea Process). YMC is a multi-year project with broad scientific scopes related to the Indo-Pacific MC, and will be discussed in Section 3.6.

Results from most studies on the MJO using in situ observations from TOGA COARE and the tropical mooring arrays were summarized by Zhang (2005) and Demott et al (2015). The following

discussions cover physical processes related to the MJO gained from in situ observations of the ARM tropical sites and DYNAMO.

The new capability of advanced polarimetric radars can detect hydrometer distributions within clouds. The radar observations made during DYNAMO were used to document the characteristics of cloud hydrometers at certain stages of the MJO: graupel near the melting level (~5 km) in actively convective towers, dry aggregates between 7-9 km increasing as convective clouds deepen, wet aggregates almost exclusively in the stratiform regions of MCSs, and small ice particles at altitudes of 9-10 km (*Barnes and Houze*, 2014; *Rowe and Houze*, 2015). Drop size distribution spectra of liquid water content and median diameter are distinct between convective and stratiform regions (*Thompson et al.*, 2015). These hydrometer distributions can be related to lightning frequencies of the MJO (*Stolz et al.*, 2017).

Radar observations of shallow clouds in conjunction with sounding observations have led to several new discoveries. During suppressed periods of the MJO, shallow convective clouds first moisten the environment (*Bellenger et al.*, 2015b). Once they start to precipitate, small cold pools form below the showers, and as the suppressed environment gained moisture, clouds are able to grow, with the deepest precipitating clouds occurring in clusters at intersections of cold pool boundaries by afternoon (*Rowe and Houze*, 2015). From the suppressed to pre-onset stage of the MJO as lower-tropospheric moisture increases, shallow/isolated convection undergoes remarkable growth (*Xu and Rutledge*, 2014). They produce about 30% of all rain events and 15% of total rain volume in the warm pool (*Thompson et al.*, 2015) because they exist in all phases of the MJO and non-MJO periods (*Zermeño-Díaz et al.*, 2015). Over the Indian Ocean, the contribution from shallow convection to total precipitation is larger in the ITCZ south of the equator than in the equatorial region where MJO deep convection is more prominent (*Xu et al.*, 2015).

During the transition from pre-convective initiation to initiation stages of the MJO, the oceanic diurnal warm layer drives a daytime increase of the air-sea fluxes of heat and moisture. In consequence, a daytime growth of cumulus clouds in both depth and areal coverage invigorates convective clouds and cumulus moistening each day leading to convective initiation of the MJO (*Ruppert and Johnson*, 2015). This shallow-to-deep convective transition can take place within a wide range of 2–20 days (*Xu and Rutledge*, 2016). During the transition, sub-MCS rainfall fraction declines from its maximum as MCS precipitation increases (*Xu and Rutledge*, 2015). The transition

393 from shallow, non-precipitating cumulus before initiation, to increasing cumulus congestus, then
394 deep convection during the initiation, to later stratiform precipitation can be consistently seen from
395 the evolution in apparent heat sources and sinks derived from sounding observations (*Johnson et*
396 *al.*, 2015). A reduction in vertical wind shear and enhanced low-level convergence induced by the
397 equatorial low-pressure system can lead to an explosive large MCS during MJO initiation (*Judt and*
398 *Chen*, 2014).

399 During rain events of 2-4 days after convective initiation, cloud evolutions follow the same
400 pattern, from shallow convection to deep convection, then wide convective systems with maximum
401 rainfall followed by broad stratiform clouds (*Zuluaga and Houze*, 2013). The cloud radiative
402 forcing, was approximately 20% of the column-integrated convective heating (*Johnson and*
403 *Ciesielski*, 2013). MCSs over the Indian Ocean were linearly organized more parallel to the low-
404 level shear with weaker but deeper updrafts and weaker cold pools than over the western Pacific
405 (*Guy and Jorgensen*, 2014). The number of cold pools, and their contribution to BL heat and
406 moisture, nearly double after convective initiation of the MJO (*de Szoeke et al.*, 2017).

407 The contrast between tropical moist air and extratropical dry air observed by aircraft
408 dropsonde data is much sharper than those in any other data (*Chen et al.*, 2016). Such contrast is a
409 result of synoptic-scale dry air intrusion from the extratropics, which can be instrumental to
410 convective initiation of the MJO (*Kerns and Chen*, 2014). At the convective initiation stage of the
411 MJO, the lower-tropospheric moistening by shallow convection is accompanied by advection as
412 low-level wind switch from westerlies to easterlies (*Sobel et al.*, 2014). After the initiation, low-
413 level dry advection by off-equatorial cyclonic gyres may act to push MJO convection moving
414 eastward (*Kerns and Chen*, 2014). Rapid increases in areal coverage of precipitating radar echo,
415 convective echo-top height, and tropospheric humidity above 850 hPa can happen over 3-7 days
416 close to MJO initiation before low-tropospheric moistening (*Powell and Houze*, 2013). Upper-
417 tropospheric moisture increases as large-scale subsidence is reduced in association with eastward
418 circumnavigating dry planetary perturbations (*Powell and Houze*, 2015). Moisture variability can
419 also be instigated by Mixed Rossby Gravity waves (*Muraleedharan et al.*, 2015) that may origin
420 from the MC (*Kubota et al.*, 2015) and Kelvin waves (*DePasquale et al.*, 2014).

421 Using sounding data to observe atmospheric BL variability, especially that of turbulence, is
422 very difficult because of uncertainties in estimating key parameters such as the eddy diffusivity

coefficient (*Bellenger et al.*, 2015a). Limited high-quality turbulence measurement has shed new lights on interactions between the BL and troposphere. Entrainment and downdraft fluxes export equal shares of moisture from the BL to the lower troposphere before MJO initiation; downdraft fluxes are found to increase by 50% and entrainment to decrease after the initiation (*de Szoeke*, 2018).

Fluctuations in air-sea heat fluxes associated with the MJO are insufficient to supply needed moisture for MJO convection after its initiation (*de Szoeke et al.*, 2015). They can be induced by, in addition to large-scale wind, perturbations in surface air temperature and local wind associated with convective cold pools (*Yokoi et al.*, 2014) and synoptic perturbations, such as Kelvin waves (*Baranowski et al.*, 2016). An unanticipated consequence of air-sea interaction associated with the MJO over the equatorial Indian Ocean is the transition from dominant BL aerosol of industrial carbon-based fine particles prior to MJO initiation to coarse particles of sea spray after initiation (*DeWitt et al.*, 2013).

Before MJO initiation, a diurnal warm layer of about 4-5 m deep forms in days of low wind ($< 6 ms^{-1}$) and high solar radiation flux ($> 80 Wm^{-2}$), with their amplitude in SST perturbations greater than 0.8˚C in the afternoon (*Matthews et al.*, 2014). Stratification caused by penetrating solar radiation initiates a decrease in turbulence dissipation rates by two orders of magnitude over 1–2 hours immediately after sunrise, leading to the change in net surface heat flux from cooling to warming (*Moulin et al.*, 2018). The entire mixed layer temperature also increases, as net surface warming becomes larger than turbulent cooling at the bottom (*Pujiana et al.*, 2018). The strength of a barrier layer can be measured by its potential energy, which is defined by the thickness of the barrier layer, the thickness of the surface mixed layer, and the density stratification across the isothermal layer (*Chi et al.*, 2014).

Ocean turbulence measurement has brought new perspectives to MJO air-sea interaction (*Moum et al.*, 2014b; *Pujiana et al.*, 2015; *Moum et al.*, 2016; *Pujiana et al.*, 2018). Over the Indian Ocean, the Yoshida-Wyrtki Jet at the equator accelerates from less than 0.5 m s^{-1} to more than 1.5 m s^{-1} in 2 days because of surface westerlies after MJO initiation. The jet energizes shear-driven entrainment at its base near the 100 m depth and advects salty water from the west. Subsurface mixing is sufficient to increase the mixed layer salinity, despite heavy precipitation after MJO initiation, by entraining salty water from the pycnocline. The turbulent salt flux across the mixed

layer base is, on average, 2 times as large as the surface salt flux. Subsurface turbulent heat fluxes related to the surface jet are comparable to atmospheric surface fluxes. The related turbulent stress, roughly 65% of the mean surface wind stress, is responsible for decelerating the jet. Nevertheless, the jet is able to sustain itself and its subsurface mixing continues reducing the heat content in the mixed layer by an amount significantly greater than atmospheric surface cooling for several weeks after an MJO event moves out of the region to the east. The resulting cooler upper ocean might affect initiation of the next MJO event.

These individual studies provided detailed perspectives of physical processes during MJO initiation using observations from different instruments. Some of these processes may be found during transitions from convectively suppressed to active periods for the mature MJO, others are unique to MJO initiation. More studies are needed to synthesize these processes and determine the degree to which these processes are critical to MJO initiation and must be adequately represented in prediction models.

3.1.2 Recent satellite observations of the MJO

Satellite observations have provided unprecedented datasets in characterizing three-dimensional structures of the MJO with a global coverage. For example, the TRMM rainfall observations has been extensively used to identify convective signals associated with the MJO (e.g., Fig. 1). The latent and radiative heating products based on the TRMM (*Masunaga et al.*, 2006; *Tao et al.*, 2006; *Jiang et al.*, 2009; *Jiang et al.*, 2011; *Ling and Zhang*, 2011), moisture and temperature estimates based on the Atmospheric Infrared Sounder (AIRS; *Tian et al.*, 2006b; *Tian et al.*, 2010), cloud products from the International Satellite Cloud Climatology Project (*Chen and Del Genio*, 2009a; *Tromeur and Rossow*, 2010), and cloud water and water vapor from the Microwave Limb Sounder (*Schwartz et al.*, 2008), among others, have been applied toward a comprehensive depiction of MJO structures as previously discussed (see a review by *Zhang*, 2012 for these earlier studies). In this subsection, we provide a brief update on observational studies of the MJO using satellite data since Zhang (2012).

Taking advantage of the explict observations of vertical cloud structure by CloudSat, Riley et al. (2011) examined evolution of cloud types during the MJO life cycle. Largely in agreement with many previous results based on reanalyses and field observations, a transition from shallow clouds along with deep, narrow, less-organized convection in the growing stage, to widespread and more

organized convection during active phases, then to more anvil and stratiform in the mature phases of the MJO is observed by CloudSat. By using a combined data from CloudSat and the Cloud–Aerosol Lidar and Infrared Pathfinder Satellite Observations (CALIPSO), Del Genio et al. (2012) also detected the deepest, tropopause-penetrating convective events during the MJO onset stage about one week before the MJO peak in convection.

Vertical temperature and specific humidity profiles associated with the MJO are also derived by the Constellation Observing System for Meteorology, Ionosphere, and Climate (COSMIC) radio occultation (RO) measurements (*Zeng et al.*, 2012; *Tian et al.*, 2012), and compared to previous results based on the AIRS observations (*Tian et al.*, 2006b; *Tian et al.*, 2010). Compared to the RO observations, MJO temperature anomalies in the upper-troposphere are underestimated by 40% in the AIRS estimates (*Tian et al.*, 2012). With a much higher vertical resolution of RO data, the RO-based results better capture the sharp temperature anomaly structures near the tropopause. Particularly, the eastward tilting of negative temperature anomalies with height in the tropopause transition layer (TTL) above the enhanced MJO convective region is well captured in RO, which is thought to be associated with the Kelvin waves excited by the "convective cold top" above the MJO convective heating as previously reported (*Kiladis et al.*, 2005; *Holloway and Neelin*, 2007; *Tian et al.*, 2010; *Virts and Wallace*, 2010; *Virts and Wallace*, 2014). These negative temperature anomalies in the TTL ahead of MJO convection can lead to increased cirrus clouds (*Del Genio et al.*, 2012; *Virts and Wallace*, 2014), indicative of a potential positive radiative feedback on the MJO (*Del Genio and Chen*, 2015; *Ciesielski et al.*, 2017).

Characteristics of separated MCSs (SMCSs) and connected MCSs (CMCSs) associated with the MJO, identified by combined data from the Moderate Resolution Imaging Spectroradiometer (MODIS) and the Advanced Microwave Scanning Radiometer for Earth Observing System (AMSR-E), were investigated by Yuan and Houze (2010; 2012). It was shown that variability in precipitation contribution from CMCSs largely matches the overall MJO precipitation variability. Meanwhile, greater occurrence frequency of CMCSs associated with enhanced large-scale MJO convection was found to be closely associated with increased mid-troposphere moisture (*Yuan and Houze*, 2012).

Using the TRMM Precipitation Radar data over the Indian Ocean and western Pacific, Barnes and Houze (2013) examined variability of precipitating cloud population associated with the MJO.

The broad stratiform regions (BSRs), which occur in connection with well-developed MCSs, are found to dominate the variability of precipitating cloud population in terms of areal coverage, and are most prevalent during the active stage of the MJO. These BSRs are favored in a large-scale environment with strong low-level shear, moderate mid-level shear, and a moist mid-to-upper troposphere.

By analyzing lightning occurrence by the World-Wide Lightning Location Network, Virts and Houze (2015) found that lightning frequency density in an MCS maximizes during the MJO transition periods at or just after the time of minimum MJO rainfall; during the MJO active periods, the zone of lightning is contracted around the centers of MCSs, and flashes are less frequent. These results are largely consistent with previous findings of an out-of-phase relationship between lightning and MJO precipitation by the TRMM-Lightning Image Sensor (*Kodama et al.*, 2006; *Morita et al.*, 2006).

3.2 Modern theories of the MJO

In this section, we review several theories that are currently being used to understand the MJO. Emphasis will be placed on the mechanisms in which the theory explains two salient features of the MJO: (1) its slow eastward propagation and (2) planetary scale. The major caveats of each theory will also be highlighted. Four of the theories discussed here are discussed in detail in recent reviews by Zhang et al. (2020) and Yang et al. (2020). The reader is referred to these review papers, as well as the original publications on these theories, for the mathematical formulation, assumptions, and comparisons with observations. Following Kim and Maloney (2017), a summary of each theory, and its essence and supporting references are shown in Table 1.

Table 1: Summary of each theory discussed in this section.

Theory	*Essence*	*Observational/Modeling Evidence*
WTG Moisture Mode+ *Sobel and Maloney, (2012, 2013), Adames and Kim (2016)*	Moisture-convection coupling is key. Moisture advection important for propagation. Cloud-radiative feedbacks cause growth and determine horizontal scale.	*Andersen & Kuang (2012), Chikira (2014), Pritchard & Bretherton (2014), Wolding & Maloney (2015), Jiang (2017), Adames et al. (2017b), Kim et al. (2017), Janiga et al. (2018), Rushley et al. (2019), Pritchard & Yang (2016)*, Kacimi & Khouider (2018)*, Chen & Wang (2018a)**
WISHE Moisture Mode+ *Fuchs and Raymond (2005, 2007, 2017)*	Moisture-convection coupling is key. WISHE determines propagation, growth and scale selection. Cloud-radiative feedbacks provide additional growth.	*Maloney and Sobel (2004), Shi et al. (2018), Sobel et al. (2008, 2010), Wang (1988)*, Zhang (1996)*, de Szoeke et al. (2015)**
BLQE Model *Khairoutdinov and Emanuel (2018; Emanuel, 2019)*	Convection adjusts to maintain BL quasi-equilibrium (BLQE). MSE evolution is key. Cloud-radiation feedback determines growth, WISHE propagation.	*Maloney & Sobel (2004), Khairoutdinov & Emanuel (2018), Arnold & Randall (2015), de Szoeke (2018), Wang (1988)*, Zhang (1996)*, de Szoeke et al. (2015)**
Trio Interaction	BL frictional moisture convergence to the east of MJO	*Maloney & Hartmann (1998), Lee et al. (2001),*

(Wang and Rui, 1990; Wang et al., 2016a)	convection center determines propagation and growth. Moisture-convection coupling slows down the MJO.	*Benedict & Randall (2007), Adames & Wallace (2014), Salby et al. (1994), Hendon and Salby (1994), Chao & Chen (2001)*, Shi et al. (2018)*, Kim et al. (2011a)**
Skeleton *Majda and Stechman (2009, 2011), Thual et al. (2014)*	MJO is an envelope of synoptic waves and mesoscale systems. MJO propagation due to interaction between low-level moisture and synoptic-scale wave activity.	*Deng and Wu (2010, 2011), Dias et al. (2013, 2017), Guo et al.(2015), Chen and Wang (2017)*, Miyakawa and Kikuchi (2018)**
Gravity Wave *Yang and Ingersoll (2013, 2014)*	MJO is an envelope of eastward and westward-propagating inertio-gravity waves. Horizontal scale is determined by interaction of waves and convection. Asymmetry between waves due to beta effect determines propagation.	*Kikuchi (2014), Pritchard & Yang (2016), Guo et al.(2015), Dias et al., (2013)*, Miyakawa and Kikuchi (2018)**
Nonlinear Solitary Wave *Yano and Tribbia (2017), Rostami and Zeitlin (2019)*	MJO is a strongly nonlinear solitary Rossby wave. MJO is explained by dry dynamics to first order. Nonlinear vorticity advection explains propagation. Large-scale modons exhibit the longest duration.	*Wang et al. (2019b), Zhang and Ling (2012)**
Large-scale Convective Vortex *Hayashi and Itoh (2017)*	MJO is an eastward-propagating pair of Rossby gyres. Propagation is due to strong low-level vortex stretching from deep convection to the east of the cyclones.	*Benedict and Randall (2009), Zhang et al. (2010), Lin et al. (2004)**

* Results contradict or are not consistent with theory.
+ These two theories offer different perspectives of a more general "moisture mode" theory.

3.2.1 Early work and observations leading to modern theories

The first attempt to understand the MJO was made by Chang (1977). His work showed that convection can slow convectively-coupled waves, although not enough to match observations. Subsequent attempts to understand the MJO include the use of a wave-driven version of the convective instability of the second kind (wave-CISK) (Lau and Peng, 1987; Chang and Lim, 1988), wind-induced surface heat exchange (WISHE) (Emanuel, 1987; Neelin et al., 1987), and a version of the wave-CISK model that includes a BL convergence feedback (frictional CISK; Wang, 1988; Wang and Rui, 1990). While many of these theories succeeded at describing some aspects of the MJO, they were unable to fully explain all of its key features. The simulated variability exhibited faster eastward propagation than observed, and often lacked the Rossby wave structures seen when the MJO is active over the warm pool. Both characteristics are more consistent with convectively-coupled Kelvin waves than the MJO. Nonetheless, many of these early theories form the building blocks of several of the modern theories discussed herein (Sections 3.2.2-3.2.4).

Observations arising from field campaigns such as TOGA-COARE (Webster and Lukas, 1992) indicate that tropical precipitation is highly sensitive to the thermodynamic environment. Precipitation occur when the free troposphere is humid, or when convective available potential energy (CAPE) is increased, or convective inhibition (CIN) is reduced (*Mapes*, 2000). These observations led to most of the modern theories of the MJO, where moist thermodynamics interact with both deep convection and the large-scale circulation. With only one exception (section 3.2.7), all of the views discussed here emphasize the role of moist thermodynamics in the MJO.

557 *3.2.2 Moisture mode theory*

558 The role that water vapor plays in regulating tropical convection was further developed into a
559 theory of the MJO, known as "moisture mode theory". A "moisture mode" can be defined as an
560 atmospheric disturbance where the evolution of moisture (i.e. inclusion of prognostic moisture)
561 plays a dominant role in its dynamics. The term was coined by Yu and Neelin (1994), who analyzed
562 a system of equations in the equatorial belt and found wave solutions driven by moisture
563 fluctuations that were unlike any previously documented wave. While Neelin and Yu (1994) and
564 Yu and Neelin (1994) documented the analytical existence of moisture modes, they did not attribute
565 the MJO to such a wave. The first studies indicating that the MJO may be a moisture mode were
566 Raymond (2001) and Sobel et al. (2001). Raymond (2001) argued that MJO-related precipitation
567 anomalies are predominantly caused by moisture fluctuations, and are destabilized by cloud-
568 radiative feedbacks, as in Hu and Randall (1995). Surface latent heat fluxes drive the propagation of
569 the disturbance. Sobel et al. (2001) obtained balanced moisture wave solutions under weak
570 temperature gradient (WTG) balance that propagated due to horizontal moisture advection. They
571 argued that the MJO may be characterized as a type of moisture wave.

572 The moisture mode framework gained further attention as studies like Grabrowski and
573 Moncrieff (2004) showed that simulating strong moisture-convection feedbacks are central to
574 simulating strong MJO activity. Subsequent studies showed that MJO simulations can be improved
575 by increasing convection's sensitivity to free tropospheric water vapor (*Kim and Kang*, 2012; *Kim*
576 *et al.*, 2012; *Del Genio et al.*, 2012; *Zhu and Hendon*, 2015; *Arnold et al.*, 2015; *Kim and Maloney*,
577 2017). Furthermore, several studies have found a link between the concentration and distribution of
578 water vapor and the ability of models to simulate the MJO (*Gonzalez and Jiang*, 2017; *Jiang*,
579 2017). Fast drying of the troposphere in forecast models has also been linked with models'
580 tendency to dissipate the MJO (*Kim et al.*, 2016, 2017; *Weber and Mass*, 2017; *Kim et al.*, 2019).
581 Due to the well-documented importance of moisture-convection feedbacks in the representation of
582 intraseasonal rainfall variability, the moisture mode framework is now one of the most well-known
583 theories of the MJO. However, even within this theory differing views exist as to which moist
584 processes determine the MJO's eastward propagation and planetary scale. Two of these views are
585 discussed here.

586 a. Moisture mode under WTG balance

587 One type of moisture mode model focuses on the role that moisture evolution alone plays in
588 the MJO. This model assumes that the MJO-related wind field instantaneously adjusts to an

equatorial heat source in the form of the Matsuno-Gill steady-state response, and that the intraseasonal heating anomalies are in WTG balance. We will refer to this model as the WTG moisture mode model. The foundations of this model were originally conceived by Sobel and Maloney (2012, 2013). They diagnosed precipitation anomalies from moisture anomalies using a simplified Betts-Miller scheme and obtained a dispersion relation using a 1-D model. Adames and Kim (2016) further developed their framework by treating the meridional and vertical structure of the MJO explicitly, and adjusted several key parameters to be more consistent with observations. Through this revision, they found that the wind anomalies in the MJO explain its eastward propagation through horizontal moisture advection, frictional convergence, and modulation of surface fluxes. The propagation mechanism also results in a westward group velocity (the extrema in the moisture/rainfall anomalies drift westward with time). Lastly, Adames and Kim (2016) showed that planetary-scale selection in the MJO can occur through a non-local feedback between convection and longwave radiative heating. Upper level clouds that spread away from regions of precipitation reduce outgoing longwave radiation. The anomalous radiative heating that results from these clouds is balanced by anomalous upward motion and adiabatic cooling. The anomalous upward motion moistens the free troposphere, which favors the development of convection.

There are several caveats to this moisture mode model. While assuming that moisture is the only prognostic variable lends analytical tractability and physical interpretation to the theory, it is unlikely that these approximations are adequate during all times in the MJO life cycle (*Kacimi and Khouider*, 2018). Several processes, such as BL moisture convergence, are parameterized based on observations. While the scale-selecting role of radiation has been demonstrated by some studies (*Shi et al.*, 2018; *Khairoutdinov and Emanuel*, 2018), the way it is incorporated into this model is based on empirical evidence, rather than first principles. It is also noteworthy that while some studies suggest that cloud-radiation feedbacks are essential to the MJO (*Andersen and Kuang*, 2012; *Shi et al.*, 2018), eliminating these feedbacks weakens but does not eliminate the MJO (*Arnold and Randall*, 2015), which suggests that it may not be the only instability mechanism. Lastly, while some studies support the notion that the MJO has a westward group velocity (*Janiga et al.*, 2018), a study based on observations does not support this type of dispersion (*Chen and Wang*, 2018a).

b. WISHE moisture mode

Another relevant moisture mode model was developed by Fuchs and Raymond (2005, 2017). Unlike the WTG-based moisture mode model, this model does not use WTG strictly and the

tendency in momentum is also included. Additionally, while the WTG moisture mode model includes multiple processes that can induce eastward propagation, this model incorporates WISHE as the only process that drives propagation. In this model, WISHE not only results in MJO eastward propagation, but also induces a planetary-scale instability. A salient feature of this model is the exclusion of the meridional wind as a fundamental feature of the MJO, with the horizontal structure of this moisture mode resembling that of a convectively coupled equatorial Kelvin wave.

There are several caveats to this model. First, while it is true that the mean tropical zonal wind is easterly, the mean zonal winds over the Indo-Pacific warm pool are weakly westerly near the equator. As a result, surface latent heat fluxes to the east of the region of enhanced MJO convection are suppressed, rather than enhanced (*Zhang*, 1996; *Kiranmayi and Maloney*, 2011; *de Szoeke et al.*, 2015). This distinction may be important since suppressing WISHE eliminates MJO-like activity in aquaplanet simulations (*Shi et al.*, 2018; *Khairoutdinov and Emanuel*, 2018), but not in most simulations with realistic topography (e.g., *Kim et al.*, 2011a; *Ma and Kuang*, 2016). It is possible that MJO propagation may instead be explained by a nonlinear WISHE mechanism over the warm pool (*Maloney and Sobel*, 2004).

3.2.3 Boundary layer quasi equilibrium (BLQE) model

Boundary layer quasi-equilibrium (BLQE, *Raymond*, 1995; *Emanuel*, 1995) assumes that regions of deep convection exhibit a balance in the BL where the net gain of MSE through surface fluxes is balanced by the import of low MSE air from the free troposphere that result from convective downdrafts. The intensity of the downdrafts are in turn related to updrafts through a precipitation efficiency parameter (*Emanuel*, 1991). When this concept is applied to the MJO (*Khairoutdinov and Emanuel*, 2018; *Emanuel*, 2019), it is found that planetary-scale instability is the result of longwave radiative heating. Like the WISHE moisture mode discussed in the previous subsection, eastward propagation of the MJO in the BLQE model is due to WISHE. To some extent, this theory can also be thought as a moisture mode model since the strict application of WTG balance still yields unstable planetary-scale modes, which indicates that the evolution of moisture may be of critical importance in this model. This is somewhat evident in the dispersion relation of this mode, which is reminiscent of the moisture mode models discussed above (*Adames and Kim*, 2016; *Fuchs and Raymond*, 2017). However, the use of BLQE does yield results that differ from the WISHE-moisture mode model. For example, in this model WISHE actually reduces the growth rate, whereas in the WISHE moisture mode model WISHE is the leading cause of instability.

While the assumption of BLQE is central to this model, it is unclear how these results would be affected if the assumption of BLQE were relaxed and BL MSE were allowed to evolve in time. Furthermore, as in all theories that rely on WISHE as a mechanism of eastward propagation, it is unclear whether this mechanism is truly applicable to the MJO when its convection is in the warm pool (*Wang*, 1988).

3.2.4 Trio interaction theory

The "trio interaction theory" can be considered to be an update to the original frictionally-coupled Kelvin-Rossby wave theory of Wang and Rui (1990), modified to include water vapor as a prognostic variable. The essence of this theory is rooted in BL convergence, equatorial wave dynamics, moisture, and diabatic heating. Cloud-radiation feedbacks, while not essential, are also included in the theory for completeness. In the trio interaction model, BL friction causes wave-driven convergence to occur to the east of the main region of convection (*Maloney and Hartmann*, 1998; *Hendon and Salby*, 1994; *Salby et al.*, 1994; *Wang and Li*, 1994; *Adames and Wallace*, 2014). This convergence results in upward motion, which moistens the atmosphere and generates available potential energy, resulting in eastward propagation and planetary-scale instability. The inclusion of moisture along with the use of a Betts-Miller parameterization scheme results in even slower eastward propagation in the most unstable mode at values that are more consistent with observations (*Wang et al.*, 2016a). The "trio" in the name is suggestive of the three-way interaction among convective heating, moisture and boundary layer dynamics. According to this theory, MJO simulations can be improved if the interactions between BL processes, moisture and large-scale waves are improved.

It is important to note that the literature is currently divided on the role of frictional convergence in the MJO. Some studies have supported its central importance using a suite of observations and modeling (*Wang and Lee*, 2017; *Wang et al.*, 2018a). Other studies indicate that removing BL friction in GCMs does not negatively impact the MJO, casting doubt on the fundamental processes of this theory (*Kim et al.*, 2011a; *Shi et al.*, 2018). It may be difficult to fully test this theory given the sensitivity of the mean state to surface friction. Furthermore, BL friction may not only be due to surface roughness, but due to other processes such as momentum damping due to turbulent entrainment (*Stevens*, 2002).

3.2.5 Skeleton model

The MJO skeleton model was originally proposed by Majda and Stechmann (2009). The theory describes the MJO as a neutrally-stable envelope of higher-frequency synoptic and

mesoscale systems. The heating driven by convection in these high-frequency systems maintain the MJO through an upscale transport of momentum. In turn, the evolution of these synoptic and mesoscale systems is driven by a planetary-scale envelope of low-level moisture. This interaction between low-level moisture and high-frequency wave activity is the essence of the skeleton model and is the basis of their representation of convective processes. This "wave activity" and low-level moisture are in quadrature, resulting in the propagation of the convective anomalies. An eastward-propagating and a westward-propagating solution arise from a shallow-water system of equations. Of these two, only the eastward propagating solution exhibits a quadrupole vortex structure consisting of Kelvin and Rossby waves, similar to what is observed during the MJO phases where there is both enhanced and suppressed convection over the warm pool. The planetary-scale disturbance propagates eastward at ~5 m s^{-1} and exhibits a dispersion relation that is approximately independent of wavenumber (i.e. constant), yielding a group velocity of zero. A study by Chen and Wang (2018a) indicates that the MJO may exhibit this type of dispersion.

There are some limitations to this view of the MJO. First, it is unclear how the formulation of the wave activity function can be quantitatively evaluated using observations. Observations also reveal that, while low-level moisture does lead MJO convection, it is not in spatial quadrature. Instead, low-level moisture is observed to slightly lead precipitation (~30° shift in phasing) (*Chen and Wang*, 2017). The literature is also divided on the role of upscale interactions in the MJO, with some studies suggesting that the MJO's momentum generation occurs at the planetary, intraseasonal scale (*Zhou et al.*, 2012a; *Dubey et al.*, 2018), while others suggest it comes from the synoptic and mesoscale (*Khouider et al.*, 2012; *Yang et al.*, 2019).

3.2.6 Gravity wave model

The gravity wave model was originally proposed by Yang and Ingersoll (2013, 2014). This view of the MJO was motivated by observations of the intermittency of convection in the tropics (*Zuluaga and Houze*, 2013). In this model, the MJO is conceived to be the result of an interference pattern between eastward and westward-propagating inertia-gravity waves. The eastward propagation is the result of the difference in propagation speed between the two inertio-gravity waves. Eastward inertia gravity waves exhibit slightly faster eastward propagation than their westward counterparts. This small difference is attributed to the gradient in planetary vorticity (beta). Thus, the eastward-propagation of the MJO can only occur in the equatorial belt of a rotating planet. The planetary scale of the MJO results from the distance that the inertia-gravity waves propagate without being dissipated by a convective storm (*Yang and Ingersoll*, 2014). This distance

717 is qualitatively determined by the phase speed of convectively-coupled gravity waves divided by
718 the density of convective events.

719 Like the skeleton model, this model suggests that multi-scale interactions are essential to the
720 MJO. However, unlike the skeleton model, where only the net upscale impact of these systems are
721 important, here the details of the interactions between the inertio-gravity waves are critical. As a
722 result, the gravity wave theory is arguably the only theory described here where the details of
723 convective organization and its interaction with the synoptic scale are of critical importance.
724 Additionally, this model treats convection as a triggered process and it is inherently nonlinear.

725 While spectral analysis reveals that gravity wave energy co-varies with the MJO (Kikuchi,
726 2014), observations have currently not observed inertio-gravity waves propagating in both eastward
727 and westward directions during an MJO life cycle (*Dias et al.*, 2017). It is unclear whether this is a
728 result of insufficient temporal resolution to fully resolve these fast waves or if these waves are not
729 central to MJO dynamics.

730 *3.2.7 Nonlinear Solitary Rossby Wave*

731 The solitary wave framework was originally proposed by Yano and Tribbia (2017), and
732 further developed by Rostami and Zeitlin (2019). The essence of this theory is that the MJO is a
733 pair of equatorially-symmetric Rossby wave vortices whose propagation is due to nonlinear
734 potential vorticity advection. This framework differs from other theories in that it completely
735 eliminates the need for deep convection as a first-order process. Their justification of a dry
736 framework arise from results such as those from Holloway et al. (2013) and Monier et al. (2010),
737 who found strong intraseasonal variations in wind even when intraseasonal fluctuations in
738 convection are weak.

739 The most unstable mode solution in this theory exhibits a scale of ~3000 km and a phase
740 speed that ranges from 8–18 m s^{-1}. This scale is slightly smaller with larger phase speed than what
741 is observed in composite MJOs. Furthermore, a potential vorticity (PV) budget analysis by Zhang
742 and Ling (2012) suggests that PV evolution in the MJO is predominantly driven by diabatic
743 processes, rather than horizontal advection of the PV field. Nonetheless, it is remarkable that a dry
744 theory for the MJO can be conceived, and more work is needed to evaluate this theory.

745 *3.2.8 Large-scale convective vortex*

746 The large-scale vortex theory was initially proposed by Hayashi and Itoh (2017) to explain the
747 eastward propagation of the MJO. They proposed that the MJO is a pair of cyclonic Rossby gyres

748 that are strongly coupled to convection. The eastward propagation can be explained by strong
749 vortex stretching that occurs in the regions of deep convection associated with strong westerly
750 winds. This mechanism exceeds the advection of planetary vorticity that would cause Rossby gyres
751 to otherwise propagate westward, a mechanism that is often disregarded in MJO theories such as
752 that of Adames and Kim (2016). This framework may serve not only as an explanation for the
753 propagation of the MJO, but may also be used as a basis to understand westerly wind bursts (*Fu*
754 *and Tziperman*, 2019).

755 *3.2.9 Overlap between the theories*

756 The diversity of the theories presented in this subsection could easily lead the reader to
757 conclude that our understanding of the MJO remains very poor. Such a conclusion is misguided. In
758 the last decade simulation of the MJO has vastly improved to the extent that many models can
759 reproduce many of its observed features (see Section 3.3). Many of the improvements have been the
760 result of a greater understanding of the processes that drive tropical convection. In particular, the
761 role that water vapor plays in the convective organization of the MJO has been especially critical.
762 An examination of each theory (Table 2) quickly reveals that moist processes are the centerpiece to
763 the majority of the theories. For example, the majority of theories include moisture as a prognostic
764 variable and consider moist processes to be crucial for understanding the propagation and growth of
765 the MJO. Additionally, the majority of the theories emphasize interactions between moisture and
766 convection in the growth and propagation of the MJO. Half of the models discussed here also
767 include cloud-radiative feedbacks, although this process has varying degrees of importance across
768 models. Out of the eight theories discussed, two can be considered to be moisture mode theories,
769 and two others (BLQE and trio interaction) contain essential elements of moisture mode theory.
770 Only the solitary Rossby wave model has its fundamental elements rooted in dry dynamics.

771 Table 2: Comparison of the role of moist processes in each of the theories discussed here.

Theory	**Conv coupling is essential**	**Prognostic moisture is key**	**Moist processes key to propagation**	**Moist processes key to MJO growth**	**Cloud- radiative heating is included**
WTG moisture mode	yes	yes	yes	yes	yes
WISHE moisture mode	yes	yes	yes	yes	yes
BLQE model	yes	yes[1]	yes	yes	yes
Trio Interaction model	yes	yes	yes	yes	yes
Skeleton model	yes	yes	yes	no	no
Gravity Wave model	yes	no	no[2]	no[2]	no
Nonlinear Solitary wave	no	no	no	no	no

Large-scale Convective Vortex	yes	no	yes	yes	no

1. This model does not have an explicit moisture equation, but a moist static energy equation. Nonetheless, they make use of the WTG approximation, which makes MSE effectively a moisture equation.
2. In this model, deep convection plays a key role in MJO propagation and scale. The "no" is because moisture-convection feedbacks are not explicit in this model.

3.3 Modeling the Madden-Julian Oscillation

In this section, we highlight recent development and activity toward process-level representation and understanding of the MJO in GCMs. These include new model intercomparison studies, development of new modeling framework and diagnostics, and an emerging area of active research – understanding the role of the mean state. The interaction of the MJO with the MC islands is another theme of active modeling studies, which are summarized in Section 3.6. Readers are referred to Sperber et al. (2012) and Kim and Maloney (2017) for a detailed summary and discussion of the achievement in MJO modeling during the earlier period.

3.3.1 Process-oriented diagnostics

Since the early 2010s, the concept of "process-oriented" diagnostics, which are distinguished from the traditional performance-oriented diagnostics by their ability to more directly guide model development, was put forward within the MJO community. In GCMs, the MJO is one of the "emerging" systems that are internally generated through the interactions among resolved and parameterized processes. The main goals of the process-oriented diagnostics are to identify processes that are key to the MJO and to provide insights into specific aspects of the model that affects the identified key processes. Various process-oriented MJO diagnostics have been developed and tested based on the processes that had been suggested to be important in the MJO dynamics: the moisture-precipitation coupling (e.g., *Kim et al.*, 2014b; *Jiang et al.*, 2015; Section 2.1), the mean GMS (e.g., *Benedict et al.*, 2014; Section 2.2), the cloud-radiation feedbacks (e.g., *Kim et al.*, 2015; Section 2.3). It was found that models with tighter moisture-convection coupling, stronger cloud-radiation feedbacks, and lower mean GMS tend to simulate a stronger MJO. Readers are referred to Jiang et al. (2020) for a more detailed review on the development of the process-oriented MJO diagnostics.

3.3.2 Recent model intercomparison studies

Model intercomparison studies have been a useful framework to gauge the overall model fidelity and to identify systematic biases that are common to many models. Prior to 2010, Slingo et

al. (1996) and Lin et al. (2006) conducted an intercomparison study focused on the MJO with more than a dozen GCMs. Slingo et al. (1996) found that all participating AMIP (Atmospheric Model Intercomparison Project) models failed to capture the observed intraseasonal spectral power in the upper level velocity potential field. Lin et al. (2006) analyzed 14 coupled GCMs participating in the 3rd coupled model intercomparison project (CMIP3) and found that the intraseasonal spectral peak in equatorial precipitation is realistically captured in only one model. The daunting conclusions of the earlier intercomparison studies - almost all models cannot simulate even the most basic features of the MJO - highlighted the need to better understand the phenomenon, for example, by making observations of key processes (Section 3.1) and via theoretical considerations (Section 3.2).

In the early 2010s, jointly led by the MJOTF and the GEWEX GASS Project, a large GCM intercomparison project that specifically focused on the MJO was successfully carried out with 27 participating models (*Petch et al.*, 2011; *Jiang et al.*, 2015; *Klingaman et al.*, 2015b; *Xavier et al.*, 2015). The model simulation data collected during the activity has been widely used for MJO studies (*Jiang et al.*, 2016; *Ling et al.*, 2019; *Wang and Lee*, 2017; *Wang et al.*, 2017; *Jiang*, 2017; *Gonzalez and Jiang*, 2017) and for developing process- and dynamics-oriented MJO diagnostics (e.g., *Wang et al.*, 2018a; *Jiang et al.*, 2016; *Maloney et al.*, 2019b). In terms of MJO simulation fidelity, Jiang et al. (2015) found that about one fourth of the participating models represented the eastward propagation of the MJO realistically (Fig. 5). For the first time, a large model intercomparison study concluded that a significant fraction (25%) of participating models simulated a reasonable MJO.

By providing standardized output variables at the daily frequency, the CMIP activity has provided an invaluable resource for MJO performance assessment. Hung et al. (2013) and Ahn et al. (2017) examined CMIP5 models in terms of their MJO simulation capability. By applying the same diagnostics that were applied to the CMIP3 models by Lin et al. (2006), Hung et al. (2013) noted a slight improvement in the performance of CMIP5 models over the CMIP3 models. Ahn et al. (2017) showed that MJO amplitude in the upper level velocity potential field in the CMIP5 models are stronger than that in the AMIP models examined in Slingo et al. (1996). Ahn et al. (2020b) analyzed the latest CMIP6 models with a focus on MJO propagation over the MC and compared them with their predecessors. They found that the CMIP6 models as a group better simulate the MJO eastward propagation over the MC, which they attributed to a reduction of dry

mean state bias near the equator. With a weaker equatorial dry bias, the CMIP6 models show a steeper mean meridional moisture gradient in the MC, which leads to a greater moisture recharging to the east of MJO convection, and provide a favorable condition for MJO eastward propagation.

3.3.3. Modeling the MJO with and without parameterized convection

It has long been known that the cumulus parameterization schemes greatly affect the simulation of tropical intraseasonal oscillations (e.g., *Tokioka et al.*, 1988; *Park et al.*, 1990). GCMs tend to produce stronger intraseasonal oscillations in the tropics as triggering of deep convection is more severely inhibited in dry conditions (e.g., *Maloney and Hartmann*, 2001; *Lee et al.*, 2003; *Zhang and Mu*, 2005; *Lin et al.*, 2008; *Bechtold et al.*, 2008; *Ling et al.*, 2009; *Zhang and Song*, 2009; also see *Kim and Maloney*, 2017 for a review). Also, it was noted that the version of convection scheme that improves the MJO does not necessarily improve the mean state (e.g., *Kim et al.*, 2011b). Efforts of improving MJO in GCMs via changes in the cumulus parameterization scheme continued during the recent decades. Most recent modeling studies that examined the effect of cumulus parameterization on the simulation of the MJO emphasized the sensitivity of parameterized convection to environmental moisture (e.g., *Chikira and Sugiyama*, 2010; *Deng and Wu*, 2010; *Kim and Kang*, 2012; *Kim et al.*, 2012; *Del Genio*, 2012; *Zhou et al.*, 2012a).

What has also long been known is that the same changes in the convection scheme that improves the MJO tend to affect the mean state significantly, often in a negative way (e.g., *Wang and Schlesinger*, 1999; *Kim et al.*, 2011b; *Mapes and Neale*, 2011a). For example, if the fractional entrainment rate in the convection scheme is increased, the convection scheme becomes more sensitive to environmental moisture, giving the parent model an enhanced variability in the tropics, including the MJO. Another consequence of increasing the fractional entrainment rate is that convective plumes become shallower and seldom reach the tropopause. The overall shoaling of convective plumes means convection becomes less efficient in removing instability from the column and therefore excessive convective activity is required. The excessive precipitation especially over the warmest part of the globe tends to distort the tropical mean climate (e.g., *Kim et al.*, 2011b). Recent modeling studies suggested that the apparent mean state-MJO trade off can be mitigated by explicitly representing mesoscale organization of convection in the convection schemes (*Mapes and Neale*, 2011a; *Chen and Mapes*, 2018; *Ahn et al.*, 2019). For example, Ahn et al. (2019) examined the mean state and MJO in a series of simulations using a GCM with a unified

convection scheme (UNICON, *Park*, 2014) in which the degree of mesoscale organization of convection is a prognostic variable whose main source is convective downdraft. They found that the GCM represented both the mean state and the MJO realistically. It was suggested that the key to the success of UNICON in mitigating the MJO-mean state tradeoff is that the plume properties (e.g., entrainment rate) are situation-adaptive: the effective entrainment rate is high for plumes in an undisturbed region (e.g., during the suppressed phase of the MJO), as the degree of organization would be lower, while it is low for the plumes within the mature systems (e.g., those embedded in the active MJO). More work is warranted in the area of developing parameterizations of mesoscale organization and its impacts on MJO simulation (e.g., *Moncrieff*, 2019; see Section 4.3).

Recently, new modeling tools that do not rely on the cumulus parameterization schemes were developed and have been used in modeling the MJO. In the so-called "superparameterization" approach, the cumulus parameterization schemes were replaced by a 2-D cloud-resolving models (CRMs) in each grid column (*Grabowski*, 2001; *Khairoutdinov and Randall*, 2003). The mesoscale organization of convection, therefore, is explicitly resolved within the 2-D CRMs. Studies have shown that the models with superparameterized convection largely showed a better performance in MJO simulation than the corresponding model with a conventional parameterization scheme (*Khairoutdinov et al.*, 2005; *Thayer-Calder and Randall*, 2009; *Benedict and Randall*, 2009; *Kim et al.*, 2009; *Zhu et al.*, 2009). It is worthwhile to note that while the models with superparameterized convection have shown to perform well in model intercomparison studies (*Kim et al.*, 2009; *Jiang et al.*, 2015), they often suffer from the same mean state biases as in the models with parameterized convection (e.g., *Kim et al.*, 2011b) and tend to exhibit too strong MJO variability (e.g., *Zhu et al.*, 2009). Moreover, not every model that employs superparameterized convection simulates a decent MJO, suggesting that employing high-resolution and resolving convective motions do not automatically improve MJO simulations.

With the aid of increasing computational power, the GCRMs became available for MJO studies (*Miura et al.*, 2007; *Liu et al.*, 2009; *Nasuno et al.*, 2009), although in most cases the use of GCRM was limited by a relatively short integration period. Nonetheless, Miura et al. (2007) demonstrated that a GCRM reproduced an observed MJO event quite realistically. After the DYNAMO field campaign (Section 3.1), many modeling studies were conducted with a focus on understanding the observed MJO events during the field campaign. The new modeling tools -

893 superparameterized GCMs and GCRMs – as well as regional CRMs were actively used to study the
894 initiation and subsequent eastward propagation of the DYNAMO MJO events in the form of
895 hindcast experiments. It was found that the models that explicitly resolves convective systems
896 realistically represent the DYNAMO MJO events (e.g., *Hannah et al.*, 2015; *Weber and Mass*,
897 2019; *Miyakawa and Kikuchi*, 2018; *Hagos et al.*, 2014; *Wang et al.*, 2015).

898 New modeling strategies that recently emerge towards improved MJO simulations will be
899 further discussed in Section 4.3.

900 *3.3.4. Role of the basic state*

901 From a point of view that defines the MJO as perturbations from the climatological seasonal
902 cycle of the mean climate, whether and to what extent the basic state affects the salient features of
903 the MJO has been a central question to many modeling and theoretical studies. Studies have
904 examined the relationship between aspects of the mean state and MJO simulation capability in
905 ensembles of GCM simulations. Such efforts recently revealed that horizontal gradient of the mean
906 moisture is a key factor that determines models' MJO simulation fidelity (*Gonzalez and Jiang*,
907 2017; *Jiang*, 2017; *DeMott et al.*, 2018; *Ahn et al.*, 2020b). In particular, GCMs that show a sharper
908 meridional mean moisture gradient in the vicinity of the MC tend to better represent the eastward
909 propagation of the MJO with a more realistic moisture recharging and discharging pattern to the
910 east and west of MJO convection (*Jiang*, 2017; *Ahn et al.*, 2020b). It is worthwhile to note that
911 earlier studies also reported that models that simulate a relatively strong MJO tend to have mean
912 precipitation confined within the area of warm sea surface temperature (*Slingo et al.*, 1996; *Wang*
913 *and Schlesinger*, 1999), indicating strong MJO is preferred in a mean state with a greater contrast
914 between moist and dry areas, i.e., a steeper horizontal mean moisture gradient (see Fig. 3 in *Wang*
915 *and Schlesinger*, 1999).

916 While the empirical relationship between the mean moisture gradient and MJO variability
917 emphasizes the central role of moisture in the MJO dynamics, supporting the moisture mode theory
918 for the MJO, isolating the role of the mean state from the effect of the convection scheme is a non-
919 trivial task in multi-model studies (*Jiang*, 2017; *Ahn et al.*, 2020b) because the convection scheme
920 affects both the mean state and the MJO. Kang and Kim (2020, Role of background meridional
921 moisture gradient on the ensemble spread of MJO simulation in CESM2, GRL, submitted
922 manuscript) analyzed a 10-member ensemble of simulations made with a single model (CESM2)

and found a marked spread among the ensemble members in their ability to represent MJO propagation over the MC. The ensemble members with a stronger MJO propagation showed enhanced moistening to the east of MJO convection that is associated with a steeper mean state meridional moisture gradient in the southern MC, highlighting the effects of background state that is independent of the effects of the convection scheme.

3.4 Predicting the MJO

Advances in theoretical understanding, improved numerical models, and collaborative international activities, such as field campaigns and multi-model ensemble prediction projects (e.g., ISVHE, S2S, SubX), have promoted remarkable improvements in MJO prediction during the past decade. Through the perfect-model assumption, the MJO predictability reaches up to 7 weeks (e.g., *Waliser et al.*, 2003; *Neena et al.*, 2014). In reality though, errors originating from the imperfect model and initial conditions make the actual prediction skill lower than the predictability; reforecasts from the recent operational and research models exhibit MJO prediction skill varying widely between 2-4.5 weeks (*Kim et al.*, 2019; *Lim et al.*, 2018). Figure 6 compares the MJO prediction skill during boreal winter from the S2S and SubX reforecasts assessed by the Real-time Multivariate MJO (RMM, *Wheeler and Hendon*, 2004) index.

To make a consistent evaluation of MJO prediction skill and fair comparison among multi-models, the majority of the studies on MJO prediction and operational forecasts use the RMM indices as a measure of the MJO. It is relatively simple to calculate and easy to implement for real-time monitoring and forecasting of the MJO. However, interpretation of the MJO prediction skill with the RMM index often needs careful consideration. It mainly reflects the skill of the predicted wind anomalies but not necessarily the predicted convective anomalies associated with the MJO (*Straub*, 2013). High prediction skill based on the RMM indices may therefore lead to an optimistic conclusion regarding our MJO prediction capabilities. A common benchmark to measure the MJO prediction skill has been scalar metrics, such as the bivariate anomaly correlation coefficient or bivariate root-mean-squared error using two RMMs which represents the skills as a function of forecast lead times (e.g., *Lim et al.*, 2018; *Rashid et al.*, 2011).

MJO prediction skill is generally higher when a model is initialized with a stronger MJO signal than with weaker or with no signal, and thus tends to be higher in boreal winter (e.g., *Rashid et al.*, 2011). During boreal winter, MJO prediction skill varies with the stratospheric low-frequency

mean state, for example during different QBO phases, which will be discussed in Section 3.8. MJO prediction skill becomes higher when the extratropical influence on the tropics is reasonably simulated (*Vitart and Jung*, 2010; *Ray and Li*, 2013). Recent studies have clearly shown that averaging multi-ensembles or multi-models extends the MJO prediction skill (e.g., *Neena et al.*, 2014; *Pegion et al.*, 2019), although including a low-performance model in the mean degrades the skill (*Green et al.*, 2017). Therefore, individual model needs to be improved in tandem with developing an optimal strategy to maximize the benefit of the multi-model mean. The importance of ocean feedback and varying SST to MJO prediction has been demonstrated (e.g., *Woolnough et al.*, 2007; *Seo et al.*, 2014), although the role of the ocean varies for individual MJO cases (*Fu et al.*, 2015) and by model configuration (e.g., *Crueger et al.*, 2013; *Wang et al.*, 2014). Ocean-atmosphere coupling may even degrade the MJO simulation due to the mean bias (*Hendon*, 2000). Understanding the role of mean state bias on MJO prediction (*Lim et al.*, 2018; *Kim et al.*, 2019) and improving the mean state is crucial to extending MJO prediction skill, since the quickly developing mean state biases over the tropics can distort the further development of the MJO (*Hannah et al.*, 2015; *Kim et al.*, 2019).

Although research and operational models have shown continuous improvement of MJO prediction, various challenges remain. Ensemble prediction systems have shown a lack of ensemble spread (i.e., under-dispersive) in MJO prediction (*Kim et al.*, 2014c; *Neena et al.*, 2014; *Vitart*, 2017; *Lim et al.*, 2018). Improving the representation of uncertainty in the model physics schemes has improved the MJO simulation (*Weisheimer et al.*, 2014) and the spread-error relationship (*Palmer et al.*, 2009; *Leutbecher et al.*, 2017; *Subramanian and Palmer*, 2017), indicating that devising ensemble generation approaches tailored for the MJO may have a considerable impact on MJO prediction. Better quality of atmospheric and ocean analyses and reanalyses for initial conditions are conducive to extending MJO prediction skill as well (*Vitart et al.*, 2007; *Dee et al.*, 2011; *Fu et al.*, 2011; *Liu et al.*, 2017).

Due to the huge computational costs for a long record of extended range reforecast experiment, only a handful of studies have performed sensitivity tests of MJO prediction skill to model physics or resolution. Studies have shown extended skill via an enhancement to the entrainment rate for deep convection, which makes the MJO amplitude stronger (*Bechtold et al.*, 2008; *Hannah and Maloney*, 2011; *Klingaman and Woolnough*, 2014), although the improvement

of the MJO often leads to degradation of the mean state (e.g., *Kim et al.*, 2011b). Using super-parameterized GCMs or GCRMs has been shown to improve the MJO skill compared to conventional cumulus parameterization (*Miyakawa et al.*, 2014; *Hannah et al.*, 2015), while the physical reasons for the improvement remain elusive. Compared to the impact of model physics or ocean-atmosphere coupling, the influence of model resolution seems to be marginal (*Vitart et al.*, 2007).

The MJO prediction skill decline after 2-3 weeks is mostly attributed to MJO phase errors, indicating that the phase change (i.e., the location) of the MJO is not accurately predicted (*Vitart*, 2017; *Lim et al.*, 2018; *Kim et al.*, 2019). In most contemporary models, the predicted MJO signal does not persist as long as it does in observations, especially when the MJO propagates across the MC, which is referred to as the MC MJO prediction barrier (e.g., *Vitart*, 2017). This MC barrier is exaggerated in forecasts; the percentage of predicted MJO events starting from the Indian Ocean and not crossing the MC is significantly higher in models compared to that in observations. This indicates the shortcoming of models to maintain MJO propagation through the MC (*Neena et al.*, 2014; *Kim et al.*, 2014c, *Kim et al.*, 2018, *Kim et al.*, 2019; *Wang et al.*, 2014; *Xiang et al.*, 2015b; *Liu et al.*, 2017; *Vitart*, 2017; *Wang et al.*, 2019c). MC-MJO interactions are further discussed in Section 3.6.

To better understand the sources of model errors in MJO propagation processes, several studies have applied the moisture mode hypothesis to the S2S and SubX reforecasts (*Lim et al.*, 2018; *Kim*, 2017; *Kim et al.*, 2019). Models generally struggle to predict MJO convection, its associated circulations, and especially the horizontal moisture advection which is a key process for eastward propagation when crossing the MC (*Kim et al.*, 2019). The error in the MJO propagation processes and the weaker moisture advection process can be partly associated with the following mean biases across the Indo-Pacific: a too-dry lower troposphere, excess surface precipitation, more frequent occurrence of light precipitation rates, and a transition to stronger precipitation rates at lower humidity than in observations (*Kim et al.*, 2019). However, errors emanating from other processes (vertical moisture advection, cloud-radiation feedback, air-sea coupling, and diurnal cycle) may also play an important role in degrading MJO propagation and prediction skill. Therefore, improved process-level understanding of model errors in MJO prediction is crucial for improving MJO prediction skill. The ongoing international projects, such as the YMC Project

(Section 3.6.3), will help improve our understanding of the critical processes involved with the MC prediction barrier issue. Also, saving 3D output fields from multi-model prediction systems will provide an opportunity to study which physical processes in the forecast models require better representation for better MJO predictions. In addition to metrics based solely on forecast skill, more focus on the process-based skill metrics could help illuminate addressable model shortcomings, which is necessary to advance MJO prediction towards its theoretical predictability.

This concise review of the latest progress on MJO prediction and predictability is largely based on the extensive review by Kim et al. (2018) where more detailed discussions can be found.

3.5 Atmosphere-ocean coupled feedbacks within the MJO

MJO convection is most often observed over SSTs greater than 28°C throughout the Indo-Pacific Warm Pool, with a secondary maximum over the eastern tropical Pacific (*Salby and Hendon*, 1994). Krishnamurti et al. (1988) first proposed that air-sea interactions over these warm waters provide energy for 30-50 day convective motions, noting that the typical intraseasonal SST fluctuations of ~0.25°C could alter fluxes by 10-15% to regulate MJO convective intensity. Ocean "coupled feedbacks" comprise the SST response to atmospheric forcing, its modulation of surface fluxes, and the effects of the modified fluxes on the atmosphere.

Understanding the role of ocean feedbacks to the MJO is beset with several challenges. The observed MJO always develops in a coupled system, but some MJO events appear more sensitive to ocean feedbacks than others (e.g., *Gottschalck et al.*, 2013; *Fu et al.*, 2015). Furthermore, the seasonal cycle (*Zhang and Dong*, 2004; *Jiang et al.*, 2018a) and modes of interannual variability, including the IOD (*Wilson et al.*, 2013), ENSO (*Pohl and Matthews*, 2007; *DeMott et al.*, 2018), and the QBO (e.g., *Nishimoto and Yoden*, 2017; *Son et al.*, 2017), influence MJO intensity and propagation.

Given the complex, multi-scale and coupled nature of the MJO, model experiments are required to test hypotheses of ocean feedbacks to the MJO. Analysis typically compares MJO behavior in coupled (CGCMs) and atmosphere-only (AGCMs) models. While coupled feedbacks almost always improve MJO simulation (*DeMott et al.*, 2015 and references therein), biases in simulated atmospheric and oceanic processes may strengthen or weaken coupled interactions in CGCMs relative to those observed, erroneously supporting or refuting the tested hypotheses. More importantly, mean-state SST biases in CGCMs alter tropical mean moisture and circulation (*Zhang*

1043 *et al.*, 2006) and may lead to incorrect conclusions about the MJO sensitivity to coupled feedbacks
1044 (*Klingaman and Woolnough*, 2014).

1045 In this section, we review MJO coupled feedbacks, report recent advances in understanding
1046 how ocean feedbacks affect the MJO, interpret these results in terms of MJO scientific issues
1047 (Section 2) and theory (Section 3.2), and conclude with recommended experimental protocols to
1048 further advance our understanding. For simplicity, we limit our discussion to extended boreal
1049 winter (November-April).

1050 *3.5.1 Summary of coupled processes within the MJO*

1051 MJO coupled feedbacks can be thought of as a cycle of atmospheric forcing of the ocean, the
1052 oceanic response to that forcing, and the atmospheric response to the resulting SST anomalies.
1053 DeMott et al. (2015) discuss these processes in detail; a brief synopsis is presented here. The
1054 atmosphere forces the ocean through fluxes of heat, fresh-water, and momentum. Reduced
1055 cloudiness and calm winds during an MJO suppressed phase increase solar heating and reduce
1056 wind-driven upper-ocean mixing, and reduce evaporative surface cooling (Fig. 7), which stabilize
1057 and thin (or shoal) the oceanic mixed layer (5~20 m deep; *Drushka et al.*, 2012). The shallower
1058 mixed layer effectively reduces upper-ocean heat capacity, yielding a larger warming per unit
1059 heating than for a deeper mixed layer. Under strongly suppressed conditions, a thin ocean mixed
1060 layer combined with intense diurnal surface heating can induce diurnal SST perturbations of 1-3 K.
1061 Nighttime surface cooling drives convective overturning of the ocean mixed layer, mixing some of
1062 the daytime-accumulated heat below the mixed layer; the remaining heat yields a warmer upper
1063 ocean at the next day's sunrise than the previous day's sunrise (*Anderson et al.*, 1996). Thus, the
1064 SST diurnal cycle rectifies onto the intraseasonal scale (e.g., *Bernie et al.*, 2005; *Zhao and Nasuno*,
1065 2020).

1066 For sufficiently strong MJO events, low-level MJO-induced easterlies may exceed low-level
1067 mean state westerlies, resulting in a net westward momentum flux into the upper ocean. As with
1068 surface heat fluxes, the strongly stratified upper ocean limits the momentum flux to the upper
1069 ocean, yielding westward surface currents, especially within about 2.5°S-2.5°N. The resulting
1070 warm-water advection augments flux-driven surface warming. Poleward of 2.5° latitude, Coriolis
1071 deflection of surface currents excites anticyclonic (downwelling) oceanic equatorial Rossby waves,

their Ekman transport forces surface water to the circulation center, suppressing the local thermocline and further maintaining the local warm SST anomaly by limiting deep-ocean mixing.

During an MJO convective transition phase, reduced subsidence and low-level easterlies promote more frequent and deeper convection and enhance evaporation, which tempers upper-ocean warming. By the onset of an MJO active phase, cloud shielding of surface solar heating and strong low-level westerlies that typically follow MJO convection (e.g., *Lin and Johnson*, 1996; *Puy et al.*, 2016) transfer accumulated upper ocean energy to the atmosphere via surface fluxes (*Zhang and McPhaden*, 2000), where it helps maintain anomalous convective heating (*Riley Dellaripa and Maloney*, 2015; *DeMott et al.*, 2016).

Fresh-water and momentum fluxes during an MJO active phase substantially affect upper-ocean stratification and surface currents. Widespread freshening from rainfall stabilizes the upper ocean, yielding a shallower salt-stratified layer over a deeper temperature-stratified layer (e.g., *Drushka et al.*, 2016; *Pei et al.*, 2018) separated by an isothermal "barrier layer" (*Sprintall and Tomczak*, 1992) that resists mixing both from above and below. Sufficiently strong barrier layers can inhibit vertical mixing of MJO-driven surface momentum fluxes, limiting them to the uppermost ocean, where they may drive anomalous surface currents that persist long after the wind forcing subsides, limiting further upper-ocean stabilization and warming before the next MJO event (*Moum et al.*, 2016; *Hong et al.*, 2017b). Equatorial current-driven Ekman transports and sea surface height anomalies forced by strong low-level westerly winds project onto oceanic shallow-water wave modes, such as oceanic upwelling Rossby and downwelling Kelvin waves. In the Indian Ocean, the downwelling Kelvin wave is partially reflected by the Sumatra coast as downwelling Rossby waves that propagate to the western Indian Ocean in roughly 70 days (*Nagura and McPhaden*, 2012), whereas in the Pacific, the downwelling Kelvin wave may initiate (*McPhaden*, 2004) or maintain (*Kapur and Zhang*, 2012; *Lopez et al.*, 2013) El Niño conditions. In less stable conditions, momentum fluxes promote mixing to the deeper ocean (e.g., *Han*, 2005).

3.5.2 Recent Progress: Direct vs indirect ocean feedbacks to the MJO

While there are event-to-event differences in MJO-linked SST anomalies, the canonical view of the ocean-atmosphere system during MJO active phases includes warm SST anomalies to the east, maximum ocean-to-atmosphere surface turbulent fluxes roughly collocated with MJO convection, and cold SST anomalies to the west (Fig. 8). Variations in surface fluxes arise from

variations in low-level winds (wind-driven fluxes) and near-surface vertical gradients of moisture or temperature (SST-driven fluxes). Since SST-driven fluxes communicate SST anomalies to the atmosphere, the most direct ocean feedbacks to the MJO are enhanced total surface flux before convective maximum, and reduced total surface flux afterward.

DeMott et al. (2016) estimated that direct SST-driven ocean feedbacks contribute up to 10% of the change in column moisture associated with MJO propagation, and roughly 2% day^{-1} of the column moistening or heating that sustains MJO convection. Since SST-driven surface fluxes tend to offset wind-driven fluxes, the *direct* effect of coupled feedbacks *reduces* the amplitude of anomalous surface fluxes within the MJO lifecycle, which seems at odds with numerous studies that report coupled feedbacks improve MJO simulation. Furthermore, MJO MSE budget analyses (Section 3.9) confirm that surface fluxes are secondary to cloud radiative feedbacks and mid-level moisture advection for MJO maintenance and propagation, respectively. It is unlikely that direct coupled feedbacks are the primary means by which ocean processes influence the MJO and its propagation.

The limited role of direct feedbacks suggests that more complex *indirect* ocean feedbacks--those that regulate an intermediate process that more effectively interacts with the MJO, or operate on temporal scales other than intraseasonal--may be important. Examples of intermediate processes include stronger MJO convection with larger anvil clouds that amplify radiative feedbacks to MJO convection (*Del Genio and Chen*, 2015); low-level convergence forced by MJO-associated sharp SST gradients (*Hsu and Li*, 2012; *Li and Carbone*, 2012); or amplified low-level convergence east of MJO convection through lower-tropospheric destabilization (*Marshall et al.*, 2008; *Benedict and Randall*, 2011; *Wang and Xie*, 1998; *Fu et al.*, 2015).

DeMott et al. (2019) explored direct and indirect ocean feedbacks to the MJO in four pairs of CGCMs and AGCMs. For each model, monthly mean SSTs from the CGCMs were prescribed to the AGCMs, to ensure that they had identical SST mean states and low-frequency variability. Consistent with previous studies, the CGCMs showed significantly enhanced MJO propagation compared to the AGCMs. However, ocean feedbacks did not uniformly (across models) improve metrics of MJO circulation or cloudiness structure (e.g., *Wang et al.*, 2018a). The CGCMs showed mixed effects of *direct* coupled feedbacks to the MJO: maintenance of the MJO heating anomalies by surface fluxes increased in two models, but decreased or unchanged in the other two. Surface

flux feedbacks to MJO propagation decreased in all four CGCMs, despite warm SST anomalies during MJO convective development, which strongly supports the role of *indirect* ocean feedbacks to MJO propagation in models.

DeMott et al. (2019) also found inconsistent evidence for "intermediate" coupled feedback processes. Coupling enhanced longwave heating and MJO maintenance in only one GCM; BL convergence east of MJO convection (akin to frictional wave-CISK; Section 3.2) was enhanced in two GCMs. In one GCM, MJO propagation improved despite weakening of both these intermediate processes.

An MSE budget analysis showed that coupled feedbacks improved MJO propagation in all CGCMs through stronger mid-level horizontal moisture advection, driven by sharper mean near-equatorial meridional moisture gradients (Fig. 9). Similar experiments with at least two other models have produced similar results (D. Kim, X. Jiang; personal communications). This implies that relatively high-frequency (<30 days) SST perturbations affect MJO propagation through the background moisture distribution, even under identical SST mean state and low-frequency variability.

Other recent studies have revealed different flavors of cross-timescale or "intermediate process" MJO coupled feedbacks. Rydbeck and Jensen (2017) found that warm SST anomalies from oceanic equatorial Rossby waves in the western Indian Ocean (generated by coastal reflection of downwelling Kelvin waves forced by earlier MJO westerly winds) create sharp SST gradients, which are responsible for up to 45% of boundary layer convergence prior to MJO convective onset. Shinoda et al. (2017) note that the reflected Rossby waves may modulate the near-Equator Somali Current or alter the thermal structure of the Seychelles thermocline ridge. Zhou and Murtugudde (2020) found that SST anomalies up to +0.6 K northwest of Australia during MJO suppressed conditions generate anomalous cyclonic circulations and moisture advection that promote the MJO convective "detour" south of the MC. In regional coupled simulations, Zhao and Nasuno (2020) found that the rectification of diurnal SST variability associated with ocean mixed- layer shoaling onto intraseasonal SST perturbations was more important for MJO propagation than the diurnal SST itself.

Advances in understanding MJO interactions with lower-frequency variability in SST and moisture have refocused efforts to understand ENSO modulation of MJO activity. ENSO-driven

Warm Pool SST anomalies modulate MJO variance, such that seasonal-scale MJO activity is enhanced near warm ENSO SST anomalies and suppressed near cold SST anomalies. Wang et al. (2018c) highlighted that western Pacific MJO activity is weaker during East Pacific (EP) El Niños and stronger during Central Pacific (CP) El Niños, associated with greater meridional advection of mean state moisture by stronger intraseasonal wind anomalies during CP events. CP events also drive stronger MJO diabatic heating anomalies (e.g., *Marshall et al.*, 2016), which may be related to the aforementioned stronger wind anomalies, MJO propagation is faster in CP events than in EP events, associated with enhanced low-level convergence east of MJO convection (Wang et al., 2019).

Klingaman and DeMott (2020) demonstrated that the MJO response to ENSO in a CGCM may lead to incorrect perceptions of how intraseasonal coupled feedbacks affect MJO. In the full CGCM, the MJO improved substantially with coupling, compared to the corresponding AGCM with prescribed CGCM SSTs (*DeMott et al.*, 2014). The authors coupled the same AGCM to a one-dimensional (1D) mixed-layer ocean model to control the background SST while retain intraseasonal coupled feedbacks. The MJO was robust when background SST was constrained to an observed climatology, but weakened substantially when background SST was constrained to the CGCM climatology, in contrast to the strong MJO in the CGCM itself. The AGCM-1D ocean model produced an MJO that resembled the CGCM MJO only when background SST was constrained to the CGCM climatology plus a repeating ENSO cycle derived from the CGCM. In both this AGCM-1D and the CGCM simulations, MJO was stronger in El Niño years, but weaker or absent in neutral or La Niña years, respectively. The El Niño background SST and moisture gradients mitigated CGCM mean-state biases, including a cold and dry equatorial Pacific. The simulated MJO is sensitive not only to intraseasonal coupled feedbacks, as often assumed, but also to (potentially erroneous) longer-scale feedbacks. Changes to model physics may affect the MJO directly, or via direct coupled feedbacks, or via indirect coupled feedbacks on scales shorter or longer than the MJO. Isolating these effects requires investing in detailed sensitivity experiments.

3.5.3 Ocean feedbacks to the MJO in the context of critical issues and existing theories

Recent studies provide the context for critical issues (Section 2) and prevailing theories (Section 3.2) of the MJO. The coupled feedbacks analyzed in DeMott et al. (2019) and Klingaman and DeMott (2020) and their effects on the mean moisture distribution strongly support the WTG

moisture mode theory of the MJO. The increased boundary-layer moisture export east of MJO convection in two CGCMs in DeMott et al. (2019) supports the trio-interaction theory; the surprising result that the two other CGCMs exhibited weaker boundary-layer moisture export, despite improved MJO propagation, suggests a need for greater scrutiny of boundary layer-moisture-convection feedbacks in models and observations. These latter models used 1D ocean mixed-layer models constrained to climatological SSTs. This eliminates ENSO and may limit MJO improvement with coupling, either through missing El Niño-induced zonal moisture gradients, the absence of an extended Warm Pool (e.g., *Pohl and Matthews*, 2007), or the lack of central Pacific warm SST anomalies to promote boundary-layer moisture export east of MJO convection (*Marshall et al.*, 2008; *Wang et al.*, 2019a). Support for skeleton model or gravity wave interference MJO theories are unclear in these studies. The results of DeMott et al. (2019) argue against the BLQE theory, as all four CGCMs show improved MJO propagation despite significantly reduced surface fluxes east of MJO convection.

3.5.4 Recommendations for future progress

Recent progress in understanding the role of ocean coupling to the MJO suggests that ocean feedbacks on scales both shorter and longer than intraseasonal are important for MJO propagation. Improved understanding of oceanic processes that affect high-frequency SST fluctuations, and how low-level atmospheric stability and free-tropospheric moisture regulate the convective response to those SST fluctuations, is essential to improve MJO in models. This objective involves two of the longest-standing challenges in atmospheric and oceanic modeling: the parameterizations of atmospheric convection and oceanic mixing, respectively. For longer scales, process-level diagnostics can shed light on how ENSO regulates MJO behavior, as well as synergistic ENSO-MJO feedbacks.

Recent work has led to a few "best practices" for related model sensitivity studies. First, the MJO in a CGCM should not be compared to that in an AGCM with prescribed CGCM daily mean SSTs, as the inability of the AGCM SST to vary in response to surface fluxes leads to strong simultaneous rainfall-SST correlations, instead of the lead-lag relationship from observations and CGCMs (e.g., *Pegion and Kirtman*, 2008). Second, CGCM and AGCM simulations should be performed with the same mean SST and low-frequency SST variability, as any differences may affect the MJO more strongly than intraseasonal or higher-frequency ocean feedbacks. It is best

practice to force the AGCM with CGCM monthly mean SSTs. Klingaman and DeMott (2020) demonstrated that it is then helpful to diagnose MJO sensitivity to ENSO. Finally, thermodynamic ocean feedbacks to the MJO are best understood in an AGCM coupled to a 1D ocean mixed-layer model constrained to observed, CGCM, or ENSO states. This framework minimizes SST mean-state changes, includes feedbacks from high-frequency SST perturbations, and maintains the observed SST-rainfall phase relationship. Furthermore, this framework can help reveal the sensitivity of the MJO, and convection in general, to diurnal SST fluctuations (e.g., *Matthews et al.*, 2014) that are captured only with fine oceanic vertical resolution (~1 m in the upper ocean) and frequent (~hourly) ocean-atmosphere coupling (e.g., *Li et al.*, 2013; *Hsu et al.*, 2019; *Zhao and Nasuno*, 2020). A collection of simulations, including fully coupled, atmosphere-only, and 1D-ocean coupled can help identify the timescales of coupled feedbacks that most strongly enable or inhibit MJO fidelity, and focus efforts to improve oceanic or atmospheric processes most relevant to those scales during model development cycles.

3.6 MJO propagation over the Maritime Continent

Situated in the heart of the Indo-Pacific warm pool between the Indian and Pacific Oceans, the MC has been recognized as a major source of heat and moisture that plays a pivotal role in driving global atmospheric circulation (*Ramage*, 1968; *Neale and Slingo*, 2003; *Slingo et al.*, 2003). Due to land-ocean contrasts and to complex topography over the mountainous MC islands, most of the total annual rainfall over the MC occurs via a vigorous diurnal cycle that is strongly coupled with land-sea breezes (e.g., *Yang and Slingo*, 2001b; *Nesbitt and Zipser*, 2003; *Mori et al.*, 2004; *Qian*, 2008; *Kikuchi and Wang*, 2008; *Love et al.*, 2011; *Peatman et al.*, 2014). Observations show that the MJO tends to be significantly weakened when propagating eastward into the MC region; the MJO also often detours around the MC via an oceanic pathway south of Sumatra Island and over the Java Sea in austral summer (*Wu and Hsu*, 2009; *Kim et al.*, 2017). Often, the MJO even completely dissipates over the MC and fails to propagate into the western Pacific, known as the MC barrier effect for MJO propagation (e.g., *Salby and Hendon*, 1994; *Seo and Kim*, 2003; *Kim et al.*, 2014a; *Kerns and Chen*, 2016; *Zhang and Ling*, 2017). About 50% of the total MJO events during the boreal winter are disrupted over the MC (*Zhang and Ling*, 2017). Due to the MJO's significant impacts on downstream high-impact weather and climate events in both the tropics and extratropics

(see Section 3.8), determining whether the MJO will propagate through the MC is crucial for climate prediction.

The MC barrier effect, however, is poorly simulated in current GCMs (e.g., *Jiang et al.*, 2015; *Ahn et al.*, 2017; *Ahn et al.*, 2020b); and most forecast systems exhibit large deficiencies in predicting the MJO propagation through the MC (see Section 3.4). These model shortcomings in simulating and predicting the MJO propagation through the MC are partially due to our poor understanding of the underlying physics responsible for the MC barrier effect (see also a recent review by *Kim et al.*, 2020a). In this subsection, we briefly review recent progress on studies of the interactions between the MC and the MJO.

3.6.1 The barrier effect of the Maritime Continent on the MJO propagation

Several factors have been proposed for the weakening of MJO amplitude over the MC, which include the topographic effect and land surface processes over the MC, upscale impacts of the local diurnal cycle, and regional and large-scale mean moisture distributions.

a. Orographic effects of MC

Hsu and Lee (2005) illustrated that the lifting and frictional effects caused by the steep topography over the major MC islands will induce near-surface moisture convergence east of the topography, where a new deep-convection region develops. This leads to a sudden shift in the deep convection from the Indian Ocean to the western Pacific. Wu and Hsu (2009) further showed that the blocking effect, as well as the mountain-wave-like structures induced by the MC topography, will lead to a southward detour of the eastward propagating MJO away from the MC mountains and a sudden shift of deep convection. In an aqua-planet AGCM study, Inness and Slingo (2006) also suggested that the topographic blocking effect on the low-level Kelvin wave leads to the observed weakening of the MJO over MC. In particular, the representation of Sumatra in the GCM, as a north-south oriented ridge straddling the equator, seems to be particularly effective at blocking the Kelvin wave signal, and thus weakening or even completely destroying the MJO signal east of the MC.

By using a full atmosphere-ocean coupled GCM that realistically simulates the major observed MJO characteristics, Tseng et al. (2017) found that the MC orography and land-sea contrast can lead to the southward detour during the eastward propagation of MJO convection. The authors also found the MC orography and land-sea contrast distorted the coupled Kelvin-Rossby

wave structure as previously hypothesized, but amplified the MJO over the MC, in contrast to the general notion of the MC damping effect on the MJO. It is argued that the MC islands strengthen the mean low-level westerlies in the eastern Indian Ocean and the western MC, which strengthens the eastward-propagating MJO. This will be further discussed.

b. MC land surface processes

Motivated by the observational and modeling evidence that the surface latent heat flux is critical to sustain MJO variability (e.g., *Maloney and Sobel*, 2004; *Kim et al.*, 2011a), the reduced MJO amplitude over the MC could be ascribed to the weak surface heat flux associated with enhanced MJO convection over the MC land, because of finite land-surface moisture holding capacity relative to ocean regions (*Sobel et al.*, 2008; *Sobel et al.*, 2010). On the other hand, an AGCM simulation suggests that transpiration in the tropical forests over the MC may play a critical role in weakening local MJO variability (*Lee et al.*, 2012). By turning off transpiration in the AGCM, the simulated precipitation variability increases substantially compared to the control experiment. It is argued that surface turbulent fluxes over tropical rainforests are highly correlated with incoming solar energy rather than wind speed as is the case over the ocean, which possibly decouples the land precipitation and large-scale disturbances like the MJO. In contrast, in the absence of transpiration, the simulated surface latent heat flux dependence on incoming solar energy decreases, while its dependence on wind increases, making land areas more coupled to MJO-like disturbances (*Lee et al.*, 2012).

c. Diurnal cycle

It has been hypothesized that reduced MJO amplitude over the MC region could result from a competition for moist energy between the diurnal cycle of convection and low-frequency variability (e.g., *Wang and Li*, 1994; *Zhang and Hendon*, 1997; *Neale and Slingo*, 2003; *Oh et al.*, 2012; *Oh et al.*, 2013). Therefore, vigorous diurnal variability over MC land limits the moist energy to support MJO convection. This dynamical link between the diurnal cycle and the MJO, however, needs to be corroborated further, as results vary on the relationship between the MJO and the diurnal rainfall rate over MC land. While several studies suggested that the amplitude of the diurnal rainfall cycle over MC islands tends to weaken during enhanced MJO convection (*Oh et al.*, 2012; *Peatman et al.*, 2014; *Sui and Lau*, 1992; *Rauniyar and Walsh*, 2011), Sakaeda et al. (2017) suggested that such a relationship is statistically insignificant, particularly over land regions away from the coasts. Jiang

et al. (2019) also suggested that the MJO does not significantly change the amplitude of diurnal rainfall cycle over MC land, but rather increases its daily mean value. Meanwhile, Tian et al. (2006a) illustrated that the diurnal cycle of tropical deep convective clouds tends to be enhanced over both MC land and ocean during the convectively active phase of the MJO.

On the other hand, several modeling studies support the hypothesis that the diurnal cycle over the MC damps the MJO amplitude as previously hypothesized. Oh et al. (2013) showed that in simulations where the diurnal cycle was suppressed by nudging toward daily averaged TRMM rain rates and reanalysis prognostic variables, the MJO amplitude is maintained rather than weakened as it moves over the MC. In an idealized modeling study, Majda and Yang (2016) proposed that the MJO temperature anomaly is cancelled by that from the upscale impact by the diurnal cycle, which suppresses MJO deep convection when it propagates into the MC. Based on CRM simulations, Hagos et al. (2016) demonstrated that the eastward propagation of an MJO event over the MC can be significantly enhanced after switching off the diurnal cycle of insolation in the model, while the model MJO is quickly damped over the MC when the diurnal effect is present.

d. Regional and large-scale mean moisture distribution

From the perspective of the moisture mode framework, Kim et al. (2017) illustrates that the southward detour of MJO convection during its propagation over the MC is primarily ascribed to stronger moistening ahead of the MJO convection over the southern MC, rather than the central MC, due to horizontal moisture advection by MJO perturbation winds acting upon the background moisture gradient. Both zonal and meridional moisture advection are greater in the southern MC region because of a stronger zonal gradient of background moisture for the former, and more organized northerly MJO wind anomalies that bring near-equatorial moist air southward for the latter (*Kim et al.*, 2017).

Meanwhile, by using high-resolution reanalysis data, it is shown that the interruption of lower-tropospheric moistening over the MC islands ahead of the MJO convection is closely associated with the topographically phase-locked mean moisture pattern over the MC (*Hung and Sui*, 2018; *Jiang et al.*, 2019). Strongly shaped by the local diurnal cycle, the low-level winter-mean moisture pattern over the MC is characterized by moisture maxima over local mountain peaks (*Jiang et al.*, 2019). Given this mean moisture distribution, the moisture advection by anomalous easterly MJO winds corresponding to the active MJO convection over the eastern Indian Ocean will

lead to a drying (moistening) effect to the east (west) of the mountain peaks, which disrupts the organization of large-scale MJO convection over the MC area.

3.6.2 Propagating versus non-propagating MJO events over the Maritime Continent

While several plausible processes responsible for the reduced MJO amplitude over the MC are described above, they do not address the question of why some MJO events pass through the MC and propagate into the western Pacific, while others are interrupted over the MC region. As previously mentioned, accurate forecasts of whether the MJO can pass over the MC is critical for prediction of downstream climate and weather extremes influenced by the MJO. This has motivated many recent studies to identify key processes underlying the propagating and non-propagating MJO events over the MC.

Kim et al. (2014a) suggested that whether MJO convection over the eastern Indian Ocean can cross over the MC is closely associated with the suppressed convective conditions over the western Pacific. The low-level off-equatorward Rossby wave circulation in response to the negative convective heating over the western Pacific induces strong moistening over the MC, which helps MJO eastward propagation over the MC. The importance of the leading suppressed convection (LSC) for Indian Ocean MJO convection to cross the MC is also suggested by Chen and Wang (2018b). The LSC enhances the low-level anomalous easterly winds, and thus increases BL convergence and promotes eastward propagation of the MJO. Higher predictive skill is also found for Indian Ocean MJO events when the LSC is present in the forecast initial conditions (*Kim*, 2017). A systematic relationship between propagating MJO events crossing the MC and suppressed convective conditions over the west Pacific, however, is not evident in the analysis by Feng et al. (2015), although MJO cases with strong LSC tend to exhibit more coherent eastward propagation than those with weak LSC. It is questionable, however, whether the LSC is independent from the enhanced MJO convection over the Indian Ocean. And what controls the strength of the LSC? The enhanced MJO convection over the Indian Ocean and the LSC over the western Pacific may be modulated by the same large-scale factors.

By using a precipitation-tracking method, Zhang and Ling (2017) also examined distinctions between MJO events that propagate across the MC and those blocked by the MC. The authors found that precipitation of propagating MJO events mainly occurs over the MC ocean area, while land precipitation dominates for the blocked MJO events. It is thus hypothesized that the strong

diurnal cycle over the MC land may inhibit convective development over the ocean and thus be a possible mechanism for the barrier effect of the MC. Ling et al. (2018) further illustrates that propagating MJO events over the MC region are characterized by a stronger vanguard of precipitation, namely, enhanced precipitation over the MC islands one week prior to the peak MJO convection, when convection over the surrounding seas is still suppressed (*Peatman et al.*, 2014; see Fig. 1b). This stronger land precipitation increases soil moisture, thus reducing the diurnal amplitude of land convection and the dominance of oceanic precipitation as the MJO convection moves over the MC, which is conducive for propagating MJO events over the MC as discussed by Zhang and Ling (2017). This process also plays a role for the more coherent model MJO eastward propagation over the MC when the diurnal cycle is turned off in Hagos et al. (2016). Weakening of MJO propagation by enhanced land convection over the MC is also illustrated by recent GCM experiments (*Ahn et al.*, 2020a), although the strong MC influences on the MJO propagation in this study are found to be associated with changes of the mean moisture distribution.

Additionally, the termination of many MJO events (~ 50%) over the MC region could result from the interruption of MJO moistening over the MC by westward propagating Rossby wave-like dry anomalies, or the so-called transient dry precursor (TDP), from the eastern / central Pacific (*Feng et al.*, 2015a; *DeMott et al.*, 2018). These TDPs tend to be more frequent during La Niña winters (*DeMott et al.*, 2018). The origin of these westward propagating TDPs, however, is not well understood. Other non-propagating MJO events over the MC that are not linked to TDPs are associated with weak moistening over the southern MC by horizontal moisture advection, due to both weak mean moisture gradients (zonal and meridional) associated with the Australian Monsoon, and easterly wind anomalies due to weak LSC over the western Pacific, largely in agreement with several previous studies (*Kim et al.*, 2014a; *Feng et al.*, 2015a; *Kim et al.*, 2017; *Chen and Wang*, 2018b).

In a recent observational study, Gonzalez and Jiang (2019) identified two prevailing intraseasonal variability modes over the western Pacific during boreal winter. In addition to the eastward propagating MJO as the leading mode, the second mode is characterized by a westward propagating intraseasonal mode (WPIM). The MJO eastward propagation tends to be largely interrupted over the MC when the WPIM is active over the western Pacific, which typically occurs under a La Niña-like condition, as for the TDPs discussed above, although the link between the

WPIM and TDP is not clear. Propagation of both the MJO and WPIM are regulated by horizontal MSE advection; their distinct propagation behaviors are largely defined by substantial differences in mean background moisture and zonal winds (*Gonzalez and Jiang*, 2019). It is thus hypothesized that the WPIM could also be a moisture mode like the MJO, but is dominated by westward propagation under a unique environment over the western Pacific, such as a typical La Niña condition with a sharp reduction in the mean moisture towards the east of the MC. Therefore, improved understanding of large-scale controls on tropical climate variability modes is needed to better understand whether MJO convection can propagate through, or get interrupted over, the MC.

On the other hand, a possible role of air-sea coupling has also been suggested for the MJO propagation over the MC. Timor Sea SSTs are observed to be warmer for propagating MJO events over the MC than for non-propagating MJO events (*Zhang and Ling*, 2017). Hirata et al. (2013) also showed that pronounced eastward propagation of the MJO across the MC is associated with locally warmer SST anomalies over the MC region associated with the subsiding Rossby wave that precedes the convective phase.

While various processes have been proposed to influence propagation of the MJO over the MC, these processes are not mutually exclusive. As the strong diurnal cycle over the MC land is proposed to damp the MJO during its passage over the MC, the diurnal cycle over MC itself is subject to strong modulations by large-scale climate variability modes, such as El Niño and La Niña (*Rauniyar and Walsh*, 2013). Therefore, the plausible impacts of the diurnal cycle on the MJO propagation could also reflect influences from large-scale conditions. Also, in the model experiments with disabled diurnal cycles or modified MC topography, the simulated changes to MJO propagation behavior are not only due to the diurnal cycle and MC topography, but also to associated changes in the large-scale mean state. For example, as previously discussed, the strong topographically phase-locked mean moisture pattern over the MC, which strongly interrupts MJO moist preconditioning over the eastern part of the MC mountains, is largely defined by the diurnal cycle (*Jiang et al.*, 2019). If the diurnal cycle is disabled in a model, the regional mean moisture gradient will be significantly weakened, which favors a smooth eastward MJO propagation over the MC (*Oh et al.*, 2013; *Hagos et al.*, 2016). The reduced MJO amplitude over the MC in Tseng et al. (2017), in which the MC orography is removed or MC land is replaced by ocean, may also result from dramatic changes in the model mean state, including the lower-tropospheric mean moisture

distribution, which have been suggested to play a critical role in regulating MJO propagation (*Gonzalez and Jiang*, 2017).

3.6.3 The Years of the Maritime Continent (YMC) Field Observations

As discussed above, MJO propagation over the MC is regulated by both large-scale conditions and regional processes over the MC, including the diurnal cycle and land-sea breezes, due to local land coverage and elevated terrain. The intricate interactions between the MJO and MC remain poorly represented in weather and climate models even at very high resolutions (e.g., cloud permitting; *Hagos et al.*, 2016; *Peatman et al.*, 2015; *Birch et al.*, 2016; *Baranowski et al.*, 2019). With an overarching goal to expedite improved understanding and prediction of local multi-scale variability of the MC weather-climate systems and its global impact, through observations and modeling exercises, the YMC field observations have been organized through international collaboration and coordination (*Yoneyama and Zhang*, 2020). One YMC focus is the barrier effect of the MC on MJO propagation.

With few YMC field campaigns conducted and others still pending, the limited in situ observations available from YMC start to provide detailed depictions of MJO modulations of the local diurnal cycle (*Wu et al.*, 2017; *Yokoi et al.*, 2017; *Yokoi et al.*, 2019; *Wu et al.*, 2018), oceanic barrier layers (*Moteki et al.*, 2018), and CCEWs (*Kubokawa et al.*, 2016; *Takasuka et al.*, 2019) over the MC region. With the progress of YMC, these observations will provide unprecedented datasets to identify model deficiencies in representing MC-MJO interactions, and to advance our understanding and prediction of MC weather-climate systems and their remote teleconnections.

3.7 Tropical-extratropical interaction associated with the MJO

In addition to the direct impact on the weather and climate in the tropics, the MJO influences a broad range of phenomena, including high impact weather events, in the extratropical regions (e.g., *Higgins et al.*, 2000; *Bond and Vecchi*, 2003; *Jones et al.*, 2004b; *Donald et al.*, 2006; *Lin and Brunet*, 2009; *Alvarez et al.*, 2016). Such global impacts of the MJO likely provide an important source of skill for subseasonal climate predictions (e.g., *NASEM*, 2016). On the other hand, the tropical MJO variability can be induced or influenced by extratropical disturbances (e.g., *Lin et al.*, 2007; *Ray and Zhang*, 2010; *Vitart and Jung*, 2010). The coherent variability between the extratropical atmosphere and the organized tropical convection, therefore, indicates a tropical-extratropical interaction on the subseasonal time scale (see a review by *Stan et al.*, 2017).

3.7.1 MJO influences on the extratropical circulation

An increasing number of studies have shown that the variability of tropical convection associated with the MJO has a considerable influence on a wide range of extratropical weather and climate events. For example, the tropical convection associated with the MJO was found to be correlated with the precipitation anomaly in the North American west coast (*Higgins et al.*, 2000; *Mo and Higgins*, 1998; *Bond and Vecchi*, 2003; *Lin et al.*, 2010; *Becker et al.*, 2011). A near-global impact of the MJO on precipitation was reported in Donald et al. (2006). Extreme rainfall over the contiguous United States was found more likely to happen when the MJO is active than inactive and most frequently when the MJO convection center is over the Indian Ocean (*Jones and Carvalho*, 2012; *Barrett and Gensini*, 2013). A modulation of U.S. West Coast atmospheric river activity is responsible for the MJO's effect on extreme rainfall there (*Guan et al.*, 2012; *Baggett et al.*, 2017; *Mundhenk et al.*, 2018). A significant influence of the MJO on subseasonal variability in wintertime surface air temperature in North America was observed (*Lin and Brunet*, 2009; *Zhou et al.*, 2012b; *Baxter et al.*, 2014; *Zheng et al.*, 2018). Surface air temperature over Canada and the eastern United States in winter tends to be anomalously warm (cold) 10-20 days following the MJO phase 2-3 (6-7), which according to Wheeler and Hendon (2004) corresponds to enhanced (reduced) convection in the tropical Indian Ocean and suppressed (enhanced) convection in the equatorial western Pacific (*Lin and Brunet*, 2009; *Lin et al.*, 2019a). It was reported that the phase of the MJO has a substantial systematic and spatially coherent effect on subseasonal variability in wintertime surface air temperature in the Arctic region (*Vecchi and Bond*, 2004; *Yoo et al.*, 2012), which contributes to the subseasonal forecast skill (*Lin*, 2020).

The influence of the MJO also extends to the Southern Hemisphere extratropics. The winter temperature and precipitation variability in southeastern South America was observed to have a coherent signal associated with different MJO phases (*Naumann and Vargas*, 2010; *Barrett et al.*, 2011). Alvarez et al. (2016) documented the influence of the MJO in South America and their marked seasonal variations. Chang and Johnson (2015) reported that several Southern Hemisphere teleconnection patterns in June-August exhibit oscillatory behavior on time scales of 20-30 days and with the frequency of occurrence modulated by the MJO phases. Flatau and Kim (2013) demonstrated that enhanced MJO convection in the Indian Ocean precedes changes in the Antarctic Oscillation (AAO). The impact of the MJO on Australian rainfall, circulation, and temperature was

also reported (*Wheeler et al.*, 2009; *Marshall et al., 2014*). Fauchereau et al. (2016) suggested that the MJO directly impacts regional circulation and climate in the New Zealand region, potentially through extratropical Rossby wave response to tropical diabatic heating. Whelan and Frederiksen (2017) found that tropical-extratropical interactions associated with the MJO contributed to the extreme rainfall and flooding in northern Australia during January 1974 and January 2011.

The MJO influence on extratropical weather and climate events is largely through its modulation of atmospheric circulation patterns. Of particular interest is the modulation of the dominant modes of variability in the wintertime Northern Hemisphere by the MJO, as these modes account for a large portion of variance on the S2S time scale and have a significant impact on extratropical weather and climate. The PNA pattern is known to be closely associated with ENSO variability on the interannual time scale (*Wallace and Gutzler*, 1981; *Horel and Wallace*, 1981). Hsu (1996) suggested that the PNA variability on the intraseasonal time scale is linked to the convective activity over the eastern Indian Ocean. Mori and Watanabe (2008) found that the development of the PNA can be triggered by the MJO convection activity in the tropical Indian Ocean and western Pacific. Seo and Lee (2017) explicitly demonstrated three different propagation ways of waves emanating from the Rossby wave source to the PNA region. Tseng et al. (2019) showed that the PNA pattern is optimally triggered when the MJO has a dipole heating structure with opposite signed convection anomalies in the west Pacific and Indian Ocean.

The NAO is another important mode of variability that influences the Northern Hemisphere weather, especially in eastern North America and Europe (e.g., *Hurrell et al.*, 2013). The NAO is usually considered as a regional expression of the Arctic Oscillation (AO), or the Northern Annular Mode (NAM; e.g., *Thompson and Wallace*, 1998; 2000). Earlier studies found that the AO/NAO variability is associated with wave-mean flow interactions and wave breaking in the extratropics (e.g., *Limpasuvan and Hartmann*, 1999; *Franzke et al.*, 2004). This indicates that the atmospheric internal dynamics of the extratropical circulation is likely the primary mechanism for the AO/NAO variability, and implies a lack of predictability for this mode beyond the synoptic weather time scale (e.g., *Greatbatch*, 2000). However, recent studies have provided evidence that part of the AO/NAO variability is associated with the tropical forcing of the MJO. The eastward progression of the convectively active phase of the MJO was found to be associated with changes in tendency and sign of the AO (*L'Heureux and Higgins*, 2008). Through time-lagged composites and

probability analysis of the NAO index with respect to different phases of the MJO, Lin et al. (2009) revealed a robust lagged connection between the MJO and NAO. About 10-15 days after the occurrence of MJO phase 2-3 (6-7), the probability of a positive (negative) NAO is significantly increased. Based on the definition of Wheeler and Hendon (2004), MJO phases 2-3 (6-7) corresponds to a dipole structure of tropical convection anomaly with enhanced convection in the tropical Indian Ocean (western Pacific) and reduced convection in the tropical western Pacific (Indian Ocean). Similar results of the association between the MJO and NAO were reported in Cassou (2008). Many S2S models are able to capture such MJO-NAO teleconnection to some extent (e.g., *Vitart*, 2017).

To illustrate the influence of the MJO on the PNA and NAO teleconnection patterns, shown in Fig. 10 are lagged composites of 500-hPa geopotential height anomalies following MJO phase 2 (Figs. 10a-c) and phase 6 (Figs. 10d-f). The calculation is performed on pentad (5-day average) data derived from the NCEP/NCAR reanalysis (*Kalnay et al.*, 1996) for extended boreal winter of November to April and the MJO phases are determined from the RMM index of Wheeler and Hendon (2004). The analysis procedure is the same as that described in Lin et al. (2009), except that data of 40 winters (1979/80-2018/19) are used here compared to 25 years (1979/80-2003/04) in the previous study. Lag *n* indicates that the 500-hPa height anomaly lags the MJO phase by *n* pentads. Indicated on the lower left and upper right corners of each panel in Fig. 10 are composite PNA and NAO indices. The results show that the MJO phases corresponding to a dipole tropical convection anomaly tend to influence the amplitude of both the PNA and NAO. A negative (positive) PNA and then a positive (negative) NAO develop following MJO phase 2 (phase 6).

The mechanism for MJO influence on the middle and high latitudes is related to atmospheric response to tropical forcing. Enhanced vertical motion associated with large-scale tropical deep convection leads to divergence in the upper tropical troposphere. The upper divergent flow near the subtropical westerly jet regions creates a source for extratropical Rossby waves (*Sardeshmukh and Hoskins*, 1988) that propagate in the middle latitude westerlies bounded by the pole and the critical latitude where the climatological zonal wind becomes easterlies (e.g., *Webster and Holton*, 1982; *Hoskins and Ambrizzi*, 1993).

The general features of extratropical atmospheric response to the MJO can be simulated using simple numerical models with idealized tropical thermal forcing (e.g., *Matthews et al.*, 2004; *Lin et*

al., 2010; *Seo and Son*, 2012; *Tseng et al.*, 2019). One important aspect of these numerical model studies is the use of realistic three-dimensional wintertime climatological mean flow. It was demonstrated that a large portion of the MJO-related teleconnection is a direct response to tropical heating and can be explained by linear dynamics. These numerical studies also show that the extratropical response pattern is established in about two weeks. A dipole tropical forcing which corresponds to MJO phases 2-3 or 6-7 is the most effective in exciting extratropical circulation anomalies (*Lin et al.*, 2010; *Tseng et al.*, 2019), consistent with several earlier studies (e.g., *Simmons et al.*, 1983; *Lau and Phillips*, 1986; *Ferranti et al.*, 1990).

Besides the Rossby wave propagation discussed above, other dynamical processes in the extratropics likely contribute to the atmospheric response to tropical heating as well. The centers of action of teleconnection patterns tend to appear in preferred locations, e.g., the eastern North Pacific and the North Atlantic. Disturbances on the time scale of 10-90 days at these locations can grow by extracting kinetic energy from the zonally asymmetric climatological flow through barotropic conversion (e.g., *Simmons et al.*, 1983; *Branstator*, 1985). The effect of synoptic-scale transients of the 2-10-day time scale is another factor that contributes to the extratropical atmospheric response to the tropical forcing. When interactions between different frequencies become strong, the nonlinear component of extratropical response becomes important. For example, Cassou (2008) noticed that the positive and negative NAO events following MJO phases 3 and 6 evolve differently. Some nonlinear aspects of the extratropical response to the MJO were discussed in Lin and Brunet (2018).

As Rossby wave propagation is dependent on the strength of the westerly mean wind (*Hoskins and Ambrizzi*, 1993; *Ting and Sardeshmukh*, 1993), the MJO teleconnection is sensitive to the background mean flow. This is reflected by the fact that the MJO teleconnection in the Northern Hemisphere extratropics is stronger in winter than in summer. Another indication of this sensitivity is that the extratropical patterns associated with the MJO vary in phase and amplitude in different phases of ENSO (*Roundy et al.*, 2010). The characteristic of the tropical thermal forcing related to the MJO is likely another important factor that influences the extratropical response. Yadav and Straus (2017) demonstrated that slow MJO events tend to have a stronger impact on NAO than fast MJO events. Henderson et al. (2017) found that GCMs with significant biases in basic state and those with poorly represented MJO forcing simulate poor MJO teleconnection patterns.

Recent studies have shown that the stratosphere may play a role in the MJO teleconnection. The MJO is observed to influence the state of the stratospheric polar vortex (e.g., *Garfinkel et al.*, 2012, 2014; *Liu et al.*, 2014; *Kang and Tziperman*, 2018b). The signal in the stratospheric polar vortex can then descend to affect the AO / NAO in a way as described in Baldwin and Dunkerton (2001). The stratospheric polar vortex may also condition the background flow of the extratropical Northern Hemisphere for the MJO-related wave propagation. Such a stratospheric pathway for the MJO-NAO connection was demonstrated in Barnes et al. (2019). Another stratospheric influence is through the QBO in the tropical stratosphere, which will discussed in Section 3.8.

3.7.2 Extratropical influences on the MJO and the global intraseasonal variability

Many previous studies have provided evidence that there is considerable extratropical influence on the tropics. Extratropical waves propagate into the tropics through regions of westerly zonal wind (e.g., *Webster and Holton*, 1982), and influence tropical convection (e.g., *Kiladis and Weickmann*, 1992; *Matthews and Kiladis*, 1999). Tropical waves can be forced by lateral forcing from the middle latitudes (e.g., *Yanai and Lu*, 1983; *Zhang and Webster*, 1989; *Hoskins and Yang*, 2000).

On the intraseasonal time scale, the extratropical influence on the tropical variability is also observed. Liebmann and Hartmann (1984) found that energy propagates from the middle latitudes to the tropics especially over the eastern Pacific. Localized intraseasonal tropical convection near the dateline and to the east was found to be forced by extratropical circulation anomalies in Lau and Phillips (1986). Again over the tropical eastern Pacific was observed the largest extratropical impact of the non-divergent component of the wind by Ferranti et al. (1990). The large extratropical impact occurs in the eastern Pacific where the extratropical westerly flow in the upper troposphere extends into the tropics, which can possibly be explained by the wave propagation mechanism as discussed in Webster and Holton (1982).

There is evidence of extratropical influence on the MJO. Lin et al. (2007) demonstrated that a tropical MJO-like wave can be generated in a long integration of a dry atmospheric model with time-independent forcing. Hong et al. (2017a) observed that the southward penetration of northerly wind anomalies associated with extratropical disturbances in the extratropical western North Pacific triggered the tropical convective instability that led to the onset of the MJO to the west of the dateline. Ray and Zhang (2010) investigated the initialization of MJO events, and found that a

1611 critical factor to the reproduction of the MJO initiation is time-varying lateral boundary conditions
1612 from the reanalysis. Hall et al. (2017) performed several experiments with different lateral
1613 boundary conditions and concluded that about half of the intraseasonal variance in the tropics can
1614 be attributed to the boundary influence of middle latitudes. The NAO variability on the subseasonal
1615 time scale was observed to influence the tropical MJO (*Lin et al.*, 2009; *Lin and Brunet*, 2011).

1616 The instability theory of Frederiksen and Frederiksen (1993,1997) and Frederiksen (2002)
1617 provides a possible explanation for the global intraseasonal variability. Based on a linearized two-
1618 level primitive equation model and simplified tropical convection representation in a three-
1619 dimensional basic state of boreal winter, the instability analysis revealed that some of the unstable
1620 modes couple the extratropics with a tropical 40-60 day disturbance, which is similar to the MJO
1621 (*Frederiksen*, 1982; 1983). The development of extratropical teleconnection patterns including the
1622 PNA and NAO is captured in this framework (*Frederiksen and Lin*, 2013). Simmons et al. (1983)
1623 calculated the most unstable normal mode of the linearized vorticity equation with a zonally
1624 varying basic state of wintertime 300-hPa flow. This mode was found to have a period of 45 days,
1625 and two of its phases project significantly onto the PNA and NAO respectively. The adjoint normal
1626 mode analysis of Ferranti et al. (1990) revealed that the tropical forcing that is optimal to excite the
1627 extratropical unstable normal mode is related to the MJO. This indicates that the atmospheric
1628 barotropic process likely plays an important role in the intraseasonal variability linking the tropical
1629 and extratropical atmosphere. The baroclinic process, on the other hand, was found to enhance the
1630 growth rate of the unstable modes (*Frederiksen*, 1983).

1631 *3.7.3 Remarks*

1632 Improved understanding of the MJO-related teleconnection and tropical-extratropical
1633 interaction is important for subseasonal to seasonal predictions (e. g., *NASEM*, 2016; *Vitart et al.*,
1634 2015). However, there remain tremendous challenges. Numerical models have great difficulties in
1635 simulating the MJO (Section 3.3). Most S2S models have significant biases in predicting the pattern
1636 and amplitude of the MJO teleconnection (e.g., *Vitart*, 2017; Section 3.4). Reducing model
1637 systematic errors, to have a realistic three-dimensional basic flow, probably is one of the most
1638 important steps to improve the MJO teleconnection simulation, although many challenges remain
1639 (e.g., *Zadra et al.*, 2018). Other aspects to explore include the role of synoptic-scale transients in
1640 generating and maintaining the MJO teleconnection. It is of interest to better understand the

processes involved in the initiation of tropical intraseasonal convection by extratropical waves. Further studies are also required to understand the role of the stratosphere in the tropical-extratropical interactions on the subseasonal time scale.

3.8 The Quasi-biennial Oscillation (QBO) - MJO connection

3.8.1 QBO influences on MJO activity

The MJO activity exhibits pronounced year-to-year variability, which has been attributed to influences by ENSO (*Hendon et al.*, 1999; *Hendon et al.*, 2007; *Marshall et al.*, 2016) in addition to the internal variability of the MJO (*Slingo et al.*, 1999； *Lin et al.*, 2015). For example, the MJO activity tends to extend farther eastward to the date line during El Niño winters. The overall level of MJO activity across the MC, however, does not change significantly in response to ENSO (*Hendon et al.*, 1999; *Son et al.*, 2017). Most recently, a strong connection between the QBO, a prevailing interannual variability mode in the tropical stratosphere, and MJO activity during boreal winter season was identified (*Liu et al.*, 2014; *Yoo and Son*, 2016), which spurred great interest in many active studies on this topic (e.g., *Son et al.*, 2017; *Nishimoto and Yoden*, 2017; *Marshall et al.*, 2017; *Hendon and Abhik*, 2018; *Wang et al.*, 2018b; *Zhang and Zhang*, 2018; *Kim et al.*, 2020c).

The QBO is an oscillation of the equatorial stratospheric zonal winds between easterlies and westerlies with an average period of 28 months. These alternating easterlies and westerlies of the QBO propagate downward with a near-constant amplitude of 20 m s^{-1} between 5 and 40 hPa (e.g., *Baldwin et al.*, 2001). It is found that about 40-50% of interannual variations of boreal winter MJO activity is attributed to the QBO (*Marshall et al.*, 2017; *Son et al.*, 2017), in contrast to only a modest (less than 10%) variance of interannual MJO activity explained by the (*Hendon et al.*, 1999; *Hendon and Abhik*, 2018; *Son et al.*, 2017). In general, boreal winter MJO activity is enhanced when the equatorial lower stratospheric winds at 50hPa are in the easterly phase of the QBO (hereafter EQBO) and decreased during the westerly phase of the QBO (WQBO; *Yoo and Son*, 2016; *Son et al.*, 2017; *Densmore et al.*, 2019; *Nishimoto and Yoden*, 2017; *Marshall et al.*, 2017). Moreover, during EQBO MJO propagates more slowly eastward with a prolonged period of active convection farther into the western Pacific, whereas the MJO convection is largely confined to the west of the MC during WQBO (*Nishimoto and Yoden*, 2017; *Son et al.*, 2017; *Zhang and Zhang*, 2018; *Wang et al.*, 2019d). The slower eastward propagation of the MJO during the EQBO phase is possibly resulted from a stronger convection-circulation coupling associated with the MJO,

particularly, due to more coherent MJO eastward propagation over the MC (*Son et al.*, 2017; *Hendon and Abhik*, 2018). In contrast, activity in CCEWs is found to be insensitive to QBO phases (*Abhik et al.*, 2019).

Whether MJO events are stronger during EQBO than WQBO or not depends on the MJO metrics used. Most studies using RMM or the outgoing longwave radiation (OLR)-based MJO index (OMI; *Kiladis et al.*, 2014) concluded that the MJO is stronger in EQBO than WQBO. By applying a precipitation tracking method to select individual MJO events and exclude non-MJO signals, Zhang and Zhang (2018) provided a minority opinion: stronger MJO activities during EQBO than WQBO are due to a greater number of MJO days during EQBO than WQBO, rather than stronger individual MJO events. While the strongest MJO events tend to occur during EQBO, the overall correlation between the strength of all tracked MJO events and a QBO index is statistically insignificant but the correlation between the number of MJO days and the QBO index is significant. The more MJO days during the EQBO period is due to more frequent initiation of MJO events over the Indian Ocean and their longer durations as a result of a weaker barrier effect of the MC on MJO propagation. The discrepancy on this issue because of different metrics used needs to be reconciled to provide solid observational evidence for understanding of the mechanism for the QBO-MJO connection.

3.8.2 QBO influences on MJO teleconnection patterns

The MJO teleconnection patterns over the North Pacific is also subject to strong modulations by the QBO. During EQBO winters, the PNA-like Rossby wave teleconnection pattern over the North Pacific is more pronounced than the WQBO winters (*Son et al.*, 2017; *Wang et al.*, 2018b; *Toms et al.*, 2020). The MJO-related North Pacific storm track (NPST) variability exhibits larger amplitude during EQBO than WQBO. Meanwhile, significant differences in the spatial distribution of the NPST change between the two QBO phases are also noticed with a zonally elongated pattern during EQBO winters but separated into two centers during WQBO winters (*Wang et al.*, 2018b). Further analysis indicates that these differences in NPST activity between the two QBO phases could be primarily caused by the baroclinic energy conversion and downstream energy propagation, possibly due to stronger MJO convection and thus associated Rossby wave sources in EQBO winters (*Wang et al.*, 2018b).

Meanwhile, over the Atlantic sector, the QBO also strongly modulates the MJO-induced NAO pattern (*Feng and Lin*, 2019). The positive (negative) NAO pattern, which usually occurs after 10 days of the MJO Phase 3 (7) as previously observed (*Lin et al.*, 2009; *Cassou*, 2008), tends to be much stronger and longer lasting during WQBO than EQBO, possibly by modulating the extratropical mean flow. During the WQBO winters, anomalous westerly winds are observed over the extratropical North Pacific as well as high-latitude over the North Atlantic, which could favor poleward propagation of extratropical Rossby waves and enhance troposphere-stratosphere interaction that promote development of the NAO (*Feng and Lin*, 2019).

3.8.3 Physical mechanisms for the QBO-MJO connection

While the physical mechanism of the QBO-MJO connection is not completely understood, it is generally considered through the QBO-related changes in the upper tropospheric static stability and the vertical zonal wind shear across the tropopause (*Son et al.*, 2017; *Nishimoto and Yoden*, 2017; *Yoo and Son*, 2016). During the EQBO phase, easterlies in the lower stratosphere are associated with cold temperature anomalies in the lower stratosphere and upper troposphere, in accord with the thermal wind balance (*Son et al.*, 2017; *Nishimoto and Yoden*, 2017). This is thought to reduce static stability near the tropopause, and destabilize tropical deep convection as supported by the recent modeling study (*Nie and Sobel*, 2015; *Martin et al.*, 2019), and thus promote stronger MJO activity (*Son et al.*, 2017; *Nishimoto and Yoden*, 2017; *Hendon and Abhik*, 2018; *Martin et al.*, 2019).

Hendon and Abhik (2018) further suggested that both positive temperature anomalies in the upper troposphere and cold anomalies near tropopause at 100hPa are stronger and more in-phase with the MJO convection during EQBO. Acting together with the reduced static instability during the EQBO phase, these MJO-induced temperature anomalies can further weaken static instability near the tropopause, and promote stronger MJO convection during EQBO, which extends further eastward past the MC (*Hendon and Abhik*, 2018).

Additional evidence of the influences of the QBO-related static stability on the MJO is provided by examining the QBO-MJO connection during the 11-year solar cycle (*Hood*, 2017). It is illustrated that the largest amplitudes and occurrence rates of the MJO during boreal winter tend to occur during EQBO under solar minimum conditions, in concert with the weakest static stability in the tropical lower stratosphere (*Hood*, 2017). It is also hypothesized that the observed strongest

QBO-MJO connection during boreal winter could be explained by the strongest influences of the tropopause by the QBO, since the tropical tropopause is highest during this season, particularly over the MC region (*Kim and Son*, 2012; *Son et al.*, 2017; *Abhik et al.*, 2019; *Klotzbach et al.*, 2019).

Note that enhanced tropical mean convection during the EQBO phase have also previously been reported (e.g., *Collimore et al.*, 2003; *Liess and Geller*, 2012). In addition to changes in static stability, strong vertical wind shear of the QBO could also play a role in affecting deep convection by disrupting the coherent structure of deep convective plumes (*Gray et al.*, 1992; *Collimore et al.*, 2003; *Nie and Sobel*, 2015). The observed QBO-MJO connection, particularly the relative role of the QBO-related static instability and vertical wind shear near the tropopause, was investigated by a limited-area CRM with idealized QBO states imposed (*Martin et al.*, 2019). In experiments only forced by the QBO temperature anomalies, stronger MJO convection during EQBO compared to WQBO is simulated although weaker than the observed. In contrast, experiments with only imposed QBO wind anomalies show much weaker effects on the MJO, suggesting that temperature anomalies could be a key pathway through which the QBO can modulate the MJO (*Martin et al.*, 2019). Sensitivity experiments also suggest that the QBO influences on MJO tend to depend on both the amplitude and the height of the QBO temperature anomalies (*Martin et al.*, 2019).

Meanwhile, it has also been suggested that the QBO's influences on MJO convective activity can also be through the cloud-radiation feedback by changing cirrus clouds near the tropopause (*Son et al.*, 2017; *Hendon and Abhik*, 2018). During EQBO, associated with reduced tropopause stability, cirrus clouds tend to form more frequently near the tropopause, especially across the MC and central Pacific (*Son et al.*, 2017). These cirrus clouds will lead to a net radiative cooling in the lower stratosphere and warming in the troposphere (e.g., *Hartmann et al.*, 2001; *Yang et al.*, 2010), thus further destabilize the tropical upper troposphere and help to amplify the MJO (*Son et al.*, 2017).

3.8.4 The QBO-MJO connection in climate model simulations and predictions

Despite the evidence on the QBO-MJO connection from both observations and idealized CRM simulations, our latest GCMs have great difficulty in representing this relationship. Lee and Klingaman (2018) illustrated that while both the QBO and MJO can be well simulated in the MetUM Global Ocean Mixed Layer coupled model (MetUM-GOML1), a rather weak QBO-MJO

connection is captured in this model compared to the reanalysis. The biased QBO-MJO relationship in MetUM-GOML1 is considered to be associated with weak QBO-induced temperature anomalies in the tropical tropopause, or to errors in MJO vertical structure (*Lee and Klingaman*, 2018). By comparing the 30 CMIP6 models, it is shown that none of the models are able to capture the observed QBO-MJO connection (*Kim et al.*, 2020b).

Due to the inability of GCMs in realistically depicting the QBO-MJO interaction, as an alternative, model representation of the QBO influences on MJO has been examined using initialized predictions based on operational models including those participated in the S2S and SubX Projects. Differences in the predicted MJO under the EQBO and WQBO phases with the forecast lead time can be examined in these hindcasts. In general, models show a higher MJO prediction skill during EQBO winters than WQBO winters. For the bivariate anomaly correlation coefficient of 0.5 or 0.6, the MJO prediction skill during EQBO winters is enhanced by up to 10 days (*Lim et al.*, 2019; *Wang et al.*, 2019d; *Marshall et al.*, 2017; *Abhik and Hendon*, 2019). This enhancement is found to be insensitive to the initial MJO amplitude, indicating that the improved MJO prediction skill is not simply the result of an initially stronger MJO during EQBO. Instead, a longer persistence of the MJO during EQBO winters, is likely responsible for a higher prediction skill (*Lim et al.*, 2019; *Marshall et al.*, 2017; *Wang et al.*, 2019d).

Particularly noteworthy is that the improved MJO predictive skill during EQBO is found even in low-top models with stratospheric processes poorly resolved (*Marshall et al.*, 2017; *Abhik and Hendon*, 2019; *Wang et al.*, 2019d). This leads to the implication that the improved MJO predictive skill during EQBO is not directly resulted from the model-predicted QBO state, or the effect of the QBO can still be felt in low-top models during the first two weeks of hindcasts. This notion is further confirmed by the higher MJO prediction skill during EQBO than WQBO in statistical models that does not contain explicit information about the stratosphere (*Wang et al.*, 2019d; *Marshall et al.*, 2017). Instead, the MJO skill dependence on QBO phases is suggested to be associated with the initial state of the MJO and/or the regularity of its propagation in the verifying observations (*Wang et al.*, 2019d).

On the other hand, by evaluating reforecasts from nine models participating in the S2S and SubX Projects, Kim et al. (2020c) illustrated that while generally higher MJO prediction skill during EQBO than WQBO is also found as in previous studies, the MJO skill difference between

the QBO phases is not statistically significant for most models. This insignificant QBO-MJO skill relationship is further confirmed by comparing two experiments by using both a high-top and low-top version of the same GCM. While there are clear differences in the forecasted QBO between the two experiments, a negligible change is shown in the MJO prediction, indicating that the QBO in this model may not directly control the MJO prediction. The insignificant QBO-MJO skill relationship could be due to model deficiencies in representing the QBO signals in tropopause static stability and vertical wind shear or the vertical structures of the MJO (*Kim et al.*, 2020c; *Lee and Klingaman*, 2018; *Abhik and Hendon*, 2019). Also, smaller sample size of QBO and MJO events in the reforecasts relative to the observation could be a reason for the insignificant QBO-MJO relationship.

Since MJO teleconnection is also strongly modulated by QBO, this thus offers an opportunity to improve the prediction skill of the MJO-related mid-latitude circulations. Based on the ECMWF reforecast ensemble system, Baggett et al. (2017) found notable differences in the prediction skill for atmospheric river (AR) activity in mid-latitude during different phases of the MJO and QBO. Particularly, it is indicated that ARs have the potential to be forecasted more accurately at lead times of 3 to 5 weeks when the phases of both the MJO and the QBO are considered (*Baggett et al.*, 2017). Therefore, future investigations are warranted for improved understanding of the QBO-MJO interaction when exploiting the untapped source of subseasonal predictability that can provide a window of opportunity for improved prediction of global climate.

3.9 MJO structure and teleconnections under a changing climate

A future climate that is warmed by increasing greenhouse gas concentrations is expected to produce fundamental changes to the tropics including warmer SSTs, an increased lower tropospheric vertical moisture gradient, and increased static stability (e.g. *Held and Soden*, 2006; *Knutson and Manabe*, 1995; see Figure 11). Given the strong dependence of MJO dynamics on the basic state (e.g. Section 3.2), it is natural to expect that MJO characteristics and associated teleconnections may be affected by these future climate changes (see *Maloney et al.*, 2019a for an extended review). A general, but not universal, finding from climate models is for the increased SST and stronger lower tropospheric vertical moisture gradient associated with climate warming to result in increased MJO precipitation variance (e.g. *Takahashi et al.*, 2011; *Arnold et al.*, 2015; *Wolding et al.*, 2017; *Bui and Maloney*, 2018; *Haertel*, 2018; *Rushley et al.*, 2019, and Figure 12).

Preferential SST warming in the eastern tropical Pacific (e.g. *Xie et al.*, 2010) may result in proportionally greater increases in MJO precipitation variance in those regions, although the tendency for models to preferentially warm the east Pacific with increasing greenhouse gas forcing does not yet have observational support (*Coats and Karnauskas*, 2017). Increased MJO precipitation amplitude in a warmer climate is consistent with reduced gross moist stability that produces a stronger MJO (e.g. *Adames et al.*, 2017a). At the end of the 21st Century under business as usual warming scenarios, some CMIP3 and CMIP5 models do indicate decreases in MJO precipitation variance (*Takahashi et al.*, 2011; *Bui and Maloney*, 2018). The modest or even decreased MJO precipitation amplitude change in some models may be due to a different SST warming pattern, or a particularly pronounced change toward top-heavy MJO heating structure with warming (*Takahashi et al.*, 2011; *Bui and Maloney*, 2019a). The latter effect would shift the vertical profile of MJO convection and associated vertical motion away from the region of strongest lower tropospheric moisture gradient, making large-scale vertical motion associated with MJO precipitation less efficient at moistening the column and hence weakening the MJO (*Bui and Maloney*, 2019a; *Wolding et al.*, 2017). Other factors that have been proposed as affecting MJO amplitude with climate warming include weaker cloud-radiation feedbacks (*Arnold et al.*, 2013; *Arnold and Randall*, 2015; *Carlson and Caballero*, 2016; *Wolding et al.*, 2017; *Adames and Kim*, 2016), stronger surface flux feedbacks (*Arnold and Randall*, 2015; *Wolding et al.*, 2017), and the onset of equatorial superrotation that reduces the equator to pole humidity gradient and weakens dry air advection into the tropics that can damp the MJO (*Carlson and Caballero*, 2016).

Even if MJO precipitation variability increases in a warmer climate, most models indicate that MJO circulation amplitude decreases more modestly or can even decrease in amplitude relative to historical conditions (Bui and Maloney 2018). This result can be explained by WTG thermodynamic energy balance. In the presence of increased static stability in a warmer climate that is consistent with a tropical temperature profile approximately determined by moist adiabatic adjustment (e.g. Figure 11; *Knutson and Manabe*, 1995), MJO apparent heating anomalies are balanced by weaker vertical motion (*Maloney and Xie*, 2013; *Bui and Maloney*, 2018). Through continuity this implies weaker MJO horizontal wind anomalies. Multimodel mean MJO wind anomalies from CMIP5 are projected to decrease in amplitude at the end of the 21st Century (Figure 12), although multimodel mean precipitation anomalies are projected to increase (*Bui and*

Maloney, 2018). A weakening of MJO wind anomalies at the end of the 21st Century would have important implications for S2S prediction of extratropical weather, given that Rossby wave generation associated with MJO teleconnections is forced by divergent flow anomalies produced by MJO heating (e.g. *Sardeshmukh and Hoskins*, 1988; *Wolding et al.*, 2017; Section 3.7).

Recent work has examined the transient response of the MJO over the 21st Century under RCP8.5 in CMIP5 models, and has provided mixed results regarding the detectability of MJO precipitation and wind amplitude changes before the end of the 21st Century. Rushley et al. (2019) examined five CMIP5 models that exhibit good MJO performance in current climate to demonstrate monotonic increases in MJO precipitation amplitude over consecutive 20 years periods of the 21st Century, although the increases in MJO precipitation amplitude changes are not distinct from increases in the background spectrum. Bui and Maloney (2019b) used a compositing technique to examine MJO precipitation and wind amplitude changes over the 21st Century in eleven simulations from models assessed to have a realistic MJO, including three ensemble members from one model. Defining a detectable change in MJO activity as the multi-model mean change being larger than the standard deviation across models (e.g. *Kirtman and coathors*, 2013), increases in MJO precipitation amplitude and decreases in MJO circulation amplitude do not become individually detectable until the last two decades of the 21st Century (Figure 12). Even different ensemble members from the same model can disagree on the sign of MJO precipitation change for a given 20-year period, consistent with substantial decadal variability in the climate system. However, decreases in the relative strength of MJO wind to precipitation anomalies can be detected as early as 2020-2040, consistent with tropical mean temperature warming and increases in static stability resulting from such warming (Figure 12). These results suggest that MJO impacts such as Rossby wave teleconnections that are initiated by divergent flow anomalies may be weaker per unit MJO precipitation anomaly over the next several decades, and also suggest the robustness of WTG theory for regulating MJO dynamics. Models from the upcoming CMIP6 database might help to resolve discrepancies between the Rushley et al. (2019) and Bui and Maloney (2019b) results on the near-term detectability of the MJO precipitation amplitude increases with climate warming, especially since several previous studies have argued that trends in MJO precipitation and wind amplitude are already detectable in the observational record (e.g. *Slingo et al.*, 1999; *Jones and Carvalho*, 2006; *Lee and Seo*, 2011; *Oliver and Thompson*, 2012; *Tao et al.*, 2015; *Jones and*

Carvalho, 2011). However, other studies have argued that natural variability may explain a large fraction of the recent changes in MJO activity (*Schubert et al.*, 2013).

Maloney et al. (2019a) also review other changes to MJO characteristics in a warmer climate that are projected by climate models. The depth of MJO convective heating and associated vertical motions are expected to increase with climate warming (e.g. *Chang et al.*, 2015; *Wolding et al.*, 2017). MJO propagation speed also tends to increase in models (e.g. *Arnold et al.*, 2013; *Adames et al.*, 2017a; *Liu et al.*, 2013; *Caballero and Huber*, 2010; *Song and Seo*, 2016; *Rushley et al.*, 2019), which shifts the MJO toward shorter period. The processes responsible for increased MJO propagation speed in a warmer climate remain unclear, although previous studies have invoked increased vertical and meridional moisture gradients as possible causes, particularly through their ability to hasten moistening through moisture advection to the east of the MJO convective center (e.g. *Arnold et al.*, 2015; *Wolding et al.*, 2017; *Chang et al.*, 2015; *Adames et al.*, 2017a). Many models also indicate an increase in the frequency of MJO events with warming, a result that is consistent with the decreased timescale of the MJO with warming (*Arnold et al.*, 2015; *Adames et al.*, 2017a; *Song and Seo*, 2016), although not all models demonstrate this behavior (*Subramanian et al.*, 2014).

Many outstanding questions about the effect of climate change on the MJO exist that deserve future emphasis by the scientific community. Changes in MJO precipitation amplitude in a warmer climate appear to be complicated by competing effects from basic state moisture profile changes, temperature profile changes, and MJO vertical structure changes (*Bui and Maloney*, 2019a), and more work is needed to understand these competing effects in single models and in the new CMIP6 database. Processes responsible for changes in the strength of various feedbacks in warmer climate as they affect MJO amplitude require scrutiny, including potentially weaker cloud-radiative feedbacks and strengthened wind-evaporation feedbacks. The effect of the pattern of SST change on MJO amplitude needs further investigation, as MJO amplitude changes show substantial sensitivity to the pattern of SST change (*Takahashi et al.*, 2011; *Maloney and Xie*, 2013). Many models do not reproduce the regional details of the tropical SST trend over the historical record (*Coats and Karnauskas*, 2017), which makes the SST pattern change a key uncertainty in future MJO projections. The processes responsible for increases in MJO propagation speed with climate warming remain relatively unclear. The separate contributions of SST warming and direct impact of

increasing greenhouse gas concentrations on the MJO should be examined, as previous modeling studies have shown potentially important direct impacts of greenhouse gas changes on the tropical hydrologic cycle (*Allen and Ingram*, 2002; *Deser and Phillips*, 2009). How MJO teleconnections change in a warmer climate requires more scrutiny, including potentially confounding effects due to changes in the amplitude of MJO divergence anomalies and basic state changes such as the strength and extent of the north Pacific jet that affect the Rossby wave source and pathway of stationary Rossby wave propagation (e.g. *Hoskins and Ambrizzi*, 1993). Finally, the CMIP6 database presents an excellent opportunity to reassess the findings of Rushley et al. (2019) and Bui and Maloney (2019b) on when changes in MJO characteristics, including the relative strength of MJO precipitation and wind anomalies, become detectable relative to the historical record in the presence of substantial decadal variability in the climate system. If the change of the ratio of MJO wind to precipitation anomalies is as robust as suggested by models, evidence for a weakening ratio over the last few decades may already be present in the observational record.

4. Outlook and recommendations

In this section, we provide a brief outlook and recommendations of MJO research in the near future (e.g., the coming years or a decade) toward further improved understanding, modeling and prediction capability of the MJO and associated high-impact weather and climate extremes.

4.1 New advanced observations of key processes associated with the MJO

Our understanding of many key processes of the MJO is hindered by a lack of accurate observations. For example, while TRMM rainfall products have been widely used to characterize convective activity associated with the MJO, the light rain and isolated convection associated with shallow and congestus cumuli during the MJO moisture preconditioning phase are largely underestimated by the TRMM precipitation radar (e.g., *Jiang et al.*, 2011; Berg et al., 2010; Short and Nakamura, 2000). The sparse spatial and diurnal sampling of the TRMM measurements also precludes analysis of the evolution of individual MJO events. The vertical profiles of precipitation of the MJO can be significantly improved by the recent GPM Mission (Hamada and Takayabu, 2016; *Skofronick-Jackson et al.*, 2018). Observations of precipitation and clouds associated with the light rain regime can be complimented by CloudSat precipitation radar (CPR) (Berg et al., 2010), although the CPR has its own limitation in retrieving the intense rain over the MJO deep convection

region, and lacks detailed information on the diurnal evolution of MJO convection owing to its sun-synchronous orbit.

Meanwhile, previous efforts on retrievals of vertical profiles of diabatic and radiative heating profiles from various satellites provided critical insights into the essential physics of the MJO (*Tao et al.*, 2006; *L'Ecuyer and McGarragh*, 2010; *Henderson et al.*, 2013; *Tao et al.*, 2016). However, these satellite-based vertical heating estimates are subject to considerable uncertainties due to limitations of satellite sensors, retrieval algorithms, as well as their dependence on reanalysis products and CRM simulations, which are further linked to physical parameterizations (*Ling and Zhang*, 2011; *Jiang et al.*, 2011; *Del Genio and Chen*, 2015).

In the near future, new revolutionary remote-sensing technology and improved retrieval algorithms will provide an unprecedented opportunity to explore various processes crucial for the MJO as previously reviewed. For example, by employing the next-generation high-performance lidar and radar technology, the EarthCARE Mission (*Illingworth et al.*, 2015), to be launched in 2021, will deliver comprehensive datasets that can be used to study the relationship among clouds, aerosols and radiation at accuracy levels that will significantly improve our understanding of MJO physics, including vertical profiles of aerosol, clouds, precipitation, and radiative cooling/heating associated with the MJO, and provides critical benchmark to constrain climate model development. The Doppler capability of the EarthCARE Project will also provide significantly improved characterization of convective motions and even entrainment processes associated with the MJO as has been explored based on CloudSat (*Luo et al.*, 2010), which have been shown to be highly sensitive to MJO behaviors in model simulations.

Advanced observing technologies will also continue to boost our capability of making in situ observations critical to MJO studies. Autonomous underwater observing technologies (e.g., seagliders, Wirewalkers, Prawlers) allow ocean profiles to be measured at spatial and temporal resolutions and locations not available from the global Argo array and the moored buoy networks (e.g., TAO, RAMA, PIRATA). The study on the diurnal cycle of the surface layer using seagliders (*Matthews et al.*, 2014) is one example. Robotic sea surface platforms (e.g., wavegliders, saildrones, and drifters) measure variables that are key to air-sea exchanges of energy and momentum but difficult to be observed by satellites. These robotic surface platforms serve to fill gaps in the moored buoy networks and are particularly useful in sampling regions of high spatial

gradients (e.g., SST fronts, ocean eddies) and coastal regions. The quality of their observations of in situ state variables for bulk estimates of air-sea turbulent fluxes and radiation fluxes have proven comparable to those of standard platforms (*Thomson and Girton*, 2017; *Zhang et al.*, 2019). It has been an even greater challenge to observe the atmospheric boundary layer over the tropical oceans than at and under the sea surface. Boundary-layer processes and their interaction with the free troposphere are deemed to play essential roles in MJO dynamics (Section 3.2). But in situ observations of the marine boundary layer are extremely rare. Traditional ways of measuring marine boundary layers using ships and airplanes are expensive, logistically difficult, and cover only limited space and time. Airdrones, which have been used widely for many purposes over land, can be an efficient and effective platform for observing the marine atmospheric boundary layer. The mobility of these platforms makes them well suited for adaptive observations for field campaign and targeted observations. Creative applications of existing and in-development technology would solve the issues of navigation, power supply, and data transmission to make a network of airdrones with moored docking devices to routinely sample the marine boundary layer over the tropical oceans for the study of the MJO and other tropical phenomena. These and other robotic or autonomous observing platforms should be widely used to fill the current observation gaps for improving understanding and predicting the MJO.

4.2 Continuous improvement of MJO understanding

The availability of new reanalysis datasets, field observations, and model simulations, particularly from those based on CRMs, will help advance understanding of the role of multi-scale interaction among convective elements on the instability and propagation of the MJO. Remaining questions that can be addressed include whether the upscale transport of momentum, moisture, and heat from small-scale convective elements is crucial for the observed MJO, and whether these processes need to be fully resolved for realistic simulations and skillful prediction of the MJO. Additionally, how smaller-scale convective systems, including the CCEWs and MCSs, and their underlying physics are regulated by the dynamic and thermodynamic environment associated with the MJO needs to be fully characterized and understood in the context of two-way interactions between the MJO and smaller-scale convective systems.

Meanwhile, despite significant progress in the most recent decade in understanding key processes of the MJO, knowledge gaps remain for explaining the observed year-to-year variability

of the MJO. Many previous studies on the interannual variability of the MJO focused on the relationship between the MJO and the ENSO, but with controversial findings. While little relationship between the interannual variability of MJO and ENSO was reported in some studies (e.g., *Slingo et al.*, 1999; *Hendon et al.*, 1999; *Jones et al.*, 2004a; *Jones and Carvalho*, 2006; *Lin et al.*, 2015; *Son et al.*, 2016), modulations of ENSO-like large-scale environment on MJO amplitude and propagation were indicated in others (e.g., *Bellenger and Duvel*, 2012; *DeMott et al.*, 2018; *Gonzalez and Jiang*, 2019). The MJO-ENSO relationship is further complicated by its seasonal dependence (e.g., *Zhang and Gottschalck*, 2002; *Teng and Wang*, 2003;*Hendon et al.*, 2007) and the diversity of ENSO events (*Gushchina and Dewitte*, 2012; *Feng et al.*, 2015b).

As discussed in Section 3.8, while strong modulation of the year-to-year MJO activity by the stratospheric QBO has been reported, our state-of-the-art climate models fail to capture this strong QBO-MJO connection. Also, although temperature stratification, wind shear, and cloud-radiative feedbacks associated with the QBO are proposed to play roles in regulating the MJO activity (*Son et al.*, 2016; *Hendon and Abhik*, 2018; *Martin et al.*, 2019), the mechanisms on the QBO-MJO connection remain largely elusive.

4.3 New modeling strategies for improved MJO simulations and predictions

4.3.1 Cloud-permitting resolution

While the use of horizontal resolution fine enough to resolve convective systems is promising for improved MJO simulations by alleviating model uncertainties in cumulus processes, this approach requires significant computing resources, making it impractical for long-term climate simulations and operational prediction purposes. Therefore, new strategies for the super-parameterization application are under development. For example, encouraging results have been reported by using a so-called ultra-parameterization method (*Parishani et al.*, 2017), in which the grid spacing of the CRM is reduced to 250m to explicitly capture the BL turbulence, clouds, and entrainment in a global climate model. A quasi-three-dimensional super-parameterization has also been tested (*Jung and Arakawa*, 2014; *Jung*, 2016), in which 3D CRMs are applied to two mutually perpendicular channel domains that extend over GCM grid cells, allowing a representation of topographic effects that could not be implemented in the 2D CRMs in the earlier super-parameterization models.

4.3.2 Stochastic convective parameterization

Stochastic convective parameterization approach in GCMs (e.g., *Deng et al.*, 2015; *Wang et al.*, 2016b; *Deng et al.*, 2016; *Wang et al.*, 2016b; *Peters et al.*, 2017; *Goswami et al.*, 2017b; *Goswami et al.*, 2017a) is a less-expensive alternative to the CRM approach for representing subgrid cumulus variability. This approach is based on the earlier stochastic modeling concept of introducing subgrid cumulus variability to the deterministic parameterization of coarse resolution GCMs (e.g., *Buizza et al.*, 1999; *Lin and Neelin*, 2003). One of these stochastic convective schemes, the stochastic multi-cloud model (SMCM), has recently been implemented into several different GCMs, yielding improved simulations of both CCEWs and the MJO (*Goswami et al.*, 2017a; *Goswami et al.*, 2017b; *Peters et al.*, 2017). Compared to the conventional ways of tuning parameters in the convection schemes, one advantage of this SMCM approach is that the dominant parameters affecting model MJO variability are different from those controlling the model mean state (*Goswami et al.*, 2017b; *Peters et al.*, 2017). Therefore, unlike the known parameter tuning strategies that give an improved MJO at the expense of the mean state (c.f., Section 3.3.3). Stochastic parameterization has the potential to retain a model's realistic mean state while improving its MJO. A drawback of the SMCM implementation to GCMs is the complicated calibration process of the SMCM which involves many parameters for depicting the transition probability among different cloud types, and many of these parameters are subject to observational constraints. Additionally, plausible dependence of these parameters on the large-scale environment needs to be considered particularly for climate projection studies.

4.3.3 Meso-scale convective system parameterization

Despite the significant role of the MCSs as a building block of large-scale convective systems, the effects of organized convection associated with the MCSs in conventional GCMs are neither resolved nor represented in the cumulus parameterization scheme. A so-called MCS parameterization (MCSP) approach has been recently implemented to represent MCS impacts in climate models. For example, Moncrieff et al. (2017) proposed an additional parameterization to represent the layered overturning of MCSs over the conventional convective parameterization scheme. This additional parameterization consists of adding a top-heavy heating profile to the convective heating profile and a corresponding momentum transport profile associated with the layered flow as derived by observations and model simulations (e.g., *Houze et al.*, 2000; *Mechem et*

2059 *al.*, 2006; *Moncrieff and Klinker*, 1997). The profiles are applied when the convective
2060 parameterization is activated and their magnitudes are controlled by the large-scale shear. It has
2061 been shown that simulations of the MJO, CCEWs, and large-scale tropical precipitation patterns are
2062 improved by implementing a minimalist version of this MCSP approach in conventional GCMs
2063 (*Moncrieff et al.*, 2017; *Moncrieff*, 2019). A recent modeling study by Ahn et al. (2019) also
2064 highlighted the ability of MCSP in climate models to mitigate the aforementioned modeling
2065 dilemmas between MJO variability and mean state.

2066 While there is still room for improving MCSP approaches to represent MCS effects in climate
2067 models, the approach holds promise for improved representation of MCS effects in coarse-
2068 resolution models needed for climate projections of Earth's water cycle, rainfall, and severe
2069 weather.

2070 *4.3.4 Machine learning*

2071 Most recently, there is increasing interest in the use of machine learning (ML) approaches to
2072 create computationally efficient parameterizations for convective and BL processes. This approach
2073 involves fitting a statistical model to the output of relatively expensive physical models (e.g.,
2074 CRMs) that more faithfully represent the subgrid processes (*Brenowitz and Bretherton*, 2018;
2075 *Gentine et al.*, 2018; *Schneider et al.*, 2017; *O'Gorman and Dwyer*, 2018; *Rasp et al.*, 2018). In
2076 contrast to conventional parameterizations that incorporate simplified physical models, such as the
2077 entraining plum for convective parameterizations, an ML-based parameterization takes a statistical
2078 approach by minimizing the error between the ML model's predictions of the parameterized
2079 model's output. The resulting GCM is then a hybrid model consisting of a physically based
2080 component and one or more ML-based components.

2081 Rasp et al. (2018) applied a deep neural network to represent all atmospheric subgrid
2082 processes in the Community Atmosphere Model v3.0 (CAM3) by learning from a super-
2083 parameterized version of this GCM (SPCAM) in which convection is treated explicitly. The
2084 traditional subgrid parameterizations in CAM3 were then replaced with the trained neural network
2085 which freely interacted with the resolved dynamics and the surface-flux scheme. The prognostic
2086 multiyear simulations closely reproduced not only the mean climate of the cloud-resolving
2087 simulation but also key aspects of variability, including a realistic MJO and equatorial wave
2088 spectrum.

As suggested by promising results from the recent studies, the coupling between the conventional GCMs and ML-trained statistical models is attractive if the most uncertain parameterizations in GCMs can be replaced with ML-based parameterizations that are trained systematically, and meanwhile greatly reduce the computational costs compared to CRMs. One caveat of this approach is that it may not be suitable for future climate projections based on training using a present-day mean state.

5. Concluding remarks

The crucial role of the MJO in the Earth's hydrological cycle has been well recognized since it was discovered five decades ago. Advanced understanding and skillful prediction of the MJO and its global influences have proven challenging, however, due to the complexity of the MJO physics which involve intricate feedbacks among clouds, circulation, moisture, and radiation. This article outlines several outstanding issues underlying fundamental MJO physics, and provides a comprehensive review of the recent progress in the observational, modeling, and theoretical study of the MJO, with a particular focus on the most recent decade since the publication of several previous review articles and books (e.g., Zhang, 2005; Lau and Waliser, 2012). Despite the exciting recent progress achieved in MJO research, significant efforts are warranted to further advance our understanding and prediction capability of the MJO. For example, our understanding remains poor on processes regulating the interannual variability of the MJO, the two-way interactions between the MJO and multi-scale convective elements, and the MJO-mean state trade-off issue in climate models. These near-future MJO research directions will be aided by the new observations and modeling strategies discussed in this review article.

Acknowledgements:

We thank Chief Editor M. Zhang for inviting this contribution, H. Hendon and two other reviewers for their insightful comments on an earlier version of this manuscript, and W. Guan for helping produce several figures. We also wish to acknowledge WMO WGNE for supporting the MJO Task Force and its activities. XJ acknowledges support by the NOAA Climate Program Office under awards NA15OAR4310098, NA15OAR4310177, and NA17OAR4310261. HK was supported by NSF grant AGS-1652289. EDM was supported by NSF Grant AGS-1841754, NOAA CVP Grant NA18OAR4310299, and NASA CYGNSS Grant NNX17AH77G. DK was supported by the NASA Grant 80NSSC17K0227, NOAA Grant NA18OAR4310300, DOE Grant DE-SC0016223, and KMA Grant KMI2018-03110. This is PMEL contribution 5063. The MJO RMM index can be accessed from the website http://www.bom.gov.au/climate/mjo/. The TRMM 3B42 3-hourly rainfall data was downloaded from the https://disc.gsfc.nasa.gov/datasets/TRMM_3B42_7/summary, and the GPM IMERG Level-3 half hourly precipitation data was downloaded from https://disc.gsfc.nasa.gov/datasets/GPM_3IMERGHH_06/summary. The SubX reforecasts can be downloaded from http://iridl.ldeo.columbia.edu/SOURCES/.Models/.SubX/, and S2S reforecasts from https://apps.ecmwf.int/datasets/data/s2s/ .

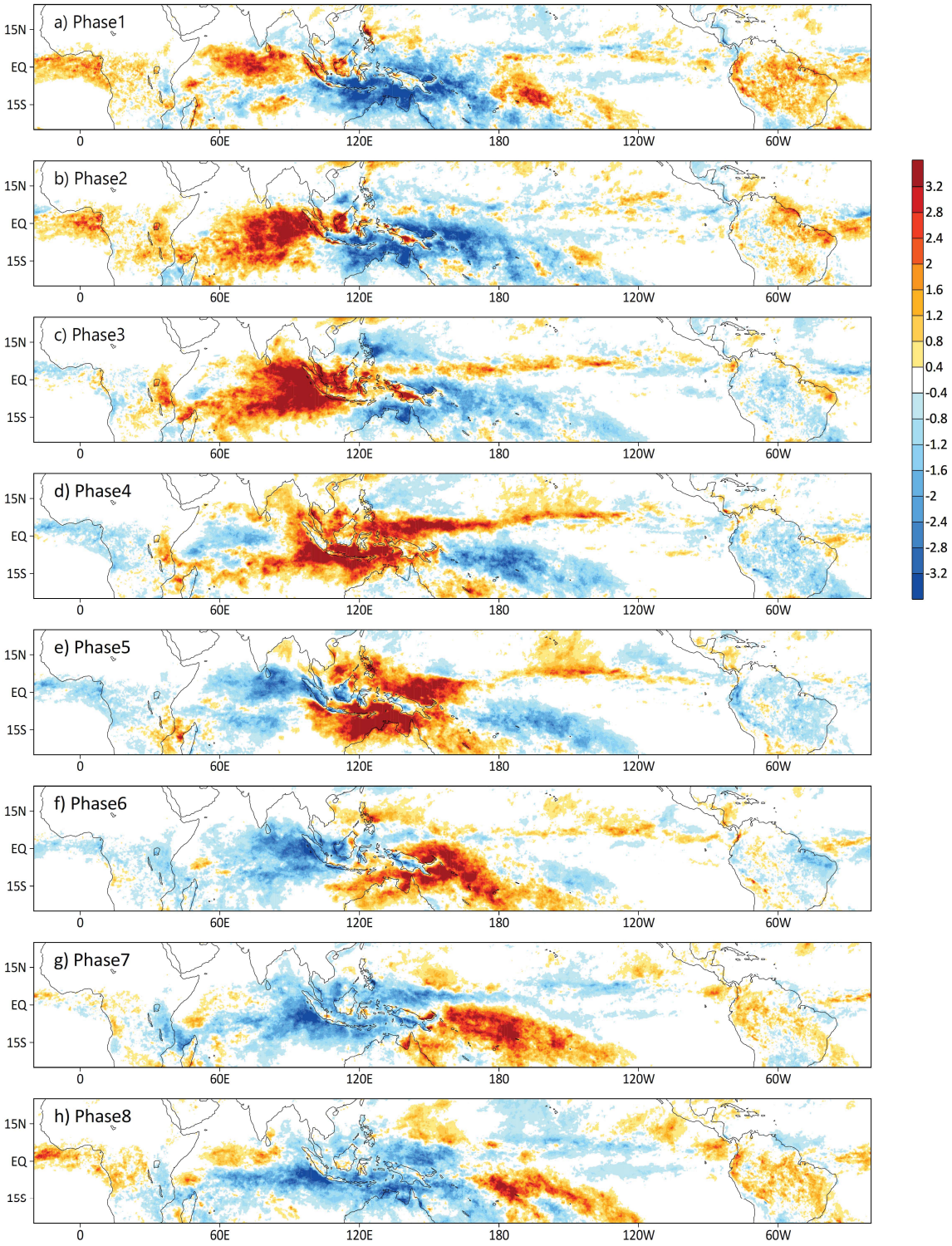


Figure 1 Evolution of composite rainfall anomalies (mm day^{-1}) during boreal winter season from November to March for MJO Phases 1-8 as defined by Wheeler and Hendon (2004). The rainfall data is based on TRMM (Version 3B42; *Huffman et al.*, 2007) from 1998 to 2016. Before used in the composite analysis, daily rainfall anomalies are derived by removing the climatological annual cycle and then applying a 20-100day bandpass filtering.

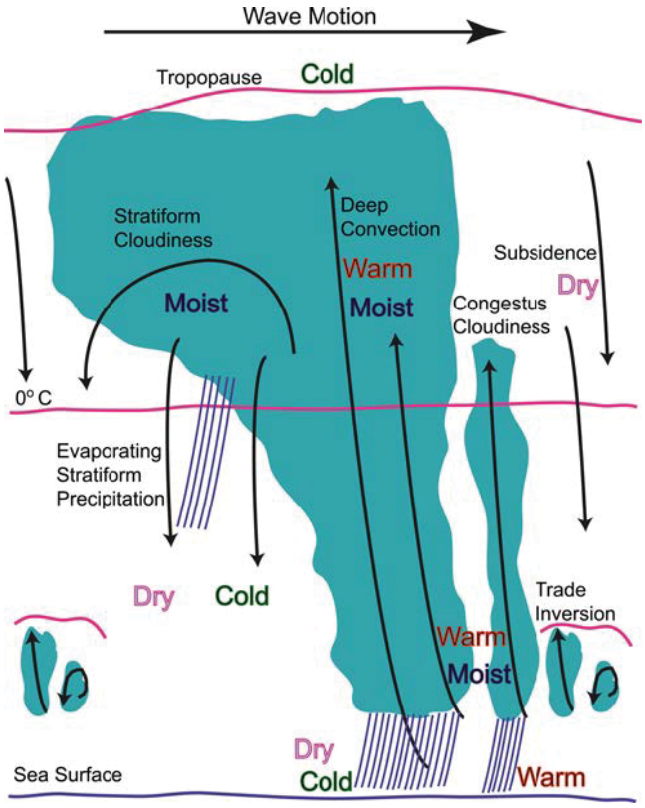


Fig. 2 Typical vertical structures in cloudiness, temperature, and humidity associated with multi-scale tropical convective systems including mesoscale convective systems (MCSs), convectively coupled equatorial waves (CCEWs), and the MJO. Wave movement is from left to right. Figure is reproduced courtesy of the American Geophysical Union from Kiladis et al. (2009).

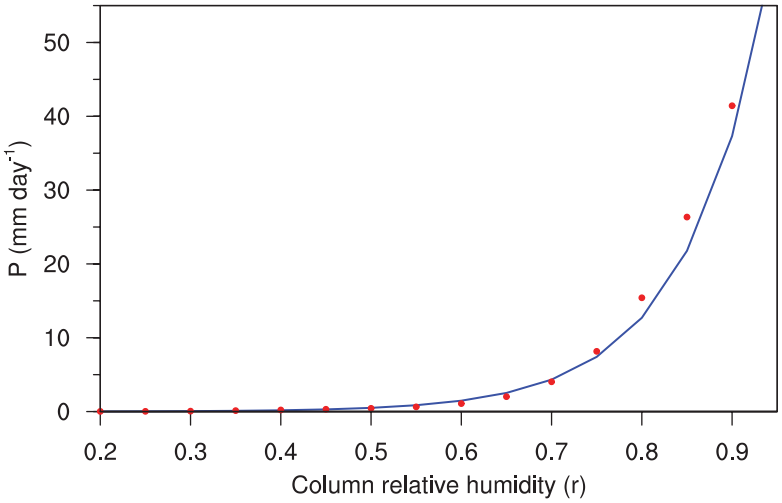


Fig. 3 Red dots: Distribution of daily precipitation P in 5% bins of column-relative humidity r over the Indian Ocean (15°S-15°N, 50°E-95°E) in all months of 1998–2016. The solid blue curve shows the exponential fit with $P = 0.00228 \exp(10.78 \cdot r)$ (mm day^{-1}). Precipitation and r data are based on TRMM 3B42 and ERA-Interim reanalysis (*Dee et al.*, 2011), respectively, and interpolated onto 2.5 by 2.5 degree grids.

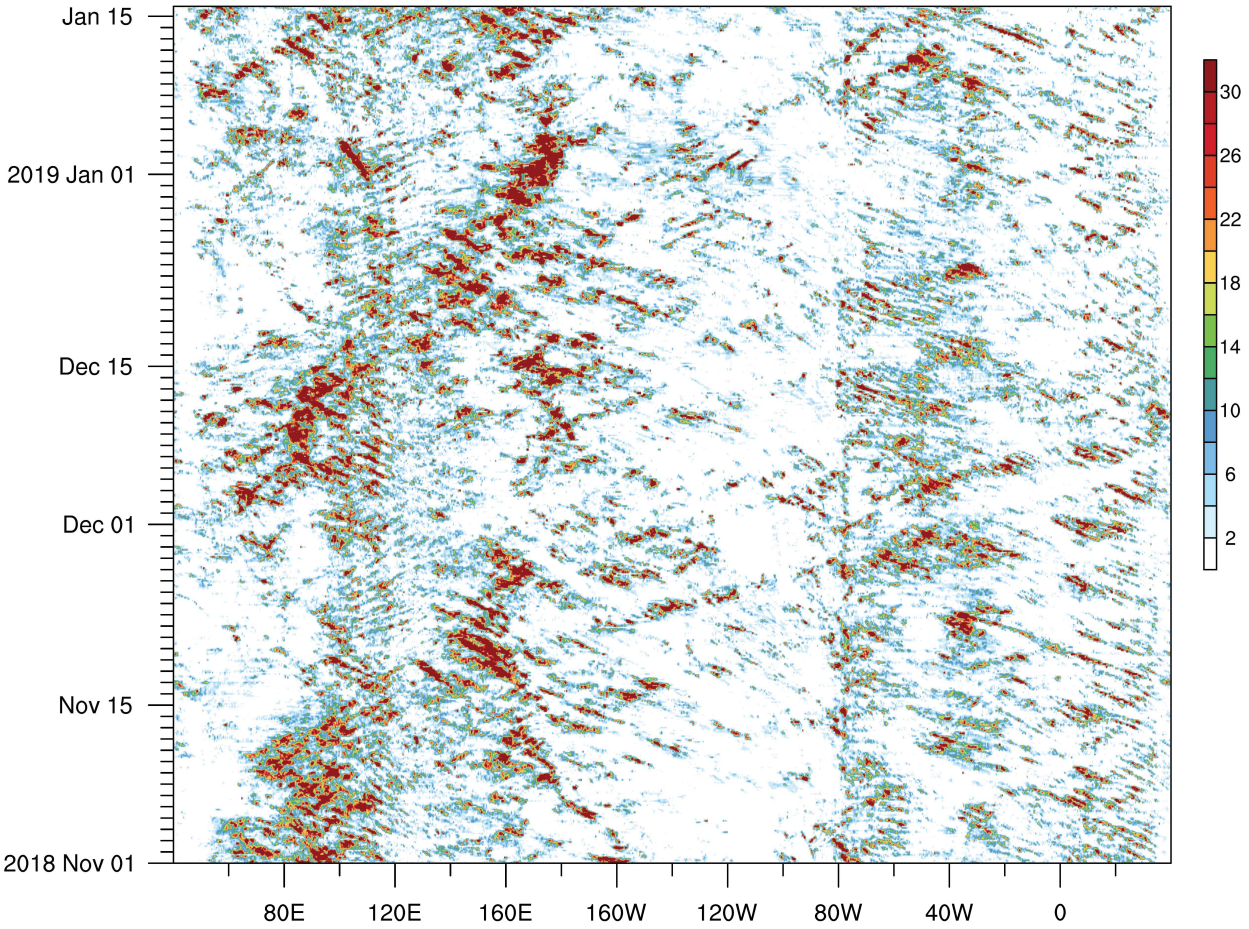


Figure 4. Time-longitude evolution of precipitation (mm day^{-1}; averaged from 5°S to 7.5°N) from 1 November 2018 through 15 January 2019. Precipitation data is based on the NASA Global Precipitation Measurement (GPM) 0.5-hourly the Integrated Multi-satellitE Retrievals for GPM (IMERG, version 6; Huffman et al., 2019) with horizontal resolution of 0.1 by 0.1 degree.

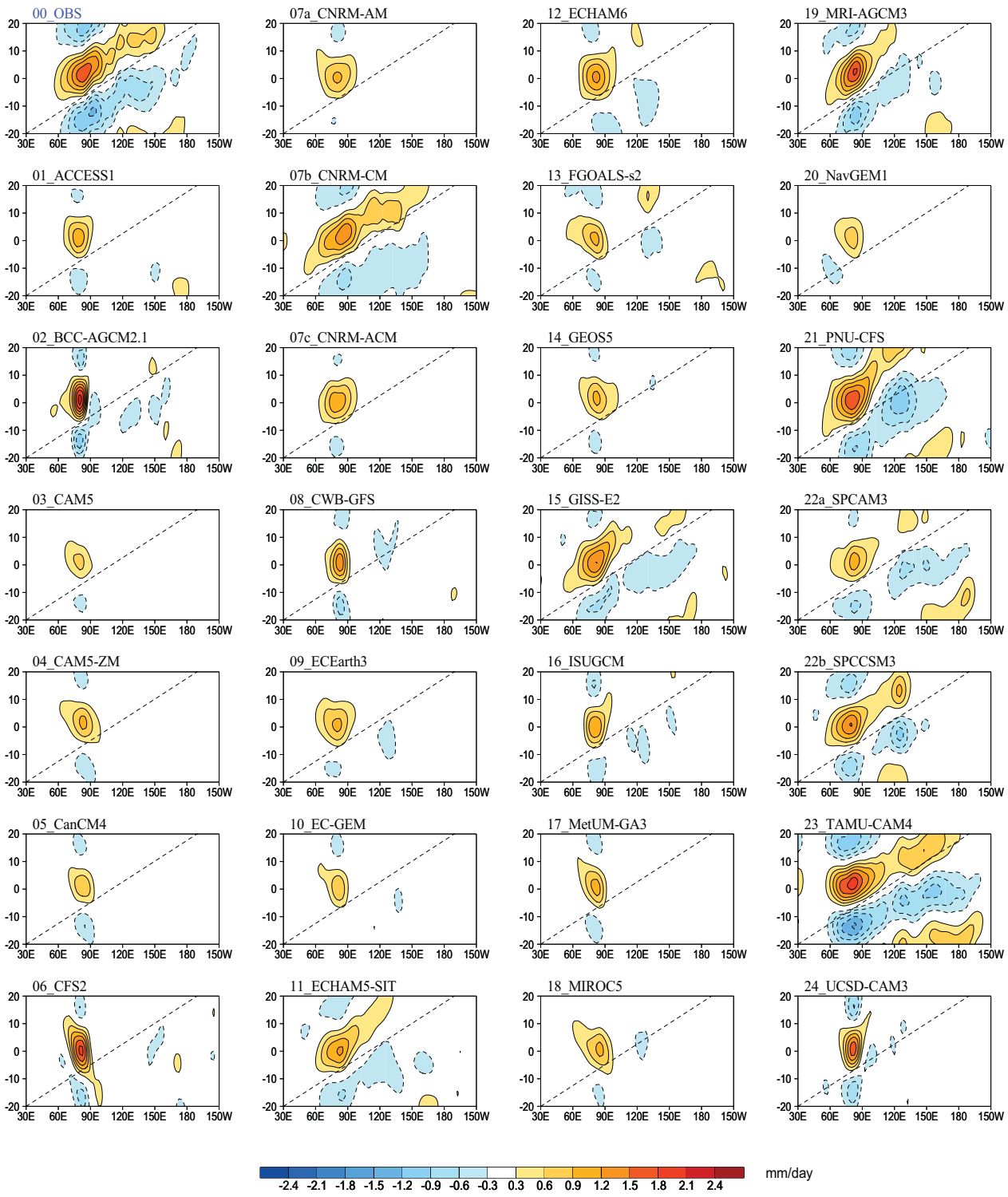


Figure 5. MJO propagation in GCMs participated in the MJOTF/GASS model comparison project represented by longitude-time evolution of rainfall anomalies (averaged over 10°S–10°N) based on lag-regression of 20-100-day filtered anomalous rainfall against itself averaged over the Eastern Indian Ocean (75–85°E; 5°S–5°N). Dashed lines in each panel denote the 5 m s^{-1} eastward propagation phase speed. Reproduced courtesy of the American Geophysical Union from Jiang et al. (2015).

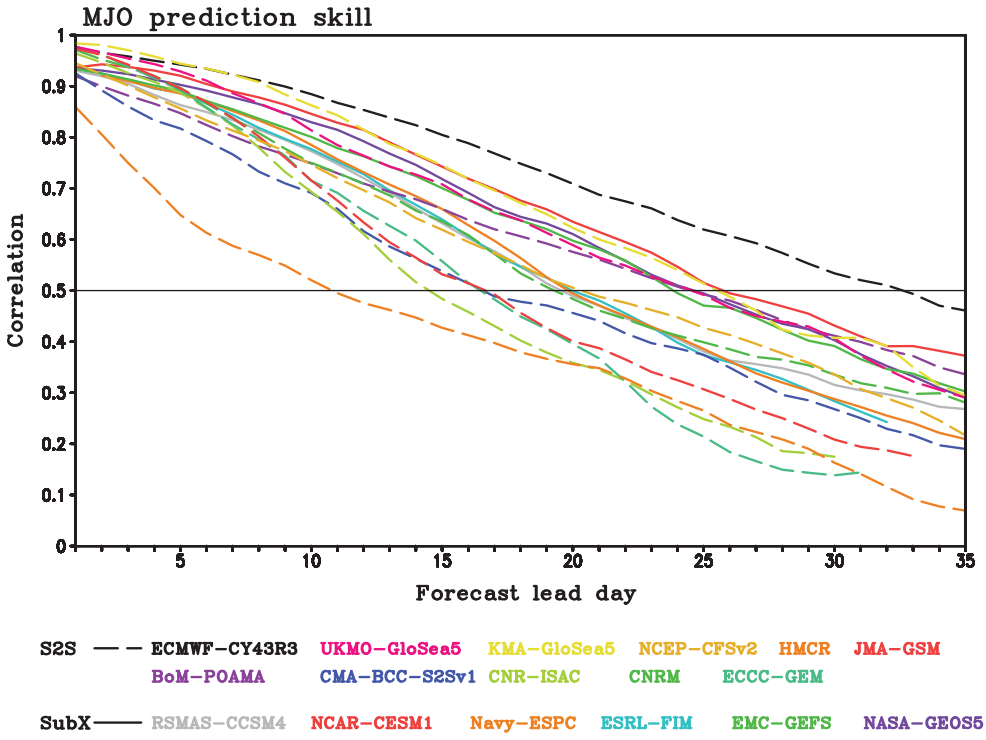


Figure 6. RMM prediction skill (bivariate correlation coefficient) for all days between the observation and ensemble means from S2S and SubX during Nov-March. Reforecasts are the same used in Lim et al. (2018) and Kim et al. (2019).

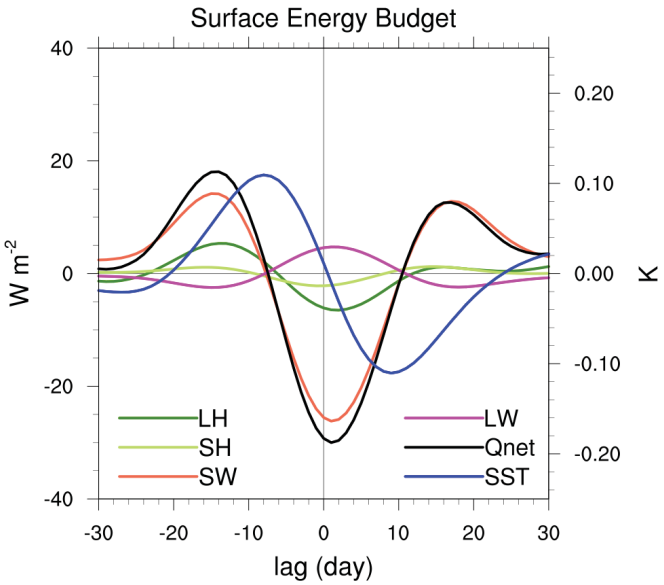


Figure 7. November through April composite surface energy budget terms obtained by regressing 1986-2013 ERA-Interim individual surface heating anomalies onto 20-100 day filtered rainfall averaged over the eastern Indian Ocean (10°S-10°N, 85°E-95°E). Surface net heating (black), net shortwave (orange) and longwave (magenta) radiative fluxes, and latent (dark green) and sensible (light green) heat fluxes are plotted so that a positive flux heats the ocean (all units are (W m^{-2})/(mm day^{-1}) of base point rainfall). The composite SST ((K)/(mm day^{-1}); blue) is plotted on the right axis. The typical MJO rainfall perturbation is about 3 mm day^{-1}. Day 0 corresponds to maximum MJO precipitation.

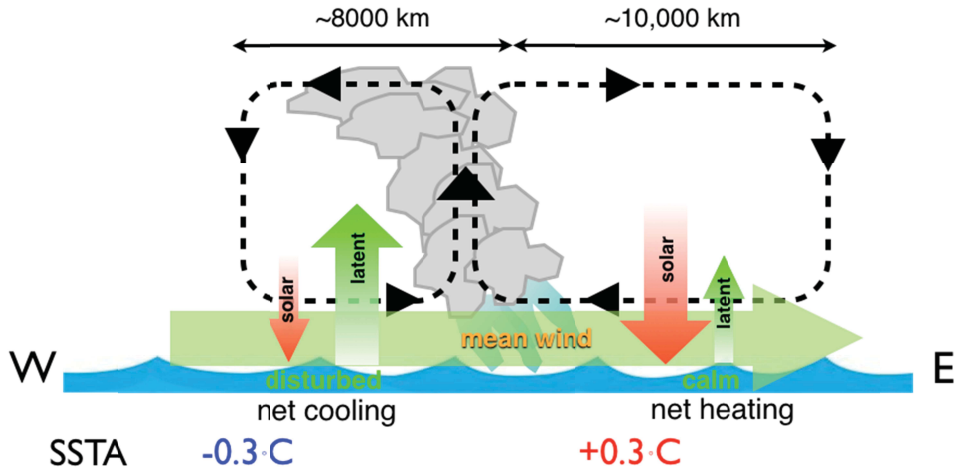


Figure 8. Schematic zonal cross section illustration of MJO convection, circulation anomalies (black dashed arrows) imposed upon Warm Pool mean low-level winds (green horizontal arrow), anomalous surface latent heat flux (green upward arrows) and net surface solar flux (red downward arrows). East (west) of MJO convection, reduced (enhanced) winds and enhanced (reduced) solar heating promote calm (disturbed) ocean conditions and ocean warming (cooling).

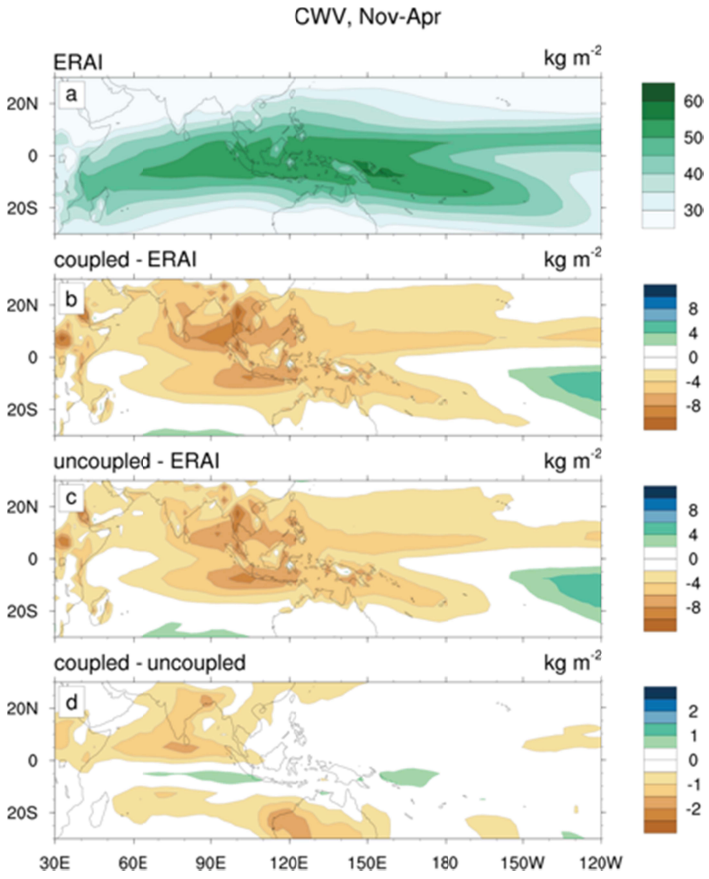


Figure 9. a) November through April 1986-2013 mean column water vapor (CWV; kg m^{-2}) from ERA-Interim. b) coupled and c) uncoupled multi-model ensemble bias, and d) coupled-uncoupled CWV mean state differences for the four models analyzed in DeMott et al. (2019).

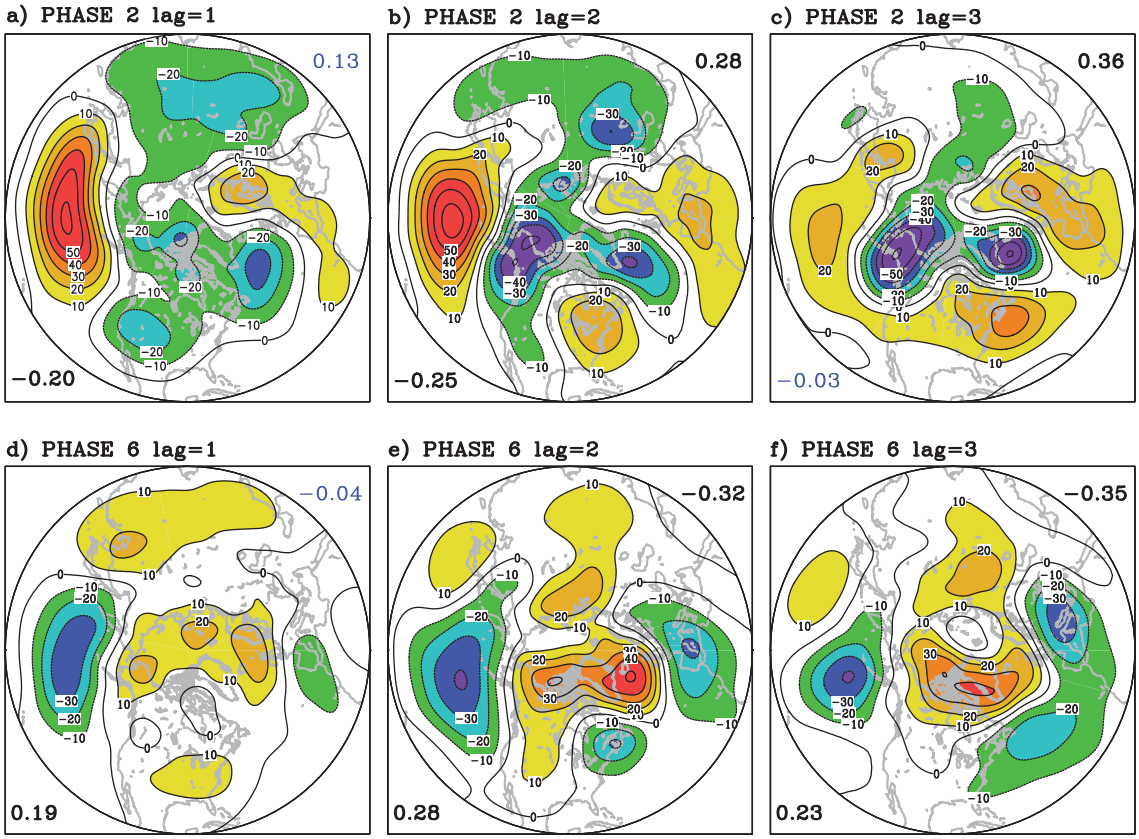


Figure 10. Lagged composites of 500-hPa geopotential height anomaly following MJO (a)-(c) phase 2 and (d)-(f) phase 6. Contour interval is 10 m. Lag=n means that the height anomaly lags the occurrence of MJO phase by n pentads. Detailed description of analysis method can be found in Lin et al. (2009). The number at the upper right (lower left) corner of each panel is the composite NAO (PNA) index which is calculated as projection to the NAO (PNA) pattern. Those in thick black font are different from zero at the 0.05 level according to a Student's t-test. 40 years of pentad data for extended winter from 1979/80 to 2018/19 are analyzed.

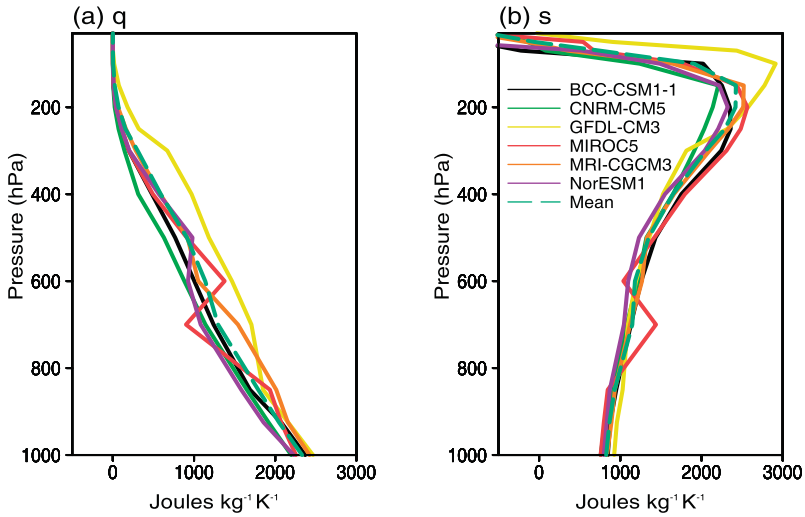


Figure 11. Changes as a function of pressure of November–April mean (a) specific humidity (q, multiplied by latent heat of condensation) and (b) dry static energy s in RCP8.5 (2081-2100) relative to the historical simulations (1986-2005) of five CMIP5 models. Fields are averaged over the warm pool from 10°S–0°, 90°E–180°. Units are J kg^{-1} K^{-1}. This figure originally found in Bui and Maloney (2019a). © American Meteorological Society. Used with permission.

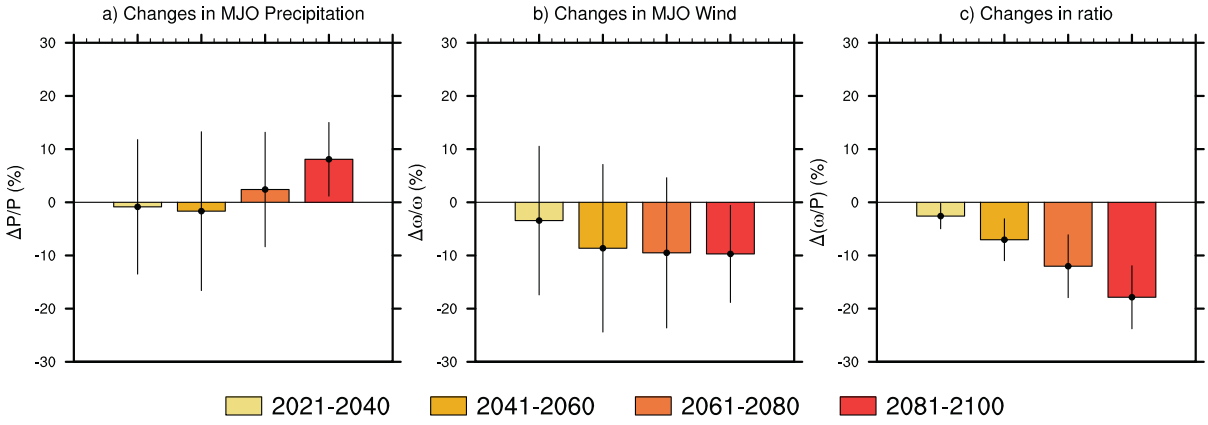


Figure 12. Multi-model mean fractional changes in (a) MJO precipitation and (b) 500 hPa omega amplitude, and (c) changes in the ratio between the two in different decades of the 21st Century relative to the historical simulation averaged over the warm pool region (15°S-15°N, 60°E-180). The bars represent the standard deviation across models. Units are %. Before averaging across the warm pool, amplitude is defined at each location as the root mean squared anomaly across all eight composite phases of the MJO defined according to Wheeler and Hendon (2004). Figure is reproduced courtesy of the American Geophysical Union from Bui and Maloney (2019b).

References

Abhik, S., and H. H. Hendon (2019), Influence of the QBO on the MJO During Coupled Model Multiweek Forecasts, *Geophys. Res. Lett.*, *46*, 10.1029/2019gl083152, 9213-9221.

Abhik, S., H. H. Hendon, and M. C. Wheeler (2019), On the Sensitivity of Convectively Coupled Equatorial Waves to the Quasi-Biennial Oscillation, *J. Clim.*, *32*, 10.1175/jcli-d-19-0010.1, 5833-5847.

Adames, Á. F., and J. M. Wallace (2014), Three-Dimensional Structure and Evolution of the Vertical Velocity and Divergence Fields in the MJO, *J. Atmos. Sci.*, *71*, 10.1175/jas-d-14-0091.1, 4661-4681.

Adames, Á. F., and J. M. Wallace (2015), Three-Dimensional Structure and Evolution of the Moisture Field in the MJO, *J. Atmos. Sci.*, *72*, doi:10.1175/JAS-D-15-0003.1, 3733-3754.

Adames, Á. F., and D. Kim (2016), The MJO as a Dispersive, Convectively Coupled Moisture Wave: Theory and Observations, *J. Atmos. Sci.*, *73*, doi:10.1175/JAS-D-15-0170.1, 913-941.

Adames, Á. F. (2017), Precipitation Budget of the Madden–Julian Oscillation, *J. Atmos. Sci.*, *74*, 10.1175/JAS-D-16-0242.1, 1799-1817.

Adames, Á. F., D. Kim, A. H. Sobel, A. Del Genio, and J. Wu (2017a), Changes in the structure and propagation of the MJO with increasing CO2, *Journal of Advances in Modeling Earth Systems*, *9*, 10.1002/2017MS000913, 1251-1268.

Adames, Á. F., D. Kim, A. H. Sobel, A. Del Genio, and J. Wu (2017b), Characterization of Moist Processes Associated With Changes in the Propagation of the MJO With Increasing CO2, *Journal of Advances in Modeling Earth Systems*, *9*, 10.1002/2017MS001040, 2946-2967.

Ahn, M.-S., D. Kim, K. R. Sperber, I.-S. Kang, E. Maloney, D. Waliser, and H. Hendon (2017), MJO simulation in CMIP5 climate models: MJO skill metrics and process-oriented diagnosis, *Climate Dyn.*10.1007/s00382-017-3558-4, 1-23.

Ahn, M.-S., D. Kim, S. Park, and Y.-G. Ham (2019), Do We Need to Parameterize Mesoscale Convective Organization to Mitigate the MJO-Mean State Trade-Off?, *Geophys. Res. Lett.*, *46*, 10.1029/2018gl080314, 2293-2301.

Ahn, M.-S., D. Kim, Y.-G. Ham, and S. Park (2020a), Role of Maritime Continent Land Convection on the Mean State and MJO Propagation, *J. Clim.*, *33*, 10.1175/jcli-d-19-0342.1, 1659-1675.

Ahn, M.-S., D. Kim, D. Kang, J. Lee, K. R. Sperber, P. J. Glecker, X. Jiang, Y.-G. Ham, and H. Kim (2020b), MJO Propagation across the Maritime Continent: Are CMIP6 Models Better than CMIP5 Models?, *Geophys Res Lett*.

Aiyyer, A., and J. Molinari (2008), MJO and Tropical Cyclogenesis in the Gulf of Mexico and Eastern Pacific: Case Study and Idealized Numerical Modeling, *J. Atmos. Sci.*, *65*, 2691-2704.

Allen, M. R., and W. J. Ingram (2002), Constraints on future changes in climate and the hydrologic cycle, *Nature*, *419*, 10.1038/nature01092, 228-232.

2443 Alvarez, M. S., C. S. Vera, G. N. Kiladis, and B. Liebmann (2016), Influence of the Madden Julian
2444 Oscillation on precipitation and surface air temperature in South America, *Climate Dyn.*, *46*,
2445 10.1007/s00382-015-2581-6, 245-262.
2446 Andersen, J. A., and Z. Kuang (2012), Moist Static Energy Budget of MJO-like Disturbances in the
2447 Atmosphere of a Zonally Symmetric Aquaplanet, *J. Clim.*, *25*, 10.1175/jcli-d-11-00168.1, 2782-2804.
2448 Anderson, S. P., R. A. Weller, and R. B. Lukas (1996), Surface Buoyancy Forcing and the Mixed Layer of
2449 the Western Pacific Warm Pool: Observations and 1D Model Results, *J. Clim.*, *9*, 10.1175/1520-
2450 0442(1996)009<3056:SBFATM>2.0.CO;2, 3056-3085.
2451 Arnold, N. P., Z. Kuang, and E. Tziperman (2013), Enhanced MJO-like Variability at High SST, *J. Clim.*,
2452 *26*, 10.1175/jcli-d-12-00272.1, 988-1001.
2453 Arnold, N. P., M. Branson, Z. Kuang, D. A. Randall, and E. Tziperman (2015), MJO Intensification with
2454 Warming in the Superparameterized CESM, *J. Clim.*, *28*, 10.1175/jcli-d-14-00494.1, 2706-2724.
2455 Arnold, N. P., and D. A. Randall (2015), Global-scale convective aggregation: Implications for the Madden-
2456 Julian Oscillation, *Journal of Advances in Modeling Earth Systems*, *7*, 10.1002/2015MS000498, 1499-
2457 1518.
2458 Baggett, C. F., E. A. Barnes, E. D. Maloney, and B. D. Mundhenk (2017), Advancing atmospheric river
2459 forecasts into subseasonal-to-seasonal time scales, *Geophys. Res. Lett.*, *44*, 10.1002/2017GL074434,
2460 7528-7536.
2461 Baggett, C. F., K. M. Nardi, S. J. Childs, S. N. Zito, E. A. Barnes, and E. D. Maloney (2018), Skillful
2462 Subseasonal Forecasts of Weekly Tornado and Hail Activity Using the Madden-Julian Oscillation,
2463 *Journal of Geophysical Research: Atmospheres*, *123*, 10.1029/2018JD029059, 12,661-612,675.
2464 Baldwin, M. P., and T. J. Dunkerton (2001), Stratospheric Harbingers of Anomalous Weather Regimes,
2465 *Science*, *294*, 10.1126/science.1063315, 581.
2466 Baldwin, M. P., L. J. Gray, T. J. Dunkerton, K. Hamilton, P. H. Haynes, W. J. Randel, J. R. Holton, M. J.
2467 Alexander, I. Hirota, T. Horinouchi, D. B. A. Jones, J. S. Kinnersley, C. Marquardt, K. Sato, and M.
2468 Takahashi (2001), The quasi-biennial oscillation, *Rev. Geophys.*, *39*, 10.1029/1999RG000073, 179-229.
2469 Baranowski, D. B., M. K. Flatau, P. J. Flatau, and A. J. Matthews (2016), Phase locking between
2470 atmospheric convectively coupled equatorial Kelvin waves and the diurnal cycle of precipitation over the
2471 Maritime Continent, *Geophys. Res. Lett.*, *43*, 10.1002/2016GL069602, 8269-8276.
2472 Baranowski, D. B., D. E. Waliser, X. Jiang, J. A. Ridout, and M. K. Flatau (2019), Contemporary GCM
2473 Fidelity in Representing the Diurnal Cycle of Precipitation Over the Maritime Continent, *Journal of*
2474 *Geophysical Research: Atmospheres*, *124*, 10.1029/2018JD029474, 747-769.
2475 Barnes, E. A., S. M. Samarasinghe, I. Ebert-Uphoff, and J. C. Furtado (2019), Tropospheric and
2476 Stratospheric Causal Pathways Between the MJO and NAO, *Journal of Geophysical Research:*
2477 *Atmospheres*, *124*, 10.1029/2019JD031024, 9356-9371.

2478 Barnes, H. C., and R. A. Houze (2013), The precipitating cloud population of the Madden-Julian Oscillation
2479 over the Indian and west Pacific Oceans, *Journal of Geophysical Research: Atmospheres*10.1002/jgrd.50375, n/a-n/a.
2481 Barnes, H. C., and R. A. Houze (2014), Precipitation hydrometeor type relative to the mesoscale airflow in
2482 mature oceanic deep convection of the Madden-Julian Oscillation, *Journal of Geophysical Research: Atmospheres*, *119*, 10.1002/2014JD022241, 13,990-914,014.
2484 Barrett, B. S., J. F. Carrasco, and A. P. Testino (2011), Madden–Julian Oscillation (MJO) Modulation of
2485 Atmospheric Circulation and Chilean Winter Precipitation, *J. Clim.*, *25*, 10.1175/JCLI-D-11-00216.1,
2486 1678-1688.
2487 Barrett, B. S., and V. A. Gensini (2013), Variability of central United States April–May tornado day
2488 likelihood by phase of the Madden-Julian Oscillation, *Geophys. Res. Lett.*, *40*, 10.1002/grl.50522, 2790-
2489 2795.
2490 Baxter, S., S. Weaver, J. Gottschalck, and Y. Xue (2014), Pentad Evolution of Wintertime Impacts of the
2491 Madden–Julian Oscillation over the Contiguous United States, *J. Clim.*, *27*, 10.1175/jcli-d-14-00105.1,
2492 7356-7367.
2493 Bechtold, P., M. Kohler, T. Jung, F. Doblas-Reyes, M. Leutbecher, M. J. Rodwell, F. Vitart, and G. Balsamo
2494 (2008), Advances in simulating atmospheric variability with the ECMWF model: From synoptic to
2495 decadal time-scales, *Quart. J. Roy. Meteor. Soc.*, *134*, Doi 10.1002/Qj.289, 1337-1351.
2496 Becker, E. J., E. H. Berbery, and R. W. Higgins (2011), Modulation of Cold-Season U.S. Daily Precipitation
2497 by the Madden–Julian Oscillation, *J. Clim.*, *24*, 10.1175/2011JCLI4018.1, 5157-5166.
2498 Bellenger, H., and J. P. Duvel (2009), An Analysis of Tropical Ocean Diurnal Warm Layers, *J. Clim.*, *22*,
2499 Doi 10.1175/2008jcli2598.1, 3629-3646.
2500 Bellenger, H., and J. P. Duvel (2012), The event-to-event variability of the boreal winter MJO, *Geophys. Res. Lett.*, *39*, 10.1029/2012GL051294, n/a-n/a.
2502 Bellenger, H., M. Katsumata, and K. Yoneyama (2015a), Turbulent mixing and its impact on lower
2503 tropospheric moisture over tropical ocean, *Geophys. Res. Lett.*, *42*, 10.1002/2015GL063868, 3030-3037.
2504 Bellenger, H., K. Yoneyama, M. Katsumata, T. Nishizawa, K. Yasunaga, and R. Shirooka (2015b),
2505 Observation of Moisture Tendencies Related to Shallow Convection, *J. Atmos. Sci.*, *72*, 10.1175/jas-d-14-
2506 0042.1, 641-659.
2507 Benedict, J. J., and D. A. Randall (2007), Observed Characteristics of the MJO Relative to Maximum
2508 Rainfall, *J. Atmos. Sci.*, *64*, 2332-2354.
2509 Benedict, J. J., and D. A. Randall (2009), Structure of the Madden-Julian Oscillation in the
2510 Superparameterized CAM, *J. Atmos. Sci.*, *66*, 3277-3296.

2511 Benedict, J. J., and D. A. Randall (2011), Impacts of Idealized Air–Sea Coupling on Madden–Julian
2512 Oscillation Structure in the Superparameterized CAM, *J. Atmos. Sci.*, *68*, 10.1175/JAS-D-11-04.1, 1990-
2513 2008.
2514 Benedict, J. J., E. D. Maloney, A. H. Sobel, and D. M. W. Frierson (2014), Gross Moist Stability and MJO
2515 Simulation Skill in Three Full-Physics GCMs, *J. Atmos. Sci.*, *71*, 10.1175/JAS-D-13-0240.1, 3327-3349.
2516 Benedict, J. J., M. S. Pritchard, and W. D. Collins (2015), Sensitivity of MJO propagation to a robust
2517 positive Indian Ocean dipole event in the superparameterized CAM, *Journal of Advances in Modeling*
2518 *Earth Systems*, *7*, 10.1002/2015MS000530, 1901-1917.
2519 Berg, W., T. L'Ecuyer, and J. M. Haynes (2010), The Distribution of Rainfall over Oceans from Spaceborne
2520 Radars, *Journal of Applied Meteorology and Climatology*, *49*, Doi 10.1175/2009jamc2330.1, 535-543.
2521 Bernie, D. J., S. J. Woolnough, J. M. Slingo, and E. Guilyardi (2005), Modeling diurnal and intraseasonal
2522 variability of the ocean mixed layer, *J. Clim.*, *18*, Doi 10.1175/Jcli3319.1, 1190-1202.
2523 Bessafi, M., and M. C. Wheeler (2006), Modulation of south Indian ocean tropical cyclones by the Madden-
2524 Julian oscillation and convectively coupled equatorial waves, *Mon. Weather Rev.*, *134*, 638-656.
2525 Biello, J. A., and A. J. Majda (2005), A new multiscale model for the Madden-Julian oscillation, *J. Atmos.*
2526 *Sci.*, *62*, 1694-1721.
2527 Birch, C. E., S. Webster, S. C. Peatman, D. J. Parker, A. J. Matthews, Y. Li, and M. E. E. Hassim (2016),
2528 Scale Interactions between the MJO and the Western Maritime Continent, *J. Clim.*, *29*, doi:10.1175/JCLI-
2529 D-15-0557.1, 2471-2492.
2530 Bond, N. A., and G. A. Vecchi (2003), The Influence of the Madden–Julian Oscillation on Precipitation in
2531 Oregon and Washington*, *Weather Forecasting*, *18*, 10.1175/1520-0434, 600-613.
2532 Bony, S., B. Stevens, D. M. W. Frierson, C. Jakob, M. Kageyama, R. Pincus, T. G. Shepherd, S. C.
2533 Sherwood, A. P. Siebesma, A. H. Sobel, M. Watanabe, and M. J. Webb (2015), Clouds, circulation and
2534 climate sensitivity, *Nature Geoscience*, *8*, 10.1038/ngeo2398, 261.
2535 Branstator, G. (1985), Analysis of General Circulation Model Sea-Surface Temperature Anomaly
2536 Simulations Using a Linear Model. Part I: Forced Solutions, *J. Atmos. Sci.*, *42*, 10.1175/1520-
2537 0469(1985)042<2225:AOGCMS>2.0.CO;2, 2225-2241.
2538 Brenowitz, N. D., and C. S. Bretherton (2018), Prognostic Validation of a Neural Network Unified Physics
2539 Parameterization, *Geophys. Res. Lett.*, *45*, 10.1029/2018gl078510, 6289-6298.
2540 Bretherton, C. S., M. E. Peters, and L. E. Back (2004), Relationships between water vapor path and
2541 precipitation over the tropical oceans, *J. Clim.*, *17*, 1517-1528.
2542 Bui, H. X., and E. D. Maloney (2018), Changes in Madden-Julian Oscillation Precipitation and Wind
2543 Variance Under Global Warming, *Geophys. Res. Lett.*, *45*, 10.1029/2018GL078504, 7148-7155.
2544 Bui, H. X., and E. D. Maloney (2019a), Mechanisms for Global Warming Impacts on Madden–Julian
2545 Oscillation Precipitation Amplitude, *J. Clim.*, *32*, 10.1175/jcli-d-19-0051.1, 6961-6975.

2546 Bui, H. X., and E. D. Maloney (2019b), Transient Response of MJO Precipitation and Circulation to
2547 Greenhouse Gas Forcing, *Geophys. Res. Lett.*, *46*, 10.1029/2019GL085328, 13546-13555.
2548 Buizza, R., M. Milleer, and T. N. Palmer (1999), Stochastic representation of model uncertainties in the
2549 ECMWF ensemble prediction system, *Quart. J. Roy. Meteor. Soc.*, *125*, 10.1002/qj.49712556006, 2887-
2550 2908.
2551 Caballero, R., and M. Huber (2010), Spontaneous transition to superrotation in warm climates simulated by
2552 CAM3, *Geophys. Res. Lett.*, *37*, 10.1029/2010GL043468, n/a-n/a.
2553 Carlson, H., and R. Caballero (2016), Enhanced MJO and transition to superrotation in warm climates,
2554 *Journal of Advances in Modeling Earth Systems*, *8*, 10.1002/2015MS000615, 304-318.
2555 Cassou, C. (2008), Intraseasonal interaction between the Madden-Julian Oscillation and the North Atlantic
2556 Oscillation, *Nature*, *455*, 523-527.
2557 Chang, C.-H., and N. C. Johnson (2015), The Continuum of Wintertime Southern Hemisphere Atmospheric
2558 Teleconnection Patterns, *J. Clim.*, *28*, 10.1175/JCLI-D-14-00739.1, 9507-9529.
2559 Chang, C.-P., and H. Lim (1988), Kelvin Wave-CISK: A Possible Mechanism for the 30-50 Day
2560 Oscillations, *J. Atmos. Sci.*, *45*, 1709-1720.
2561 Chang, C.-W. J., W.-L. Tseng, H.-H. Hsu, N. Keenlyside, and B.-J. Tsuang (2015), The Madden-Julian
2562 Oscillation in a warmer world, *Geophys. Res. Lett.*, *42*, 10.1002/2015GL065095, 6034-6042.
2563 Chang, C. P. (1977), Viscous Internal Gravity-Waves and Low-Frequency Oscillations in the Tropics, *J.*
2564 *Atmos. Sci.*, *34*, 901-910.
2565 Chao, W. C., and B. Chen (2001), The Role of Surface Friction in Tropical Intraseasonal Oscillation, *Mon.*
2566 *Weather Rev.*, *129*, 10.1175/1520-0493(2001)129<0896:TROSFI>2.0.CO;2, 896-904.
2567 Chen, B., and B. E. Mapes (2018), Effects of a Simple Convective Organization Scheme in a Two-Plume
2568 GCM, *Journal of Advances in Modeling Earth Systems*, *10*, 10.1002/2017MS001106, 867-880.
2569 Chen, G., and B. Wang (2017), Reexamination of the Wave Activity Envelope Convective Scheme in
2570 Theoretical Modeling of MJO, *J. Clim.*, *30*, 10.1175/JCLI-D-16-0325.1, 1127-1138.
2571 Chen, G., and B. Wang (2018a), Does the MJO Have a Westward Group Velocity?, *J. Clim.*, *31*,
2572 10.1175/JCLI-D-17-0446.1, 2435-2443.
2573 Chen, G., and B. Wang (2018b), Effects of Enhanced Front Walker Cell on the Eastward Propagation of the
2574 MJO, *J. Clim.*, *31*, 10.1175/jcli-d-17-0383.1, 7719-7738.
2575 Chen, S. S., and R. A. Houze (1997), Diurnal variation and life-cycle of deep convective systems over the
2576 Tropical Pacific warm pool, *Quart. J. Roy. Meteor. Soc.*, *123*, DOI 10.1002/qj.49712353806, 357-388.
2577 Chen, S. S., B. W. Kerns, N. Guy, D. P. Jorgensen, J. Delanoë, N. Viltard, C. J. Zappa, F. Judt, C.-Y. Lee,
2578 and A. Savarin (2016), Aircraft Observations of Dry Air, the ITCZ, Convective Cloud Systems, and Cold
2579 Pools in MJO during DYNAMO, *97*, 10.1175/bams-d-13-00196.1, 405-423.

2580 Chen, Y., and A. D. Del Genio (2009a), Evaluation of tropical cloud regimes in observations and a general
2581 circulation model, *Climate Dyn.*, *32*, 10.1007/s00382-008-0386-6, 355-369.
2582 Chen, Y. H., and A. D. Del Genio (2009b), Evaluation of tropical cloud regimes in observations and a
2583 general circulation model, *Climate Dyn.*, *32*, doi:10.1007/S00382-008-0386-6, 355-369.
2584 Chi, N.-H., R.-C. Lien, E. A. D'Asaro, and B. B. Ma (2014), The surface mixed layer heat budget from
2585 mooring observations in the central Indian Ocean during Madden–Julian Oscillation events, *Journal of*
2586 *Geophysical Research: Oceans*, *119*, 10.1002/2014JC010192, 4638-4652.
2587 Chikira, M., and M. Sugiyama (2010), A Cumulus Parameterization with State-Dependent Entrainment Rate.
2588 Part I: Description and Sensitivity to Temperature and Humidity Profiles, *J. Atmos. Sci.*, *67*, Doi
2589 10.1175/2010jas3316.1, 2171-2193.
2590 Chikira, M. (2014), Eastward-Propagating Intraseasonal Oscillation Represented by Chikira–Sugiyama
2591 Cumulus Parameterization. Part II: Understanding Moisture Variation under Weak Temperature Gradient
2592 Balance, *J. Atmos. Sci.*, *71*, 10.1175/JAS-D-13-038.1, 615-639.
2593 Ciesielski, P. E., R. H. Johnson, X. Jiang, Y. Zhang, and S. Xie (2017), Relationships Between Radiation,
2594 Clouds, and Convection During DYNAMO, *Journal of Geophysical Research:*
2595 *Atmospheres*10.1002/2016JD025965.
2596 Coats, S., and K. B. Karnauskas (2017), Are Simulated and Observed Twentieth Century Tropical Pacific
2597 Sea Surface Temperature Trends Significant Relative to Internal Variability?, *Geophys. Res. Lett.*, *44*,
2598 10.1002/2017GL074622, 9928-9937.
2599 Collimore, C. C., D. W. Martin, M. H. Hitchman, A. Huesmann, and D. Waliser (2003), On The
2600 Relationship between the QBO and Tropical Deep Convection, *J. Clim.*, *16*, 10.1175/1520-
2601 0442(2003)016<2552:otrbtq>2.0.co;2, 2552-2568.
2602 Crueger, T., B. Stevens, and R. Brokopf (2013), The Madden–Julian Oscillation in ECHAM6 and the
2603 Introduction of an Objective MJO Metric, *J. Clim.*, *26*, 10.1175/jcli-d-12-00413.1, 3241-3257.
2604 de Szoeke, S. P., J. B. Edson, J. R. Marion, C. W. Fairall, and L. Bariteau (2015), The MJO and Air–Sea
2605 Interaction in TOGA COARE and DYNAMO, *J. Clim.*, *28*, 10.1175/jcli-d-14-00477.1, 597-622.
2606 de Szoeke, S. P., E. D. Skyllingstad, P. Zuidema, and A. S. Chandra (2017), Cold Pools and Their Influence
2607 on the Tropical Marine Boundary Layer, *J. Atmos. Sci.*, *74*, 10.1175/jas-d-16-0264.1, 1149-1168.
2608 de Szoeke, S. P. (2018), Variations of the Moist Static Energy Budget of the Tropical Indian Ocean
2609 Atmospheric Boundary Layer, *J. Atmos. Sci.*, *75*, 10.1175/jas-d-17-0345.1, 1545-1551.
2610 Dee, D. P., S. M. Uppala, A. J. Simmons, P. Berrisford, P. Poli, S. Kobayashi, U. Andrae, M. A. Balmaseda,
2611 G. Balsamo, P. Bauer, P. Bechtold, A. C. M. Beljaars, L. van de Berg, J. Bidlot, N. Bormann, C. Delsol,
2612 R. Dragani, M. Fuentes, A. J. Geer, L. Haimberger, S. B. Healy, H. Hersbach, E. V. Hólm, L. Isaksen, P.
2613 Kållberg, M. Köhler, M. Matricardi, A. P. McNally, B. M. Monge-Sanz, J. J. Morcrette, B. K. Park, C.
2614 Peubey, P. de Rosnay, C. Tavolato, J. N. Thépaut, and F. Vitart (2011), The ERA-Interim reanalysis:

configuration and performance of the data assimilation system, *Quart. J. Roy. Meteor. Soc.*, *137*, 10.1002/qj.828, 553-597.

DeFlorio, M. J., D. E. Waliser, B. Guan, F. M. Ralph, and F. Vitart (2019), Global evaluation of atmospheric river subseasonal prediction skill, *Climate Dyn.*, *52*, 10.1007/s00382-018-4309-x, 3039-3060.

Del Genio, A. D. (2012), Representing the Sensitivity of Convective Cloud Systems to Tropospheric Humidity in General Circulation Models, *Surveys in Geophysics*, *33*, 10.1007/s10712-011-9148-9, 637-656.

Del Genio, A. D., Y. Chen, D. Kim, and M.-S. Yao (2012), The MJO Transition from Shallow to Deep Convection in CloudSat/CALIPSO Data and GISS GCM Simulations, *J. Clim.*, *25*, 10.1175/JCLI-D-11-00384.1, 3755-3770.

Del Genio, A. D., and Y. Chen (2015), Cloud-radiative driving of the Madden-Julian oscillation as seen by the A-Train, *Journal of Geophysical Research: Atmospheres*, *120*, 10.1002/2015JD023278, 5344-5356.

DeMott, C. A., C. Stan, D. A. Randall, and M. D. Branson (2014), Intraseasonal Variability in Coupled GCMs: The Roles of Ocean Feedbacks and Model Physics, *J. Clim.*, *27*, doi:10.1175/JCLI-D-13-00760.1, 4970-4995.

DeMott, C. A., N. P. Klingaman, and S. J. Woolnough (2015), Atmosphere-ocean coupled processes in the Madden-Julian oscillation, *Rev. Geophys.*10.1002/2014RG000478, n/a-n/a.

DeMott, C. A., J. J. Benedict, N. P. Klingaman, S. J. Woolnough, and D. A. Randall (2016), Diagnosing ocean feedbacks to the MJO: SST-modulated surface fluxes and the moist static energy budget, *Journal of Geophysical Research: Atmospheres*, *121*, 10.1002/2016JD025098, 8350-8373.

DeMott, C. A., B. O. Wolding, E. D. Maloney, and D. A. Randall (2018), Atmospheric Mechanisms for MJO Decay Over the Maritime Continent, *Journal of Geophysical Research: Atmospheres*, *123*, 10.1029/2017jd026979, 5188-5204.

DeMott, C. A., N. P. Klingaman, W.-L. Tseng, M. A. Burt, Y. Gao, and D. A. Randall (2019), The convection connection: How ocean feedbacks affect tropical mean moisture and MJO propagation, *Journal of Geophysical Research: Atmospheres*, *n/a*, 10.1029/2019JD031015.

Deng, L., and X. Wu (2010), Effects of Convective Processes on GCM Simulations of the Madden–Julian Oscillation, *J. Clim.*, *23*, 10.1175/2009jcli3114.1, 352-377.

Deng, L., and X. Wu (2011), Physical Mechanisms for the Maintenance of GCM-Simulated Madden–Julian Oscillation over the Indian Ocean and Pacific, *J. Clim.*, *24*, 10.1175/2010JCLI3759.1, 2469-2482.

Deng, Q., B. Khouider, and A. J. Majda (2015), The MJO in a Coarse-Resolution GCM with a Stochastic Multicloud Parameterization, *J. Atmos. Sci.*, *72*, 10.1175/jas-d-14-0120.1, 55-74.

Deng, Q., B. Khouider, A. J. Majda, and R. S. Ajayamohan (2016), Effect of Stratiform Heating on the Planetary-Scale Organization of Tropical Convection, *J. Atmos. Sci.*, *73*, 10.1175/jas-d-15-0178.1, 371-392.

Densmore, C. R., E. R. Sanabia, and B. S. Barrett (2019), QBO Influence on MJO Amplitude over the Maritime Continent: Physical Mechanisms and Seasonality, *Mon. Weather Rev.*, *147*, 10.1175/mwr-d-18-0158.1, 389-406.

DePasquale, A., C. Schumacher, and A. Rapp (2014), Radar observations of MJO and Kelvin wave interactions during DYNAMO/CINDY2011/AMIE, *Journal of Geophysical Research: Atmospheres*, *119*, 10.1002/2013JD021031, 6347-6367.

Derbyshire, S. H., I. Beau, P. Bechtold, J.-Y. Grandpeix, J.-M. Piriou, J.-L. Redelsperger, and P. M. M. Soares (2004), Sensitivity of moist convection to environmental humidity, *Quart. J. Roy. Meteor. Soc.*, *130*, 3055-3079.

Deser, C., and A. S. Phillips (2009), Atmospheric Circulation Trends, 1950–2000: The Relative Roles of Sea Surface Temperature Forcing and Direct Atmospheric Radiative Forcing, *J. Clim.*, *22*, 10.1175/2008jcli2453.1, 396-413.

DeWitt, L. H., D. J. Coffman, K. J. Schulz, W. Alan Brewer, T. S. Bates, and P. K. Quinn (2013), Atmospheric aerosol properties over the equatorial Indian Ocean and the impact of the Madden-Julian Oscillation, *Journal of Geophysical Research: Atmospheres*, *118*, 10.1002/jgrd.50419, 5736-5749.

Dias, J., S. Leroux, S. N. Tulich, and G. N. Kiladis (2013), How systematic is organized tropical convection within the MJO?, *Geophys. Res. Lett.*, *40*, 10.1002/grl.50308, 1420-1425.

Dias, J., N. Sakaeda, G. N. Kiladis, and K. Kikuchi (2017), Influences of the MJO on the space-time organization of tropical convection, *Journal of Geophysical Research: Atmospheres*, *122*, 10.1002/2017JD026526, 8012-8032.

Ding, R. Q., J. P. Li, and K. H. Seo (2010), Predictability of the Madden-Julian Oscillation Estimated Using Observational Data, *Mon. Weather Rev.*, *138*, Doi 10.1175/2009mwr3082.1, 1004-1013.

Donald, A., H. Meinke, B. Power, A. d. H. N. Maia, M. C. Wheeler, N. White, R. C. Stone, and J. Ribbe (2006), Near-global impact of the Madden-Julian Oscillation on rainfall, *Geophys. Res. Lett.*, *33*, 10.1029/2005GL025155, n/a-n/a.

Drushka, K., J. Sprintall, S. T. Gille, and S. Wijffels (2012), In Situ Observations of Madden–Julian Oscillation Mixed Layer Dynamics in the Indian and Western Pacific Oceans, *J. Clim.*, *25*, 10.1175/jcli-d-11-00203.1, 2306-2328.

Drushka, K., W. E. Asher, B. Ward, and K. Walesby (2016), Understanding the formation and evolution of rain-formed fresh lenses at the ocean surface, *Journal of Geophysical Research: Oceans*, *121*, 10.1002/2015JC011527, 2673-2689.

Dubey, S., T. N. Krishnamurti, and V. Kumar (2018), On scale interactions between the MJO and synoptic scale, *Quart. J. Roy. Meteor. Soc.*, *144*, 10.1002/qj.3400, 2727-2747.

Emanuel, K. (2019), Inferences from Simple Models of Slow, Convectively Coupled Processes, *J. Atmos. Sci.*, *76*, 10.1175/JAS-D-18-0090.1, 195-208.

Emanuel, K. A. (1987), An Air-Sea Interaction-Model of Intraseasonal Oscillations in the Tropics, *J. Atmos. Sci.*, *44*, 2324-2340.

Emanuel, K. A. (1991), A Scheme for Representing Cumulus Convection in Large-Scale Models, *J. Atmos. Sci.*, *48*, 10.1175/1520-0469(1991)048<2313:ASFRCC>2.0.CO;2, 2313-2329.

Emanuel, K. A. (1995), The Behavior of a Simple Hurricane Model Using a Convective Scheme Based on Subcloud-Layer Entropy Equilibrium, *J. Atmos. Sci.*, *52*, 10.1175/1520-0469(1995)052<3960:TBOASH>2.0.CO;2, 3960-3968.

Fauchereau, N., B. Pohl, and A. Lorrey (2016), Extra-tropical impacts of the Madden-Julian Oscillation over New Zealand from a weather regime perspective, *J. Clim.*, *29*, 10.1175/JCLI-D-15-0152.1, 2161-2175.

Feng, J., T. Li, and W. Zhu (2015a), Propagating and Nonpropagating MJO Events over Maritime Continent, *J. Clim.*, *28*, 10.1175/JCLI-D-15-0085.1, 8430-8449.

Feng, J., P. Liu, W. Chen, and X. Wang (2015b), Contrasting Madden–Julian Oscillation activity during various stages of EP and CP El Niños, *Atmospheric Science Letters*, *16*, 10.1002/asl2.516, 32-37.

Feng, P.-N., and H. Lin (2019), Modulation of the MJO-Related Teleconnections by the QBO, *Journal of Geophysical Research: Atmospheres*, *124*, 10.1029/2019jd030878, 12022-12033.

Ferranti, L., T. N. Palmer, F. Molteni, and E. Klinker (1990), Tropical-Extratropical Interaction Associated with the 30-60 Day Oscillation and Its Impact on Medium and Extended Range Prediction, *J. Atmos. Sci.*, *47*, 2177-2199.

Flatau, M., and Y.-J. Kim (2013), Interaction between the MJO and Polar Circulations, *J. Clim.*, *26*, 10.1175/jcli-d-11-00508.1, 3562-3574.

Franzke, C., S. Lee, and S. Feldstein (2004), Is the North Atlantic Oscillation a Breaking Wave, *J. Atmos. Sci.*, *61*, 10.1175/1520-0469(2004)061<0145:ITNAOA>2.0.CO;2, 145-160.

Frederiksen, J. S. (1982), A Unified Three-Dimensional Instability Theory of the Onset of Blocking and Cyclogenesis, *J. Atmos. Sci.*, *39*, 10.1175/1520-0469(1982)039<0969:AUTDIT>2.0.CO;2, 969-982.

Frederiksen, J. S. (1983), A Unified Three-Dimensional Instability Theory of the Onset of Blocking and Cyclogenesis. II. Teleconnection Patterns, *J. Atmos. Sci.*, *40*, 10.1175/1520-0469(1983)040<2593:AUTDIT>2.0.CO;2, 2593-2609.

Frederiksen, J. S., and C. S. Frederiksen (1993), Monsoon Disturbances, Intraseasonal Oscillations, Teleconnection Patterns, Blocking, and Storm Tracks of the Global Atmosphere during January 1979 - Linear-Theory, *J. Atmos. Sci.*, *50*, 1349-1372.

Frederiksen, J. S., and C. S. Frederiksen (1997), Mechanism of the formation of intraseasonal oscillations and Australian monsoon disturbances: The roles of convection, barotropic and baroclinic instability. Contributions to Atmospheric Physics, 70, 39–56.

Frederiksen, J. S. (2002), Genesis of Intraseasonal Oscillations and Equatorial Waves, *J. Atmos. Sci.*, *59*, 10.1175/1520-0469(2002)059<2761:GOIOAE>2.0.CO;2, 2761-2781.

Frederiksen, J. S., and H. Lin (2013), Tropical–Extratropical Interactions of Intraseasonal Oscillations, *J. Atmos. Sci.*, *70*, 10.1175/JAS-D-12-0302.1, 3180-3197.

Fu, M., and E. Tziperman (2019), Essential Ingredients to the Dynamics of Westerly Wind Bursts, *J. Clim.*, *32*, 10.1175/JCLI-D-18-0584.1, 5549-5565.

Fu, X., B. Wang, J.-Y. Lee, W. Wang, and L. Gao (2011), Sensitivity of Dynamical Intraseasonal Prediction Skills to Different Initial Conditions*, *Mon. Weather Rev.*, *139*, 10.1175/2011MWR3584.1, 2572-2592.

Fu, X., W. Wang, J.-Y. Lee, B. Wang, K. Kikuchi, J. Xu, J. Li, and S. Weaver (2015), Distinctive Roles of Air–Sea Coupling on Different MJO Events: A New Perspective Revealed from the DYNAMO/CINDY Field Campaign, *Mon. Weather Rev.*, *143*, 10.1175/mwr-d-14-00221.1, 794-812.

Fuchs, Z., and D. J. Raymond (2005), Large-Scale Modes in a Rotating Atmosphere with Radiative–Convective Instability and WISHE, *J. Atmos. Sci.*, *62*, 10.1175/JAS3582.1, 4084-4094.

Fuchs, ž., and D. J. Raymond (2007), A simple, vertically resolved model of tropical disturbances with a humidity closure, *Tellus A: Dynamic Meteorology and Oceanography*, *59*, 10.1111/j.1600-0870.2007.00230.x, 344-354.

Fuchs, Ž., and D. J. Raymond (2017), A simple model of intraseasonal oscillations, *Journal of Advances in Modeling Earth Systems*, *9*, 10.1002/2017MS000963, 1195-1211.

Garfinkel, C. I., S. B. Feldstein, D. W. Waugh, C. Yoo, and S. Lee (2012), Observed connection between stratospheric sudden warmings and the Madden-Julian Oscillation, *Geophys. Res. Lett.*, *39*, 10.1029/2012GL053144, L18807.

Garfinkel, C. I., J. J. Benedict, and E. D. Maloney (2014), Impact of the MJO on the boreal winter extratropical circulation, *Geophys. Res. Lett.*, *41*, 10.1002/2014gl061094, 6055-6062.

Garfinkel, C. I., and C. Schwartz (2017), MJO-Related Tropical Convection Anomalies Lead to More Accurate Stratospheric Vortex Variability in Subseasonal Forecast Models, *Geophys. Res. Lett.*, *44*, 10.1002/2017gl074470, 10,054-010,062.

Gensini, V. A., D. Gold, J. T. Allen, and B. S. Barrett (2019), Extended U.S. Tornado Outbreak During Late May 2019: A Forecast of Opportunity, *Geophys. Res. Lett.*, *46*, 10.1029/2019gl084470, 10150-10158.

Gentine, P., M. Pritchard, S. Rasp, G. Reinaudi, and G. Yacalis (2018), Could Machine Learning Break the Convection Parameterization Deadlock?, *Geophys. Res. Lett.*, *45*, 10.1029/2018gl078202, 5742-5751.

Gonzalez, A. O., and X. Jiang (2017), Winter Mean Lower-Tropospheric Moisture over the Maritime Continent as a Climate Model Diagnostic Metric for the Propagation of the Madden-Julian Oscillation, *Geophys. Res. Lett.*10.1002/2016GL072430.

Gonzalez, A. O., and X. Jiang (2019), Distinct Propagation Characteristics of Intraseasonal Variability Over the Tropical West Pacific, *Journal of Geophysical Research: Atmospheres*, *0*, 10.1029/2018JD029884.

Goswami, B. B., B. Khouider, R. Phani, P. Mukhopadhyay, and A. Majda (2017a), Improving synoptic and intraseasonal variability in CFSv2 via stochastic representation of organized convection, *Geophys. Res. Lett.*, *44*, 10.1002/2016GL071542, 1104-1113.

Goswami, B. B., B. Khouider, R. Phani, P. Mukhopadhyay, and A. J. Majda (2017b), Implementation and calibration of a stochastic multicloud convective parameterization in the NCEP Climate Forecast System (CFSv2), *Journal of Advances in Modeling Earth Systems*, *9*, 10.1002/2017MS001014, 1721-1739.

Gottschalck, J., M. Wheeler, K. Weickmann, F. Vitart, N. Savage, H. Lin, H. Hendon, D. Waliser, K. Sperber, M. Nakagawa, C. Prestrelo, M. Flatau, and W. Higgins (2010), A Framework for Assessing Operational Madden–Julian Oscillation Forecasts: A CLIVAR MJO Working Group Project, *Bull. Am. Meteorol. Soc.*, *91*, doi:10.1175/2010BAMS2816.1, 1247-1258.

Gottschalck, J., P. E. Roundy, C. J. Schreck Iii, A. Vintzileos, and C. Zhang (2013), Large-Scale Atmospheric and Oceanic Conditions during the 2011–12 DYNAMO Field Campaign, *Mon. Weather Rev.*, *141*, 10.1175/MWR-D-13-00022.1, 4173-4196.

Grabowski, W. W. (2001), Coupling Cloud Processes with the Large-Scale Dynamics Using the Cloud-Resolving Convection Parameterization (CRCP), *J. Atmos. Sci.*, *58*, 10.1175/1520-0469(2001)058<0978:Ccpwtl>2.0.Co;2, 978-997.

Grabowski, W. W., and M. W. Moncrieff (2004), Moisture–convection feedback in the tropics, *Quart. J. Roy. Meteor. Soc.*, *130*, 10.1256/qj.03.135, 3081-3104.

Gray, W. M., J. D. Sheaffer, and J. A. Knaff (1992), Influence of the Stratospheric QBO on ENSO Variability, *Journal of the Meteorological Society of Japan. Ser. II*, *70*, 10.2151/jmsj1965.70.5_975, 975-995.

Greatbatch, R. J. (2000), The North Atlantic Oscillation, *Stochastic Environmental Research and Risk Assessment*, *14*, 10.1007/s004770000047, 213-242.

Green, B. W., S. Sun, R. Bleck, S. G. Benjamin, and G. A. Grell (2017), Evaluation of MJO Predictive Skill in Multiphysics and Multimodel Global Ensembles, *Mon. Weather Rev.*, *145*, 10.1175/mwr-d-16-0419.1, 2555-2574.

Guan, B., D. E. Waliser, N. P. Molotch, E. J. Fetzer, and P. J. Neiman (2012), Does the Madden–Julian Oscillation Influence Wintertime Atmospheric Rivers and Snowpack in the Sierra Nevada?, *Mon. Weather Rev.*, *140*, 10.1175/MWR-D-11-00087.1, 325-342.

Guo, Y., X. Jiang, and D. E. Waliser (2014), Modulation of the Convectively Coupled Kelvin Waves over South America and the Tropical Atlantic Ocean in Association with the Madden–Julian Oscillation, *J. Atmos. Sci.*, *71*, 10.1175/JAS-D-13-0215.1, 1371-1388.

Guo, Y., D. E. Waliser, and X. Jiang (2015), A Systematic Relationship between the Representations of Convectively Coupled Equatorial Wave Activity and the Madden–Julian Oscillation in Climate Model Simulations, *J. Clim.*, *28*, 10.1175/JCLI-D-14-00485.1, 1881-1904.

Gushchina, D., and B. Dewitte (2012), Intraseasonal Tropical Atmospheric Variability Associated with the Two Flavors of El Niño, *Mon. Weather Rev.*, *140*, 10.1175/mwr-d-11-00267.1, 3669-3681.

Guy, N., and D. P. Jorgensen (2014), Kinematic and Precipitation Characteristics of Convective Systems Observed by Airborne Doppler Radar during the Life Cycle of a Madden–Julian Oscillation in the Indian Ocean, *Mon. Weather Rev.*, *142*, 10.1175/mwr-d-13-00252.1, 1385-1402.

Haertel, P. (2018), Sensitivity of the Madden Julian Oscillation to Ocean Warming in a Lagrangian Atmospheric Model, *Climate*, *6*, 45.

Haertel, P. T., and G. N. Kiladis (2004), Dynamics of 2-day equatorial waves, *J. Atmos. Sci.*, *61*, 2707-2721.

Hagos, S., Z. Feng, C. D. Burleyson, K.-S. S. Lim, C. N. Long, D. Wu, and G. Thompson (2014), Evaluation of convection-permitting model simulations of cloud populations associated with the Madden-Julian Oscillation using data collected during the AMIE/DYNAMO field campaign, *Journal of Geophysical Research: Atmospheres*, *119*, 10.1002/2014JD022143, 12,052-012,068.

Hagos, S. M., C. Zhang, Z. Feng, C. D. Burleyson, C. De Mott, B. Kerns, J. J. Benedict, and M. N. Martini (2016), The impact of the diurnal cycle on the propagation of Madden-Julian Oscillation convection across the Maritime Continent, *Journal of Advances in Modeling Earth Systems*10.1002/2016MS000725.

Hall, N. M. J., S. Thibaut, and P. Marchesiello (2017), Impact of the observed extratropics on climatological simulations of the MJO in a tropical channel model, *Climate Dyn.*, *48*, 10.1007/s00382-016-3221-5, 2541-2555.

Hamada, A., and Y. N. Takayabu (2016), Improvements in Detection of Light Precipitation with the Global Precipitation Measurement Dual-Frequency Precipitation Radar (GPM DPR), *Journal of Atmospheric and Oceanic Technology*, *33*, 10.1175/jtech-d-15-0097.1, 653-667.

Han, W. (2005), Origins and Dynamics of the 90-Day and 30–60-Day Variations in the Equatorial Indian Ocean, *J. Phys. Oceanogr.*, *35*, 10.1175/jpo2725.1, 708-728.

Han, Y., and B. Khouider (2010), Convectively Coupled Waves in a Sheared Environment, *J. Atmos. Sci.*, *67*, doi:10.1175/2010JAS3335.1, 2913-2942.

Hannah, W. M., and E. D. Maloney (2011), The Role of Moisture–Convection Feedbacks in Simulating the Madden–Julian Oscillation, *J. Clim.*, *24*, 10.1175/2011jcli3803.1, 2754-2770.

Hannah, W. M., and E. D. Maloney (2014), The moist static energy budget in NCAR CAM5 hindcasts during DYNAMO, *Journal of Advances in Modeling Earth Systems*, *6*, 10.1002/2013MS000272, 420-440.

Hannah, W. M., E. D. Maloney, and M. S. Pritchard (2015), Consequences of systematic model drift in DYNAMO MJO hindcasts with SP-CAM and CAM5, *Journal of Advances in Modeling Earth Systems*, *7*, 10.1002/2014MS000423, 1051-1074.

Hartmann, D. L., J. R. Holton, and Q. Fu (2001), The heat balance of the tropical tropopause, cirrus, and stratospheric dehydration, *Geophys. Res. Lett.*, *28*, 10.1029/2000GL012833, 1969-1972.

Hayashi, M., and H. Itoh (2017), A New Mechanism of the Slow Eastward Propagation of Unstable Disturbances with Convection in the Tropics: Implications for the MJO, *J. Atmos. Sci.*, *74*, 10.1175/JAS-D-16-0300.1, 3749-3769.

Hayes, S. P., L. J. Mangum, J. Picaut, A. Sumi, and K. Takeuchi (1991), TOGA-TAO: A Moored Array for Real-time Measurements in the Tropical Pacific Ocean, *Bull. Am. Meteorol. Soc.*, *72*, 10.1175/1520-0477(1991)072<0339:Ttamaf>2.0.Co;2, 339-347.

Held, I. M., and B. J. Soden (2006), Robust Responses of the Hydrological Cycle to Global Warming, *J. Clim.*, *19*, 10.1175/JCLI3990.1, 5686-5699.

Henderson, D. S., T. L'Ecuyer, G. Stephens, P. Partain, and M. Sekiguchi (2013), A Multisensor Perspective on the Radiative Impacts of Clouds and Aerosols, *Journal of Applied Meteorology and Climatology*, *52*, 10.1175/JAMC-D-12-025.1, 853-871.

Henderson, S. A., E. D. Maloney, and E. A. Barnes (2016), The Influence of the Madden–Julian Oscillation on Northern Hemisphere Winter Blocking, *J. Clim.*, *29*, 10.1175/jcli-d-15-0502.1, 4597-4616.

Henderson, S. A., E. D. Maloney, and S.-W. Son (2017), Madden–Julian Oscillation Pacific Teleconnections: The Impact of the Basic State and MJO Representation in General Circulation Models, *J. Clim.*, *30*, 10.1175/jcli-d-16-0789.1, 4567-4587.

Hendon, H. H., and B. Liebmann (1990), The Intraseasonal (30-50 day) Oscillation of the Australian Summer Monsoon, *J. Atmos. Sci.*, *47*, 2909-2924.

Hendon, H. H., and B. Liebmann (1994), Organization of Convection within the Madden-Julian Oscillation, *J. Geophys. Res.*, *99*, 8073-8083.

Hendon, H. H., and M. L. Salby (1994), The Life-Cycle of the Madden-Julian Oscillation, *J. Atmos. Sci.*, *51*, 2225-2237.

Hendon, H. H., and J. Glick (1997), Intraseasonal Air–Sea Interaction in the Tropical Indian and Pacific Oceans, *J. Clim.*, *10*, 10.1175/1520-0442(1997)010<0647:IASIIT>2.0.CO;2, 647-661.

Hendon, H. H., C. Zhang, and J. D. Glick (1999), Interannual Variation of the Madden–Julian Oscillation during Austral Summer, *J. Clim.*, *12*, 10.1175/1520-0442(1999)012<2538:Ivotmj>2.0.Co;2, 2538-2550.

Hendon, H. H. (2000), Impact of Air–Sea Coupling on the Madden–Julian Oscillation in a General Circulation Model, *J. Atmos. Sci.*, *57*, 10.1175/1520-0469(2001)058<3939:IOASCO>2.0.CO;2, 3939-3952.

Hendon, H. H., M. C. Wheeler, and C. Zhang (2007), Seasonal Dependence of the MJO–ENSO Relationship, *J. Clim.*, *20*, 10.1175/jcli4003.1, 531-543.

Hendon, H. H., and S. Abhik (2018), Differences in Vertical Structure of the Madden-Julian Oscillation Associated With the Quasi-Biennial Oscillation, *Geophys. Res. Lett.*, *45*, 10.1029/2018gl077207, 4419-4428.

Higgins, R. W., J. K. E. Schemm, W. Shi, and A. Leetmaa (2000), Extreme precipitation events in the western United States related to tropical forcing, *J. Clim.*, *13*, 793-820.

Higgins, R. W., and W. Shi (2001), Intercomparison of the Principal Modes of Interannual and Intraseasonal Variability of the North American Monsoon System, *J. Clim.*, *14*, 403-417.

Holloway, C. E., and J. D. Neelin (2007), The Convective Cold Top and Quasi Equilibrium, *J. Atmos. Sci.*, *64*, 10.1175/jas3907.1, 1467-1487.

Holloway, C. E., S. J. Woolnough, and G. M. S. Lister (2013), The Effects of Explicit versus Parameterized Convection on the MJO in a Large-Domain High-Resolution Tropical Case Study. Part I: Characterization of Large-Scale Organization and Propagation, *J. Atmos. Sci.*, *70*, 10.1175/jas-d-12-0227.1, 1342-1369.

Hong, C.-C., H.-H. Hsu, W.-L. Tseng, M.-Y. Lee, C.-H. Chow, and L.-C. Jiang (2017a), Extratropical Forcing Triggered the 2015 Madden–Julian Oscillation–El Niño Event, *Scientific Reports*, *7*, 10.1038/srep46692, 46692.

Hong, X., C. A. Reynolds, J. D. Doyle, P. May, and L. O'Neill (2017b), Assessment of upper-ocean variability and the Madden-Julian Oscillation in extended-range air-ocean coupled mesoscale simulations, *Dynamics of Atmospheres and Oceans*, *78*, https://doi.org/10.1016/j.dynatmoce.2017.03.002, 89-105.

Hood, L. L. (2017), QBO/solar modulation of the boreal winter Madden-Julian oscillation: A prediction for the coming solar minimum, *Geophys. Res. Lett.*, *44*, 10.1002/2017GL072832, 3849-3857.

Horel, J. D., and J. M. Wallace (1981), Planetary-Scale Atmospheric Phenomena Associated with the Southern Oscillation, *Mon. Weather Rev.*, *109*, 10.1175/1520-0493(1981)109<0813:Psapaw>2.0.Co;2, 813-829.

Hoskins, B. J., and T. Ambrizzi (1993), Rossby Wave Propagation on a Realistic Longitudinally Varying Flow, *J. Atmos. Sci.*, *50*, 10.1175/1520-0469(1993)050<1661:Rwpoar>2.0.Co;2, 1661-1671.

Hoskins, B. J., and G.-Y. Yang (2000), The Equatorial Response to Higher-Latitude Forcing, *J. Atmos. Sci.*, *57*, 10.1175/1520-0469(2000)057<1197:Terthl>2.0.Co;2, 1197-1213.

Houze, R. A., S. S. Chen, D. E. Kingsmill, Y. Serra, and S. E. Yuter (2000), Convection over the Pacific warm pool in relation to the atmospheric Kelvin-Rossby wave, *J. Atmos. Sci.*, *57*, 3058-3089.

Hsu, H.-H. (1996), Global View of the intraseasonal Oscillation during Northern Winter, *J. Clim.*, *9*, 10.1175/1520-0442(1996)009<2386:Gvotio>2.0.Co;2, 2386-2406.

Hsu, H.-H., and M.-Y. Lee (2005), Topographic Effects on the Eastward Propagation and Initiation of the Madden–Julian Oscillation, *J. Clim.*, *18*, doi:10.1175/JCLI-3292.1, 795-809.

Hsu, J.-Y., H. Hendon, M. Feng, and X. Zhou (2019), Magnitude and Phase of Diurnal SST Variations in the ACCESS-S1 Model During the Suppressed Phase of the MJOs, *Journal of Geophysical Research: Oceans*, *124*, 10.1029/2019JC015458, 9553-9571.

Hsu, P. C., and T. Li (2012), Role of the Boundary Layer Moisture Asymmetry in Causing the Eastward Propagation of the Madden-Julian Oscillation, *J. Clim.*, *25*, Doi 10.1175/Jcli-D-11-00310.1, 4914-4931.

Hu, Q., and D. A. Randall (1995), Low-Frequency Oscillations in Radiative Convective Systems .2. An Idealized Model, *J. Atmos. Sci.*, *52*, 478-490.

Huffman, G., E. Stocker, D. T. Bolvin, E. J. Nelkin, and J. Tan (2019), GPM IMERG Final Precipitation L3 1 day 0.1 degree x 0.1 degree V06, Edited by Andrey Savtchenko, Greenbelt, MD, Goddard Earth Sciences Data and Information Services Center (GES DISC), Accessed: [Data Access Date], 10.5067/GPM/IMERGDF/DAY/06.

Huffman, G. J., R. F. Adler, D. T. Bolvin, G. Gu, E. J. Nelkin, K. P. Bowman, Y. Hong, E. F. Stocker, and D. B. Wolff (2007), The TRMM Multisatellite Precipitation Analysis (TMPA): Quasi-Global, Multiyear, Combined-Sensor Precipitation Estimates at Fine Scales, *J. Hydrometeorol*, *8*, 38-55.

Hung, C.-S., and C.-H. Sui (2018), A Diagnostic Study of the Evolution of the MJO from Indian Ocean to Maritime Continent: Wave Dynamics versus Advective Moistening Processes, *J. Clim.*, *31*, 10.1175/jcli-d-17-0139.1, 4095-4115.

Hung, M.-P., J.-L. Lin, W. Wang, D. Kim, T. Shinoda, and S. J. Weaver (2013), MJO and Convectively Coupled Equatorial Waves Simulated by CMIP5 Climate Models, *J. Clim.*, *26*, 10.1175/JCLI-D-12-00541.1, 6185-6214.

Hurrell, J. W., Y. Kushnir, G. Ottersen, and M. Visbeck (2013), An Overview of the North Atlantic Oscillation, in *The North Atlantic Oscillation: Climatic Significance and Environmental Impact*, edited, pp. 1-35, American Geophysical Union.

ICTP (2006), Workshop on the Organization and Maintenance of Tropical Convection and the Madden Julian Oscillation: Sponsors: ITCP, WCRP, Thorpex. Organizers: J. Slingo, F. Molteni, M. Moncrieff, M. Shapiro, edited by F.M. J. Slingo, M. Moncrieff, M. Shapiro, International Centre for Theoretical Physics, Tieste, Italy, March 13-17, 2006.

Illingworth, A. J., H. W. Barker, A. Beljaars, M. Ceccaldi, H. Chepfer, N. Clerbaux, J. Cole, J. Delanoë, C. Domenech, D. P. Donovan, S. Fukuda, M. Hirakata, R. J. Hogan, A. Huenerbein, P. Kollias, T. Kubota, T. Nakajima, T. Y. Nakajima, T. Nishizawa, Y. Ohno, H. Okamoto, R. Oki, K. Sato, M. Satoh, M. W. Shephard, A. Velázquez-Blázquez, U. Wandinger, T. Wehr, and G.-J. v. Zadelhoff (2015), The EarthCARE Satellite: The Next Step Forward in Global Measurements of Clouds, Aerosols, Precipitation, and Radiation, *Bull. Am. Meteorol. Soc.*, *96*, 10.1175/bams-d-12-00227.1, 1311-1332.

Inness, P. M., and J. M. Slingo (2006), The interaction of the Madden-Julian Oscillation with the Maritime Continent in a GCM, *Quart. J. Roy. Meteor. Soc.*, *132*, 1645-1667.

Inoue, K., and L. Back (2015a), Column-Integrated Moist Static Energy Budget Analysis on Various Time Scales during TOGA COARE, *J. Atmos. Sci.*, *72*, doi:10.1175/JAS-D-14-0249.1, 1856-1871.

2926 Inoue, K., and L. E. Back (2015b), Gross Moist Stability Assessment during TOGA COARE: Various
2927 Interpretations of Gross Moist Stability, *J. Atmos. Sci.*, *72*, doi:10.1175/JAS-D-15-0092.1, 4148-4166.
2928 Janiga, M. A., C. J. S. III, J. A. Ridout, M. Flatau, N. P. Barton, E. J. Metzger, and C. A. Reynolds (2018),
2929 Subseasonal Forecasts of Convectively Coupled Equatorial Waves and the MJO: Activity and Predictive
2930 Skill, *Mon. Weather Rev.*, *146*, 10.1175/mwr-d-17-0261.1, 2337-2360.
2931 Jeong, J.-H., C.-H. Ho, B.-M. Kim, and W.-T. Kwon (2005), Influence of the Madden-Julian Oscillation on
2932 wintertime surface air temperature and cold surges in east Asia, *Journal of Geophysical Research:*
2933 *Atmospheres*, *110*, 10.1029/2004JD005408, D11104.
2934 Jiang, X., T. Li, and B. Wang (2004), Structures and Mechanisms of the Northward Propagating Boreal
2935 Summer Intraseasonal Oscillation, *J. Clim.*, *17*, 1022-1039.
2936 Jiang, X., D. E. Waliser, W. S. Olson, W.-K. Tao, T. S. L'Ecuyer, J.-L. Li, B. Tian, Y. L. Yung, A. M.
2937 Tompkins, S. E. Lang, and M. Grecu (2009), Vertical Heating Structures Associated with the MJO as
2938 Characterized by TRMM Estimates, ECMWF Reanalyses, and Forecasts: A Case Study during 1998/99
2939 Winter, *J. Clim.*, *22*, doi:10.1175/2009JCLI3048.1, 6001-6020.
2940 Jiang, X., D. E. Waliser, W. S. Olson, W.-K. Tao, T. S. L'Ecuyer, K.-F. Li, Y. L. Yung, S. Shige, S. Lang,
2941 and Y. N. Takayabu (2011), Vertical Diabatic Heating Structure of the MJO: Intercomparison between
2942 Recent Reanalyses and TRMM Estimates, *Mon. Weather Rev.*, *139*, 10.1175/2011mwr3636.1, 3208-
2943 3223.
2944 Jiang, X., M. Zhao, and D. E. Waliser (2012), Modulation of Tropical Cyclones over the Eastern Pacific by
2945 the Intraseasonal Variability Simulated in an AGCM, *J. Clim.*, *25*, 10.1175/jcli-d-11-00531.1, 6524-6538.
2946 Jiang, X., D. E. Waliser, P. K. Xavier, J. Petch, N. P. Klingaman, S. J. Woolnough, B. Guan, G. Bellon, T.
2947 Crueger, C. DeMott, C. Hannay, H. Lin, W. Hu, D. Kim, C.-L. Lappen, M.-M. Lu, H.-Y. Ma, T.
2948 Miyakawa, J. A. Ridout, S. D. Schubert, J. Scinocca, K.-H. Seo, E. Shindo, X. Song, C. Stan, W.-L.
2949 Tseng, W. Wang, T. Wu, X. Wu, K. Wyser, G. J. Zhang, and H. Zhu (2015), Vertical structure and
2950 physical processes of the Madden-Julian oscillation: Exploring key model physics in climate simulations,
2951 *Journal of Geophysical Research: Atmospheres*, *120*, 10.1002/2014JD022375, 4718-4748.
2952 Jiang, X., M. Zhao, E. D. Maloney, and D. E. Waliser (2016), Convective moisture adjustment time scale as
2953 a key factor in regulating model amplitude of the Madden-Julian Oscillation, *Geophys. Res. Lett.*, *43*,
2954 10.1002/2016GL070898, 10,412-410,419.
2955 Jiang, X. (2017), Key processes for the eastward propagation of the Madden-Julian Oscillation based on
2956 multimodel simulations, *Journal of Geophysical Research: Atmospheres*10.1002/2016JD025955.
2957 Jiang, X., Á. F. Adames, M. Zhao, D. Waliser, and E. Maloney (2018a), A Unified Moisture Mode
2958 Framework for Seasonality of the Madden–Julian Oscillation, *J. Clim.*, *31*, 10.1175/jcli-d-17-0671.1,
2959 4215-4224.

2960 Jiang, X., B. Xiang, M. Zhao, T. Li, S.-J. Lin, Z. Wang, and J.-H. Chen (2018b), Intraseasonal Tropical
2961 Cyclogenesis Prediction in a Global Coupled Model System, *J. Clim.*, *31*, 10.1175/JCLI-D-17-0454.1,
2962 6209-6227.
2963 Jiang, X., H. Su, and D. E. Waliser (2019), A Damping Effect of the Maritime Continent for the Madden-
2964 Julian Oscillation, *Journal of Geophysical Research: Atmospheres*10.1029/2019JD031503.
2965 Jiang, X., D. Kim, and E. Maloney (2020), Progress and Status of MJO Simulation in Climate Models and
2966 Process-Oriented Diagnostics, Chapter 25 in The Multiscale Global Monsoon System, eds :C.P. Chang,
2967 K.J. Ha, R. H. Johnson, D. Kim, G.N. Lau, B. Wang. World Scientific Series on Asia-Pacific Weather
2968 and Climate, Vol. 11. World Scientific, Singapore., edited.
2969 Johnson, R. H., T. M. Rickenbach, S. A. Rutledge, P. E. Ciesielski, and W. H. Schubert (1999), Trimodal
2970 Characteristics of Tropical Convection, *J. Clim.*, *12*, 2397-2418.
2971 Johnson, R. H., and P. E. Ciesielski (2013), Structure and Properties of Madden–Julian Oscillations Deduced
2972 from DYNAMO Sounding Arrays, *J. Atmos. Sci.*, *70*, 10.1175/JAS-D-13-065.1, 3157-3179.
2973 Johnson, R. H., P. E. Ciesielski, J. H. Ruppert, and M. Katsumata (2015), Sounding-Based Thermodynamic
2974 Budgets for DYNAMO, *J. Atmos. Sci.*, *72*, 10.1175/JAS-D-14-0202.1, 598-622.
2975 Jones, C., L. M. V. Carvalho, R. Wayne Higgins, D. E. Waliser, and J. K. E. Schemm (2004a), Climatology
2976 of Tropical Intraseasonal Convective Anomalies: 1979–2002, *J. Clim.*, *17*, 10.1175/1520-
2977 0442(2004)017<0523:COTICA>2.0.CO;2, 523-539.
2978 Jones, C., D. E. Waliser, K. M. Lau, and W. Stern (2004b), Global occurrences of extreme precipitation and
2979 the Madden-Julian oscillation: Observations and predictability, *J. Clim.*, *17*, 4575-4589.
2980 Jones, C., and L. M. V. Carvalho (2006), Changes in the Activity of the Madden–Julian Oscillation during
2981 1958–2004, *J. Clim.*, *19*, 10.1175/JCLI3972.1, 6353-6370.
2982 Jones, C., and L. M. V. Carvalho (2011), Will global warming modify the activity of the Madden–Julian
2983 Oscillation?, *Quart. J. Roy. Meteor. Soc.*, *137*, 10.1002/qj.765, 544-552.
2984 Jones, C., and L. M. V. Carvalho (2012), Spatial–Intensity Variations in Extreme Precipitation in the
2985 Contiguous United States and the Madden–Julian Oscillation, *J. Clim.*, *25*, 10.1175/jcli-d-11-00278.1,
2986 4898-4913.
2987 Judt, F., and S. S. Chen (2014), An explosive convective cloud system and its environmental conditions in
2988 MJO initiation observed during DYNAMO, *Journal of Geophysical Research: Atmospheres*, *119*,
2989 10.1002/2013JD021048, 2781-2795.
2990 Kacimi, A., and B. Khouider (2018), The transient response to an equatorial heat source and its convergence
2991 to steady state: implications for MJO theory, *Climate Dyn.*, *50*, 10.1007/s00382-017-3807-6, 3315-3330.
2992 Kalnay, E., M. Kanamitsu, R. Kistler, W. Collins, D. Deaven, L. Gandin, M. Iredell, S. Saha, G. White, J.
2993 Woollen, Y. Zhu, M. Chelliah, W. Ebisuzaki, W. Higgins, J. Janowiak, K. C. Mo, C. Ropelewski, J.

Wang, A. Leetmaa, R. Reynolds, R. Jenne, and D. Joseph (1996), The NCEP/NCAR 40-year reanalysis project, *Bull. Am. Meteorol. Soc.*, *77*, 437-471.

Kang, W., and E. Tziperman (2017), More Frequent Sudden Stratospheric Warming Events due to Enhanced MJO Forcing Expected in a Warmer Climate, *J. Clim.*, *30*, 10.1175/jcli-d-17-0044.1, 8727-8743.

Kang, W., and E. Tziperman (2018a), The Role of Zonal Asymmetry in the Enhancement and Suppression of Sudden Stratospheric Warming Variability by the Madden–Julian Oscillation, *J. Clim.*, *31*, 10.1175/jcli-d-17-0489.1, 2399-2415.

Kang, W., and E. Tziperman (2018b), The MJO-SSW Teleconnection: Interaction Between MJO-Forced Waves and the Midlatitude Jet, *Geophys. Res. Lett.*, *45*, 10.1029/2018GL077937, 4400-4409.

Kapur, A., and C. Zhang (2012), Multiplicative MJO Forcing of ENSO, *J. Clim.*, *25*, 10.1175/jcli-d-11-00609.1, 8132-8147.

Kemball-Cook, S. R., and B. C. Weare (2001), The onset of convection in the Madden-Julian oscillation, *J. Clim.*, *14*, 780-793.

Kerns, B. W., and S. S. Chen (2014), Equatorial Dry Air Intrusion and Related Synoptic Variability in MJO Initiation during DYNAMO, *Mon. Weather Rev.*, *142*, 10.1175/MWR-D-13-00159.1, 1326-1343.

Kerns, B. W., and S. S. Chen (2016), Large-scale precipitation tracking and the MJO over the Maritime Continent and Indo-Pacific warm pool, *Journal of Geophysical Research: Atmospheres*, *121*, 10.1002/2015JD024661, 8755-8776.

Kessler, W. S., and R. Kleeman (2000), Rectification of the Madden-Julian Oscillation into the ENSO Cycle, *J. Clim.*, *13*, 3560-3575.

Khairoutdinov, M., D. Randall, and C. DeMott (2005), Simulations of the atmospheric general circulation using a cloud-resolving model as a superparameterization of physical processes, *J. Atmos. Sci.*, *62*, 2136-2154.

Khairoutdinov, M. F., and D. A. Randall (2003), Cloud resolving modeling of the ARM summer 1997 IOP: Model formulation, results, uncertainties, and sensitivities, *J. Atmos. Sci.*, *60*, 607-625.

Khairoutdinov, M. F., and K. Emanuel (2018), Intraseasonal Variability in a Cloud-Permitting Near-Global Equatorial Aquaplanet Model, *J. Atmos. Sci.*, *75*, 10.1175/jas-d-18-0152.1, 4337-4355.

Khouider, B., and A. J. Majda (2006), A Simple Multicloud Parameterization for Convectively Coupled Tropical Waves. Part I: Linear Analysis, *J. Atmos. Sci.*, *63*, 1308-1323.

Khouider, B., Y. Han, A. J. Majda, and S. N. Stechmann (2012), Multiscale Waves in an MJO Background and Convective Momentum Transport Feedback, *J. Atmos. Sci.*, *69*, 10.1175/JAS-D-11-0152.1, 915-933.

Kikuchi, K., and Y. N. Takayabu (2004), The development of organized convection associated with the MJO during TOGA COARE IOP: Trimodal characteristics, *Geophys. Res. Lett.*, *31*.

Kikuchi, K., and B. Wang (2008), Diurnal Precipitation Regimes in the Global Tropics, *J. Clim.*, *21*, doi:10.1175/2007JCLI2051.1, 2680-2696.

Kikuchi, K. (2014), An introduction to combined Fourier–wavelet transform and its application to convectively coupled equatorial waves, *Climate Dyn.*, *43*, 10.1007/s00382-013-1949-8, 1339-1356.

Kiladis, G. N., and K. M. Weickmann (1992), Extratropical Forcing of Tropical Pacific Convection during Northern Winter, *Mon. Weather Rev.*, *120*, 1924-1938.

Kiladis, G. N., K. H. Straub, and P. T. Haertel (2005), Zonal and Vertical Structure of the Madden-Julian Oscillation, *J. Atmos. Sci.*, *62*, 2790-2809.

Kiladis, G. N., M. C. Wheeler, P. T. Haertel, K. H. Straub, and P. E. Roundy (2009), Convectively Coupled Equatorial Waves, *Rev. Geophys.*, *47*, RG2003, DOI:10.1029/2008RG000266

Kiladis, G. N., J. Dias, K. H. Straub, M. C. Wheeler, S. N. Tulich, K. Kikuchi, K. M. Weickmann, and M. J. Ventrice (2014), A Comparison of OLR and Circulation-Based Indices for Tracking the MJO, *Mon. Weather Rev.*, *142*, 10.1175/mwr-d-13-00301.1, 1697-1715.

Kim, D., K. Sperber, W. Stern, D. Waliser, I. S. Kang, E. Maloney, W. Wang, K. Weickmann, J. Benedict, M. Khairoutdinov, M. I. Lee, R. Neale, M. Suarez, K. Thayer-Calder, and G. Zhang (2009), Application of MJO Simulation Diagnostics to Climate Models, *J. Clim.*, *22*, Doi 10.1175/2009jcli3063.1, 6413-6436.

Kim, D., A. H. Sobel, and I.-S. Kang (2011a), A mechanism denial study on the Madden-Julian Oscillation, *Journal of Advances in Modeling Earth Systems*, *3*, 10.1029/2011MS000081, n/a-n/a.

Kim, D., A. H. Sobel, E. D. Maloney, D. M. W. Frierson, and I. S. Kang (2011b), A Systematic Relationship between Intraseasonal Variability and Mean State Bias in AGCM Simulations, *J. Clim.*, *24*, Doi 10.1175/2011jcli4177.1, 5506-5520.

Kim, D., and I.-S. Kang (2012), A bulk mass flux convection scheme for climate model: description and moisture sensitivity, *Climate Dyn.*, *38*, 10.1007/s00382-010-0972-2, 411-429.

Kim, D., A. H. Sobel, A. D. Del Genio, Y. Chen, S. J. Camargo, M.-S. Yao, M. Kelley, and L. Nazarenko (2012), The Tropical Subseasonal Variability Simulated in the NASA GISS General Circulation Model, *J. Clim.*, *25*, 10.1175/JCLI-D-11-00447.1, 4641-4659.

Kim, D., J.-S. Kug, and A. H. Sobel (2014a), Propagating versus Nonpropagating Madden–Julian Oscillation Events, *J. Clim.*, *27*, 10.1175/JCLI-D-13-00084.1, 111-125.

Kim, D., P. Xavier, E. Maloney, M. Wheeler, D. Waliser, K. Sperber, H. Hendon, C. Zhang, R. Neale, Y.-T. Hwang, and H. Liu (2014b), Process-Oriented MJO Simulation Diagnostic: Moisture Sensitivity of Simulated Convection, *J. Clim.*, *27*, 10.1175/jcli-d-13-00497.1, 5379-5395.

Kim, D., M.-S. Ahn, I.-S. Kang, and A. D. D. Genio (2015), Role of Longwave Cloud–Radiation Feedback in the Simulation of the Madden–Julian Oscillation, *J. Clim.*, *28*, doi:10.1175/JCLI-D-14-00767.1, 6979-6994.

Kim, D., H. Kim, and M.-I. Lee (2017), Why does the MJO detour the Maritime Continent during austral summer?, *Geophys. Res. Lett.*10.1002/2017GL072643, n/a-n/a.

Kim, D., and E. Maloney (2017), Simulation of the Madden-Julian Oscillation Using General Circulation Models, in *The Global Monsoon System*, edited, pp. 161-172, World Scientific.

Kim, D., E. Maloney, and C. Zhang (2020a), Review: MJO propagation over the Maritime Continent. The Multiscale Global Monsoon System, C. P. Chang et al., Eds., Vol. 11, World Scientific Series on Asia-Pacific Weather and Climate, World Scientific.

Kim, H.-M., P. J. Webster, V. E. Toma, and D. Kim (2014c), Predictability and Prediction Skill of the MJO in Two Operational Forecasting Systems, *J. Clim.*, *27*, doi:10.1175/JCLI-D-13-00480.1, 5364-5378.

Kim, H.-M., D. Kim, F. Vitart, V. E. Toma, J.-S. Kug, and P. J. Webster (2016), MJO Propagation across the Maritime Continent in the ECMWF Ensemble Prediction System, *J. Clim.*, *29*, doi:10.1175/JCLI-D-15-0862.1, 3973-3988.

Kim, H.-M. (2017), The Impact of the Mean Moisture Bias on the Key Physics of MJO Propagation in the ECMWF Reforecast, *Journal of Geophysical Research: Atmospheres*10.1002/2017JD027005, 2017JD027005.

Kim, H., F. Vitart, and D. E. Waliser (2018), Prediction of the Madden–Julian Oscillation: A Review, *J. Clim.*, *31*, 10.1175/JCLI-D-18-0210.1, 9425-9443.

Kim, H., M. A. Janiga, and K. Pegion (2019), MJO Propagation Processes and Mean Biases in the SubX and S2S Reforecasts, *Journal of Geophysical Research: Atmospheres*, *124*, 10.1029/2019JD031139, 9314-9331.

Kim, H., J. M. Caron, J. H. Richter, and I. R. Simpson (2020b), The lack of QBO-MJO connection in CMIP6 models, *Geophys. Res. Lett.*, *n/a*, 10.1029/2020GL087295, e2020GL087295.

Kim, H., J. H. Richter, and Z. Martin (2020c), Insignificant QBO-MJO Prediction Skill Relationship in the SubX and S2S Subseasonal Reforecasts, *Journal of Geophysical Research: Atmospheres*, *124*, 10.1029/2019jd031416, 12655-12666.

Kim, J., and S.-W. Son (2012), Tropical Cold-Point Tropopause: Climatology, Seasonal Cycle, and Intraseasonal Variability Derived from COSMIC GPS Radio Occultation Measurements, *J. Clim.*, *25*, 10.1175/jcli-d-11-00554.1, 5343-5360.

Kiranmayi, L., and E. D. Maloney (2011), Intraseasonal moist static energy budget in reanalysis data, *Journal of Geophysical Research: Atmospheres*, *116*, 10.1029/2011JD016031, D21117.

Kirtman, B., and coathors (2013), Near-term Climate Change: Projections and Predictability. In: Climate Change 2013: The Physical Science Basis. Contribution of Working Group I to the Fifth Assessment Report of the Intergovernmental Panel on Climate Change [Stocker, T.F., D. Qin, G.-K. Plattner, M. Tignor, S.K. Allen, J. Boschung, A. Nauels, Y. Xia, V. Bex and P.M. Midgley (eds.)]. Cambridge University Press, Cambridge, United Kingdom and New York, NY, USA. , edited.

Klingaman, N. P., and S. J. Woolnough (2014), The role of air–sea coupling in the simulation of the Madden–Julian oscillation in the Hadley Centre model, *Quart. J. Roy. Meteor. Soc.*10.1002/qj.2295.

Klingaman, N. P., X. Jiang, P. K. Xavier, J. Petch, D. Waliser, and S. J. Woolnough (2015a), Vertical structure and physical processes of the Madden-Julian oscillation: Synthesis and summary, *Journal of Geophysical Research: Atmospheres*, *120*, 10.1002/2015JD023196, 4671-4689.

Klingaman, N. P., S. J. Woolnough, X. Jiang, D. Waliser, P. K. Xavier, J. Petch, M. Caian, C. Hannay, D. Kim, H.-Y. Ma, W. J. Merryfield, T. Miyakawa, M. Pritchard, J. A. Ridout, R. Roehrig, E. Shindo, F. Vitart, H. Wang, N. R. Cavanaugh, B. E. Mapes, A. Shelly, and G. J. Zhang (2015b), Vertical structure and physical processes of the Madden-Julian oscillation: Linking hindcast fidelity to simulated diabatic heating and moistening, *Journal of Geophysical Research: Atmospheres*, *120*, 10.1002/2014JD022374, 4690-4717.

Klingaman, N. P., and C. A. Demott (2020), Mean State Biases and Interannual Variability Affect Perceived Sensitivities of the Madden-Julian Oscillation to Air-Sea Coupling, *Journal of Advances in Modeling Earth Systems*, *12*, 10.1029/2019MS001799, e2019MS001799.

Klotzbach, P., S. Abhik, H. H. Hendon, M. Bell, C. Lucas, A. G. Marshall, and E. C. J. Oliver (2019), On the emerging relationship between the stratospheric Quasi-Biennial oscillation and the Madden-Julian oscillation, *Scientific Reports*, *9*, 10.1038/s41598-019-40034-6, 2981.

Klotzbach, P. J. (2010), On the Madden-Julian Oscillation-Atlantic Hurricane Relationship, *J. Clim.*, *23*, doi:10.1175/2009JCLI2978.1, 282-293.

Knutson, T. R., and S. Manabe (1995), Time-Mean Response over the Tropical Pacific to Increased C02 in a Coupled Ocean-Atmosphere Model, *J. Clim.*, *8*, 10.1175/1520-0442(1995)008<2181:Tmrott>2.0.Co;2, 2181-2199.

Kodama, Y.-M., M. Tokuda, and F. Murata (2006), Convective Activity Over the Indonesian Maritime Continent During CPEA-I as Evaluated by Lightning Activity and Q1 and Q2 Profiles, *Journal of the Meteorological Society of Japan. Ser. II*, *84A*, 10.2151/jmsj.84A.133, 133-149.

Krishnamurti, T. N., D. K. Oosterhof, and A. V. Mehta (1988), Air–Sea Interaction on the Time Scale of 30 to 50 Days, *J. Atmos. Sci.*, *45*, 10.1175/1520-0469(1988)045<1304:Aiotts>2.0.Co;2, 1304-1322.

Kuang, Z. (2008), A moisture-stratiform instability for convectively coupled waves, *J. Atmos. Sci.*, *65*, Doi 10.1175/2007jas2444.1, 834-854.

Kubokawa, H., M. Satoh, J. Suzuki, and M. Fujiwara (2016), Influence of topography on temperature variations in the tropical tropopause layer, *Journal of Geophysical Research: Atmospheres*, *121*, 10.1002/2016JD025569, 11,556-511,574.

Kubota, H., K. Yoneyama, J.-I. Hamada, P. Wu, A. Sudaryanto, and I. B. Wahyono (2015), Role of Maritime Continent Convection during the Preconditioning Stage of the Madden-Julian Oscillation Observed in CINDY2011/DYNAMO, *Journal of the Meteorological Society of Japan. Ser. II*, *93A*, 10.2151/jmsj.2015-050, 101-114.

Kuo, Y.-H., J. D. Neelin, C.-C. Chen, W.-T. Chen, L. J. Donner, A. Gettelman, X. Jiang, K.-T. Kuo, E. Maloney, C. R. Mechoso, Y. Ming, K. A. Schiro, C. J. Seman, C.-M. Wu, and M. Zhao (2019), Convective transition statistics over tropical oceans for climate model diagnostics: GCM evaluation, *J. Atmos. Sci.*, *0*, 10.1175/jas-d-19-0132.1, null.

L'Ecuyer, T. S., and G. McGarragh (2010), A 10-Year Climatology of Tropical Radiative Heating and Its Vertical Structure from TRMM Observations, *J. Clim.*, *23*, Doi 10.1175/2009jcli3018.1, 519-541.

L'Heureux, M. L., and R. W. Higgins (2008), Boreal winter links between the Madden-Julian oscillation and the Arctic oscillation, *J. Clim.*, *21*, Doi 10.1175/2007jcli1955.1, 3040-3050.

L'Heureux, M. L., and R. W. Higgins (2008), Boreal Winter Links between the Madden–Julian Oscillation and the Arctic Oscillation, *J. Clim.*, *21*, 10.1175/2007jcli1955.1, 3040-3050.

Lau, K.-M., and P. H. Chan (1986), Aspects of the 40-50 Day Oscillation during the Northern Summer as Inferred from Outgoing Longwave Radiation, *Mon. Weather Rev.*, *114*, 1354-1367.

Lau, K.-M., and T. J. Phillips (1986), Coherent Fluctuations of Fxtratropical Geopotential Height and Tropical Convection in Intraseasonal Time Scales, *J. Atmos. Sci.*, *43*, 10.1175/1520-0469(1986)043<1164:Cfofgh>2.0.Co;2, 1164-1181.

Lau, K.-M., and L. Peng (1987), Origin of Low-Frequency (Intraseasonal) Oscillations in the Tropical Atmosphere. Part I: Basic Theory, *J. Atmos. Sci.*, *44*, 950-972.

Lau, W. K.-M., and D. E. Waliser (2012), *Intraseasonal Variability in the Atmosphere-Ocean Climate System*, Second ed., Springer, 613p, Heidelberg, Germany.

Lee, C.-Y., S. J. Camargo, F. Vitart, A. H. Sobel, and M. K. Tippett (2018), Sub-seasonal tropical cyclone genesis prediction and MJO in the S2S dataset, *Weather Forecasting*, *33*, 10.1175/waf-d-17-0165.1.

Lee, H.-J., and K.-H. Seo (2019), Impact of the Madden-Julian oscillation on Antarctic sea ice and its dynamical mechanism, *Scientific Reports*, *9*, 10.1038/s41598-019-47150-3, 10761.

Lee, J.-E., B. R. Lintner, J. D. Neelin, X. Jiang, P. Gentine, C. K. Boyce, J. B. Fisher, J. T. Perron, T. L. Kubar, J. Lee, and J. Worden (2012), Reduction of tropical land region precipitation variability via transpiration, *Geophys. Res. Lett.*, *39*, 10.1029/2012GL053417, n/a-n/a.

Lee, J. C. K., and N. P. Klingaman (2018), The effect of the quasi-biennial oscillation on the Madden–Julian oscillation in the Met Office Unified Model Global Ocean Mixed Layer configuration, *Atmospheric Science Letters*, *19*, 10.1002/asl.816, e816.

Lee, M. I., I. S. Kang, J. K. Kim, and B. E. Mapes (2001), Influence of cloud-radiation interaction on simulating tropical intraseasonal oscillation with an atmospheric general circulation model, *J. Geophys. Res.*, *106*, 14219-14233.

Lee, M. I., I. S. Kang, and B. E. Mapes (2003), Impacts of cumulus convection parameterization on aqua-planet AGCM Simulations of tropical intraseasonal variability, *J. Meteorol. Soc. Japan*, *81*, 963-992.

Lee, S.-H., and K.-H. Seo (2011), A multi-scale analysis of the interdecadal change in the Madden-Julian Oscillation, *Atmosphere*, *21*.

Lee, S., T. Gong, N. Johnson, S. B. Feldstein, and D. Pollard (2011), On the Possible Link between Tropical Convection and the Northern Hemisphere Arctic Surface Air Temperature Change between 1958 and 2001, *J. Clim.*, *24*, 10.1175/2011jcli4003.1, 4350-4367.

Leutbecher, M., S.-J. Lock, P. Ollinaho, S. T. K. Lang, G. Balsamo, P. Bechtold, M. Bonavita, H. M. Christensen, M. Diamantakis, E. Dutra, S. English, M. Fisher, R. M. Forbes, J. Goddard, T. Haiden, R. J. Hogan, S. Juricke, H. Lawrence, D. MacLeod, L. Magnusson, S. Malardel, S. Massart, I. Sandu, P. K. Smolarkiewicz, A. Subramanian, F. Vitart, N. Wedi, and A. Weisheimer (2017), Stochastic representations of model uncertainties at ECMWF: state of the art and future vision, *Quart. J. Roy. Meteor. Soc.*, *143*, 10.1002/qj.3094, 2315-2339.

Li, K.-F., B. Tian, D. E. Waliser, and Y. L. Yung (2010), Tropical mid-tropospheric CO2 variability driven by the Madden–Julian oscillation, *Proceedings of the National Academy of Sciences*, *107*, 10.1073/pnas.1008222107, 19171-19175.

Li, Y., and R. E. Carbone (2012), Excitation of Rainfall over the Tropical Western Pacific, *J. Atmos. Sci.*, *69*, 10.1175/jas-d-11-0245.1, 2983-2994.

Li, Y., W. Han, T. Shinoda, C. Wang, R.-C. Lien, J. N. Moum, and J.-W. Wang (2013), Effects of the diurnal cycle in solar radiation on the tropical Indian Ocean mixed layer variability during wintertime Madden-Julian Oscillations, *Journal of Geophysical Research: Oceans*, *118*, 10.1002/jgrc.20395, 4945-4964.

Liebmann, B., and D. L. Hartmann (1984), An Observational Study of Tropical-Midlatitude Interaction on Intraseasonal Time Scales during Winter, *J. Atmos. Sci.*, *41*, 3333-3350.

Liebmann, B., H. H. Hendon, and J. D. Glick (1994), The Relationship between Tropical Cyclones of the Western Pacific and Indian Oceans and the Madden-Julian Oscillation, *J. Meteorol. Soc. Japan*, *72*, 401-412.

Liebmann, B., H. H. Hendon, and J. D. Glick (1997), On the generation of two-day convective disturbances across the western equatorial Pacific, *J. Meteorol. Soc. Japan*, *75*, 939-946.

Liess, S., and M. A. Geller (2012), On the relationship between QBO and distribution of tropical deep convection, *Journal of Geophysical Research: Atmospheres*, *117*, 10.1029/2011JD016317.

Lim, Y., S.-W. Son, and D. Kim (2018), MJO Prediction Skill of the Subseasonal-to-Seasonal Prediction Models, *J. Clim.*, *31*, 10.1175/JCLI-D-17-0545.1, 4075-4094.

Lim, Y., S.-W. Son, A. G. Marshall, H. H. Hendon, and K.-H. Seo (2019), Influence of the QBO on MJO prediction skill in the subseasonal-to-seasonal prediction models, *Climate Dyn.*, *53*, 10.1007/s00382-019-04719-y, 1681-1695.

Limpasuvan, V., and D. L. Hartmann (1999), Eddies and the annular modes of climate variability, *Geophys. Res. Lett.*, *26*, 10.1029/1999GL010478, 3133-3136.

Lin, H., G. Brunet, and J. Derome (2007), Intraseasonal Variability in a Dry Atmospheric Model, *J. Atmos. Sci.*, *64*, 10.1175/JAS3955.1, 2422-2441.

Lin, H., and G. Brunet (2009), The Influence of the Madden–Julian Oscillation on Canadian Wintertime Surface Air Temperature, *Mon. Weather Rev.*, *137*, 10.1175/2009mwr2831.1, 2250-2262.

Lin, H., G. Brunet, and J. Derome (2009), An Observed Connection between the North Atlantic Oscillation and the Madden-Julian Oscillation, *J. Clim.*, *22*, Doi 10.1175/2008jcli2515.1, 364-380.

Lin, H., G. Brunet, and R. Mo (2010), Impact of the Madden–Julian Oscillation on Wintertime Precipitation in Canada, *Mon. Weather Rev.*, *138*, 10.1175/2010MWR3363.1, 3822-3839.

Lin, H., and G. Brunet (2011), Impact of the North Atlantic Oscillation on the forecast skill of the Madden-Julian Oscillation, *Geophys. Res. Lett.*, *38*, 10.1029/2010GL046131.

Lin, H., G. Brunet, and B. Yu (2015), Interannual variability of the Madden-Julian Oscillation and its impact on the North Atlantic Oscillation in the boreal winter, *Geophys. Res. Lett.*, *42*, 10.1002/2015GL064547, 5571-5576.

Lin, H. (2018), Predicting the Dominant Patterns of Subseasonal Variability of Wintertime Surface Air Temperature in Extratropical Northern Hemisphere, *Geophys. Res. Lett.*, *45*, 10.1029/2018GL077509, 4381-4389.

Lin, H., and G. Brunet (2018), Extratropical Response to the MJO: Nonlinearity and Sensitivity to the Initial State, *J. Atmos. Sci.*, *75*, 10.1175/jas-d-17-0189.1, 219-234.

Lin, H., J. S. Frederiksen, D. M. Straus, and C. Stan (2019a), Tropical-extratropical interactions and teleconnections. Chapter 7, Pages 143-164, Sub-Seasonal to Seasonal Prediction: The Gap Between Weather and Climate Forecasting, Editor(s): Andrew W. Robertson, Frederic Vitart, Elsevier, 2019., edited.

Lin, H., R. Mo, F. Vitart, and C. Stan (2019b), Eastern Canada Flooding 2017 and its Subseasonal Predictions, *Atmosphere-Ocean*, *57*, 10.1080/07055900.2018.1547679, 195-207.

Lin, H. (2020), Subseasonal Forecast Skill over the Northern Polar Region in Boreal Winter, *J. Clim.*, *33*, 10.1175/jcli-d-19-0408.1, 1935-1951.

Lin, J.-L., G. N. Kiladis, B. E. Mapes, K. M. Weickmann, K. R. Sperber, W. Lin, M. C. Wheeler, S. D. Schubert, A. Del Genio, L. J. Donner, S. Emori, J.-F. Gueremy, F. Hourdin, P. J. Rasch, E. Roeckner, and J. F. Scinocca (2006), Tropical Intraseasonal Variability in 14 IPCC AR4 Climate Models. Part I: Convective Signals, *J. Clim.*, *19*, 2665-2690.

Lin, J.-L., M.-I. Lee, D. Kim, I.-S. Kang, and D. M. W. Frierson (2008), The Impacts of Convective Parameterization and Moisture Triggering on AGCM-Simulated Convectively Coupled Equatorial Waves, *J. Clim.*, *21*, 10.1175/2007jcli1790.1, 883-909.

Lin, J., B. Mapes, M. Zhang, and M. Newman (2004), Stratiform Precipitation, Vertical Heating Profiles, and the Madden-Julian Oscillation, *J. Atmos. Sci.*, *61*, 296-309.

Lin, J. L., and B. E. Mapes (2004), Radiation budget of the tropical intraseasonal oscillation, *J. Atmos. Sci.*, *61*, 2050-2062.

Lin, J. W.-B., and J. D. Neelin (2003), Toward stochastic deep convective parameterization in general circulation models, *Geophys. Res. Lett.*, *30*, 10.1029/2002GL016203, n/a-n/a.

Lin, X., and R. H. Johnson (1996), Kinematic and thermodynamic characteristics of the flow over the western Pacific warm pool during TOGA COARE, *J. Atmos. Sci.*, *53*, 695-715.

Ling, J., C. Li, and X. Jia (2009), Impacts of cumulus momentum transport on MJO simulation, *Advances in Atmospheric Sciences*, *26*, 10.1007/s00376-009-8016-8, 864-876.

Ling, J., and C. Zhang (2011), Structural Evolution in Heating Profiles of the MJO in Global Reanalyses and TRMM Retrievals, *J. Clim.*, *24*, 10.1175/2010jcli3826.1, 825-842.

Ling, J., Y. Zhao, and G. Chen (2019), Barrier Effect on MJO Propagation by the Maritime Continent in the MJO Task Force/GEWEX Atmospheric System Study Models, *J. Clim.*, *32*, 10.1175/jcli-d-18-0870.1, 5529-5547.

Liu, C., B. Tian, K.-F. Li, G. L. Manney, N. J. Livesey, Y. L. Yung, and D. E. Waliser (2014), Northern Hemisphere mid-winter vortex-displacement and vortex-split stratospheric sudden warmings: Influence of the Madden-Julian Oscillation and Quasi-Biennial Oscillation, *Journal of Geophysical Research: Atmospheres*, *119*, 10.1002/2014JD021876, 12,599-512,620.

Liu, P., M. Satoh, B. Wang, H. Fudeyasu, T. Nasuno, T. Li, H. Miura, H. Taniguchi, H. Masunaga, X. Fu, and H. Annamalai (2009), An MJO Simulated by the NICAM at 14- and 7-km Resolutions, *Mon. Weather Rev.*, *137*, 10.1175/2009mwr2965.1, 3254-3268.

Liu, P., T. Li, B. Wang, M. Zhang, J.-j. Luo, Y. Masumoto, X. Wang, and E. Roeckner (2013), MJO change with A1B global warming estimated by the 40-km ECHAM5, *Climate Dyn.*, *41*, 10.1007/s00382-012-1532-8, 1009-1023.

Liu, X., T. Wu, S. Yang, T. Li, W. Jie, L. Zhang, Z. Wang, X. Liang, Q. Li, Y. Cheng, H. Ren, Y. Fang, and S. Nie (2017), MJO prediction using the sub-seasonal to seasonal forecast model of Beijing Climate Center, *Climate Dyn.*, *48*, 10.1007/s00382-016-3264-7, 3283-3307.

Long, C. N., S. A. McFarlane, A. D. Genio, P. Minnis, T. P. Ackerman, J. Mather, J. Comstock, G. G. Mace, M. Jensen, and C. Jakob (2013), ARM Research In The Equatorial Western Pacific: A Decade And Counting, *Bull. Am. Meteorol. Soc.*, *94*, 10.1175/BAMS-D-11-00137.1, 695-708.

Lopez, H., B. P. Kirtman, E. Tziperman, and G. Gebbie (2013), Impact of interactive westerly wind bursts on CCSM3, *Dynamics of Atmospheres and Oceans*, *59*, https://doi.org/10.1016/j.dynatmoce.2012.11.001, 24-51.

Lorenz, D. J., and D. L. Hartmann (2006), The Effect of the MJO on the North American Monsoon, *J. Clim.*, *19*, 333-343.

Love, B. S., A. J. Matthews, and G. M. S. Lister (2011), The diurnal cycle of precipitation over the Maritime Continent in a high-resolution atmospheric model, *Quart. J. Roy. Meteor. Soc.*, *137*, 10.1002/qj.809, 934-947.

Luo, Z. J., G. Y. Liu, and G. L. Stephens (2010), Use of A-Train data to estimate convective buoyancy and entrainment rate, *Geophys. Res. Lett.*, *37*, 10.1029/2010gl042904.

Ma, D., and Z. M. Kuang (2011), Modulation of radiative heating by the Madden-Julian Oscillation and convectively coupled Kelvin waves as observed by CloudSat, *Geophys. Res. Lett.*, *38*, Doi 10.1029/2011gl049734.

Ma, D., and Z. Kuang (2016), A mechanism-denial study on the Madden-Julian Oscillation with reduced interference from mean state changes, *Geophys. Res. Lett.*, *43*, 10.1002/2016GL067702, 2989-2997.

Madden, R. A., and P. R. Julian (1971), Detection of a 40-50 Day Oscillation in Zonal Wind in Tropical Pacific, *J. Atmos. Sci.*, *28*, 702-&.

Madden, R. A., and P. R. Julian (1972), Description of Global-Scale Circulation Cells in Tropics with a 40-50 Day Period, *J. Atmos. Sci.*, *29*, 1109-&.

Madden, R. A., and P. R. Julian (1994), Observations of the 40-50-Day Tropical Oscillation: A Review, *Mon. Weather Rev.*, *122*, 814-837.

Majda, A. J., and J. A. Biello (2004), A multiscale model for tropical intraseasonal oscillations, *Proc. Natl. Acad. Sci.*, *101*, 4736-4741.

Majda, A. J., and S. N. Stechmann (2009), A Simple Dynamical Model with Features of Convective Momentum Transport, *J. Atmos. Sci.*, *66*, 373-392.

Majda, A. J., and S. N. Stechmann (2011), Nonlinear Dynamics and Regional Variations in the MJO Skeleton, *J. Atmos. Sci.*, *68*, 10.1175/JAS-D-11-053.1, 3053-3071.

Majda, A. J., and S. N. Stechmann (2012), Multi-scale theories for the MJO, in *Intraseasonal Variability in the Atmosphere-Ocean Climate System*, edited by W. K. M. Lau and D. E. Waliser, Springer, Heidelberg, Germany.

Majda, A. J., and Q. Yang (2016), A Multiscale Model for the Intraseasonal Impact of the Diurnal Cycle over the Maritime Continent on the Madden–Julian Oscillation, *J. Atmos. Sci.*, *73*, doi:10.1175/JAS-D-15-0158.1, 579-604.

Maloney, E. D., and D. L. Hartmann (1998), Frictional Moisture Convergence in a Composite Life Cycle of the Madden-Julian Oscillation, *J. Clim.*, *11*, 2387-2403.

Maloney, E. D., and D. L. Hartmann (2000), Modulation of Eastern North Pacific Hurricanes by the Madden-Julian Oscillation, *J. Clim.*, *13*, 1451-1460.

Maloney, E. D., and D. L. Hartmann (2001), The sensitivity of intraseasonal variability in the NCAR CCM3 to changes in convective parameterization, *J. Clim.*, *14*, 2015-2034.

Maloney, E. D., and A. H. Sobel (2004), Surface Fluxes and Ocean Coupling in the Tropical Intraseasonal Oscillation, *J. Clim.*, *17*, 4368-4386.

Maloney, E. D. (2009), The Moist Static Energy Budget of a Composite Tropical Intraseasonal Oscillation in a Climate Model, *J. Clim.*, *22*, 711-729.

Maloney, E. D., A. H. Sobel, and W. M. Hannah (2010), Intraseasonal variability in an aquaplanet general circulation model, *Journal of Advances in Modeling Earth Systems*, *2*, 10.3894/james.2010.2.5.

Maloney, E. D., and S.-P. Xie (2013), Sensitivity of tropical intraseasonal variability to the pattern of climate warming, *Journal of Advances in Modeling Earth Systems*, *5*, 10.1029/2012MS000171, 32-47.

Maloney, E. D., Á. F. Adames, and H. X. Bui (2019a), Madden–Julian oscillation changes under anthropogenic warming, *Nature Climate Change*, *9*, 10.1038/s41558-018-0331-6, 26-33.

Maloney, E. D., A. Gettelman, Y. Ming, J. D. Neelin, D. Barrie, A. Mariotti, C. C. Chen, D. R. B. Coleman, Y.-H. Kuo, B. Singh, H. Annamalai, A. Berg, J. F. Booth, S. J. Camargo, A. Dai, A. Gonzalez, J. Hafner, X. Jiang, X. Jing, D. Kim, A. Kumar, Y. Moon, C. M. Naud, A. H. Sobel, K. Suzuki, F. Wang, J. Wang, A. A. Wing, X. Xu, and M. Zhao (2019b), Process-Oriented Evaluation of Climate and Weather Forecasting Models, *Bull. Am. Meteorol. Soc.*, *100*, 10.1175/BAMS-D-18-0042.1, 1665-1686.

Mapes, B., S. Tulich, J. Lin, and P. Zuidema (2006), The mesoscale convection life cycle: Building block or prototype for large-scale tropical waves?, *Dynamics of Atmospheres and Oceans*, *42*, Doi 10.1016/J.Dynatmoce.2006.03.003, 3-29.

Mapes, B., and R. Neale (2011a), Parameterizing Convective Organization to Escape the Entrainment Dilemma, *Journal of Advances in Modeling Earth Systems*, *3*, 10.1029/2011ms000042.

Mapes, B. E. (2000), Convective Inhibition, Subgrid-Scale Triggering Energy, and Stratiform Instability in a Toy Tropical Wave Model, *J. Atmos. Sci.*, *57*, 1515-1535.

Mapes, B. E., and R. B. Neale (2011b), Parameterizing convective organization, *Journal of Advances in Modeling Earth Systems*, *3*, 10.1029/2011ms000042, 20 pp.

Marshall, A. G., O. Alves, and H. H. Hendon (2008), An Enhanced Moisture Convergence–Evaporation Feedback Mechanism for MJO Air–Sea Interaction, *J. Atmos. Sci.*, *65*, 10.1175/2007jas2313.1, 970-986.

Marshall, A. G., D. Hudson, M. C. Wheeler, O. Alves, H. H. Hendon, M. J. Pook, and J. S. Risbey (2014), Intra-seasonal drivers of extreme heat over Australia in observations and POAMA-2, *Climate Dyn.*, *43*, 10.1007/s00382-013-2016-1, 1915-1937.

Marshall, A. G., H. H. Hendon, and G. Wang (2016), On the role of anomalous ocean surface temperatures for promoting the record Madden-Julian Oscillation in March 2015, *Geophys. Res. Lett.*, *43*, 10.1002/2015GL066984, 472-481.

Marshall, A. G., H. H. Hendon, S.-W. Son, and Y. Lim (2017), Impact of the quasi-biennial oscillation on predictability of the Madden–Julian oscillation, *Climate Dyn.*10.1007/s00382-016-3392-0, 1-13.

Martin, Z., S. Wang, J. Nie, and A. Sobel (2019), The Impact of the QBO on MJO Convection in Cloud-Resolving Simulations, *J. Atmos. Sci.*, *76*, 10.1175/jas-d-18-0179.1, 669-688.

Masunaga, H., T. S. L'Ecuyer, and C. D. Kummerow (2006), The Madden-Julian oscillation recorded in early observations from the Tropical Rainfall Measuring Mission (TRMM), *J. Atmos. Sci.*, *63*, 2777-2794.

Matsuno, T. (1966), Quasi-Geostrophic Motions in the Equatorial Area, *J. Meteorol. Soc. Japan*, *44*, 25-42.

Matthews, A. J., and G. N. Kiladis (1999), The Tropical–Extratropical Interaction between High-Frequency Transients and the Madden–Julian Oscillation, *Mon. Weather Rev.*, *127*, 10.1175/1520-0493, 661-677.

Matthews, A. J., B. J. Hoskins, and M. Masutani (2004), The global response to tropical heating in the Madden–Julian oscillation during the northern winter, *Quart. J. Roy. Meteor. Soc.*, *130*, 10.1256/qj.02.123, 1991-2011.

Matthews, A. J., D. B. Baranowski, K. J. Heywood, P. J. Flatau, and S. Schmidtko (2014), The Surface Diurnal Warm Layer in the Indian Ocean during CINDY/DYNAMO, *J. Clim.*, *27*, 10.1175/jcli-d-14-00222.1, 9101-9122.

McPhaden, M. J. (1999), Genesis and evolution of the 1997-98 El Nino, *Science*, *283*, 950-954.

McPhaden, M. J. (2004), Evolution of the 2002/03 El Niño*, *Bull. Am. Meteorol. Soc.*, *85*, 10.1175/bams-85-5-677, 677-696.

Mechem, D. B., S. S. Chen, and R. A. Houze Jr. (2006), Momentum transport processes in the stratiform regions of mesoscale convective systems over the western Pacific warm pool, *Quart. J. Roy. Meteor. Soc.*, *132*, 10.1256/qj.04.141, 709-736.

Miura, H., M. Satoh, T. Nasuno, A. T. Noda, and K. Oouchi (2007), A Madden-Julian Oscillation event realistically simulated by a global cloud-resolving model, *Science*, *318*, Doi 10.1126/Science.1148443, 1763-1765.

Miyakawa, T., M. Satoh, H. Miura, H. Tomita, H. Yashiro, A. T. Noda, Y. Yamada, C. Kodama, M. Kimoto, and K. Yoneyama (2014), Madden–Julian Oscillation prediction skill of a new-generation global model demonstrated using a supercomputer, *Nat Commun*, *5*, 10.1038/ncomms4769.

Miyakawa, T., and K. Kikuchi (2018), CINDY2011/DYNAMO Madden-Julian oscillation successfully reproduced in global cloud/cloud-system resolving simulations despite weak tropical wavelet power, *Scientific Reports*, *8*, 10.1038/s41598-018-29931-4, 11664.

Mo, K. C., and R. W. Higgins (1998), Tropical Convection and Precipitation Regimes in the Western United States, *J. Clim.*, *11*, 2404-2423.

Mo, K. C. (2000), Intraseasonal Modulation of Summer Precipitation over North America, *Mon. Weather Rev.*, *128*, 1490-1505.

Mo, K. C., C. Jones, and J. Nogues-Paegle (2012), Pan-America, in *Intraseasonal Variability in the Atmosphere-Ocean Climate System*, edited by W. K. M. Lau and D. E. Waliser, pp. 111-145, Springer, Heidelberg, Germany.

Moncrieff, M. W. (1992), Organized Convective Systems - Archetypal Dynamic-Models, Mass and Momentum Flux Theory, and Parametrization, *Quart. J. Roy. Meteor. Soc.*, *118*, 819-850.

Moncrieff, M. W., and E. Klinker (1997), Organized convective systems in the tropical western Pacific as a process in general circulation models: A TOGA COARE case-study, *Quart. J. Roy. Meteor. Soc.*, *123*, 10.1002/qj.49712354002, 805-827.

Moncrieff, M. W., D. E. Waliser, M. J. Miller, M. A. Shapiro, G. R. Asrar, and J. Caughey (2012), Multiscale Convective Organization and the YOTC Virtual Global Field Campaign, *Bull. Am. Meteorol. Soc.*, *93*, 10.1175/bams-d-11-00233.1, 1171-1187.

Moncrieff, M. W. (2019), Toward a Dynamical Foundation for Organized Convection Parameterization in GCMs, *Geophys. Res. Lett.*10.1029/2019gl085316.

Monier, E., B. C. Weare, and W. I. Gustafson (2010), The Madden–Julian oscillation wind-convection coupling and the role of moisture processes in the MM5 model, *Climate Dyn.*, *35*, 10.1007/s00382-009-0626-4, 435-447.

Mori, M., and M. Watanabe (2008), The Growth and Triggering Mechanisms of the PNA: A MJO-PNA Coherence, *Journal of the Meteorological Society of Japan. Ser. II*, *86*, 10.2151/jmsj.86.213, 213-236.

Mori, S., H. Jun-Ichi, Y. I. Tauhid, M. D. Yamanaka, N. Okamoto, F. Murata, N. Sakurai, H. Hashiguchi, and T. Sribimawati (2004), Diurnal Land–Sea Rainfall Peak Migration over Sumatera Island, Indonesian Maritime Continent, Observed by TRMM Satellite and Intensive Rawinsonde Soundings, *Mon. Weather Rev.*, *132*, doi:10.1175/1520-0493(2004)132<2021:DLRPMO>2.0.CO;2, 2021-2039.

Morita, J., Y. N. Takayabu, S. Shige, and Y. Kodama (2006), Analysis of rainfall characteristics of the Madden–Julian oscillation using TRMM satellite data, *Dynamics of Atmospheres and Oceans*, *42*, https://doi.org/10.1016/j.dynatmoce.2006.02.002, 107-126.

Moteki, Q., M. Katsumata, K. Yoneyama, K. Ando, and T. Hasegawa (2018), Drastic thickening of the barrier layer off the western coast of Sumatra due to the Madden-Julian oscillation passage during the Pre-Years of the Maritime Continent campaign, *Progress in Earth and Planetary Science*, *5*, 10.1186/s40645-018-0190-9, 35.

Moulin, A. J., J. N. Moum, and E. L. Shroyer (2018), Evolution of Turbulence in the Diurnal Warm Layer, *J. Phys. Oceanogr.*, *48*, 10.1175/jpo-d-17-0170.1, 383-396.

Moum, J. N., S. P. de Szoeke, W. D. Smyth, J. B. Edson, H. L. DeWitt, A. J. Moulin, E. J. Thompson, C. J. Zappa, S. A. Rutledge, R. H. Johnson, and C. W. Fairall (2014a), Air-Sea Interactions from Westerly Wind Bursts during the November 2011 MJO in the Indian Ocean, *Bull. Am. Meteorol. Soc.*10.1175/BAMS-D-12-00225.1.

Moum, J. N., S. P. d. Szoeke, W. D. Smyth, J. B. Edson, H. L. DeWitt, A. J. Moulin, E. J. Thompson, C. J. Zappa, S. A. Rutledge, R. H. Johnson, and C. W. Fairall (2014b), Air–Sea Interactions from Westerly Wind Bursts During the November 2011 MJO in the Indian Ocean, *Bull. Am. Meteorol. Soc.*, *95*, 10.1175/bams-d-12-00225.1, 1185-1199.

Moum, J. N., K. Pujiana, R.-C. Lien, and W. D. Smyth (2016), Ocean feedback to pulses of the Madden–Julian Oscillation in the equatorial Indian Ocean, *Nature Communications*, *7*, 10.1038/ncomms13203, 13203.

Mundhenk, B. D., E. A. Barnes, E. D. Maloney, and C. F. Baggett (2018), Skillful empirical subseasonal prediction of landfalling atmospheric river activity using the Madden–Julian oscillation and quasi-biennial oscillation, *npj Climate and Atmospheric Science*, *1*, 10.1038/s41612-017-0008-2, 20177.

Muraleedharan, P. M., S. Prasanna Kumar, K. Mohana kumar, S. Sijikumar, K. U. Sivakumar, and T. Mathew (2015), Observational evidence of Mixed Rossby Gravity waves at the central equatorial Indian Ocean, *Meteorol. Atmos. Phys.*, *127*, 10.1007/s00703-015-0376-2, 407-417.

Nagura, M., and M. J. McPhaden (2012), The dynamics of wind-driven intraseasonal variability in the equatorial Indian Ocean, *Journal of Geophysical Research: Oceans*, *117*, 10.1029/2011JC007405.

Nakazawa, T. (1988), Tropical Super Clusters within Intraseasonal Variations over the Western Pacific, *J. Meteorol. Soc. Japan*, *66*, 823-839.

NAS (2010), Assessment of Intraseasonal to Interannual Climate Prediction and Predictability. The National Academies Press, Washington, D.C. ISBN-0-309-15184-8, 192 pages.

NASEM (2016), Next Generation Earth System Prediction: Strategies for Subseasonal to Seasonal Forecasts, *National Research Council, National Academy of Sciences*, Washington DC, ISBN-978-0-309-38880-1, 290 pages.

Nasuno, T., H. Miura, M. Satoh, A. T. Noda, and K. Oouchi (2009), Multi-scale Organization of Convection in a Global Numerical Simulation of the December 2006 MJO Event Using Explicit Moist Processes, *Journal of the Meteorological Society of Japan. Ser. II*, *87*, 10.2151/jmsj.87.335, 335-345.

Naumann, G., and W. M. Vargas (2010), Joint Diagnostic of the Surface Air Temperature in Southern South America and the Madden–Julian Oscillation, *Weather Forecasting*, *25*, 10.1175/2010waf2222418.1, 1275-1280.

Neale, R., and J. Slingo (2003), The Maritime Continent and Its Role in the Global Climate: A GCM Study, *J. Clim.*, *16*, 10.1175/1520-0442(2003)016<0834:TMCAIR>2.0.CO;2, 834-848.

Neelin, J. D., and I. M. Held (1987), Modeling Tropical Convergence Based on the Moist Static Energy Budget, *Mon. Weather Rev.*, *115*, 3-12.

Neelin, J. D., I. M. Held, and K. H. Cook (1987), Evaporation-Wind Feedback and Low-Frequency Variability in the Tropical Atmosphere, *J. Atmos. Sci.*, *44*, 2341-2348.

Neelin, J. D., and J. Y. Yu (1994), Modes of Tropical Variability under Convective Adjustment and the Madden-Julian Oscillation .1. Analytical Theory, *J. Atmos. Sci.*, *51*, 1876-1894.

Neena, J. M., J. Y. Lee, D. Waliser, B. Wang, and X. Jiang (2014), Predictability of the Madden–Julian Oscillation in the Intraseasonal Variability Hindcast Experiment (ISVHE), *J. Clim.*, *27*, 10.1175/JCLI-D-13-00624.1, 4531-4543.

Nesbitt, S. W., and E. J. Zipser (2003), The Diurnal Cycle of Rainfall and Convective Intensity according to Three Years of TRMM Measurements, *J. Clim.*, *16*, doi:10.1175/1520-0442(2003)016<1456:TDCORA>2.0.CO;2, 1456-1475.

Nie, J., and A. H. Sobel (2015), Responses of Tropical Deep Convection to the QBO: Cloud-Resolving Simulations, *J. Atmos. Sci.*, *72*, doi:10.1175/JAS-D-15-0035.1, 3625-3638.

Nishimoto, E., and S. Yoden (2017), Influence of the Stratospheric Quasi-Biennial Oscillation on the Madden–Julian Oscillation during Austral Summer, *J. Atmos. Sci.*, *74*, 10.1175/JAS-D-16-0205.1, 1105-1125.

O'Gorman, P. A., and J. G. Dwyer (2018), Using Machine Learning to Parameterize Moist Convection: Potential for Modeling of Climate, Climate Change, and Extreme Events, *Journal of Advances in Modeling Earth Systems*, *10*, 10.1029/2018ms001351, 2548-2563.

Oh, J.-H., B.-M. Kim, K.-Y. Kim, H.-J. Song, and G.-H. Lim (2013), The impact of the diurnal cycle on the MJO over the Maritime Continent: a modeling study assimilating TRMM rain rate into global analysis, *Climate Dyn.*, *40*, 10.1007/s00382-012-1419-8, 893-911.

Oh, J.-H., X. Jiang, D. E. Waliser, M. W. Moncrieff, and R. H. Johnson (2015a), Convective Momentum Transport Associated with the Madden–Julian Oscillation Based on a Reanalysis Dataset, *J. Clim.*, *28*, 10.1175/JCLI-D-14-00570.1, 5763-5782.

Oh, J.-H., X. Jiang, D. E. Waliser, M. W. Moncrieff, R. H. Johnson, and P. Ciesielski (2015b), A Momentum Budget Analysis of Westerly Wind Events Associated with the Madden–Julian Oscillation during DYNAMO, *J. Atmos. Sci.*, *72*, 10.1175/JAS-D-15-0044.1, 3780-3799.

Oh, J. H., K. Y. Kim, and G. H. Lim (2012), Impact of MJO on the diurnal cycle of rainfall over the western Maritime Continent in the austral summer, *Climate Dyn.*, *38*, DOI 10.1007/s00382-011-1237-4, 1167-1180.

Oliver, E. C. J., and K. R. Thompson (2012), A Reconstruction of Madden–Julian Oscillation Variability from 1905 to 2008, *J. Clim.*, *25*, 10.1175/jcli-d-11-00154.1, 1996-2019.

Palmer, T., R. Buizza, F. Doblas-Reyes, T. Jung, M. Leutbecher, G. Shutts, M. Steinheimer, and A. Weisheimer (2009), Stochastic parametrization and model uncertainty. Tech. Memo. 598, ECMWF, Reading, UK, edited.

Parishani, H., M. S. Pritchard, C. S. Bretherton, M. C. Wyant, and M. Khairoutdinov (2017), Toward low-cloud-permitting cloud superparameterization with explicit boundary layer turbulence, *Journal of Advances in Modeling Earth Systems*, *9*, 10.1002/2017ms000968, 1542-1571.

Park, C. K., D. M. Straus, and K. M. Lau (1990), An Evaluation of the Structure of Tropical Intraseasonal Oscillations in 3 General-Circulation Models, *J. Meteorol. Soc. Japan*, *68*, 403-417.

Park, S. (2014), A Unified Convection Scheme (UNICON). Part I: Formulation, *J. Atmos. Sci.*, *71*, 10.1175/jas-d-13-0233.1, 3902-3930.

Park, T.-W., C.-H. Ho, S. Yang, and J.-H. Jeong (2010), Influences of Arctic Oscillation and Madden-Julian Oscillation on cold surges and heavy snowfalls over Korea: A case study for the winter of 2009–2010, *Journal of Geophysical Research: Atmospheres*, *115*, 10.1029/2010JD014794, D23122.

Peatman, S. C., A. J. Matthews, and D. P. Stevens (2014), Propagation of the Madden–Julian Oscillation through the Maritime Continent and scale interaction with the diurnal cycle of precipitation, *Quart. J. Roy. Meteor. Soc.*, *140*, 10.1002/qj.2161, 814-825.

Peatman, S. C., A. J. Matthews, and D. P. Stevens (2015), Propagation of the Madden–Julian Oscillation and scale interaction with the diurnal cycle in a high-resolution GCM, *Climate Dyn.*, *45*, 10.1007/s00382-015-2513-5, 2901-2918.

Pegion, K., and B. P. Kirtman (2008), The Impact of Air–Sea Interactions on the Simulation of Tropical Intraseasonal Variability, *J. Clim.*, *21*, 10.1175/2008jcli2180.1, 6616-6635.

Pegion, K., B. P. Kirtman, E. Becker, D. C. Collins, E. LaJoie, R. Burgman, R. Bell, T. DelSole, D. Min, Y. Zhu, W. Li, E. Sinsky, H. Guan, J. Gottschalck, E. J. Metzger, N. P. Barton, D. Achuthavarier, J. Marshak, R. D. Koster, H. Lin, N. Gagnon, M. Bell, M. K. Tippett, A. W. Robertson, S. Sun, S. G. Benjamin, B. W. Green, R. Bleck, and H. Kim (2019), The Subseasonal Experiment (SubX): A Multimodel Subseasonal Prediction Experiment, *Bull. Am. Meteorol. Soc.*, *100*, 10.1175/bams-d-18-0270.1, 2043-2060.

Pei, S., T. Shinoda, A. Soloviev, and R.-C. Lien (2018), Upper Ocean Response to the Atmospheric Cold Pools Associated With the Madden-Julian Oscillation, *Geophys. Res. Lett.*, *45*, 10.1029/2018GL077825, 5020-5029.

Petch, J., D. Waliser, X. Jiang, P. Xavier, and S. Woolnough (2011), A global model inter-comparison of the physical processes associated with the MJO, *GEWEX News*, August. .

Peters, K., T. Crueger, C. Jakob, and B. Möbis (2017), Improved MJO-simulation in ECHAM6.3 by coupling a Stochastic Multicloud Model to the convection scheme, *Journal of Advances in Modeling Earth Systems*, *9*, 10.1002/2016MS000809, 193-219.

Peters, O., and J. D. Neelin (2006), Critical phenomena in atmospheric precipitation, *Nat Phys*, *2*, 393-396.

Pohl, B., and A. J. Matthews (2007), Observed Changes in the Lifetime and Amplitude of the Madden–Julian Oscillation Associated with Interannual ENSO Sea Surface Temperature Anomalies, *J. Clim.*, *20*, 10.1175/jcli4230.1, 2659-2674.

Powell, S. W., and R. A. Houze (2013), The cloud population and onset of the Madden-Julian Oscillation over the Indian Ocean during DYNAMO-AMIE, *Journal of Geophysical Research: Atmospheres*, *118*, 10.1002/2013JD020421, 2013JD020421.

Powell, S. W., and R. A. Houze (2015), Effect of dry large-scale vertical motions on initial MJO convective onset, *Journal of Geophysical Research: Atmospheres*, *120*, 10.1002/2014JD022961, 4783-4805.

Pritchard, M. S., and C. S. Bretherton (2014), Causal Evidence that Rotational Moisture Advection is Critical to the Superparameterized Madden–Julian Oscillation, *J. Atmos. Sci.*, *71*, 10.1175/JAS-D-13-0119.1, 800-815.

Pritchard, M. S., and D. Yang (2016), Response of the Superparameterized Madden–Julian Oscillation to Extreme Climate and Basic-State Variation Challenges a Moisture Mode View, *J. Clim.*, *29*, 10.1175/jcli-d-15-0790.1, 4995-5008.

Pujiana, K., J. N. Moum, W. D. Smyth, and S. J. Warner (2015), Distinguishing ichthyogenic turbulence from geophysical turbulence, *Journal of Geophysical Research: Oceans*, *120*, 10.1002/2014JC010659, 3792-3804.

Pujiana, K., J. N. Moum, and W. D. Smyth (2018), The Role of Turbulence in Redistributing Upper-Ocean Heat, Freshwater, and Momentum in Response to the MJO in the Equatorial Indian Ocean, *J. Phys. Oceanogr.*, *48*, 10.1175/jpo-d-17-0146.1, 197-220.

Puy, M., J. Vialard, M. Lengaigne, and E. Guilyardi (2016), Modulation of equatorial Pacific westerly/easterly wind events by the Madden–Julian oscillation and convectively-coupled Rossby waves, *Climate Dyn.*, *46*, 10.1007/s00382-015-2695-x, 2155-2178.

Qian, J.-H. (2008), Why Precipitation Is Mostly Concentrated over Islands in the Maritime Continent, *J. Atmos. Sci.*, *65*, doi:10.1175/2007JAS2422.1, 1428-1441.

Ramage, C. S. (1968), ROLE OF A TROPICAL "MARITIME CONTINENT" IN THE ATMOSPHERIC CIRCULATION, *Mon. Weather Rev.*, *96*, doi:10.1175/1520-0493(1968)096<0365:ROATMC>2.0.CO;2, 365-370.

Randall, D., M. Khairoutdinov, A. Arakawa, and W. Grabowski (2003), Breaking the Cloud Parameterization Deadlock, *Bull. Am. Meteorol. Soc.*, *84*, 10.1175/BAMS-84-11-1547, 1547-1564.

Rashid, H. A., H. H. Hendon, M. C. Wheeler, and O. Alves (2011), Prediction of the Madden-Julian oscillation with the POAMA dynamical prediction system, *Climate Dyn.*, *36*, 10.1007/s00382-010-0754-x, 649-661.

Rasp, S., M. S. Pritchard, and P. Gentine (2018), Deep learning to represent subgrid processes in climate models, *Proceedings of the National Academy of Sciences*, *115*, 10.1073/pnas.1810286115, 9684-9689.

Rauniyar, S. P., and K. J. E. Walsh (2011), Scale Interaction of the Diurnal Cycle of Rainfall over the Maritime Continent and Australia: Influence of the MJO, *J. Clim.*, *24*, doi:10.1175/2010JCLI3673.1, 325-348.

Rauniyar, S. P., and K. J. E. Walsh (2013), Influence of ENSO on the Diurnal Cycle of Rainfall over the Maritime Continent and Australia, *J. Clim.*, *26*, 10.1175/jcli-d-12-00124.1, 1304-1321.

Ray, P., and C. Zhang (2010), A Case Study of the Mechanics of Extratropical Influence on the Initiation of the Madden–Julian Oscillation, *J. Atmos. Sci.*, *67*, 10.1175/2009jas3059.1, 515-528.

Ray, P., and T. Li (2013), Relative Roles of Circumnavigating Waves and Extratropics on the MJO and Its Relationship with the Mean State, *J. Atmos. Sci.*, *70*, 10.1175/jas-d-12-0153.1, 876-893.

Raymond, D. J. (1995), Regulation of Moist Convection over the West Pacific Warm Pool, *J. Atmos. Sci.*, *52*, 3945-3959.

Raymond, D. J. (2001), A new model of the Madden-Julian oscillation, *J. Atmos. Sci.*, *58*, 2807-2819.

Raymond, D. J., and Ž. Fuchs (2009), Moisture Modes and the Madden–Julian Oscillation, *J. Clim.*, *22*, 10.1175/2008jcli2739.1, 3031-3046.

Raymond, D. J., S. Sessions, A. Sobel, and Z. Fuchs (2009), The Mechanics of Gross Moist Stability, *Journal of Advances in Modeling Earth Systems*, *1*, 10.3894/james.2009.1.9, 20 pp.

Reed, R. J., W. J. Campbell, L. A. Rasmussen, and D. G. Rogers (1961), Evidence of a downward-propagating, annual wind reversal in the equatorial stratosphere, *Journal of Geophysical Research (1896-1977)*, *66*, 10.1029/JZ066i003p00813, 813-818.

Riley Dellaripa, E. M., and E. Maloney (2015), Riley Dellaripa, E. M., and E. D. Maloney, 2014: Analysis of MJO Wind-Flux Feedbacks in the Indian Ocean Using RAMA Buoy Observations. *J. Meteor. Soc. Japan*, doi:10.2151/jmsj.2015-021.

Riley, E. M., B. E. Mapes, and S. N. Tulich (2011), Clouds Associated with the Madden–Julian Oscillation: A New Perspective from CloudSat, *J. Atmos. Sci.*, *68*, 10.1175/JAS-D-11-030.1, 3032-3051.

Rostami, M., and V. Zeitlin (2019), Eastward-moving convection-enhanced modons in shallow water in the equatorial tangent plane, *Physics of Fluids*, *31*, 10.1063/1.5080415, 021701.

Roundy, P. E., K. MacRitchie, J. Asuma, and T. Melino (2010), Modulation of the Global Atmospheric Circulation by Combined Activity in the Madden–Julian Oscillation and the El Niño–Southern Oscillation during Boreal Winter, *J. Clim.*, *23*, 10.1175/2010JCLI3446.1, 4045-4059.

Rowe, A. K., and R. A. Houze (2015), Cloud organization and growth during the transition from suppressed to active MJO conditions, *Journal of Geophysical Research: Atmospheres*, *120*, 10.1002/2014JD022948, 10,324-310,350.

Ruppert, J. H., and R. H. Johnson (2015), Diurnally Modulated Cumulus Moistening in the Pre-Onset Stage of the Madden–Julian Oscillation during DYNAMO, *J. Atmos. Sci.*10.1175/JAS-D-14-0218.1.

Rushley, S. S., D. Kim, C. S. Bretherton, and M. S. Ahn (2018), Reexamining the Nonlinear Moisture - Precipitation Relationship Over the Tropical Oceans, *Geophys. Res. Lett.*, *45*, doi:10.1002/2017GL076296, 1133-1140.

Rushley, S. S., D. Kim, and Á. F. Adames (2019), Changes in the MJO under Greenhouse Gas–Induced Warming in CMIP5 Models, *J. Clim.*, *32*, 10.1175/jcli-d-18-0437.1, 803-821.

Rydbeck, A. V., and T. G. Jensen (2017), Oceanic Impetus for Convective Onset of the Madden–Julian Oscillation in the Western Indian Ocean, *J. Clim.*, *30*, 10.1175/jcli-d-16-0595.1, 4299-4316.

Sakaeda, N., G. Kiladis, and J. Dias (2017), The Diurnal Cycle of Tropical Cloudiness and Rainfall Associated with the Madden–Julian Oscillation, *J. Clim.*, *30*, 10.1175/jcli-d-16-0788.1, 3999-4020.

Salby, M. L., and H. H. Hendon (1994), Intraseasonal Behavior of Clouds, Temperature, and Motion in the Tropics, *J. Atmos. Sci.*, *51*, 2207-2224.

Salby, M. L., H. H. Hendon, and R. R. Garcia (1994), Planetary-Scale Circulations in the Presence of Climatological and Wave-Induced Heating, *J. Atmos. Sci.*, *51*, 3365-3365.

Sardeshmukh, P. D., and B. J. Hoskins (1988), The Generation of Global Rotational Flow by Steady Idealized Tropical Divergence, *J. Atmos. Sci.*, *45*, 10.1175/1520-0469(1988)045<1228:Tgogrf>2.0.Co;2, 1228-1251.

Schneider, T., J. Teixeira, C. S. Bretherton, F. Brient, K. G. Pressel, C. Schär, and A. P. Siebesma (2017), Climate goals and computing the future of clouds, *Nature Climate Change*, *7*, 10.1038/nclimate3190, 3-5.

Schubert, J. J., B. Stevens, and T. Crueger (2013), Madden-Julian oscillation as simulated by the MPI Earth System Model: Over the last and into the next millennium, *Journal of Advances in Modeling Earth Systems*, *5*, 10.1029/2012MS000180, 71-84.

Schwartz, M. J., D. E. Waliser, B. Tian, D. L. Wu, J. H. Jiang, and W. G. Read (2008), Characterization of MJO-related upper tropospheric hydrological processes using MLS, *Geophys. Res. Lett.*, *35*, Doi 10.1029/2008gl033675.

Seo, H., A. C. Subramanian, A. J. Miller, and N. R. Cavanaugh (2014), Coupled Impacts of the Diurnal Cycle of Sea Surface Temperature on the Madden–Julian Oscillation, *J. Clim.*, *27*, 10.1175/jcli-d-14-00141.1, 8422-8443.

Seo, K.-H., W. Wang, J. Gottschalck, Q. Zhang, J.-K. E. Schemm, W. R. Higgins, and A. Kumar (2009), Evaluation of MJO Forecast Skill from Several Statistical and Dynamical Forecast Models, *J. Clim.*, *22*, doi:10.1175/2008JCLI2421.1, 2372-2388.

Seo, K.-H., H.-J. Lee, and D. M. W. Frierson (2016), Unraveling the Teleconnection Mechanisms that Induce Wintertime Temperature Anomalies over the Northern Hemisphere Continents in Response to the MJO, *J. Atmos. Sci.*, *73*, 10.1175/JAS-D-16-0036.1, 3557-3571.

Seo, K.-H., and H.-J. Lee (2017), Mechanisms for a PNA-Like Teleconnection Pattern in Response to the MJO, *J. Atmos. Sci.*, *74*, 10.1175/jas-d-16-0343.1, 1767-1781.

Seo, K. H., and K. Y. Kim (2003), Propagation and initiation mechanisms of the Madden-Julian oscillation, *J. Geophys. Res.*, *108*, Doi 10.1029/2002jd002876, -.

Seo, K. H., and W. Q. Wang (2010), The Madden-Julian Oscillation Simulated in the NCEP Climate Forecast System Model: The Importance of Stratiform Heating, *J. Clim.*, *23*, Doi 10.1175/2010jcli2983.1, 4770-4793.

Seo, K. H., and S. W. Son (2012), The Global Atmospheric Circulation Response to Tropical Diabatic Heating Associated with the Madden-Julian Oscillation during Northern Winter, *J. Atmos. Sci.*, *69*, Doi 10.1175/2011jas3686.1, 79-96.

Shi, X., D. Kim, Á. F. Adames-Corraliza, and J. Sukhatme (2018), WISHE-moisture mode in an aquaplanet simulation, *Journal of Advances in Modeling Earth Systems*, *0*, 10.1029/2018MS001441.

Shinoda, T., H. H. Hendon, and J. Glick (1998), Intraseasonal Variability of Surface Fluxes and Sea Surface Temperature in the Tropical Western Pacific and Indian Oceans, *J. Clim.*, *11*, 10.1175/1520-0442(1998)011<1685:Ivosfa>2.0.Co;2, 1685-1702.

Shinoda, T., W. Han, L. Zamudio, R.-C. Lien, and M. Katsumata (2017), Remote Ocean Response to the Madden–Julian Oscillation during the DYNAMO Field Campaign: Impact on Somali Current System and the Seychelles–Chagos Thermocline Ridge, *Atmosphere*, *8*, 171.

Short, D. A., and K. Nakamura (2000), TRMM radar observations of shallow precipitation over the tropical oceans, *J. Clim.*, *13*, 4107-4124.

Simmons, A. J., J. M. Wallace, and G. W. Branstator (1983), Barotropic Wave Propagation and Instability, and Atmospheric Teleconnection Patterns, *J. Atmos. Sci.*, *40*, 10.1175/1520-0469(1983)040<1363:Bwpaia>2.0.Co;2, 1363-1392.

Skofronick-Jackson, G., D. Kirschbaum, W. Petersen, G. Huffman, C. Kidd, E. Stocker, and R. Kakar (2018), The Global Precipitation Measurement (GPM) mission's scientific achievements and societal contributions: reviewing four years of advanced rain and snow observations, *Quart. J. Roy. Meteor. Soc.*, *144*, 10.1002/qj.3313, 27-48.

Slingo, J., P. Inness, R. Neale, S. Woolnough, and G. Y. Yang (2003), Scale interactions on diurnal to seasonal timescales and their relevance to model systematic errors, *Annals of Geophysics*, *46*, 139-155.

Slingo, J. M., K. R. Sperber, J. S. Boyle, J. P. Ceron, M. Dix, B. Dugas, W. Ebisuzaki, J. Fyfe, D. Gregory, J. F. Gueremy, J. Hack, A. Harzallah, P. Inness, A. Kitoh, W. K. M. Lau, B. McAvaney, R. Madden, A. Matthews, T. N. Palmer, C. K. Park, D. Randall, and N. Renno (1996), Intraseasonal oscillations in 15 atmospheric general circulation models: Results from an AMIP diagnostic subproject, *Climate Dyn.*, *12*, 325-357.

Slingo, J. M., D. P. Rowell, K. R. Sperber, and F. Nortley (1999), On the predictability of the interannual behaviour of the Madden-Julian oscillation and its relationship with el Niño, *Quart. J. Roy. Meteor. Soc.*, *125*, 10.1002/qj.49712555411, 583-609.

Sobel, A., and E. Maloney (2012), An Idealized Semi-Empirical Framework for Modeling the Madden–Julian Oscillation, *J. Atmos. Sci.*, *69*, 10.1175/jas-d-11-0118.1, 1691-1705.

Sobel, A., and E. Maloney (2013), Moisture Modes and the Eastward Propagation of the MJO, *J. Atmos. Sci.*, *70*, Doi 10.1175/Jas-D-12-0189.1, 187-192.

Sobel, A., S. Wang, and D. Kim (2014), Moist Static Energy Budget of the MJO during DYNAMO, *J. Atmos. Sci.*, *71*, 10.1175/JAS-D-14-0052.1, 4276-4291.

Sobel, A. H., J. Nilsson, and L. M. Polvani (2001), The weak temperature gradient approximation and balanced tropical moisture waves, *J. Atmos. Sci.*, *58*, 3650-3665.

Sobel, A. H., and H. Gildor (2003), A simple time-dependent model of SST hot spots, *J. Clim.*, *16*, 3978-3992.

Sobel, A. H., E. D. Maloney, G. Bellon, and D. M. Frierson (2008), The role of surface heat fluxes in tropical intraseasonal oscillations, *Nature Geoscience*, *1*, Doi 10.1038/Ngeo312, 653-657.

Sobel, A. H., E. D. Maloney, G. Bellon, and D. M. Frierson (2010), Surface Fluxes and Tropical Intraseasonal Variability: a Reassessment, *Journal of Advances in Modeling Earth Systems*, *2*, 10.3894/JAMES.2010.2.2, 2.

Son, S.-W., Y. Lim, C. Yoo, H. H. Hendon, and J. Kim (2016), Stratospheric Control of the Madden–Julian Oscillation, *J. Clim.*, *30*, 10.1175/JCLI-D-16-0620.1, 1909-1922.

Son, S.-W., Y. Lim, C. Yoo, H. H. Hendon, and J. Kim (2017), Stratospheric Control of the Madden–Julian Oscillation, *J. Clim.*, *30*, 10.1175/jcli-d-16-0620.1, 1909-1922.

Song, E.-J., and K.-H. Seo (2016), Past- and present-day Madden-Julian Oscillation in CNRM-CM5, *Geophys. Res. Lett.*, *43*, 10.1002/2016GL068771, 4042-4048.

Sperber, K., J. Slingo, and P. Inness (2012), Modeling intraseasonal variability, in *Intraseasonal Variability in the Atmosphere-Ocean Climate System*, edited by W. K. M. Lau and D. E. Waliser, Springer, Heidelberg, Germany.

Sperber, K. R. (2003), Propagation and the vertical structure of the Madden-Julian oscillation, *Mon. Weather Rev.*, *131*, 3018-3037.

Sprintall, J., and M. Tomczak (1992), Evidence of the barrier layer in the surface layer of the tropics, *Journal of Geophysical Research: Oceans*, *97*, 10.1029/92JC00407, 7305-7316.

Stan, C., D. M. Straus, J. S. Frederiksen, H. Lin, E. D. Maloney, and C. Schumacher (2017), Review of Tropical-Extratropical Teleconnections on Intraseasonal Time Scales, *Rev. Geophys.*, *55*, 10.1002/2016RG000538, 902-937.

Stephens, G. L., P. J. Webster, R. H. Johnson, R. Engelen, and T. L'Ecuyer (2004), Observational evidence for the mutual regulation of the tropical hydrological cycle and tropical sea surface temperatures, *J. Clim.*, *17*, 2213-2224.

Stevens, B. (2002), Entrainment in stratocumulus-topped mixed layers, *Quart. J. Roy. Meteor. Soc.*, *128*, 10.1256/qj.01.202, 2663-2690.

Stolz, D. C., S. A. Rutledge, W. Xu, and J. R. Pierce (2017), Interactions between the MJO, Aerosols, and Convection over the Central Indian Ocean, *J. Atmos. Sci.*, *74*, 10.1175/jas-d-16-0054.1, 353-374.

Straub, K. H., and G. N. Kiladis (2003), The observed structure of convectively coupled Kelvin waves: Comparison with simple models of coupled wave instability, *J. Atmos. Sci.*, *60*, 1655-1668.

Straub, K. H. (2013), MJO Initiation in the Real-Time Multivariate MJO Index, *J. Clim.*, *26*, 10.1175/JCLI-D-12-00074.1, 1130-1151.

Subramanian, A., M. Jochum, A. J. Miller, R. Neale, H. Seo, D. Waliser, and R. Murtugudde (2014), The MJO and global warming: a study in CCSM4, *Climate Dyn.*, *42*, 10.1007/s00382-013-1846-1, 2019-2031.

Subramanian, A. C., and T. N. Palmer (2017), Ensemble superparameterization versus stochastic parameterization: A comparison of model uncertainty representation in tropical weather prediction, *Journal of Advances in Modeling Earth Systems*, *9*, 10.1002/2016MS000857, 1231-1250.

Sui, C.-H., and K.-M. Lau (1992), Multiscale Phenomena in the Tropical Atmosphere over the Western Pacific, *Mon. Weather Rev.*, *120*, 10.1175/1520-0493(1992)120<0407:Mpitta>2.0.Co;2, 407-430.

Sultan, B., S. Janicot, and A. Diedhiou (2003), The West African monsoon dynamics. Part I: Documentation of intraseasonal variability, *J. Clim.*, *16*, 3389-3406.

Takahashi, C., N. Sato, A. Seiki, K. Yoneyama, and R. Shirooka (2011), Projected Future Change of MJO and its Extratropical Teleconnection in East Asia during the Northern Winter Simulated in IPCC AR4 Models, *SOLA*, *7*, 10.2151/sola.2011-051, 201-204.

Takasuka, D., M. Satoh, and S. Yokoi (2019), Observational Evidence of Mixed Rossby-Gravity Waves as a Driving Force for the MJO Convective Initiation and Propagation, *Geophys. Res. Lett.*, *46*, 10.1029/2019GL083108, 5546-5555.

Takayabu, Y. N. (1994), Large-Scale Cloud Disturbances Associated with Equatorial Waves .2. Westward-Propagating Inertio-Gravity Waves, *J. Meteorol. Soc. Japan*, *72*, 451-465.

Takayabu, Y. N., T. Iguchi, M. Kachi, A. Shibata, and H. Kanzawa (1999), Abrupt termination of the 1997-98 El Nino in response to a Madden-Julian oscillation, *Nature*, *402*, 279-282.

Tao, L., J. Zhao, and T. Li (2015), Trend analysis of tropical intraseasonal oscillations in the summer and winter during 1982–2009, *International Journal of Climatology*, *35*, 10.1002/joc.4258, 3969-3978.

Tao, W.-K., E. A. Smith, R. F. Adler, Z. S. Haddad, A. Y. Hou, T. Iguchi, R. Kakar, T. N. Krishnamurti, C. D. Kummerow, S. Lang, R. Meneghini, K. Nakamura, T. Nakazawa, K. Okamoto, W. S. Olson, S. Satoh, S. Shige, J. Simpson, Y. Takayabu, G. J. Tripoli, and S. Yang (2006), Retrieval of Latent Heating from TRMM Measurements, *Bull. Am. Meteorol. Soc.*, *87*, 1555-1572.

Tao, W.-K., Y. N. Takayabu, S. Lang, S. Shige, W. Olson, A. Hou, G. Skofronick-Jackson, X. Jiang, C. Zhang, W. Lau, T. Krishnamurti, D. Waliser, M. Grecu, P. E. Ciesielski, R. H. Johnson, R. Houze, R. Kakar, K. Nakamura, S. Braun, S. Hagos, R. Oki, and A. Bhardwaj (2016), TRMM Latent Heating Retrieval: Applications and Comparisons with Field Campaigns and Large-Scale Analyses, *Meteorological Monographs*, *56*, doi:10.1175/AMSMONOGRAPHS-D-15-0013.1, 2.1-2.34.

Teng, H. Y., and B. Wang (2003), Interannual variations of the boreal summer intraseasonal oscillation in the Asian-Pacific region, *J. Clim.*, *16*, 3572-3584.

Thayer-Calder, K., and D. A. Randall (2009), The Role of Convective Moistening in the Madden-Julian Oscillation, *J. Atmos. Sci.*, *66*, Doi 10.1175/2009jas3081.1, 3297-3312.

Thompson, D. W. J., and J. M. Wallace (1998), The Arctic oscillation signature in the wintertime geopotential height and temperature fields, *Geophys. Res. Lett.*, *25*, 10.1029/98GL00950, 1297-1300.

Thompson, D. W. J., and J. M. Wallace (2000), Annular modes in the extratropical circulation. Part I: Month-to-month variability, *J. Clim.*, *13*, 1000-1016.

Thompson, E. J., S. A. Rutledge, B. Dolan, and M. Thurai (2015), Drop Size Distributions and Radar Observations of Convective and Stratiform Rain over the Equatorial Indian and West Pacific Oceans, *J. Atmos. Sci.*, *72*, 10.1175/jas-d-14-0206.1, 4091-4125.

Thomson, J., and J. Girton (2017), Sustained Measurements of Southern Ocean Air-Sea Coupling from a Wave Glider Autonomous Surface Vehicle, *Oceanography*, *30*, 10.5670/oceanog.2017.228, 104-109.

Thual, S., A. J. Majda, and S. N. Stechmann (2014), A Stochastic Skeleton Model for the MJO, *J. Atmos. Sci.*, *71*, 10.1175/JAS-D-13-0186.1, 697-715.

Tian, B., Y. L. Yung, D. E. Waliser, T. Tyranowski, L. Kuai, E. J. Fetzer, and F. W. Irion (2007), Intraseasonal variations of the tropical total ozone and their connection to the Madden-Julian Oscillation, *Geophys. Res. Lett.*, *34*, 10.1029/2007GL029451.

Tian, B., D. E. Waliser, E. J. Fetzer, and Y. L. Yung (2010), Vertical Moist Thermodynamic Structure of the Madden–Julian Oscillation in Atmospheric Infrared Sounder Retrievals: An Update and a Comparison to ECMWF Interim Re-Analysis, *Mon. Weather Rev.*, *138*, doi:10.1175/2010MWR3486.1, 4576-4582.

Tian, B., D. E. Waliser, R. A. Kahn, and S. Wong (2011), Modulation of Atlantic aerosols by the Madden-Julian Oscillation, *Journal of Geophysical Research: Atmospheres*, *116*, 10.1029/2010JD015201.

Tian, B., C. O. Ao, D. E. Waliser, E. J. Fetzer, A. J. Mannucci, and J. Teixeira (2012), Intraseasonal temperature variability in the upper troposphere and lower stratosphere from the GPS radio occultation measurements, *Journal of Geophysical Research: Atmospheres*, *117*, 10.1029/2012JD017715.

Tian, B. J., D. E. Waliser, and E. J. Fetzer (2006a), Modulation of the diurnal cycle of tropical deep convective clouds by the MJO, *Geophys. Res. Lett.*, *33*, Doi 10.1029/2006gl027752.

Tian, B. J., D. E. Waliser, E. J. Fetzer, B. H. Lambrigtsen, Y. L. Yung, and B. Wang (2006b), Vertical moist thermodynamic structure and spatial-temporal evolution of the MJO in AIRS observations, *J. Atmos. Sci.*, *63*, 2462-2485.

Ting, M., and P. D. Sardeshmukh (1993), Factors Determining the Extratropical Response to Equatorial Diabatic Heating Anomalies, *J. Atmos. Sci.*, *50*, 10.1175/1520-0469(1993)050<0907:Fdtert>2.0.Co;2, 907-918.

Tippett, M. K. (2018), Robustness of Relations between the MJO and U.S. Tornado Occurrence, *Mon. Weather Rev.*, *146*, 10.1175/mwr-d-18-0207.1, 3873-3884.

Tokioka, T., K. Yamazaki, A. Kitoh, and T. Ose (1988), The Equatorial 30-60 Day Oscillation and the Arakawa-Schubert Penetrative Cumulus Parameterization, *J. Meteorol. Soc. Japan*, *66*, 883-901.

Toms, B. A., E. A. Barnes, E. D. Maloney, and S. C. van den Heever (2020), The Global Teleconnection Signature of the Madden-Julian Oscillation and Its Modulation by the Quasi-Biennial Oscillation, *Journal of Geophysical Research: Atmospheres*, *125*, 10.1029/2020JD032653, e2020JD032653.

Tromeur, E., and W. B. Rossow (2010), Interaction of Tropical Deep Convection with the Large-Scale Circulation in the MJO, *J. Clim.*, *23*, Doi 10.1175/2009jcli3240.1, 1837-1853.

Tseng, K.-C., E. Maloney, and E. Barnes (2019), The Consistency of MJO Teleconnection Patterns: An Explanation Using Linear Rossby Wave Theory, *J. Clim.*, *32*, 10.1175/jcli-d-18-0211.1, 531-548.

Tseng, W.-L., H.-H. Hsu, N. Keenlyside, C.-W. J. Chang, B.-J. Tsuang, C.-Y. Tu, and L.-C. Jiang (2017), Effects of Surface Orography and Land–Sea Contrast on the Madden–Julian Oscillation in the Maritime Continent: A Numerical Study Using ECHAM5-SIT, *J. Clim.*, *30*, 10.1175/jcli-d-17-0051.1, 9725-9741.

Tung, W. W., and M. Yanai (2002a), Convective momentum transport observed during the TOGA COARE IOP. Part II: Case studies, *J. Atmos. Sci.*, *59*, 2535-2549.

Tung, W. W., and M. Yanai (2002b), Convective momentum transport observed during the TOGA COARE IOP. Part I: General features, *J. Atmos. Sci.*, *59*, 1857-1871.

Vecchi, G. A., and N. A. Bond (2004), The Madden-Julian Oscillation (MJO) and northern high latitude wintertime surface air temperatures, *Geophys. Res. Lett.*, *31*, L04104, Doi 10.1029/2003gl018645, -.

Virts, K. S., and J. M. Wallace (2010), Annual, Interannual, and Intraseasonal Variability of Tropical Tropopause Transition Layer Cirrus, *J. Atmos. Sci.*, *67*, doi:10.1175/2010JAS3413.1, 3097-3112.

Virts, K. S., and J. M. Wallace (2014), Observations of Temperature, Wind, Cirrus, and Trace Gases in the Tropical Tropopause Transition Layer during the MJO, *J. Atmos. Sci.*, *71*, 10.1175/jas-d-13-0178.1, 1143-1157.

Virts, K. S., and R. A. Houze (2015), Variation of Lightning and Convective Rain Fraction in Mesoscale Convective Systems of the MJO, *J. Atmos. Sci.*, *72*, 10.1175/jas-d-14-0201.1, 1932-1944.

Vitart, F., S. Woolnough, M. A. Balmaseda, and A. M. Tompkins (2007), Monthly forecast of the Madden-Julian oscillation using a coupled GCM, *Mon. Weather Rev.*, *135*, Doi 10.1175/Mwr3415.1, 2700-2715.

Vitart, F., and T. Jung (2010), Impact of the Northern Hemisphere extratropics on the skill in predicting the Madden Julian Oscillation, *Geophys. Res. Lett.*, *37*, 10.1029/2010GL045465.

Vitart, F., and F. Molteni (2010), Simulation of the Madden-Julian Oscillation and its teleconnections in the ECMWF forecast system, *Quart. J. Roy. Meteor. Soc.*, *136*, Doi 10.1002/Qj.623, 842-855.

Vitart, F., A. Robertson, A. Kumar, H. Hendon, Y. Takaya, H. Lin, A. Arribas, J.-Y. Lee, D. Waliser, B. Kirtman, and H.-K. Kinm (2012), Subseasonal To Seasonal Prediction: Research Implementation Plan, WWRP/THORPEX-WCRP Report.

Vitart, F., A. Robertson, and S2S Steering Group (2015), Sub-seasonal to seasonal prediction: Linking weather and climate. Seamless Prediction of the Earth System: From Minutes to Months, G. Brunet, S. Jones, and P. M. Ruti, Eds., WMO-1156, World Meteorological Organization, 385–401. [Available online at http://library.wmo.int/pmb_ged/wmo_1156_en.pdf.].

Vitart, F. (2017), Madden—Julian Oscillation prediction and teleconnections in the S2S database, *Quart. J. Roy. Meteor. Soc.*, *143*, 10.1002/qj.3079, 2210-2220.

Vitart, F., C. Ardilouze, A. Bonet, A. Brookshaw, M. Chen, C. Codorean, M. Déqué, L. Ferranti, E. Fucile, M. Fuentes, H. Hendon, J. Hodgson, H.-S. Kang, A. Kumar, H. Lin, G. Liu, X. Liu, P. Malguzzi, I. Mallas, M. Manoussakis, D. Mastrangelo, C. MacLachlan, P. McLean, A. Minami, R. Mladek, T. Nakazawa, S. Najm, Y. Nie, M. Rixen, A. W. Robertson, P. Ruti, C. Sun, Y. Takaya, M. Tolstykh, F. Venuti, D. Waliser, S. Woolnough, T. Wu, D.-J. Won, H. Xiao, R. Zaripov, and L. Zhang (2017), The Subseasonal to Seasonal (S2S) Prediction Project Database, *Bull. Am. Meteorol. Soc.*, *98*, 10.1175/bams-d-16-0017.1, 163-173.

Vitart, F., and A. W. Robertson (2018), The sub-seasonal to seasonal prediction project (S2S) and the prediction of extreme events, *npj Climate and Atmospheric Science*, *1*, 10.1038/s41612-018-0013-0, 3.

Waliser, D., K. Sperber, H. Hendon, D. Kim, M. Wheeler, K. Weickmann, C. Zhang, L. Donner, J. Gottschalck, W. Higgins, I. S. Kang, D. Legler, M. Moncrieff, F. Vitart, B. Wang, W. Wang, S. Woolnough, E. Maloney, S. Schubert, W. Stern, and C. M.-J. Oscillation (2009), MJO Simulation Diagnostics, *J. Clim.*, *22*, Doi 10.1175/2008jcli2731.1, 3006-3030.

Waliser, D. E., W. Stern, S. Schubert, and K. M. Lau (2003), Dynamic predictability of intraseasonal variability associated with the Asian summer monsoon, *Quart. J. Roy. Meteor. Soc.*, *129*, Doi 10.1256/Qj.02.51, 2897-2925.

Waliser, D. E., R. Murtugudde, P. Strutton, and J.-L. Li (2005), Subseasonal organization of ocean chlorophyll: Prospects for prediction based on the Madden-Julian Oscillation, *Geophys. Res. Lett.*, *32*, 10.1029/2005GL024300.

Waliser, D. E. (2012), Predictability and Forecasting, in *Intraseasonal Variability in the Atmosphere-Ocean Climate System*, edited by W. K. M. Lau and D. E. Waliser, Springer, Heidelberg, Germany.

Waliser, D. E., M. W. Moncrieff, D. Burridge, A. H. Fink, D. Gochis, B. N. Goswami, B. Guan, P. Harr, J. Heming, H.-H. Hsu, C. Jakob, M. Janiga, R. Johnson, S. Jones, P. Knippertz, J. Marengo, H. Nguyen, M. Pope, Y. Serra, C. Thorncroft, M. Wheeler, R. Wood, and S. Yuter (2012), The "Year" of Tropical Convection (May 2008–April 2010): Climate Variability and Weather Highlights, *Bull. Am. Meteorol. Soc.*, *93*, doi:10.1175/2011BAMS3095.1, 1189-1218.

Wallace, J. M., and D. S. Gutzler (1981), Teleconnections in the Geopotential Height Field during the Northern Hemisphere Winter, *Mon. Weather Rev.*, *109*, 10.1175/1520-0493(1981)109<0784:TITGHF>2.0.CO;2, 784-812.

Wang, B. (1988), Dynamics of Tropical Low-Frequency Waves - an Analysis of the Moist Kelvin Wave, *J. Atmos. Sci.*, *45*, 2051-2065.

Wang, B., and H. Rui (1990), Dynamics of the Coupled Moist Kelvin-Rossby Wave on an Equatorial Beta-Plane, *J. Atmos. Sci.*, *47*, 397-413.

Wang, B., and T. M. Li (1994), Convective Interaction with Boundary-Layer Dynamics in the Development of a Tropical Intraseasonal System, *J. Atmos. Sci.*, *51*, 1386-1400.

Wang, B., and X. S. Xie (1998), Coupled modes of the warm pool climate system. Part 1: The role of air-sea interaction in maintaining Madden-Julian oscillation, *J. Clim.*, *11*, 2116-2135.

Wang, B. (2006), *The Asian Monsoon*, Springer, Heidelberg, Germany.

Wang, B., and F. Liu (2011), A Model for Scale Interaction in the Madden–Julian Oscillation, *J. Atmos. Sci.*, *68*, 10.1175/2011jas3660.1, 2524-2536.

Wang, B., F. Liu, and G. Chen (2016a), A trio-interaction theory for Madden–Julian oscillation, *Geoscience Letters*, *3*, 10.1186/s40562-016-0066-z, 34.

Wang, B., and S.-S. Lee (2017), MJO Propagation Shaped by Zonal Asymmetric Structures: Results from 24 GCM Simulations, *J Clim*, *30*, 10.1175/jcli-d-16-0873.1, 7933-7952.

Wang, B., S.-S. Lee, D. E. Waliser, C. Zhang, A. Sobel, E. Maloney, T. Li, X. Jiang, and K.-J. Ha (2018a), Dynamics-Oriented Diagnostics for the Madden–Julian Oscillation, *J. Clim.*, *31*, 10.1175/jcli-d-17-0332.1, 3117-3135.

Wang, B., G. Chen, and F. Liu (2019a), Diversity of the Madden-Julian Oscillation, *Science Advances*, *5*, 10.1126/sciadv.aax0220, eaax0220.

Wang, D., J.-I. Yano, and Y. Lin (2019b), Madden–Julian Oscillations Seen in the Upper-Troposphere Vorticity Field: Interactions with Rossby Wave Trains, *J. Atmos. Sci.*, *76*, 10.1175/JAS-D-18-0172.1, 1785-1807.

Wang, J., H.-M. Kim, E. K. M. Chang, and S.-W. Son (2018b), Modulation of the MJO and North Pacific Storm Track Relationship by the QBO, *Journal of Geophysical Research: Atmospheres*, *123*, 10.1029/2017JD027977, 3976-3992.

Wang, L., T. Li, E. Maloney, and B. Wang (2017), Fundamental Causes of Propagating and Nonpropagating MJOs in MJOTF/GASS Models, *J. Clim.*, *30*, 10.1175/jcli-d-16-0765.1, 3743-3769.

Wang, L., T. Li, L. Chen, S. K. Behera, and T. Nasuno (2018c), Modulation of the MJO intensity over the equatorial western Pacific by two types of El Niño, *Climate Dyn.*, *51*, 10.1007/s00382-017-3949-6, 687-700.

Wang, S., A. H. Sobel, A. Fridlind, Z. Feng, J. M. Comstock, P. Minnis, and M. L. Nordeen (2015), Simulations of cloud-radiation interaction using large-scale forcing derived from the CINDY/DYNAMO northern sounding array, *Journal of Advances in Modeling Earth Systems*, *7*, 10.1002/2015MS000461, 1472-1498.

Wang, S., A. H. Sobel, M. K. Tippett, and F. Vitart (2019c), Prediction and predictability of tropical intraseasonal convection: seasonal dependence and the Maritime Continent prediction barrier, *Climate Dyn.*, *52*, 10.1007/s00382-018-4492-9, 6015-6031.

Wang, S., M. K. Tippett, A. H. Sobel, Z. K. Martin, and F. Vitart (2019d), Impact of the QBO on Prediction and Predictability of the MJO Convection, *Journal of Geophysical Research: Atmospheres*, *124*, 10.1029/2019jd030575, 11766-11782.

Wang, W., M.-P. Hung, S. Weaver, A. Kumar, and X. Fu (2014), MJO prediction in the NCEP Climate Forecast System version 2, *Climate Dyn.*10.1007/s00382-013-1806-9, 1-12.

Wang, W. Q., and M. E. Schlesinger (1999), The dependence on convection parameterization of the tropical intraseasonal oscillation simulated by the UIUC 11-layer atmospheric GCM, *J. Clim.*, *12*, 1423-1457.

Wang, Y., G. J. Zhang, and G. C. Craig (2016b), Stochastic convective parameterization improving the simulation of tropical precipitation variability in the NCAR CAM5, *Geophys. Res. Lett.*, *43*, 10.1002/2016GL069818, 6612-6619.

Wang, Z., W. Li, M. S. Peng, X. Jiang, R. McTaggart-Cowan, and C. A. Davis (2018d), Predictive Skill and Predictability of North Atlantic Tropical Cyclogenesis in Different Synoptic Flow Regimes, *J. Atmos. Sci.*, *75*, 10.1175/jas-d-17-0094.1, 361-378.

Weber, N. J., and C. F. Mass (2017), Evaluating CFSv2 Subseasonal Forecast Skill with an Emphasis on Tropical Convection, *Mon. Weather Rev.*, *145*, 10.1175/MWR-D-17-0109.1, 3795-3815.

Weber, N. J., and C. F. Mass (2019), Subseasonal Weather Prediction in a Global Convection-Permitting Model, *Bull. Am. Meteorol. Soc.*, *100*, 10.1175/bams-d-18-0210.1, 1079-1089.

Webster, P. J., and J. R. Holton (1982), Cross-Equatorial Response to Middle-Latitude Forcing in a Zonally Varying Basic State, *J. Atmos. Sci.*, *39*, 10.1175/1520-0469(1982)039<0722:Certml>2.0.Co;2, 722-733.

Webster, P. J., and R. Lukas (1992), TOGA COARE: The Coupled Ocean–Atmosphere Response Experiment, *Bull. Am. Meteorol. Soc.*, *73*, 1377-1416.

Webster, P. J., V. O. Magana, T. N. Palmer, J. Shukla, R. A. Tomas, M. Yanai, and T. Yasunari (1998), Monsoons: Processes, predictability, and the prospects for prediction, *J. Geophys. Res.*, *103*, 14451-14510.

Weisheimer, A., S. Corti, T. Palmer, and F. Vitart (2014), Addressing model error through atmospheric stochastic physical parametrizations: impact on the coupled ECMWF seasonal forecasting system, *Philosophical Transactions of the Royal Society A: Mathematical, Physical and Engineering Sciences*, *372*, 10.1098/rsta.2013.0290, 20130290.

Wheeler, M., and G. N. Kiladis (1999), Convectively coupled equatorial waves: Analysis of clouds and temperature in the wavenumber-frequency domain, *J. Atmos. Sci.*, *56*, 374-399.

Wheeler, M., and E. Maloney (2013), Madden-Julian Oscillation (MJO) Task Force: a joint effort of the climate and weather communities, *CLIVAR Exchanges*. No. 61 (Vol 18 No.1).

Wheeler, M. C., and H. H. Hendon (2004), An All-Season Real-Time Multivariate MJO Index: Development of an Index for Monitoring and Prediction, *Mon. Weather Rev.*, *132*, 1917-1932.

Wheeler, M. C., H. H. Hendon, S. Cleland, H. Meinke, and A. Donald (2009), Impacts of the Madden–Julian Oscillation on Australian Rainfall and Circulation, *J. Clim.*, *22*, 10.1175/2008jcli2595.1, 1482-1498.

Whelan, J., and J. S. Frederiksen (2017), Dynamics of the perfect storms: La Niña and Australia's extreme rainfall and floods of 1974 and 2011, *Climate Dyn.*, *48*, 10.1007/s00382-016-3312-3, 3935-3948.

Wilson, E. A., A. L. Gordon, and D. Kim (2013), Observations of the Madden Julian Oscillation during Indian Ocean Dipole events, *Journal of Geophysical Research: Atmospheres*, *118*, 10.1002/jgrd.50241, 2588-2599.

Wolding, B. O., and E. D. Maloney (2015), Objective Diagnostics and the Madden–Julian Oscillation. Part II: Application to Moist Static Energy and Moisture Budgets, *J. Clim.*, *28*, 10.1175/jcli-d-14-00689.1, 7786-7808.

Wolding, B. O., E. D. Maloney, S. Henderson, and M. Branson (2017), Climate change and the Madden-Julian oscillation: A vertically resolved weak temperature gradient analysis, *Journal of Advances in Modeling Earth Systems*10.1002/2016MS000843, n/a-n/a.

Woolnough, S. J., J. M. Slingo, and B. J. Hoskins (2000), The Relationship between Convection and Sea Surface Temperature on Intraseasonal Timescales, *J. Clim.*, *13*, 2086-2104.

Woolnough, S. J., F. Vitart, and M. A. Balmaseda (2007), The role of the ocean in the Madden–Julian Oscillation: Implications for MJO prediction, *Quart. J. Roy. Meteor. Soc.*, *133*, 10.1002/qj.4, 117-128.

Wu, C.-H., and H.-H. Hsu (2009), Topographic Influence on the MJO in the Maritime Continent, *J. Clim.*, *22*, doi:10.1175/2009JCLI2825.1, 5433-5448.

Wu, P., D. Ardiansyah, S. Yokoi, S. Mori, F. Syamsudin, and K. Yoneyama (2017), Why Torrential Rain Occurs on the Western Coast of Sumatra Island at the Leading Edge of the MJO Westerly Wind Bursts, *SOLA*, *13*, 10.2151/sola.2017-007, 36-40.

Wu, P., S. Mori, and F. Syamsudin (2018), Land-sea surface air temperature contrast on the western coast of Sumatra Island during an active phase of the Madden-Julian Oscillation, *Progress in Earth and Planetary Science*, *5*, 10.1186/s40645-017-0160-7, 4.

Xavier, P. K., J. C. Petch, N. P. Klingaman, S. J. Woolnough, X. Jiang, D. E. Waliser, M. Caian, J. Cole, S. M. Hagos, C. Hannay, D. Kim, T. Miyakawa, M. S. Pritchard, R. Roehrig, E. Shindo, F. Vitart, and H. Wang (2015), Vertical structure and physical processes of the Madden-Julian Oscillation: Biases and uncertainties at short range, *Journal of Geophysical Research: Atmospheres*, *120*, 10.1002/2014JD022718, 4749-4763.

Xiang, B., S.-J. Lin, M. Zhao, S. Zhang, G. Vecchi, T. Li, X. Jiang, L. Harris, and J.-H. Chen (2015a), Beyond Weather Time-Scale Prediction for Hurricane Sandy and Super Typhoon Haiyan in a Global Climate Model, *Mon. Weather Rev.*, *143*, 10.1175/MWR-D-14-00227.1, 524-535.

Xiang, B., M. Zhao, X. Jiang, S.-J. Lin, T. Li, X. Fu, and G. Vecchi (2015b), 3-4 week MJO prediction skill in a GFDL Coupled Model, *J. Clim.*10.1175/JCLI-D-15-0102.1.

Xiang, B., Q. Sun, J.-H. Chen, N. C. Johnson, and X. Jiang (2020), Subseasonal prediction of land cold extremes in boreal wintertime, *Journal of Geophysical Research: Atmospheres*.

Xie, S.-P., C. Deser, G. A. Vecchi, J. Ma, H. Teng, and A. T. Wittenberg (2010), Global Warming Pattern Formation: Sea Surface Temperature and Rainfall, *J. Clim.*, *23*, 10.1175/2009jcli3329.1, 966-986.

Xu, W., and S. A. Rutledge (2014), Convective Characteristics of the Madden–Julian Oscillation over the Central Indian Ocean Observed by Shipborne Radar during DYNAMO, *J. Atmos. Sci.*, *71*, 10.1175/JAS-D-13-0372.1, 2859-2877.

Xu, W., and S. A. Rutledge (2015), Morphology, Intensity, and Rainfall Production of MJO Convection: Observations from DYNAMO Shipborne Radar and TRMM, *J. Atmos. Sci.*, *72*, 10.1175/jas-d-14-0130.1, 623-640.

Xu, W., S. A. Rutledge, C. Schumacher, and M. Katsumata (2015), Evolution, Properties, and Spatial Variability of MJO Convection near and off the Equator during DYNAMO, *J. Atmos. Sci.*, *72*, 10.1175/jas-d-15-0032.1, 4126-4147.

Xu, W., and S. A. Rutledge (2016), Time scales of shallow-to-deep convective transition associated with the onset of Madden-Julian Oscillations, *Geophys. Res. Lett.*, *43*, 10.1002/2016GL068269, 2880-2888.

Yadav, P., and D. M. Straus (2017), Circulation Response to Fast and Slow MJO Episodes, *Mon. Weather Rev.*, *145*, 10.1175/mwr-d-16-0352.1, 1577-1596.

Yanai, M., and M.-M. Lu (1983), Equatorially Trapped Waves at the 200 mb Level and Their Association with Meridional Convergence of Wave Energy Flux, *J. Atmos. Sci.*, *40*, 10.1175/1520-0469(1983)040<2785:Etwatm>2.0.Co;2, 2785-2803.

Yang, D., and A. P. Ingersoll (2013), Triggered Convection, Gravity Waves, and the MJO: A Shallow-Water Model, *J. Atmos. Sci.*, *70*, 10.1175/JAS-D-12-0255.1, 2476-2486.

Yang, D., and A. P. Ingersoll (2014), A theory of the MJO horizontal scale, *Geophys. Res. Lett.*, *41*, 10.1002/2013GL058542, 1059-1064.

Yang, D., Á. F. Adames-Corraliza, B. Khouider, B. Wang, and C. Zhang (2020), A Review of MJO Theories. Chap. 19 in The Multiscale Global Monsoon System, eds: C.P. Chang, K.J. Ha, R. H. Johnson, D. Kim, G.N. Lau, B. Wang. World Scientific Series on Asia-Pacific Weather and Climate, Vol. 11. World Scientific, Singapore., edited.

Yang, G.-Y., and J. Slingo (2001a), The Diurnal Cycle in the Tropics, *Mon. Weather Rev.*, *129*, 10.1175/1520-0493(2001)129<0784:Tdcitt>2.0.Co;2, 784-801.

Yang, G. Y., and J. Slingo (2001b), The diurnal cycle in the Tropics, *Mon. Weather Rev.*, *129*, 784-801.

Yang, Q., Q. Fu, and Y. Hu (2010), Radiative impacts of clouds in the tropical tropopause layer, *Journal of Geophysical Research: Atmospheres*, *115*, 10.1029/2009JD012393.

Yang, Q., A. J. Majda, and M. W. Moncrieff (2019), Upscale Impact of Mesoscale Convective Systems and Its Parameterization in an Idealized GCM for an MJO Analog above the Equator, *J. Atmos. Sci.*, *76*, 10.1175/jas-d-18-0260.1, 865-892.

Yano, J.-I., and J. J. Tribbia (2017), Tropical Atmospheric Madden–Julian Oscillation: A Strongly Nonlinear Free Solitary Rossby Wave?, *J. Atmos. Sci.*, *74*, 10.1175/JAS-D-16-0319.1, 3473-3489.

Yasunaga, K., and B. Mapes (2012), Differences between More Divergent and More Rotational Types of Convectively Coupled Equatorial Waves. Part II: Composite Analysis based on Space–Time Filtering, *J. Atmos. Sci.*, *69*, 10.1175/jas-d-11-034.1, 17-34.

Yokoi, S., M. Katsumata, and K. Yoneyama (2014), Variability in surface meteorology and air-sea fluxes due to cumulus convective systems observed during CINDY/DYNAMO, *Journal of Geophysical Research: Atmospheres*, *119*, 10.1002/2013JD020621, 2013JD020621.

Yokoi, S., and A. H. Sobel (2015), Intraseasonal Variability and Seasonal March of the Moist Static Energy Budget over the Eastern Maritime Continent during CINDY2011/DYNAMO, *Journal of the Meteorological Society of Japan. Ser. II*, *93A*, 10.2151/jmsj.2015-041, 81-100.

Yokoi, S., S. Mori, M. Katsumata, B. Geng, K. Yasunaga, F. Syamsudin, Nurhayati, and K. Yoneyama (2017), Diurnal Cycle of Precipitation Observed in the Western Coastal Area of Sumatra Island: Offshore Preconditioning by Gravity Waves, *Mon. Weather Rev.*, *145*, 10.1175/mwr-d-16-0468.1, 3745-3761.

Yokoi, S., S. Mori, F. Syamsudin, U. Haryoko, and B. Geng (2019), Environmental Conditions for Nighttime Offshore Migration of Precipitation Area as Revealed by In Situ Observation off Sumatra Island, *Mon. Weather Rev.*, *147*, 10.1175/mwr-d-18-0412.1, 3391-3407.

Yoneyama, K., C. Zhang, and C. N. Long (2013), Tracking Pulses of the Madden–Julian Oscillation, *Bull. Am. Meteorol. Soc.*, *94*, 10.1175/BAMS-D-12-00157.1, 1871-1891.

Yoneyama, K., and C. Zhang (2020), Years of the Maritime Continent, *Geophys. Res. Lett.*, *47*, 10.1029/2020GL087182, e2020GL087182.

Yoo, C., S. Feldstein, and S. Lee (2011), The impact of the Madden-Julian Oscillation trend on the Arctic amplification of surface air temperature during the 1979–2008 boreal winter, *Geophys. Res. Lett.*, *38*, 10.1029/2011GL049881, L24804.

Yoo, C., S. Lee, and S. B. Feldstein (2012), Mechanisms of Arctic Surface Air Temperature Change in Response to the Madden–Julian Oscillation, *J. Clim.*, *25*, 10.1175/JCLI-D-11-00566.1, 5777-5790.

Yoo, C., and S.-W. Son (2016), Modulation of the boreal wintertime Madden-Julian oscillation by the stratospheric quasi-biennial oscillation, *Geophys. Res. Lett.*, *43*, 10.1002/2016GL067762, 1392-1398.

Yu, J. Y., and J. D. Neelin (1994), Modes of Tropical Variability under Convective Adjustment and the Madden-Julian Oscillation .2. Numerical Results, *J. Atmos. Sci.*, *51*, 1895-1914.

Yuan, J., and R. A. Houze (2010), Global Variability of Mesoscale Convective System Anvil Structure from A-Train Satellite Data, *J. Clim.*, *23*, 10.1175/2010jcli3671.1, 5864-5888.

Yuan, J., and R. A. Houze (2012), Deep Convective Systems Observed by A-Train in the Tropical Indo-Pacific Region Affected by the MJO, *J. Atmos. Sci.*, *70*, 10.1175/jas-d-12-057.1, 465-486.

Zadra, A., K. Williams, A. Frassoni, M. Rixen, Á. F. Adames, J. Berner, F. Bouyssel, B. Casati, H. Christensen, M. B. Ek, G. Flato, Y. Huang, F. Judt, H. Lin, E. Maloney, W. Merryfield, A. V. Niekerk, T. Rackow, K. Saito, N. Wedi, and P. Yadav (2018), Systematic Errors in Weather and Climate Models: Nature, Origins, and Ways Forward, *Bull. Am. Meteorol. Soc.*, *99*, 10.1175/bams-d-17-0287.1, ES67-ES70.

Zeng, Z., S.-P. Ho, S. Sokolovskiy, and Y.-H. Kuo (2012), Structural evolution of the Madden-Julian Oscillation from COSMIC radio occultation data, *Journal of Geophysical Research: Atmospheres*, *117*, 10.1029/2012JD017685, D22108.

Zermeño-Díaz, D. M., C. Zhang, P. Kollias, and H. Kalesse (2015), The Role of Shallow Cloud Moistening in MJO and Non-MJO Convective Events over the ARM Manus Site, *J. Atmos. Sci.*, *72*, 10.1175/jas-d-14-0322.1, 4797-4820.

Zhang, C., and P. J. Webster (1989), Effects of Zonal Flows on Equatorially Trapped Waves, *J. Atmos. Sci.*, *46*, 10.1175/1520-0469(1989)046<3632:Eozfoe>2.0.Co;2, 3632-3652.

Zhang, C. (1996), Atmospheric Intraseasonal Variability at the Surface in the Tropical Western Pacific Ocean, *J. Atmos. Sci.*, *53*, 739-758.

Zhang, C., and H. H. Hendon (1997), Propagating and Standing Components of the Intraseasonal Oscillationin Tropical Convection, *J. Atmos. Sci.*, *54*, doi:10.1175/1520-0469(1997)054<0741:PASCOT>2.0.CO;2, 741-752.

Zhang, C., and J. Gottschalck (2002), SST Anomalies of ENSO and the Madden–Julian Oscillation in the Equatorial Pacific, *J. Clim.*, *15*, 10.1175/1520-0442(2002)015<2429:SAOEAT>2.0.CO;2, 2429-2445.

Zhang, C., J. Ling, S. Hagos, W.-K. Tao, S. Lang, Y. N. Takayabu, S. Shige, M. Katsumata, W. S. Olson, and T. L'Ecuyer (2010), MJO Signals in Latent Heating: Results from TRMM Retrievals, *J. Atmos. Sci.*, *67*, 10.1175/2010jas3398.1, 3488-3508.

Zhang, C. (2012), Vertical structure from recent observations, in *Intraseasonal Variability in the Atmosphere-Ocean Climate System*, edited by W. K. M. Lau and D. E. Waliser, Springer, Heidelberg, Germany.

Zhang, C., and J. Ling (2012), Potential Vorticity of the Madden–Julian Oscillation, *J. Atmos. Sci.*, *69*, 10.1175/JAS-D-11-081.1, 65-78.

Zhang, C. (2013), Madden–Julian Oscillation: Bridging Weather and Climate, *Bull. Am. Meteorol. Soc.*, *94*, 10.1175/bams-d-12-00026.1, 1849-1870.

Zhang, C., J. Gottschalck, E. D. Maloney, M. W. Moncrieff, F. Vitart, D. E. Waliser, B. Wang, and M. C. Wheeler (2013), Cracking the MJO nut, *Geophys. Res. Lett.*, *40*, 10.1002/grl.50244, 1223-1230.

Zhang, C., and J. Ling (2017), Barrier Effect of the Indo-Pacific Maritime Continent on the MJO: Perspectives from Tracking MJO Precipitation, *J. Clim.*, *30*, 10.1175/JCLI-D-16-0614.1, 3439-3459.

Zhang, C., and B. Zhang (2018), QBO-MJO Connection, *Journal of Geophysical Research: Atmospheres*, *123*, 10.1002/2017jd028171, 2957-2967.

Zhang, C., Á. F. Adames, B. Khouider, B. Wang, and D. Yang (2020), FOUR THEORIES OF THE MADDEN-JULIAN OSCILLATION, *Rev. Geophys.*10.1029/2019RG000685, e2019RG000685.

Zhang, C. D., and M. J. McPhaden (2000), Intraseasonal surface cooling in the equatorial western Pacific, *J. Clim.*, *13*, 2261-2276.

Zhang, C. D., and M. Dong (2004), Seasonality in the Madden-Julian oscillation, *J. Clim.*, *17*, 3169-3180.

Zhang, C. D. (2005), Madden-Julian oscillation, *Rev. Geophys.*, *43*, RG2003, DOI: 10.1029/2004RG000158, 36.

Zhang, C. D., M. Dong, S. Gualdi, H. H. Hendon, E. D. Maloney, A. Marshall, K. R. Sperber, and W. Q. Wang (2006), Simulations of the Madden-Julian oscillation in four pairs of coupled and uncoupled global models, *Climate Dyn.*, *27*, 573-592.

Zhang, D., M. F. Cronin, C. Meinig, J. T. Farrar, R. Jenkins, D. Peacock, J. Keene, A. Sutton, and Q. Yang (2019), Comparing Air-Sea Flux Measurements from a New Unmanned Surface Vehicle and Proven Platforms During the SPURS-2 Field Campaign, *Oceanography*, *32*, https://doi.org/10.5670/oceanog.2019.220, 122-133.

Zhang, G. J., and M. Mu (2005), Simulation of the Madden–Julian Oscillation in the NCAR CCM3 Using a Revised Zhang–McFarlane Convection Parameterization Scheme, *J. Clim.*, *18*, 10.1175/jcli3508.1, 4046-4064.

Zhang, G. J., and X. L. Song (2009), Interaction of deep and shallow convection is key to Madden-Julian Oscillation simulation, *Geophys. Res. Lett.*, *36*, Doi 10.1029/2009gl037340.

Zhao, N., and T. Nasuno (2020), How Does the Air-Sea Coupling Frequency Affect Convection During the MJO Passage?, *Journal of Advances in Modeling Earth Systems*, *12*, 10.1029/2020MS002058, e2020MS002058.

Zheng, C., E. K.-M. Chang, H.-M. Kim, M. Zhang, and W. Wang (2018), Impacts of the Madden–Julian Oscillation on Storm-Track Activity, Surface Air Temperature, and Precipitation over North America, *J. Clim.*, *31*, 10.1175/jcli-d-17-0534.1, 6113-6134.

Zhou, L., R. B. Neale, M. Jochum, and R. Murtugudde (2012a), Improved Madden-Julian Oscillations with Improved Physics: The Impact of Modified Convection Parameterizations, *J. Clim.*, *25*, Doi 10.1175/2011jcli4059.1, 1116-1136.

Zhou, L., and R. Murtugudde (2020), Oceanic Impacts on MJOs Detouring near the Maritime Continent, *J. Clim.*, *33*, 10.1175/jcli-d-19-0505.1, 2371-2388.

Zhou, S., M. L'Heureux, S. Weaver, and A. Kumar (2012b), A composite study of the MJO influence on the surface air temperature and precipitation over the Continental United States, *Climate Dyn.*, *38*, 10.1007/s00382-011-1001-9, 1459-1471.

Zhu, C., T. Nakazawa, J. Li, and L. Chen (2003), The 30–60 day intraseasonal oscillation over the western North Pacific Ocean and its impacts on summer flooding in China during 1998, *Geophys. Res. Lett.*, *30*, 10.1029/2003GL017817, 1952.

Zhu, H., and H. H. Hendon (2015), Role of large-scale moisture advection for simulation of the MJO with increased entrainment, *Quart. J. Roy. Meteor. Soc.*, *141*, 10.1002/qj.2510, 2127-2136.

Zhu, H. Y., H. Hendon, and C. Jakob (2009), Convection in a Parameterized and Superparameterized Model and Its Role in the Representation of the MJO, *J. Atmos. Sci.*, *66*, Doi 10.1175/2009jas3097.1, 2796-2811.

Zuluaga, M. D., and R. A. Houze (2013), Evolution of the Population of Precipitating Convective Systems over the Equatorial Indian Ocean in Active Phases of the Madden–Julian Oscillation, *J. Atmos. Sci.*, *70*, 10.1175/JAS-D-12-0311.1, 2713-2725.

Figure 01.

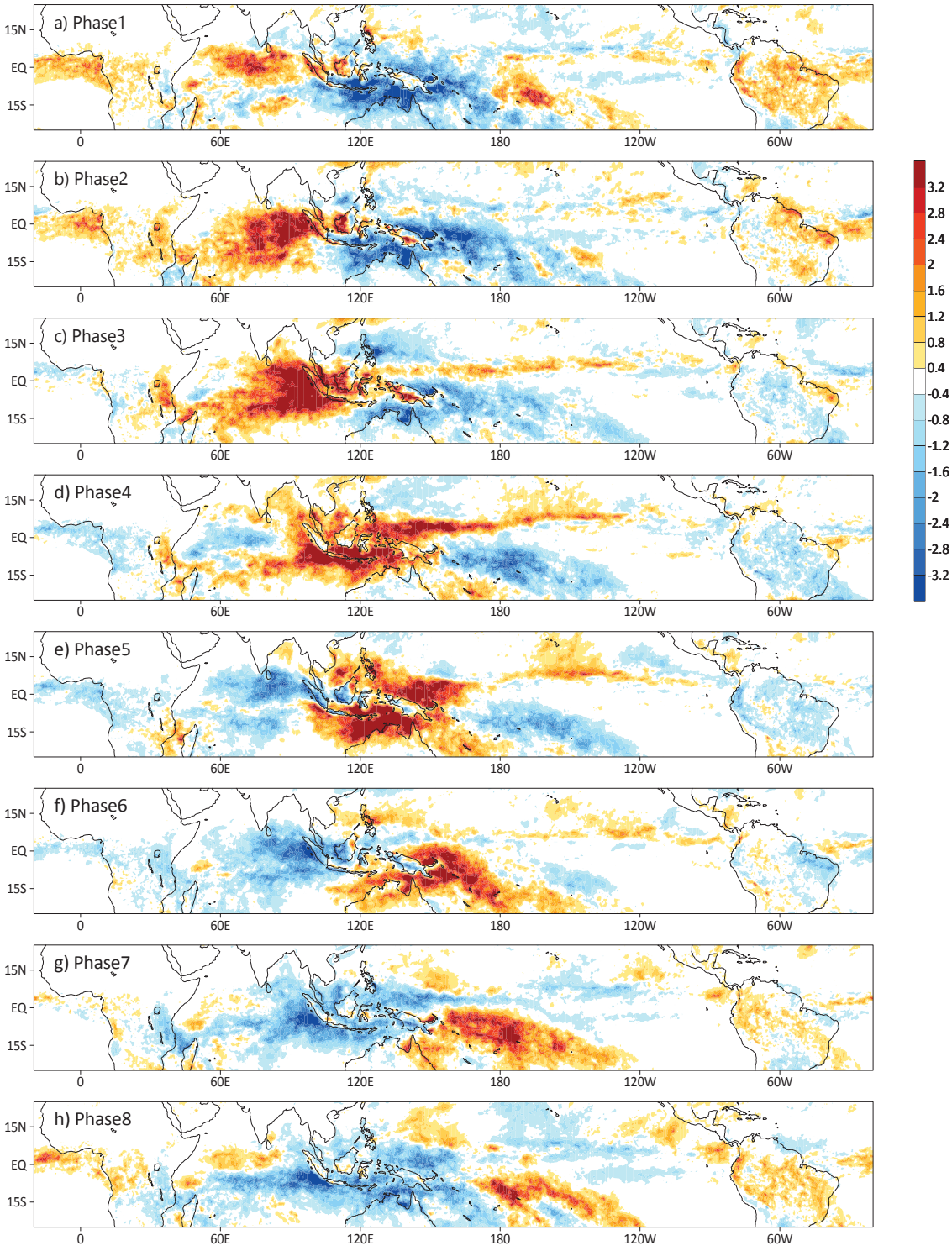

a) Phase1
b) Phase2
c) Phase3
d) Phase4
e) Phase5
f) Phase6
g) Phase7
h) Phase8
15N
EQ
15S
0
60E
120E
180
120W
60W
3.2
2.8
2.4
2
1.6
1.2
0.8
0.4
-0.4
-0.8
-1.2
-1.6
-2
-2.4
-2.8
-3.2

Figure 02.

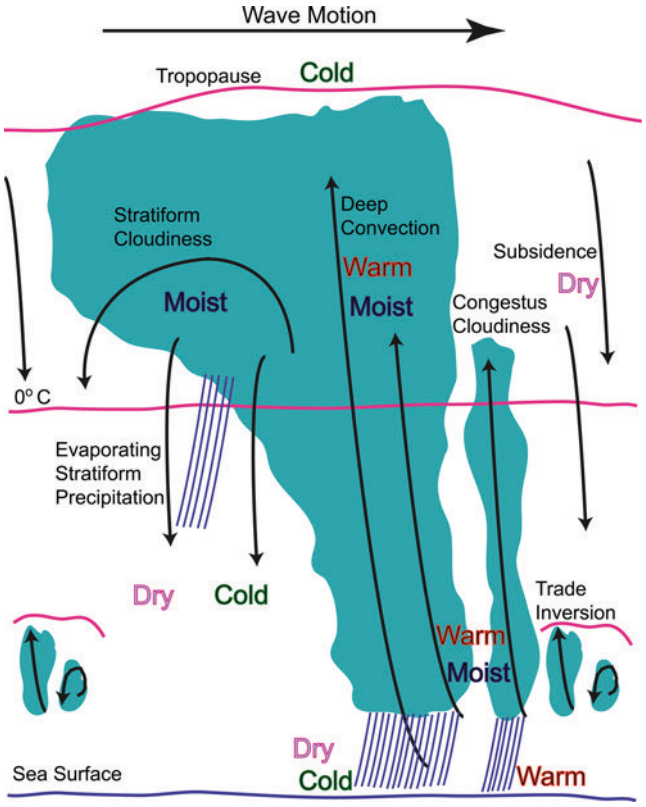

Wave Motion
Tropopause
Cold
Stratiform
Cloudiness
Moist
Deep
Convection
Warm
Moist
Subsidence
Dry
Congestus
Cloudiness
0° C
Evaporating
Stratiform
Precipitation
Dry
Cold
Trade
Inversion
Warm
Moist
Dry
Cold
Warm
Sea Surface

Figure 03.

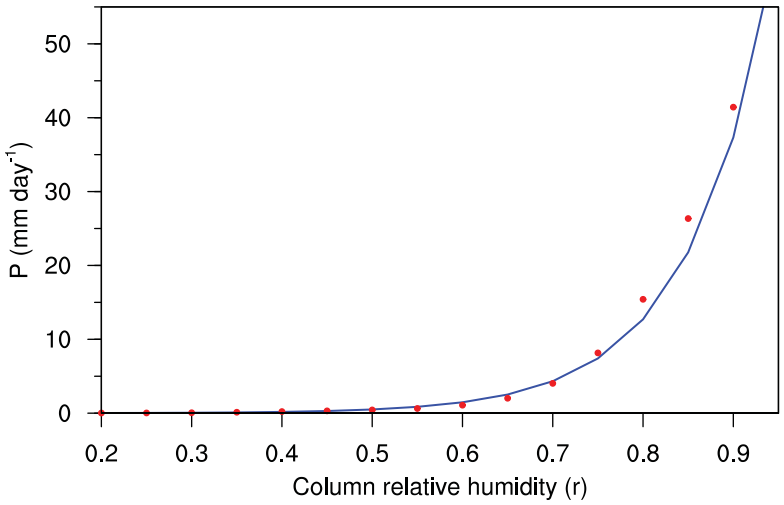

50
40
30
20
10
0
P (mm day-1)
0.2
0.3
0.4
0.5
0.6
0.7
0.8
0.9
Column relative humidity (r)

Figure 04.

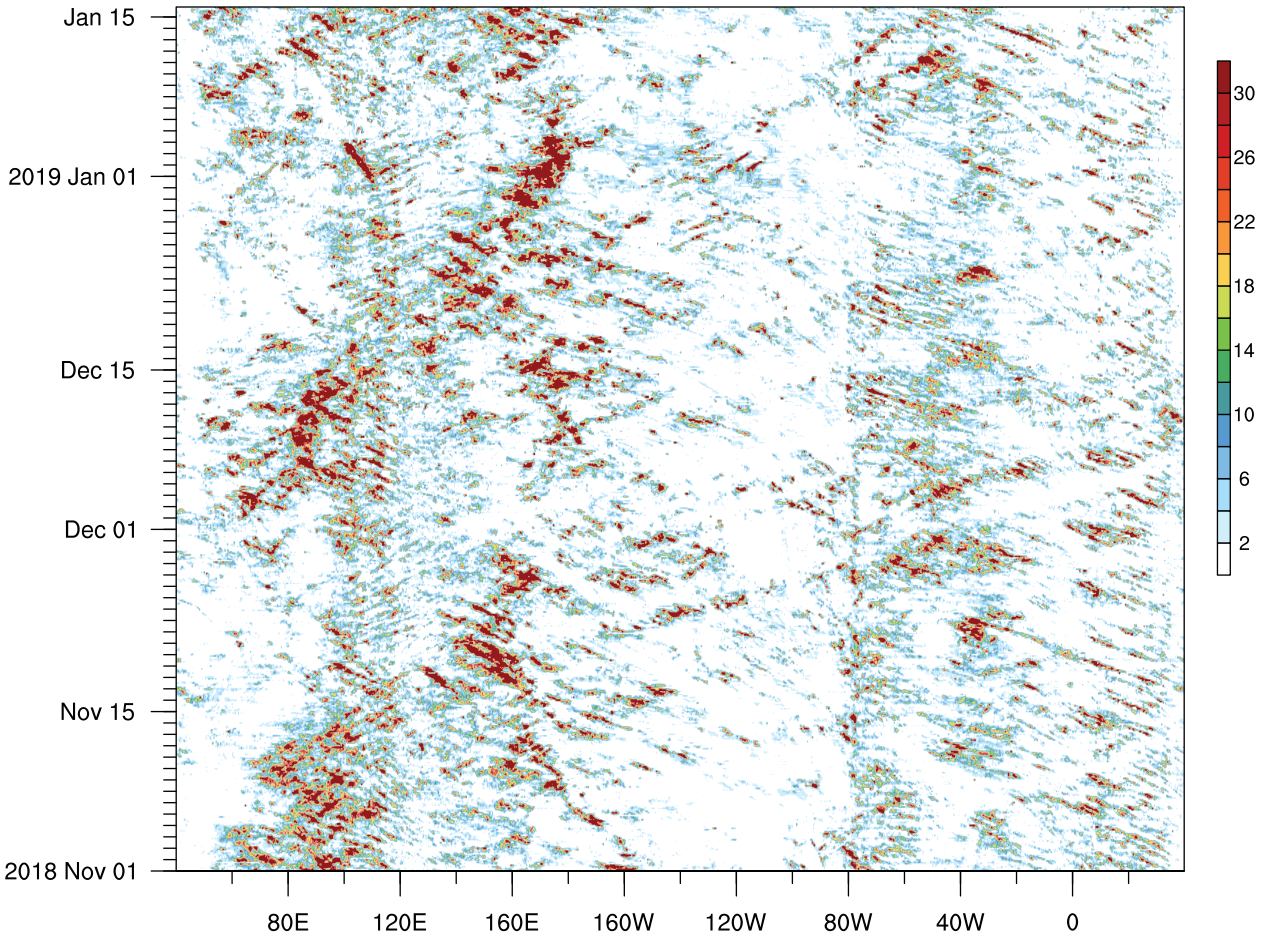

Jan 15
2019 Jan 01
Dec 15
Dec 01
Nov 15
2018 Nov 01
80E
120E
160E
160W
120W
80W
40W
0
30
26
22
18
14
10
6
2

Figure 05.

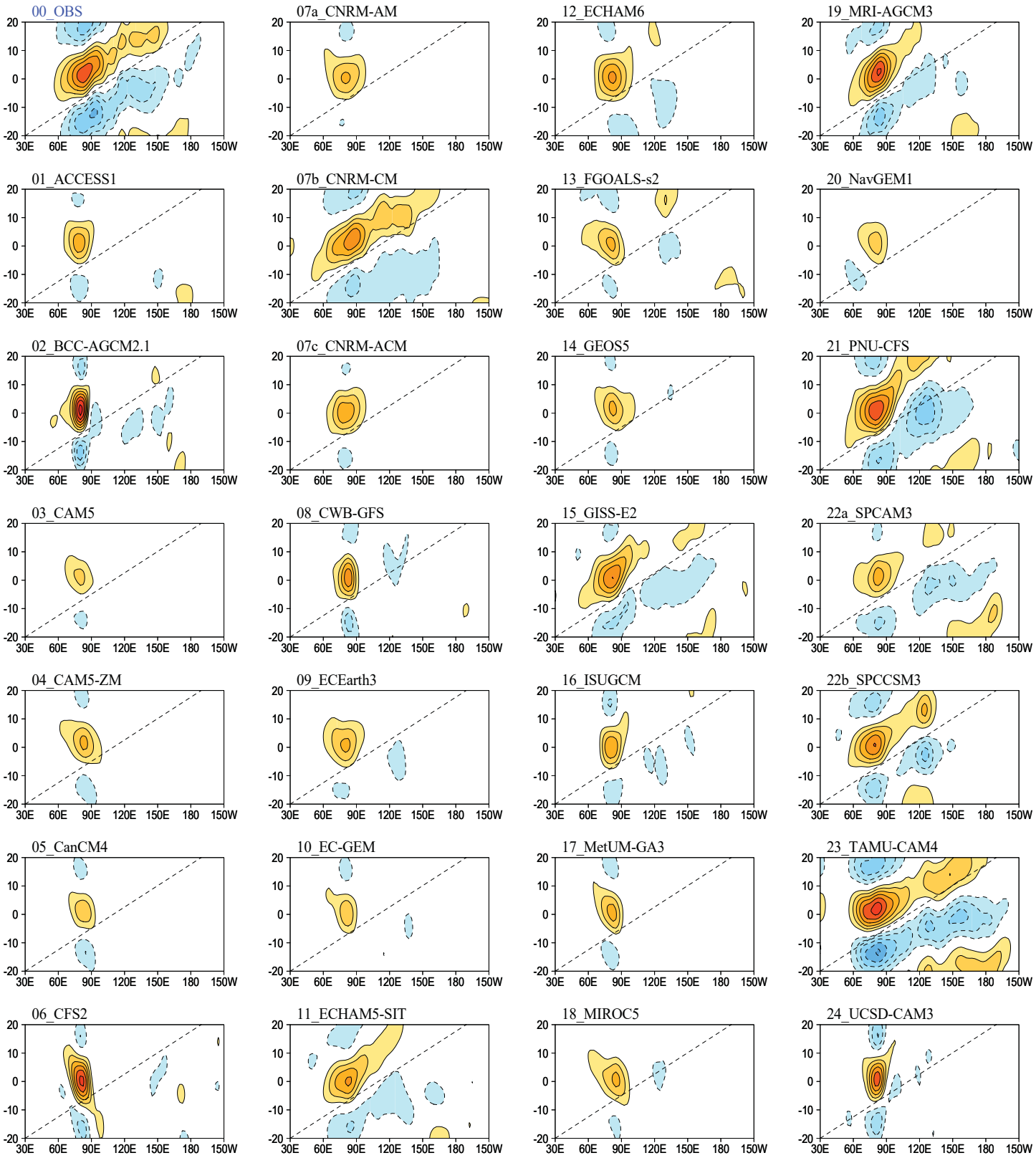

00_OBS
07a_CNRM-AM
12_ECHAM6
19_MRI-AGCM3
01_ACCESS1
07b_CNRM-CM
13_FGOALS-s2
20_NavGEM1
02_BCC-AGCM2.1
07c_CNRM-ACM
14_GEOS5
21_PNU-CFS
03_CAM5
08_CWB-GFS
15_GISS-E2
22a_SPCAM3
04_CAM5-ZM
09_ECEarth3
16_ISUGCM
22b_SPCCSM3
05_CanCM4
10_EC-GEM
17_MetUM-GA3
23_TAMU-CAM4
06_CFS2
11_ECHAM5-SIT
18_MIROC5
24_UCSD-CAM3
20 10 0 -10 -20
30E 60E 90E 120E 150E 180 150W
-2.4 -2.1 -1.8 -1.5 -1.2 -0.9 -0.6 -0.3 0.3 0.6 0.9 1.2 1.5 1.8 2.1 2.4
mm/day

Figure 06.

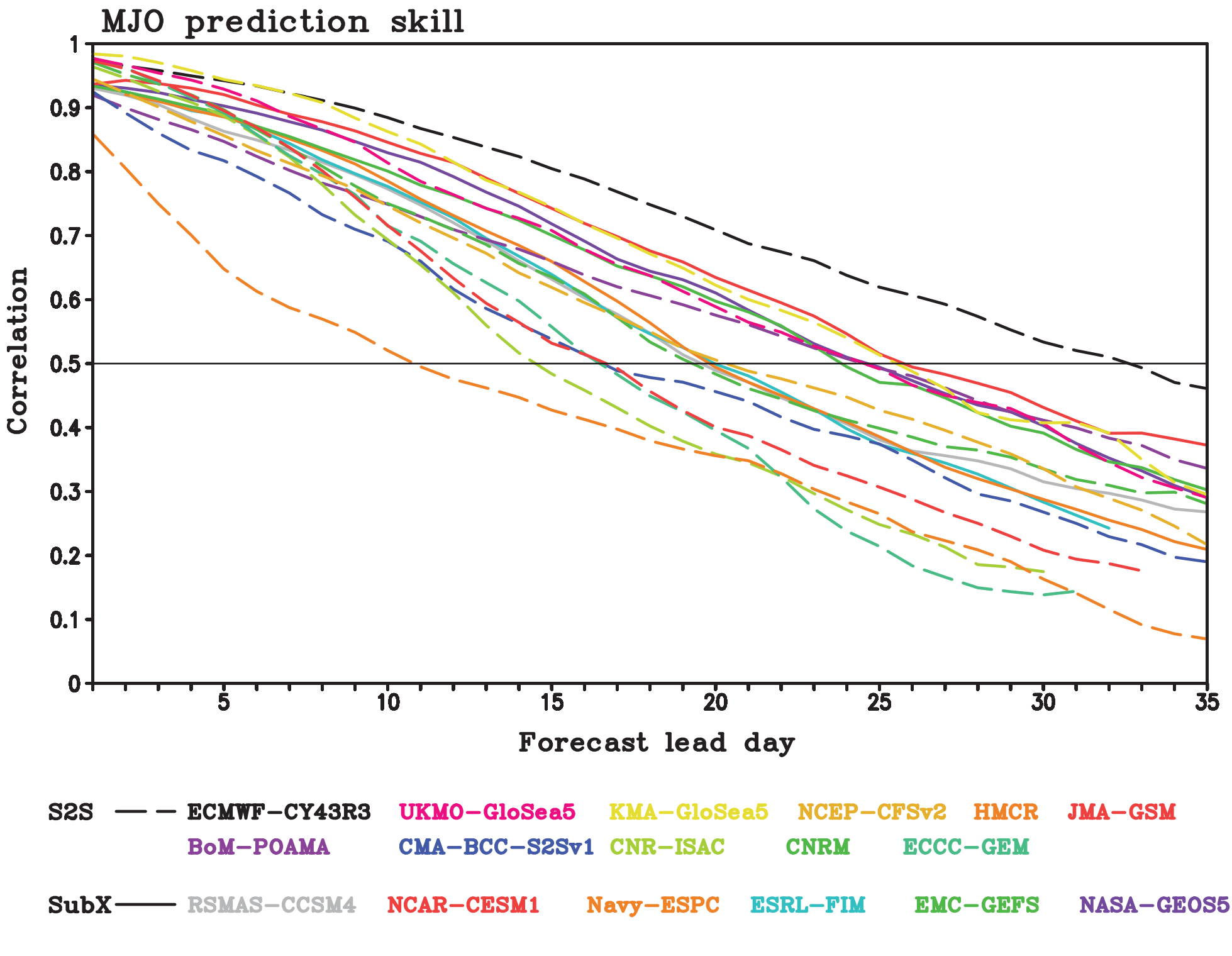

MJO prediction skill
Correlation
1
0.9
0.8
0.7
0.6
0.5
0.4
0.3
0.2
0.1
0
5
10
15
20
25
30
35
Forecast lead day
S2S
ECMWF-CY43R3
UKMO-GloSea5
KMA-GloSea5
NCEP-CFSv2
HMCR
JMA-GSM
BoM-POAMA
CMA-BCC-S2Sv1
CNR-ISAC
CNRM
ECCC-GEM
SubX
RSMAS-CCSM4
NCAR-CESM1
Navy-ESPC
ESRL-FIM
EMC-GEFS
NASA-GEOS5

Figure 07.

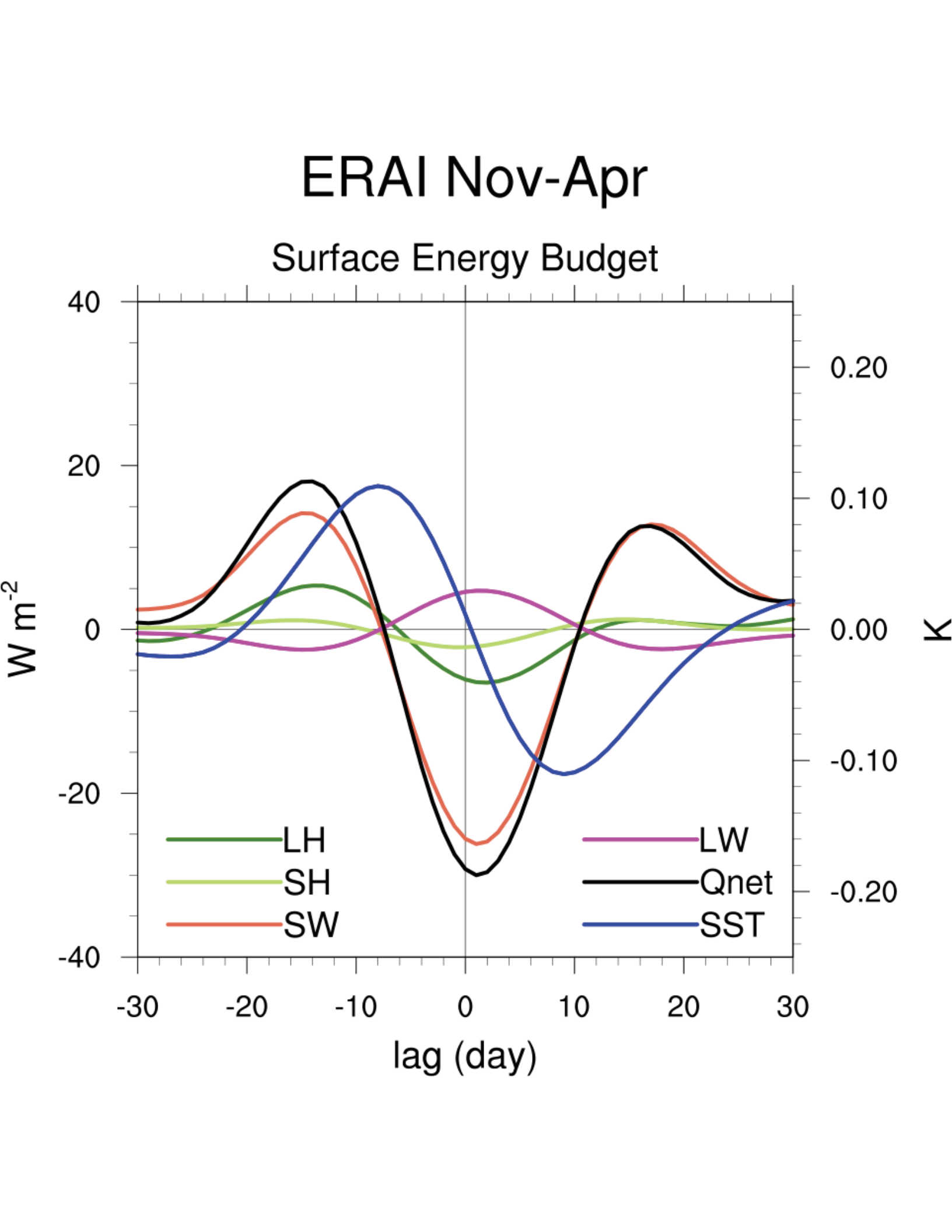

ERAI Nov-Apr
Surface Energy Budget
40
20
0
-20
-40
W m-2
0.20
0.10
0.00
-0.10
-0.20
K
-30
-20
-10
0
10
20
30
lag (day)
LH
SH
SW
LW
Qnet
SST

Figure 08.

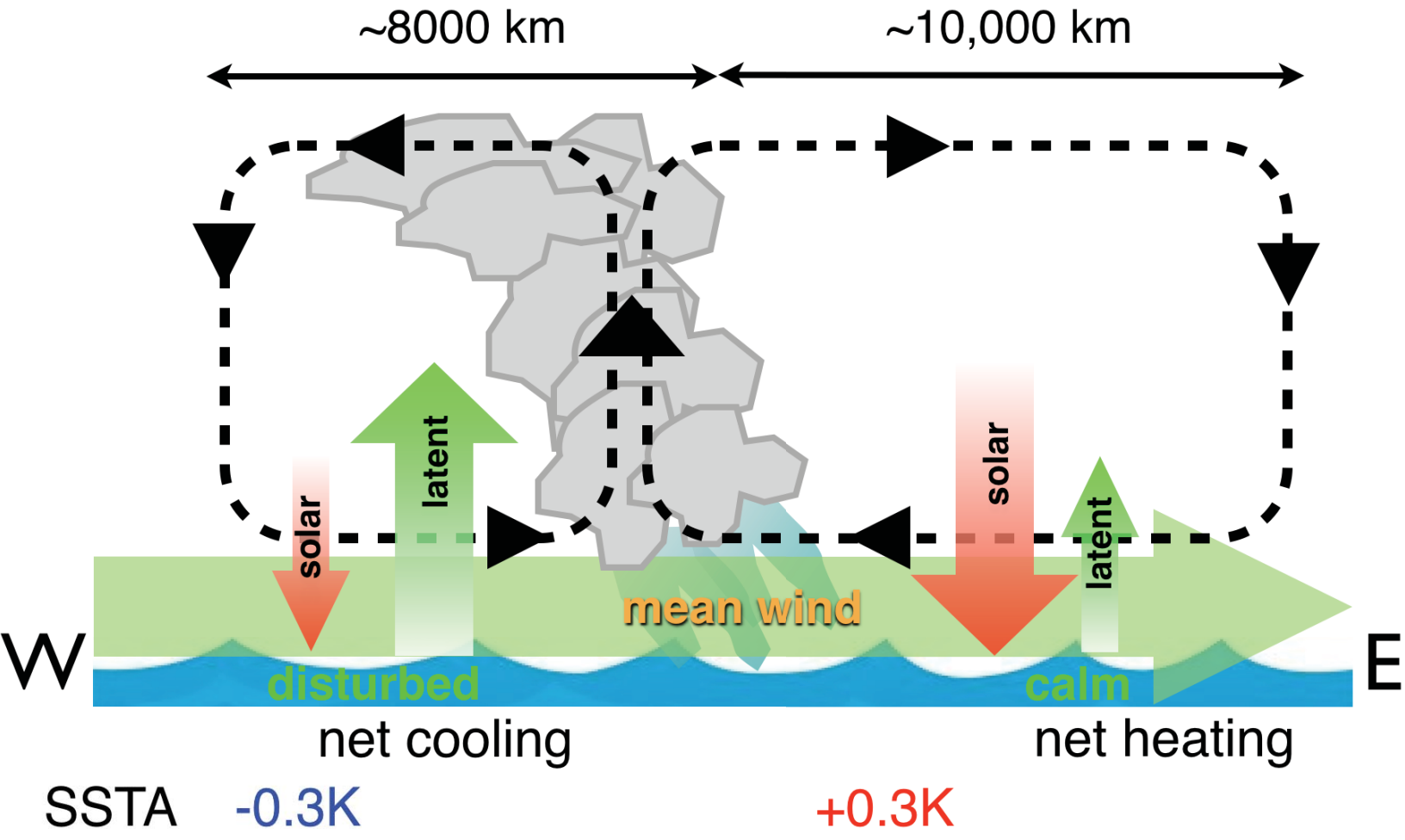

~8000 km
~10,000 km
solar
latent
solar
latent
mean wind
W
E
disturbed
calm
net cooling
net heating
SSTA
-0.3K
+0.3K

Figure 09.

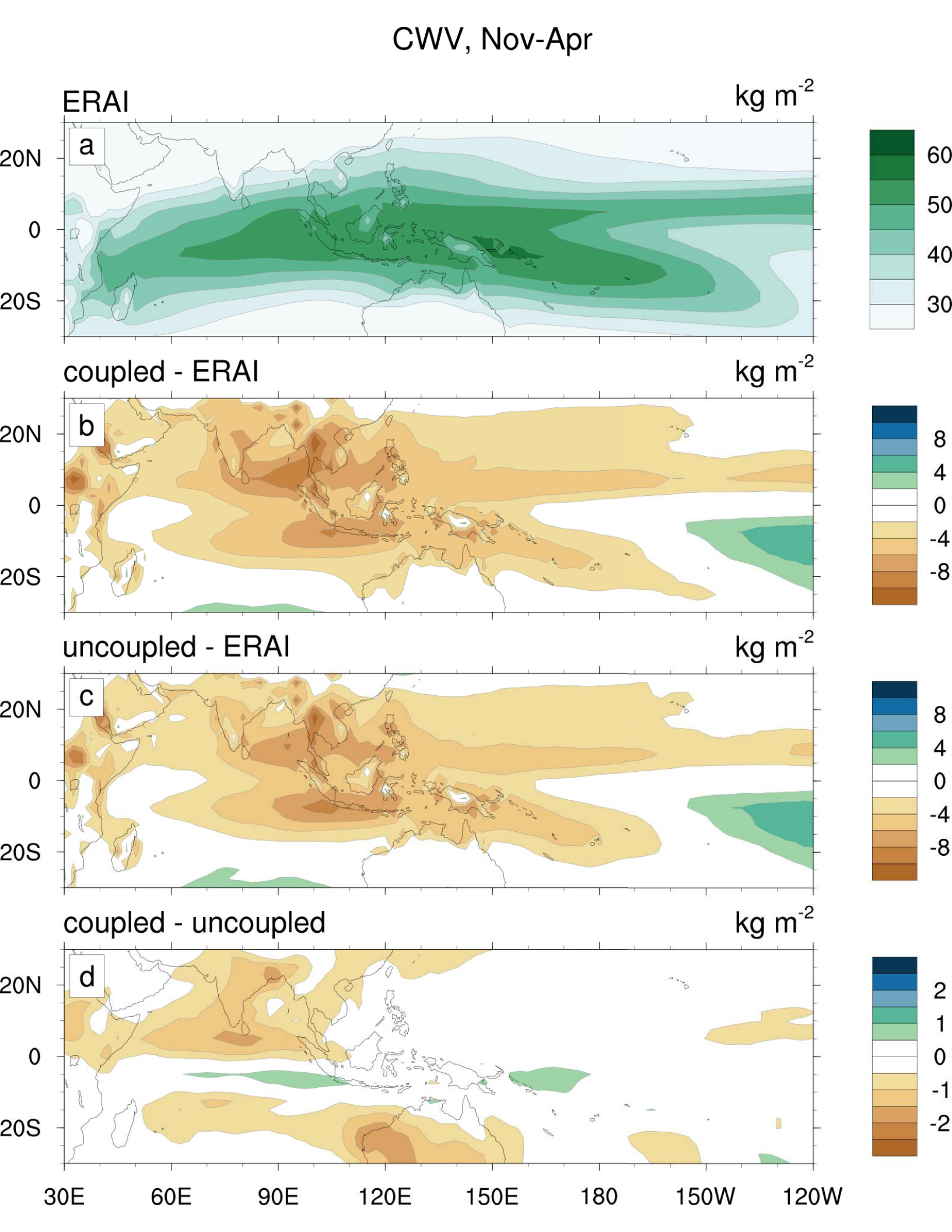

CWV, Nov-Apr
ERAI
kg m-2
a
20N
0
20S
60
50
40
30
coupled - ERAI
kg m-2
b
20N
0
20S
8
4
0
-4
-8
uncoupled - ERAI
kg m-2
c
20N
0
20S
8
4
0
-4
-8
coupled - uncoupled
kg m-2
d
20N
0
20S
2
1
0
-1
-2
30E
60E
90E
120E
150E
180
150W
120W

Figure 01.

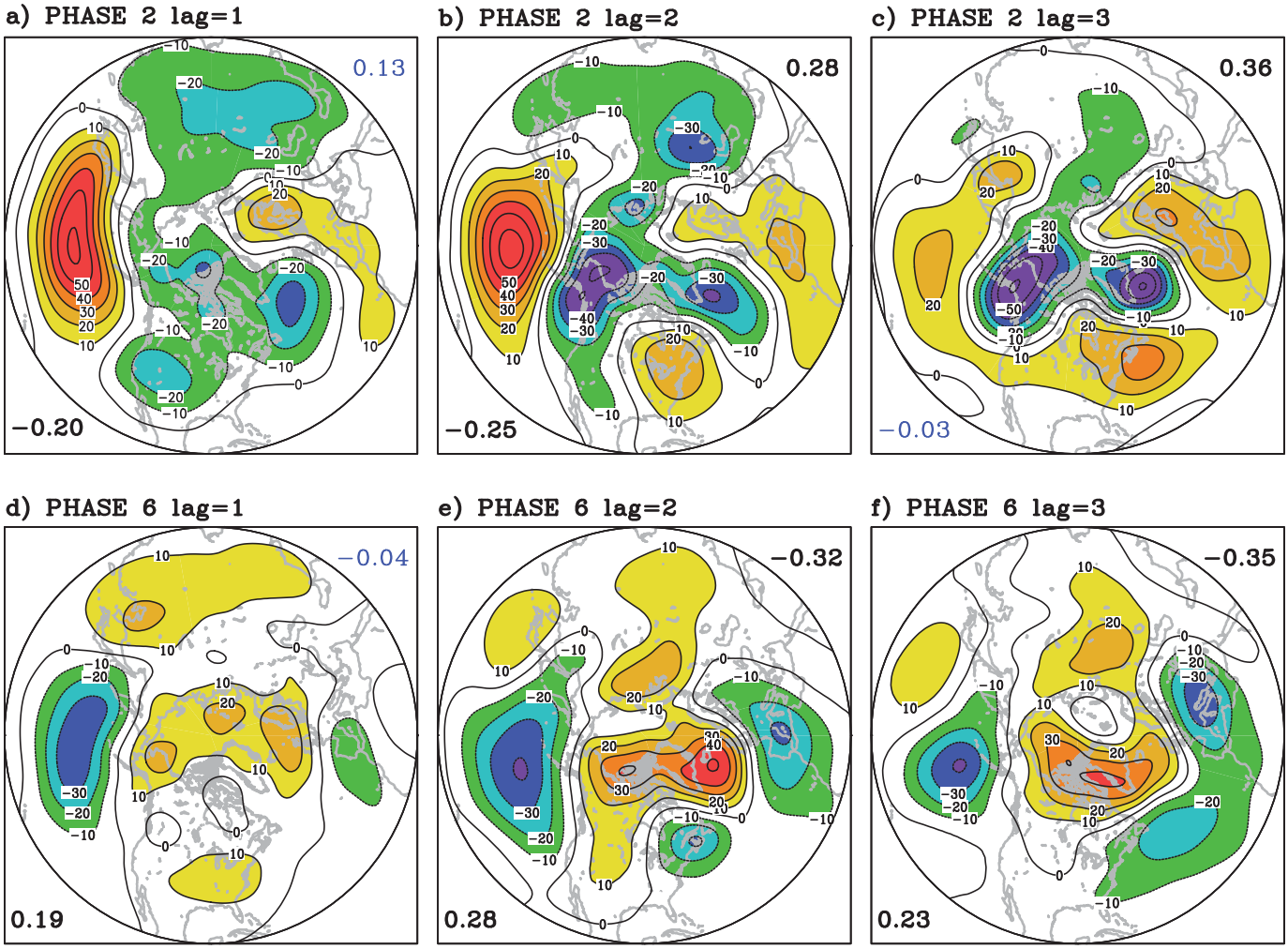

a) PHASE 2 lag=1
0.13
−0.20
b) PHASE 2 lag=2
0.28
−0.25
c) PHASE 2 lag=3
0.36
−0.03
d) PHASE 6 lag=1
−0.04
0.19
e) PHASE 6 lag=2
−0.32
0.28
f) PHASE 6 lag=3
−0.35
0.23

Figure 11.

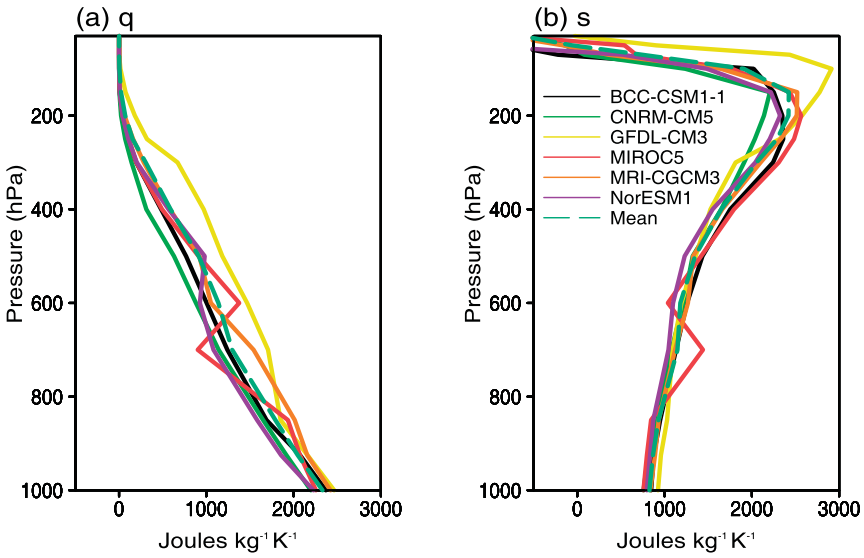
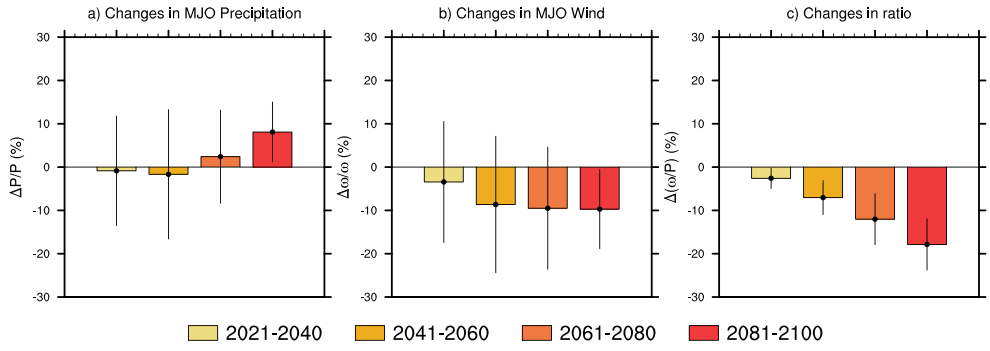

(a) q
(b) s
Pressure (hPa)
200
400
600
800
1000
0
1000
2000
3000
Joules kg-1 K-1
BCC-CSM1-1
CNRM-CM5
GFDL-CM3
MIROC5
MRI-CGCM3
NorESM1
Mean

Figure 12.


a) Changes in MJO Precipitation
b) Changes in MJO Wind
c) Changes in ratio
ΔP/P (%)
Δω/ω (%)
Δ(ω/P) (%)
30
20
10
0
-10
-20
-30
2021-2040
2041-2060
2061-2080
2081-2100